RECENT SEDIMENTS IN THE FIRTH OF TAY REGION

by

SHARAD KUMAR MISHRA, M.Tech., B.Sc.

Thesis presented for the degree of DOCTOR OF PHILOSOPHY of the UNIVERSITY OF EDINBURGH in the FACULTY OF SCIENCE

1964

CONTENTS

Section 1. INTRODUCTION

1.1 General

The present investigation of the sedimentation in the Tay Estuary Region has been undertaken to study the processes of erosion, transport and deposition in various environments. The recent sediments are studied to find out their source, and modes of transport and deposition by considerable attention to the grain-size frequency distributions. A number of methods of analysing the results are used and their relative advantages in separating sands from different environments assessed. Studies of the sedimentary structures are used to decipher the processes of transport and environments of deposition. The nature of source rocks is deduced from heavy mineral studies and the character of transporting medium and the distance of transport are visualised from the roundness of grains, grain size, sorting and mineral content.

1.2 Description of the area

The river Tay flows into the sea, after a winding course of about 180 miles, between Budden Ness and Tentsmuir point. The total catchment area is approximately 2,000 square miles and the nearby River Earn draws about 380 square miles. The area under study stretches from Perth to Budden Ness, a distance of 29 miles on the northern side

FIG. 1

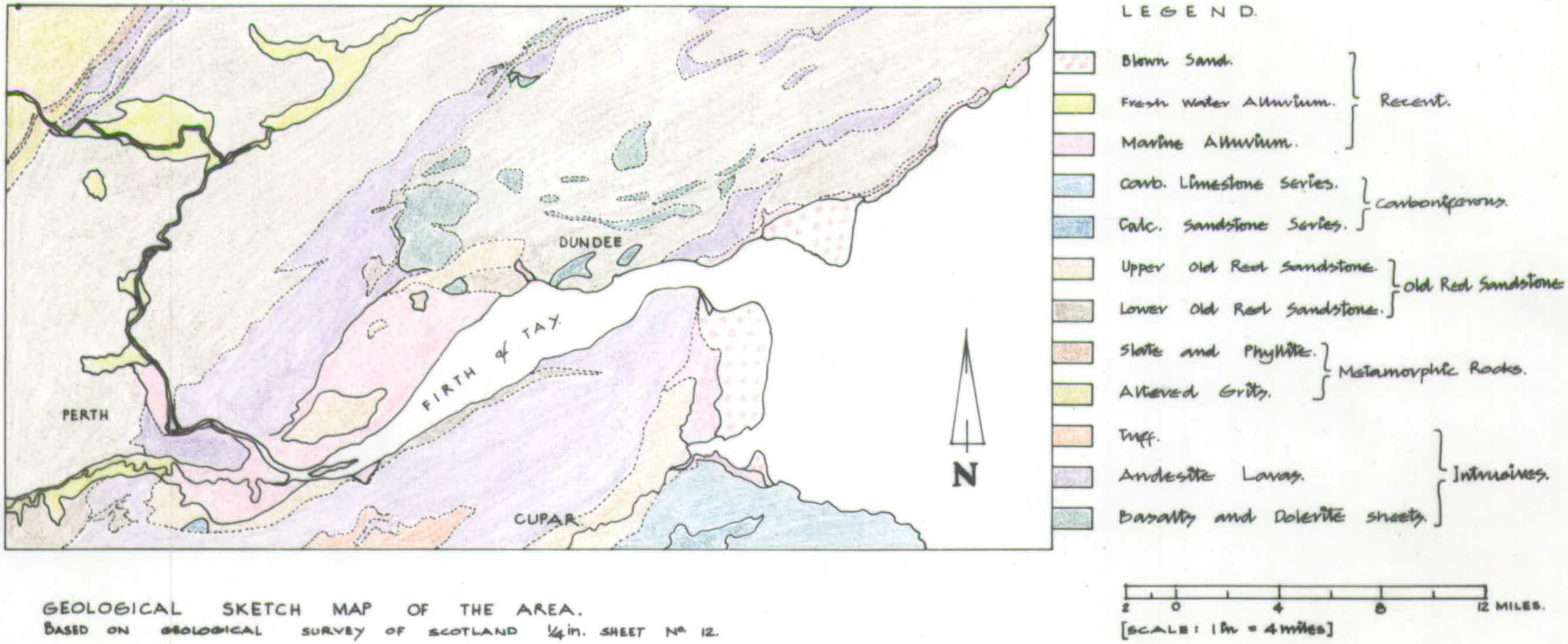

GEOLOGICAL SKETCH MAP OF THE AREA.
BASED ON GEOLOGICAL SURVEY OF SCOTLAND ¼ in. SHEET No. 12.

FIG. 2

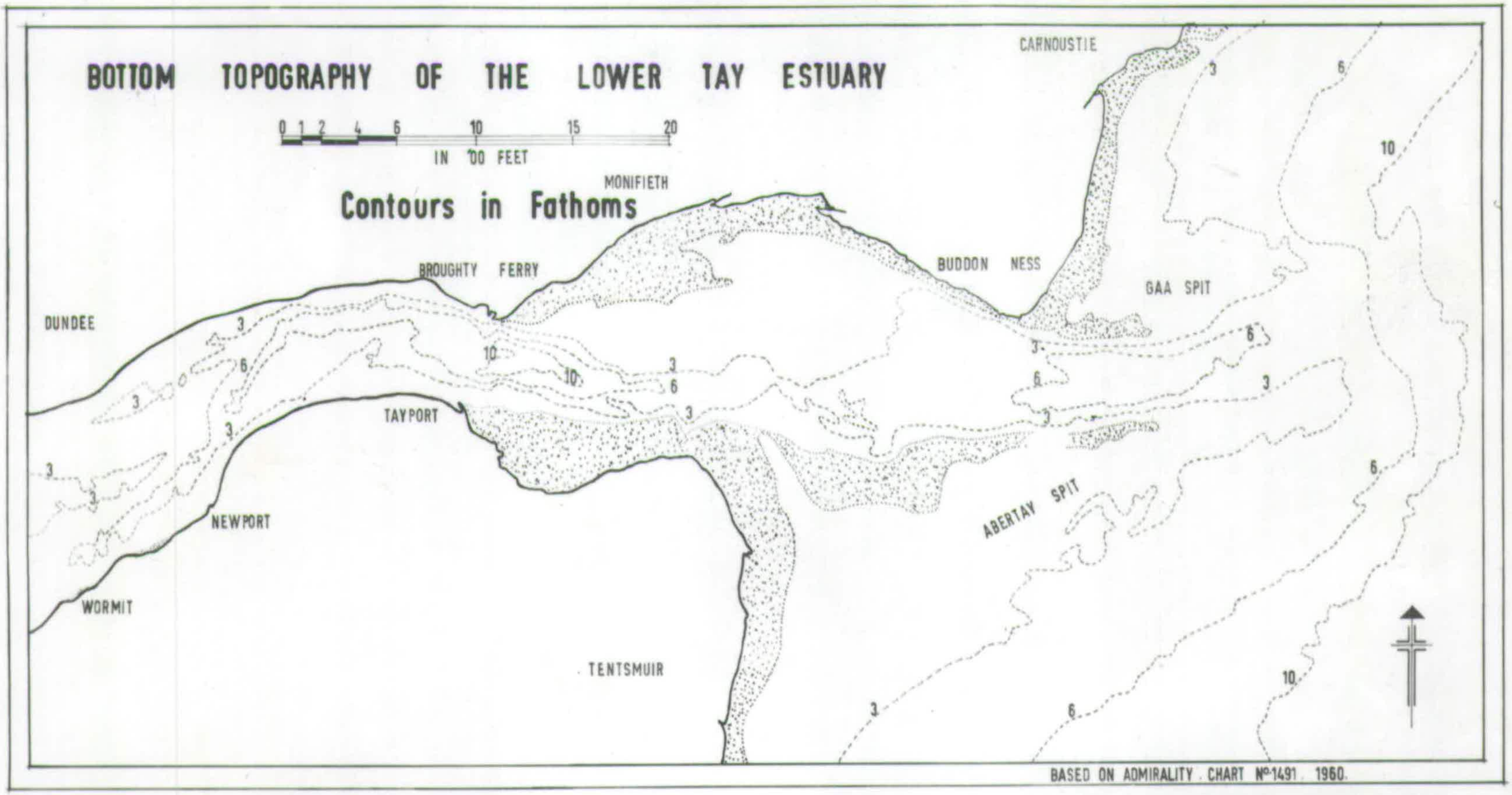

BOTTOM TOPOGRAPHY OF THE LOWER TAY ESTUARY
0 1 2 4 6 10 15 20
IN '00 FEET
Contours in Fathoms
CARNOUSTIE
MONIFIETH
BROUGHTY FERRY
BUDDON NESS
GAA SPIT
DUNDEE
TAYPORT
NEWPORT
WORMIT
ABERTAY SPIT
TENTSMUIR
BASED ON ADMIRALITY CHART No 1491. 1960.

of the river and up to Tentsmuir sands in the southern side (fig. 2). The greater part of the area lies below 500 ft. level with Ochil Hills (2,363 ft.) in the south-west and Sidlaw Hills (1,235 ft.) to the north. The Tay enters the lower reaches of the estuary from the Grampian Highlands in a deeply trenched valley with a general south-easterly direction representing an earlier river system produced by the regional tilting in the Tertiary times (Macgregor and Macgregor, 1948). The bottom topography of the lower estuarine region is given in figs. 2 & 3 and the longitudinal section (fig. 4) shows the base of the Recent and the andesite of the Lower Old Red Sandstone series near Dundee.

1.3 Lithology

Fig. 1 gives a lithological sketch map of the area of investigation. Most of the lower part of the estuary lies in the Lower Old Red Sandstone series with andesitic lavas. Recent marine deposits underly the blown sands of Tentsmuir and Barry Links; these marine deposits are also exposed in the Earn valley, the Tay valley around Perth and the northern parts of the estuary. Most of the other formations are those of Upper Old Red Sandstone series in the west and northern side of the estuary. These beds are intruded by the basaltic, doleristic and andesitic lavas. The Carboniferous sandstone and limestone beds are present in the St. Andrews region and the Upper Old Red Sandstone series around Cupar and Glendoick. Across the Highland Boundary fault are the Dalradian

FIG. 3

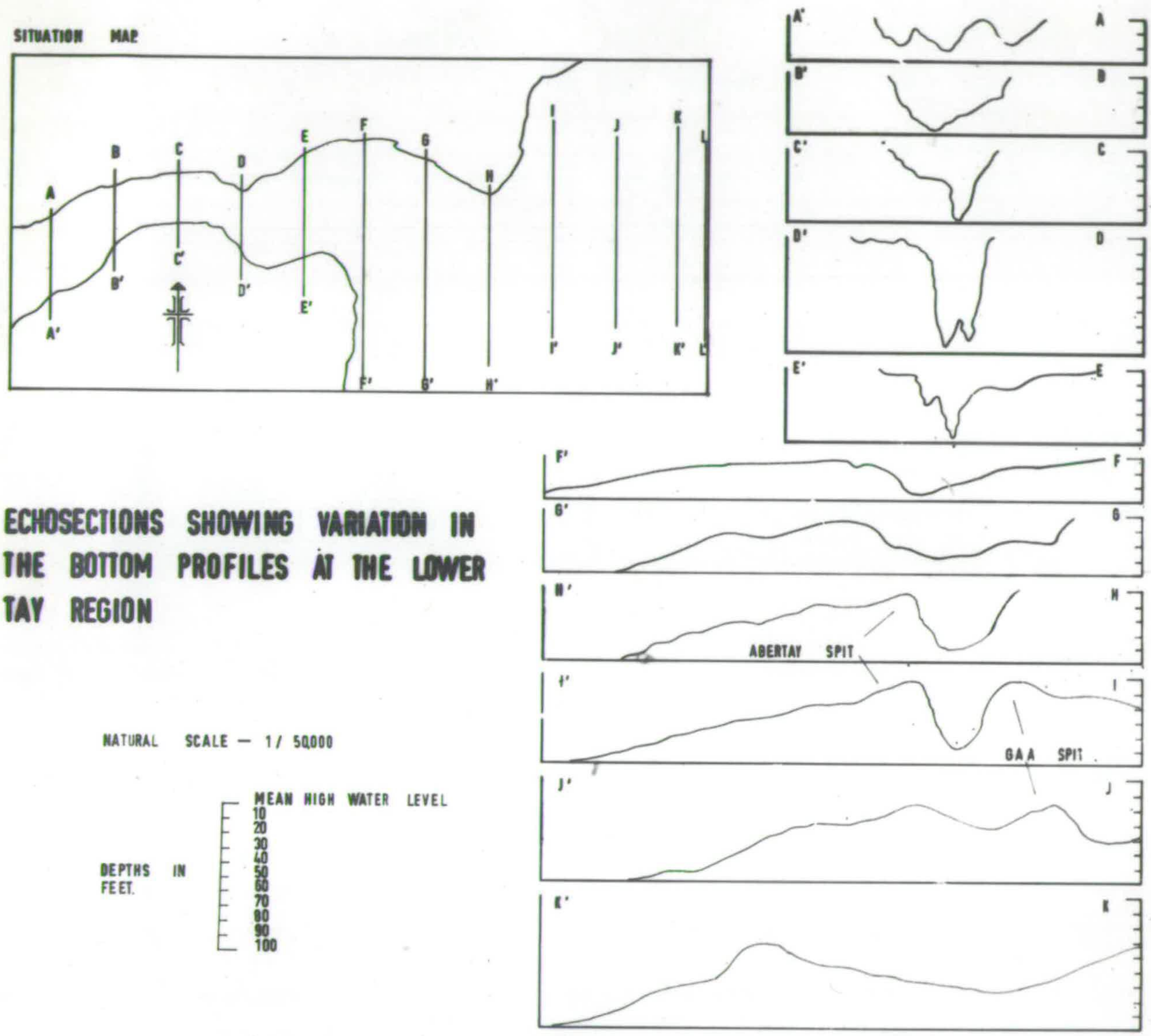

ECHOSECTIONS SHOWING VARIATION IN THE BOTTOM PROFILES AT THE LOWER TAY REGION

NATURAL SCALE — 1/ 50,000

BASED ON THE ECHO SOUNDING DATA FROM THE ADMIRALTY CHART Nº 1481. 1960.

FIG. 4

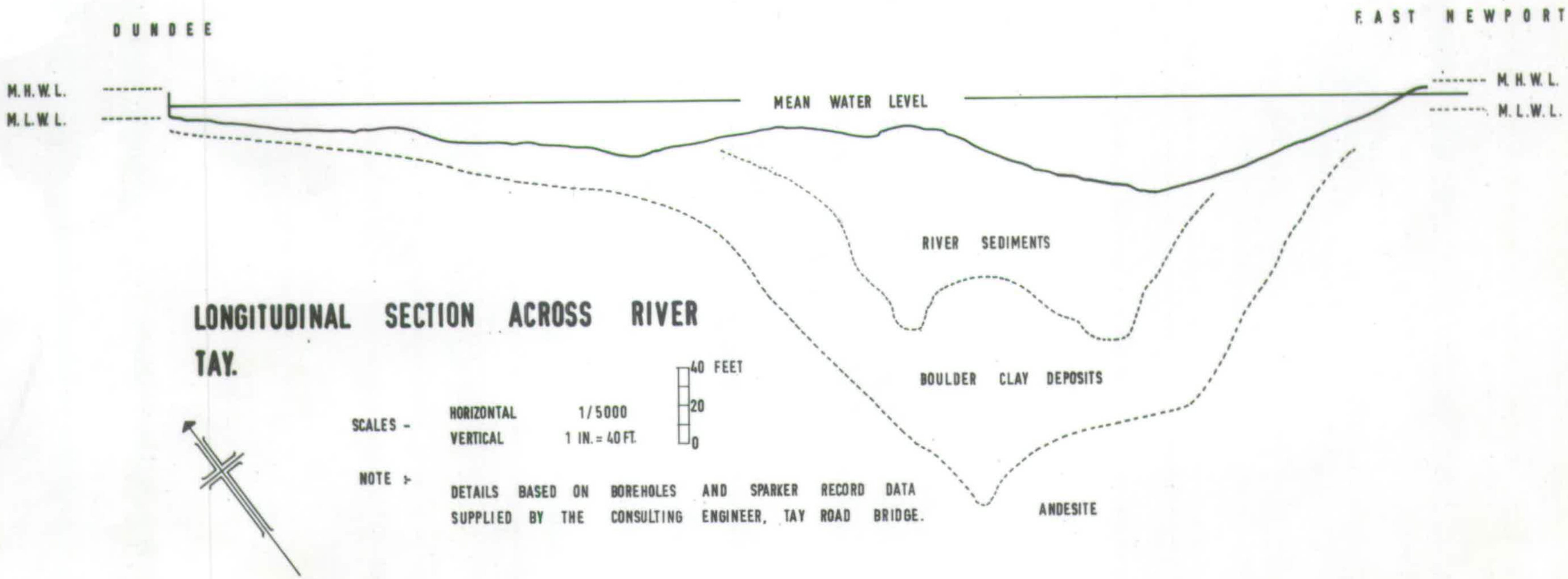

LONGITUDINAL SECTION ACROSS RIVER TAY.

and Moine metamorphics with various granitic and gabbroic intrusives. Most of the catchment area lies in this metamorphic region and thus most of the material is derived from the Dalradian and Moine horizons.

1.4 Environments

The location of various environments is given in the fig. 5 and these are classified on the basis of Twenhofel (1950), and Van Straaten (1954). The environments consist of fluvial; estuarine with salt marshes, tidal flats and sand banks; dune; and marine with beaches or beaches with tidal flats in the littoral zone. The structures and sedimentation in various environments are discussed in later sections.

1.5 Previous work in the area

The only previous work on the mineralogy of the recent sediments was done by Davidson (1937) on the concentration of garnet sands in the Budden ness region. He reported only the concentration of garnets and the source from the garnetiferous mica-schists from the Highlands. Jamieson (1865), Bremner (1916, 1939), Gregory (1926), Callender (1929), Simpson (1933, 1940) ~~and McCullen (1935)~~ have discussed the glaciation and raised beaches in the region. The lithology has been described in the various Geological Survey publications and other papers (see References).

1.6 Acknowledgements

I wish to acknowledge the help and encouragements of Dr. E.K. Walton and Professor F.H. Stewart during this research project. Dr. Walton suggested the problem and supervised the research; for his guidance and constructive criticism of the manuscript I am very grateful.

I am indebted to numerous individuals for the assistance in the project; Dr. T.V. Loudon of the Department of Geology, Northwestern University for the computer programming and Ft. Lt. Russell of the University Air Squadron for the flights over the area.

The research was carried out with the aid of Assam Oil/ Burmah Shell Scholarship from the Government of India.

Section 2. SEDIMENTARY STRUCTURES

2.1 Introduction

Important structures of recent sediments include stratification, cross-lamination, ripple-structures and wave marks. The term lamination is restricted to units smaller than one c.m. and larger units are termed beds (Payne, 1942; McKee and Weir, 1953). Internal structures can be studied by cutting L- and T- shaped sections in various selected localities. Undisturbed tray samples were collected during field work and some of the samples were impregnated by bakelite and other polyester resins to study minor internal structures.

2.2 Laminations have been studied in their natural habitat as well as by experimental tests (McKee, 1957; Brush, 1958). In the present study laminations are classified on the basis of environments as proposed by Van Straaten (1954) and McKee (1953).

2.2.1 Beach Laminations

Most of the beach sands are finely laminated and the material well sorted in different laminae. The direction of the dip and value vary according to its location on the beach. Light and dark-coloured laminae are formed due to mineral sorting; 'light-coloured laminae' are mostly composed of quartz, felspar, shell-fragments and other light-coloured minerals while the 'dark-coloured laminae' are mostly composed of heavy minerals like, garnet, hornblende, iron ores,

FIG.5

DISTRIBUTION OF VARIOUS ENVIRONMENTS IN THE AREA.

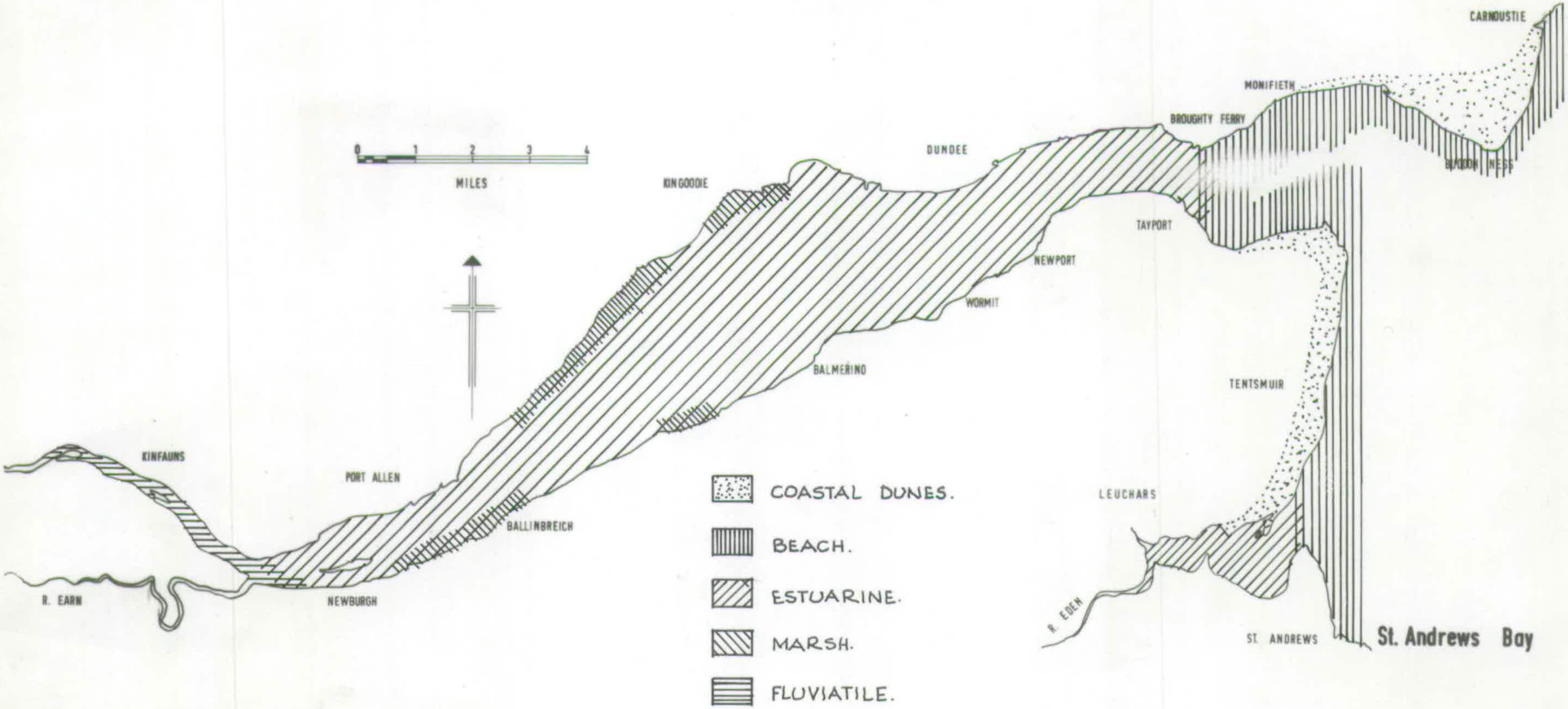

epidote, zircon etc. The beach laminations are classified into three groups and they are

(i) Backshore laminations

(ii) Upper Foreshore laminations, and

(iii) Lower Foreshore laminations.

Backshore lamination - Laminae of backshore sands have gentle landwards dips varying from 1° to 5°; the most common dip is 4°. Laminae are formed of medium to fine grained sands. The laminations are very distinct in this part of the beach due to the higher frequency of dark-mineral bands. Adjacent light-coloured laminae have different medium grain size and sorting from the dark-coloured laminae. There is no statistical significant difference in the grain-size parameters between the individual light-coloured laminae but the 't' test shows a significant difference ($P = 0{\cdot}02-0{\cdot}06$) between the grain-size parameters of the light and dark-coloured laminae. The dark-coloured laminae are better sorted and have a smaller mean size than the adjacent light-coloured laminae.

The thickness of individual laminae range from 1mm to 1cm with an average mean value of 8mm. In few cases thin beds of heavy mineral concentrates, varying between 1 to 4 c.m. are observed near the upper parts of the backshore at the foot of the coastal dunes. The average thickness of the dark-coloured laminae is 6mm and 1 c.m. for the light-coloured laminae. In this part of the beach the percentage of dark-coloured laminae usually varies from 5 to 20 but in one section

FIG. 6

A

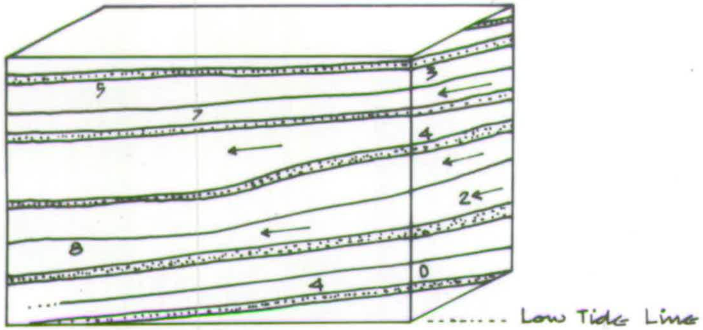

Longitudinal section in the Backshore beach deposits of Barry sands. Both regular to irregular laminae are observed. They have characteristic low value of landward dip. Various distinct dark coloured laminae composed of heavy minerals are seen. Ripple laminae are absent.

B

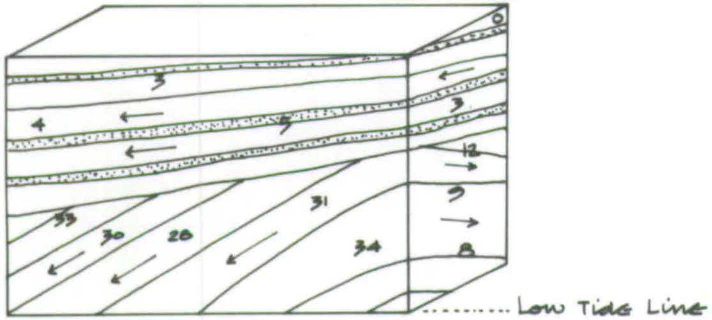

Longitudinal section in the Backshore Barry sands. The upper parts of the section shows typical backshore lamination but the lower part of the section shows high angle dune lamination. The section is from the upper part of the backshore region near the coastal dunes.

C

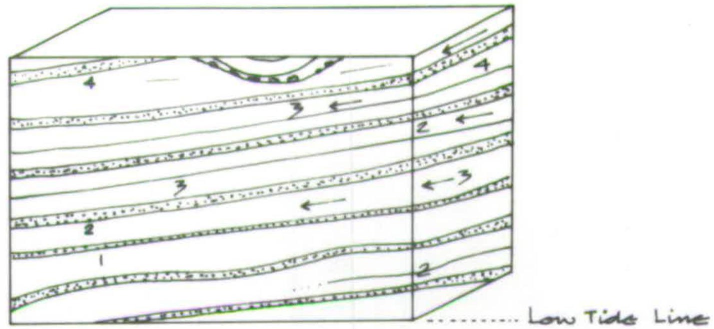

Backshore section in the Tentsmuir sands with the characteristic backshore shoreward dipping low angle laminations. The section also show part of a burried channel.

D

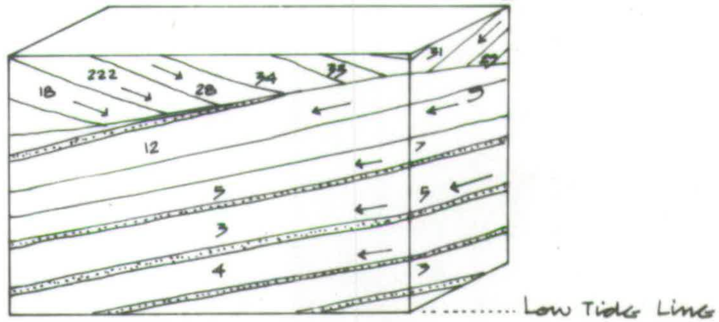

Backshore section near the coastal dune showing the typical high angle laminae overlying the low landward dipping backshore laminations in the Buddenness a much higher value of 27% was observed. The 't' test does indicate no significant difference in the thickness of laminae between the backshore and foreshore deposits. But the frequency of dark laminae shows a significant difference ($P = 0.05$) from backshore to foreshore sands. The foreshore laminations have a higher frequency of dark laminae than the backshore laminations while backshore laminations are better developed than those in the foreshore.

Individual laminae can be traced a few meters parallel to the coast line but their lateral continuity is much smaller in the direction right angles to the coast line. The individual laminae pinch out or are cut off by other laminae along frequent erosion surfaces. Fig. 6 shows the relationship between various laminations and large-scale stratification.

Upper Foreshore Lamination - The average thickness of the upper foreshore laminae is 6mm in the area and it ranges between 2 to 10 mm. The light-coloured laminae have an average thickness of 9 mm while the dark laminae show a very considerable variation with an average thickness of 5 mm. Thin beds of dark-coloured minerals 1 to 6 cm. in thickness are frequent in the Buddenness area. In most of the sections the light-coloured laminae dominate over the dark laminae but nearer the top of the sections the frequency of dark laminae increases sharply. The frequencies of dark laminae range between

FIG. 7

A

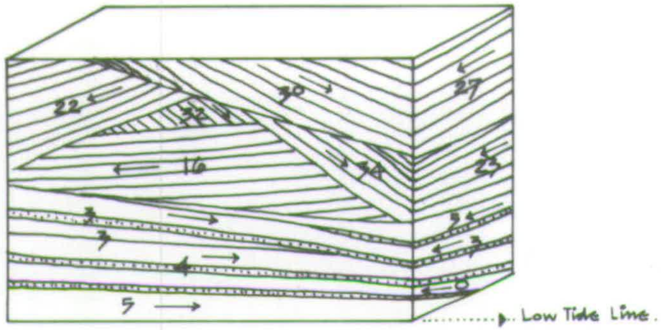

Longitudinal section in the Tentsmuir sands showing dune cross-lamination in the upper part of the section. Typical upper foreshore laminations are seen in the lower part of the section.

C

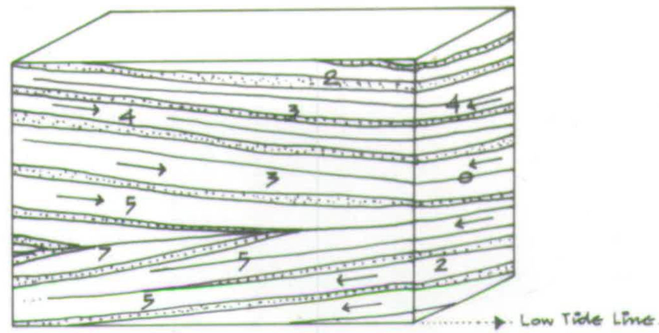

Upper Foreshore Longitudinal section in Barry Sands. Upper parts of the section show regular laminae with gentle seaward dips, while the lower part of the section show shoreward dipping laminae of the backshore lamination.

B

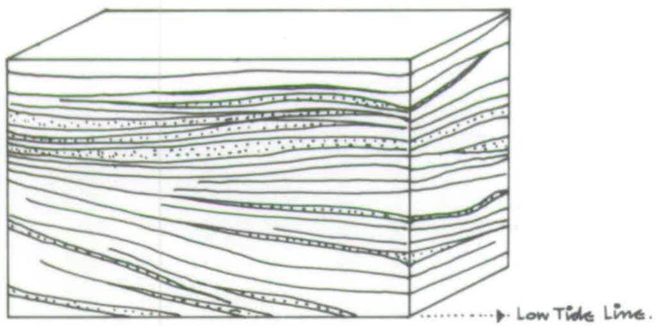

Section in the Tentsmuir sands showing the irregular upper foreshore laminations.

D

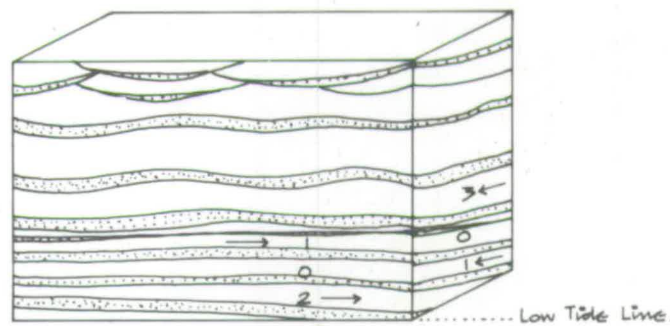

Section in Upper Foreshore showing ripple laminations and dark heavy-mineral laminae. Lamination have normal trend of gentle seaward dip.

10 to 35 percent from one part of foreshore to another and are more concentrated near the upper and lower edges of the zone.

In general the laminae have a gentle seaward dip; the values range between 0° to 5° with most of the values nearer 3° (see fig. 7). Similar foreshore laminations are observed by Thompson (1937), McKee (1957) and others. The individual laminae can seldom be traced lateraly for more than 5 - 10 meters while the sections normal to the shoreline show their terminations in 2 to 4 meters. Thicker laminae have slightly coarser grains but the 't' test shows no significant difference in the sorting of the adjacent laminae of same compositions. The dark laminae are made up of finer and better sorted grains than the light-coloured laminae. The dark laminae have a very high concentration of heavy minerals, ranging between 67 to 97%, with garnet the most predominant mineral. The average grains size of the chief minerals decreases in the order; quartz, felspar, hornblende, epidote, garnet, iron-ores, zircon, etc. De Vries (1949) has observed similar trends in the mineral size in the beach laminations. The observed relationship between the thickness of the unit and the average grain size has been shown by various workers, i.e., Pettijohn (1949), Allen (1962, 1963) etc.

One notable feature of the beach lamination is the complete absence of any appreciable amount of silt/clay fraction (less than 63 microns.)). Most of the fine suspended material brought by the river Tay is either concentrated inside the estuary or is carried away to

FIG. 8

A

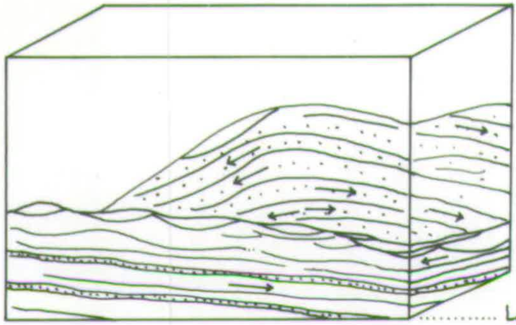

Section across the beach ridge in lower part of the upper foreshore. The normal low angle seaward dipping laminations are overlain by high angle soft sands poor in dark minerals and indistinct laminae.

C

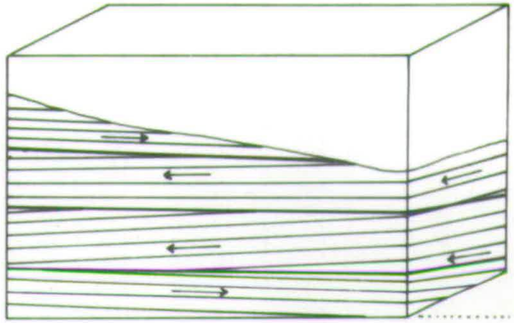

Diagram of cross-lamination. The surface truncating the underlying laminae is also the floor of deposition for the overlying laminae. This surface dips seaward more steeply than the truncated laminae

B

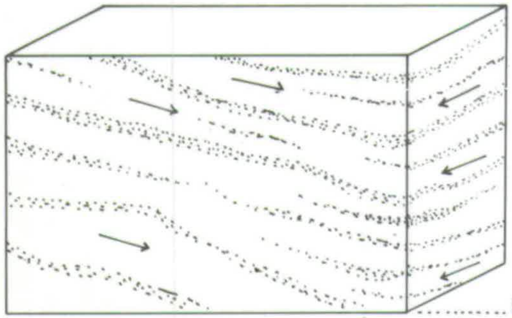

Section in the lower foreshore sands of Barry sands. Sediment is usually too saturated and distinct laminae are absent. Some faint traces of seaward dipping laminae are visible with higher dip values than the upper foreshore laminae.

D

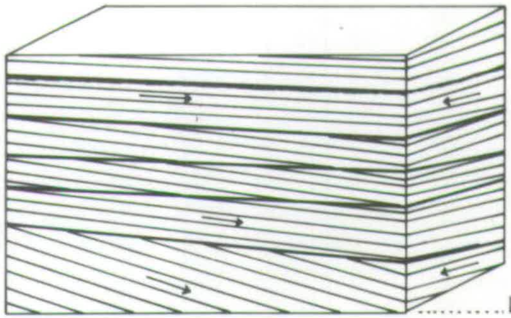

Diagram of cross-lamination. The truncating surface dips seaward less steeply than the truncated laminae. As in the other type these laminae and truncating surfaces have the same strike almost parallel to the coast line.

the deeper parts of the sea. Unlike the Dutch coasts, the North sea in this region does not bring in appreciable amount of fine suspended material to be deposited.

<u>Lower Foreshore Lamination</u> - Sediments in this zone are normally very much saturated and sections cut in the zone cave in quickly. But in some sections steeply dipping laminations (12^{o} - 21^{o} seaward dip) have been observed. These inclinations seem to follow the general slope of that part of the beach. The sands are coarse to medium grade and relatively poorly sorted than those of the upper foreshore. Lamination are irregular and indistinct, poor in dark-mineral laminae and have thicker light-coloured laminae. Due to saturation and the texture of the light-coloured sands it is normally difficult to distinguish between adjacent laminae.

Laminations and other wave formed structures on a beach depend upon the type of beach. The relationship between the value of dip of laminations and the slope of the beach profile has been emphasised by Martens (1939/1959), Van Straaten (1953) and Doeglas (1955). With the change in beach profile due to seasonal tidal variations, different modifications in the beach structures take place i. e., formation and modification of laminations, formations of ripple patterns, appearance and disappearance of beach cusps, etc.. Laminae are formed due to a complexity of variables like sediment types and their specific gravity,

FIG.9

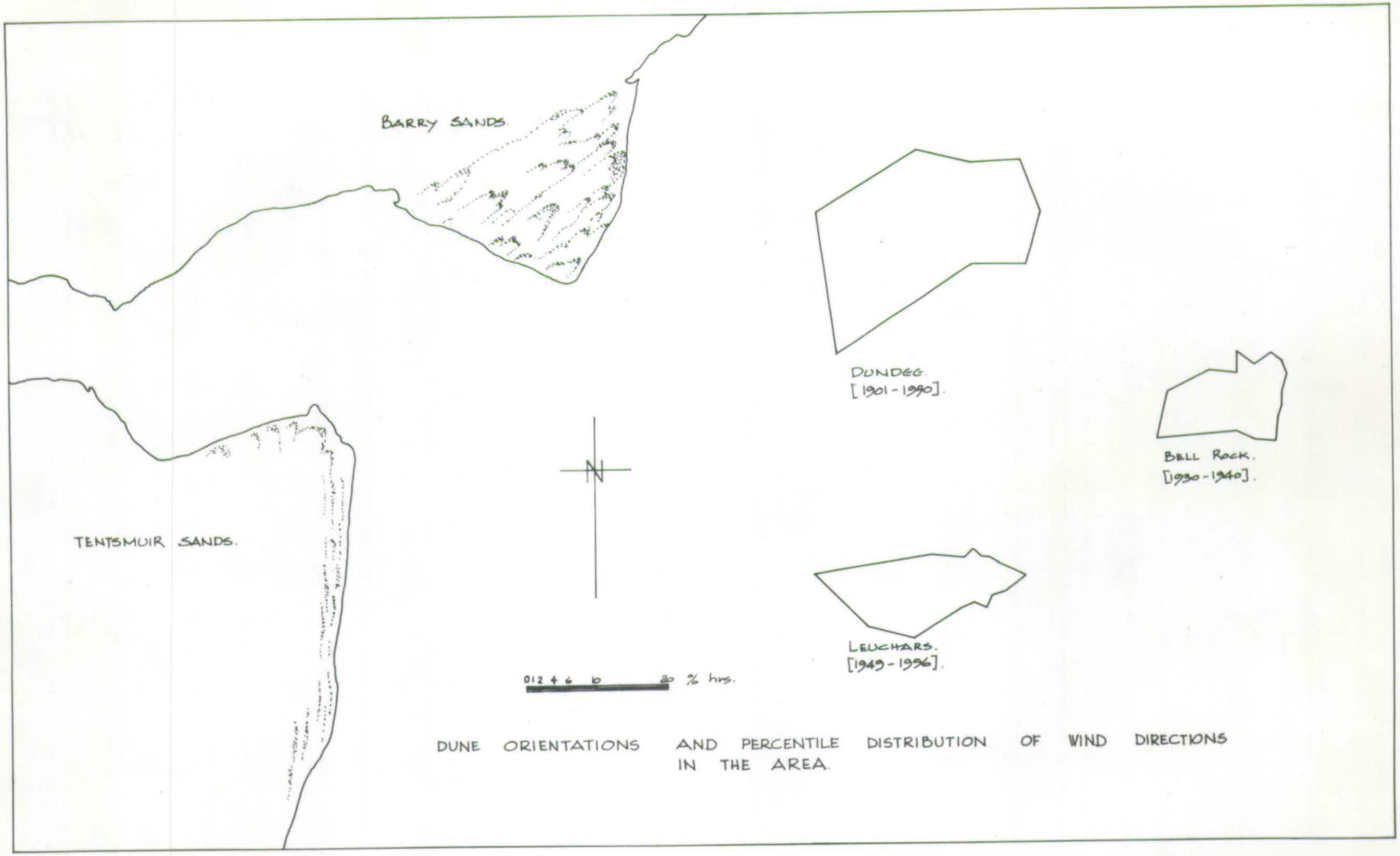

DUNE ORIENTATIONS AND PERCENTILE DISTRIBUTION OF WIND DIRECTIONS IN THE AREA.

transporting medium and their strength, beach profile and their seasonal variations, etc. All these factors are extensively treated (e.g. Hantzschel, 1936; Thompson, 1937; etc.). The degree of prominence of individual laminae is partly dependent on the depositional currents and their fluctuations in the region. Slight changes in the currents directions and salinity also play an important part in the prominence of individual laminae.

Cross-laminations presumably are produced by currents of different strength and orientations. They appear in the change in the dip of laminations over an erosion surface. Figs. 6 - 8 show the types of laminations found in the beach sands.

2.2.2 Coastal Dune Lamination

Coastal dunes are present in the Tentsmuir and Barry areas. The dunes are of barchan type at Barry and of transverse ridge type in the Tentsmuir area; the dune classification is on the basis of schemes suggested by Hack (1941) and Bagnold (1941). The orientation of the dunes corresponds to the most frequent wind direction according to the data available on the area (fig. 9; see also Landsberg 1956;).

The dune laminations are related to the shape and size of the dunes. Low-angle laminations are observed in the windward sides while higher angle values are obtained in the lee side. In the wind-

FIG.10

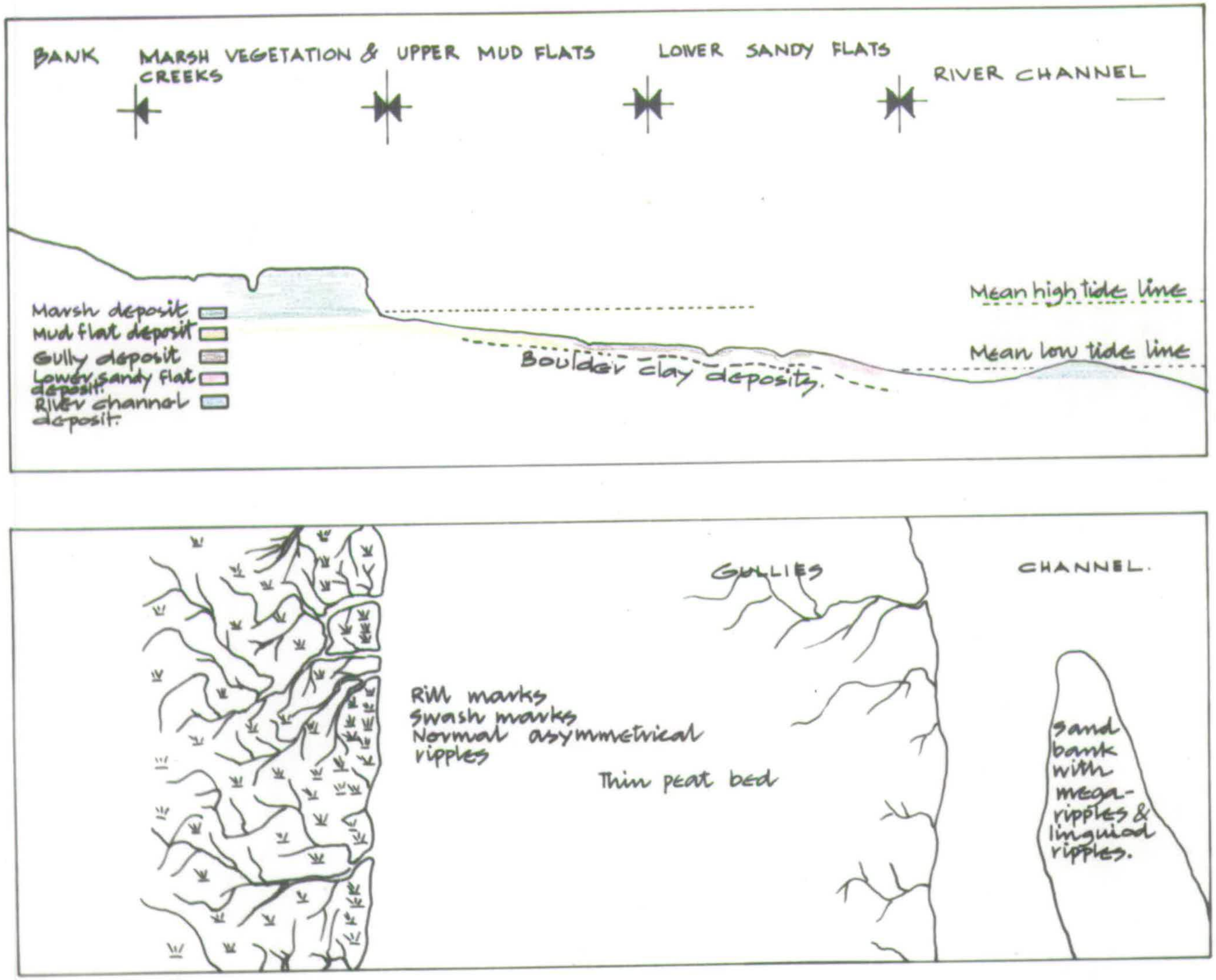

IDEALIZED CROSS SECTION AND SKETCH MAP NEAR BALLINBREICH, TAY ESTUARY.

ward side the laminae dip from 5^{o} - 14^{o} while it ranges between 24^{o} - 34^{o} in the lee side. These variations in the dip values are due to the location of the laminae in a particular part of the dune (Bagnold, 1937, 1943; McKee, 1945, 1957;). The sets of cross-laminae are characteristic of the dunes with larger variations in the dip values. Ripple laminae are quite common. Dune laminae are thin and not so distinct as that of the beach due to the absence of distinctive dark laminae. Individual laminae are 0.5 mm. to 5.0 mm. thick with a mean value of 3.0 mm. Most of the minerals in the laminae are light minerals while very thin streaks of dark minerals are observed in a few cases . The dark minerals are usually concentrated at the lee side of the ripple laminae as well as in the leeward side of the dunes. There is a complete absence of horizontal laminae. Individual laminae can seldom be traced more than one or two meters. Generally laminae dip in almost all directions on a dune.

2.2.3 Estuarine Lamination.

The laminations and other structures found in the estuarine environments are divided into three sub-groups corresponding to three sub-environments (Van Straaten, 1953; 1959). They are:

(i) Salt Marshes - these are situated just above the mean high water level,

(ii) Tidal Flats - this zone extends from the mean high tide level to the mean low tide level, and

(iii) Tidal Channels - these are below the mean low tide level with occasional sand banks in the channels. (See fig. 10).

Marsh Lamination - The marsh sediments show regular to irregular wavy laminations, at times nodular in nature (fig. 11). The wavy nature of the laminae is due to deposition of fine-grained sediment on the uneven surfaces of the plants as well as by the variable oscillatory currents. The nodules are formed from small pebbles trapped in the halophyte plants during the storm tides and successive mud coating around them. A few of the nodules are entirely made up of mud with previous dried mud forming the nucleus for later nodules; while others are also formed by mud coating around thick pieces of roots. Fine-grained sediment is brought in during the storm tides and is trapped in the marsh plants and in times is bound together with extensive root systems. Marsh sediments are undisturbed by the absence of burrowing fauna and there is also a complete absence of ripple lamination.

Marsh sediments are composed of sandy silts and near Ballinbreich are seen overlying the boulder-clay deposits (Plate 2). The sediment is very dark in colour due to abundance of organic material. High values up to 18% organic content were determined from the samples in the estuary. The organic content decreases towards the tidal channel. In a few cases due to high organic content and silt it

FIG.11

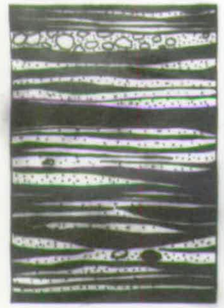

A

Tidal flat deposit with mud laminations due to strong variations in tidal currents. Pebble beds are seen in some sections. Strong affect of migration of gullies and channels. Sediment mostly sandy mud and silty very fine sand.

C

Section in the Marsh upper zone with nodular laminae and silty sediment. Abundance of plant rootlets in the upper parts. In some sections former places of roots have been completely replaced by the filling of fine mud.

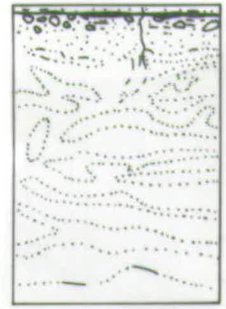

E

Tray sample from the upper part of the Tidal flat. Mottled fine grained sandy silt; original laminar structures destroyed by the burrowing organisms.

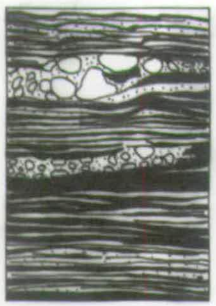

B

Lower part of Tidal Flat deposit with some ripple laminations and pebble conglomerate. Regular laminae of mud and very fine sand. Little effect of burrowing organisms.

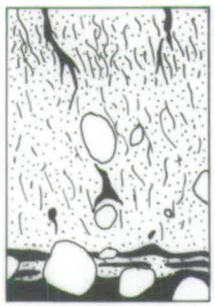

D

Marsh section from a Tray sample showing fine grained marsh sediment with abundance of plant rootlets. In the lower part of the section the marsh sediments are seen exposed resting on the in-situ Boulder clay deposit.

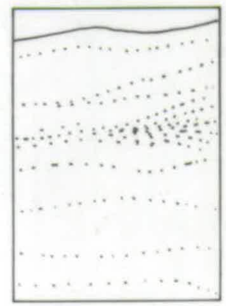

F

Tray sample from the tidal channel bar. Sample collected from a mega ripple. Upper part of the section shows indistinct ripple lamination but most of the sample is homogeneous medium sand. Indistinct 'herring bone structure' is seen in the section.

was very difficult to distinguish between individual laminae.

Tidal Flat Lamination - In the tidal flats more regular, sandy laminae are observed than the salt marshes. Laminae are more distinct and vary in composition, mean size and sorting. The grain size varies from fine sandy silts to very fine silty sands. Thickness of individual laminae range from 1 mm. to 1 cm. In the upper parts of the tidal flats more silty laminae are observed while the frequency of sandy laminae increases towards the lower tidal flats. A few thin beds of peat 2 - 7 cm. in thickness occur in the upper-middle parts of the flats near Balmerino. Some of the sands bands show ripple laminations. Mottled structures resultant from the burrowing organisms are present in a few cases in the upper tidal flats (Van Straaten, 1954; Moore and Scruton, 1957).

The deposition of mud laminae takes place mainly in quiet waters inside the estuary, in the parts sheltered from strong currents. Most of the fine material is deposited at the turn of the tides when current velocity drops below the value at which sediment of 40 microns or more is no longer transported (3 mm/sec according to Hulstroem). Van Straaten and Kuenen (1957) have held the 'settling-lag effect' to be responsible for the deposition of fine suspended material in the Dutch Tidal flats. Settling-lag is the delay between the moment at which a current of decreasing velocity is no longer able to hold a particle in suspension and the moment at which this particle reaches the bottom. The sudden decrease in the current velocity may be due to the fanning of the quantity of the river discharge in the estuary and also due to the effect of tidal currents which act against the forces of river discharge. This 'settling lag' phenomenon postulates a very delicate condition of suspended load as if there is too much lag then no material would be deposited at all.

Tidal Channel Lamination

Normally no study of structures in the tidal channels was possible due to the depth of water, but in extreme conditions of low tides some sand banks were exposed. The sands of these estuarine banks are homogeneous, medium to medium-fine grade, fairly well sorted with abundant ripple structures. The types of ripple structures found in these sand banks are described in the later pages. Sections cut in these sand bodies failed to reveal distinct internal structures, only in one section vague "herring-bone" type structure was seen in the mega-ripple. Tray samples from this locality were later subjected to bakelite impregnations but the peels also failed to show any internal structures. Absence of any dark laminae makes it very difficult to distinguish any laminations. It is possible that X-ray radiographic methods (Hamblin, 1962) may bring out structures from these homogeneous looking sands.

FIG.12

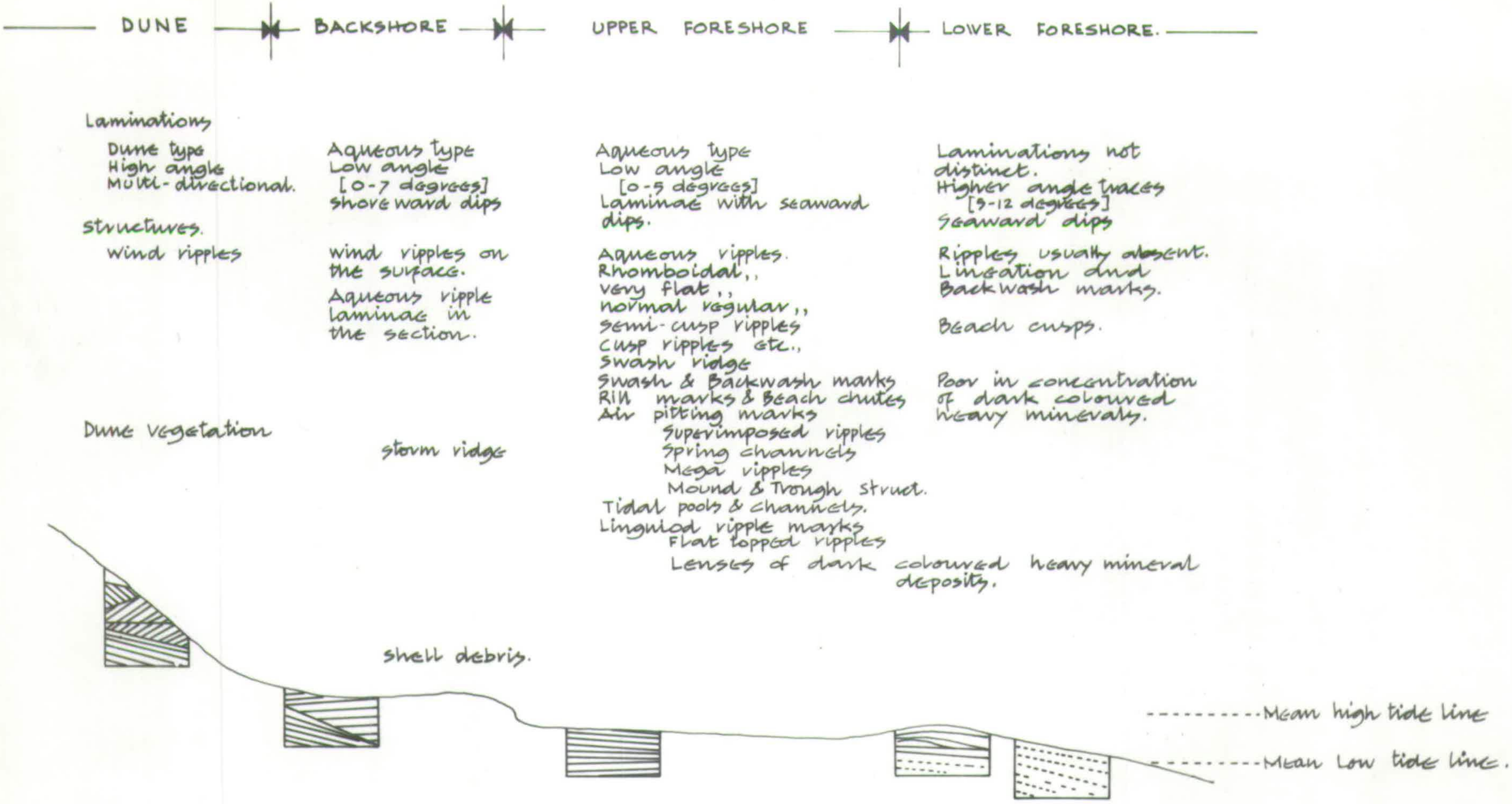

DIAGRAMATIC SECTION ACROSS THE BARRY SANDS ILLUSTRATING THE RELATIONSHIP BETWEEN VARIOUS STRUCTURAL FEATURES AND THE ENVIRONMENTAL REGIONS.

2.3 Ripple Structures

There is a bewildering array of ripple terminology available to describe these structures but in the present investigation the terms suggested by Gilbert (1899), Kindle (1919), Evans (1941, 1949), Van Straaten (1953), Tanner (1960), and Allen (1963) are used. The ripples are described in terms of size and shape; the mega-ripple term is used to designate ripples with wave lengths of more than one meter. Mega-ripples and allied mega-structures are described first and then the minor ripple structures. The ripple structures are naturally best developed in the sandy part of the area.

2.3.1 Mega - Structures

Longitudinal mega-ripples

To the area east of Tayport, the tidal flats show straight symmetrical mega-ripple structures in a very shallow environment. The ripple ridges have a symmetrical cross-section and the crests are slightly angular (see Plate 3). The wave length varies between 5 - 20 metres and the amplitude from a few cm. to several dm. The ripple crests are perpendicular to the coast line and are seasonal in nature. They were observed in the later half of 1961, but since then they have disappeared.

The origin of this type of mega-ripples is not yet clear. Hantzschel (1936, 1938, 1939), Hulsemann (1955), and Van Straaten (1950, 1951 1953) have described these structures and Van Straaten has put forward a

FIG.13

DISTRIBUTION OF VARIOUS MEGA STRUCTURES IN THE AREA.

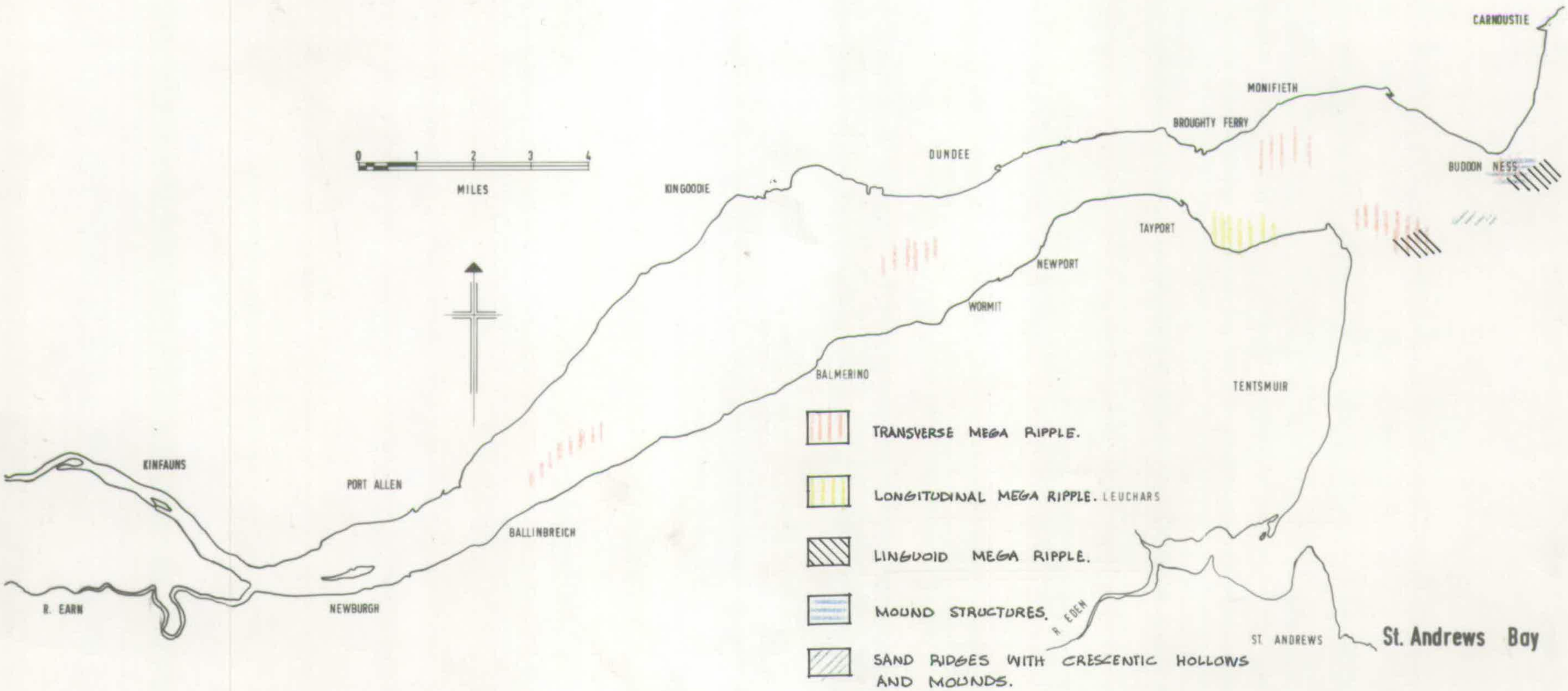

tentative theory on their origin. According to Van Straaten (1951), the ripple troughs are formed due to the erosion behind some obstacle. With the gradual scouring of several troughs, the areas between form ridges. But it seems to be too much to assume regular arrangement of obstacles in the currents to give this type of regular arrangement of ripple ridges. Probably the wave theory by Vanoni (1941, 1946) may explain the origin of these longitudinal structures. The presence of secondary spiral flow was observed during the flume experiments; this secondary double spiral flow is superimposed on the forward flow which carries the slow moving water from bottom up along the sides and out along the top of the centre. In the presence of double spiral flow, sediment can easily form symmetrical ridges. These spiral flows can be formed by the ebb and flow tidal currents on a gently sloping shallow tidal flats.

Transverse mega-ripples

Transverse mega-ripples are mostly asymmetrical, have varying wave lengths, and are observed usually lying in parallel trains with few bifurcating ridges. Mega-ripples of this type are found in different forms at various localities in the area (Fig. 13). The ripples observed on the sand bank off Ballinbreich and west of Wormit have a varying wave length from 5 to 15 metres and amplitude from few dm. to a metre or two (Plate 4). The ripple index of these ripple structures is much higher than that of the longitudinal ripples of Tayport sands. The river current is the stronger one as the lee-side of the ripples is towards the downstream; the crests of the ripples are well rounded due to the ebb and flow of the tidal currents. Plate 4 shows these ripples curved upstream near the secondary channels due to the stronger force of the tidal currents near the south bank of the Tay. Similarly the ripple ridges towards the main river channel are curved slightly downstream due to stronger river flow. The strong river current has also affected the rounding of the crests; the crests are not so well rounded nearer the main channel as they are towards the secondary channels nearer the south bank of the Tay. All the ripples are not fully exposed as some are observed clearly in the shallow parts of the channels in the aerial photographs. No significant change is observed in these ripples in the last three years except slight variations in the ripple crests. Muller (1941), Escher (1948), and Van Straaten (1950) have shown the changes which take place in the ripple crests by the "age" of these ripple structures.

Another set of asymmetrical transverse mega-ripples is seen in the tidal channel south of Monifieth at low tides (see plate 5A). At this locality the westward movement of the tides and waves is stronger than inside the estuary and the mega-ripples have steeper sides towards west. All these mega-ripples are superposed by other sets of minor ripple structures. These mega-ripples are seasonal and are best developed in the late summer at the cycle of low tides.

In the Barry Sands, mega-ripples are observed after the spring high tides, the wave lengths vary between 1 to 3 metres and amplitude in few dm. The ripple crests are covered by sets of superposed minor ripples; the ripple crests run in the N - S direction. The mega-ripples are of a very temporary nature, produced during the extensive reworking of the sediment in the Buddenness area during the cycle of high tides.

Abertay Spit, at the mouth of river has an assemblage of mega-ripples and are produced by the shoreward waves as they have lee-sides towards west. The main train of the transverse mega-ripples is in the centre of the spit (fig. 5.B), with ripple crests running in N - S but due to lateral reworking by the waves, they are slightly modified on the sides of the spit. The wave length varies from a meter to 5 meters and the amplitudes from few dm. to a meter. All these measurements are approximate as they are calculated from the aerial photographs. The amplitudes are directly proportional to the length of the ripples as illustrated by Allen (1963), who has also shown the relationship between the ripple amplitudes and the depth of water. This is the cause that large scale ripple structures are better developed in the deeper waters while in the shallow waters nearer the shores, the magnitude of the ripples decreases.

Similar mega-ripple structures are very common in different parts of the world in the tidal flats, estuaries, off-shore bars, sandy parts of seas and rivers. Aerial photographs, echograms and flights over the area have revealed the presence of these asymmetrical mega-ripples off the coast and near the mouth of the Tay. The existence of similar structures over the floor of the North Sea and around the British Isles is quite well known

(Luders, 1929, 1930; Van Veen, 1935, 1938; Cloet, 1954; Stride, 1963 and Allen, 1963).

Linguoid Mega Ripples

Cuspate ripples (McKee, 1957), or linguoid ripples (Bucher, 1919) have a tongue like projection towards the lee-side. Some of the modified forms of the transverse mega-ripples with these tongue like projections in the area can be termed semi-cusp or semi-linguoid mega-ripples. The crest line of the ripple is usually curved back in the up-current directions. Thus the cusps or the tongue like projections point down current directions. The arrangement and the shape of these ripples vary from semi-linguoid to linguoid mega-ripples. These tongue like lobes can be a single lobe or a series of lobes (see Plate 7A). The structures are found in the Abertay spit and bar, and also in the Gaa sands off Buddenness. In both these areas the structures are formed by the westward waves. The development of the structure is related to the intensity and distribution of the currents, both wave as well as tidal. They are best developed in the central part of the Gaa sands.

In the Abertay spit, the transverse mega-ripples are developed best in the middle part of the sands with semi-cuspate forms in the turbulent marginal parts. Some of the ripple ridges are well rounded, the wave lengths vary between 2 to 6 meters and amplitudes in few dm. The general orientation of the ripple trains is N.- S. but a few minor variations are also observed.

In the Gaa sands, the linguoid mega-ripples are observed at very low tides (Plate 7B). Strong westward currents are indicated by the steeper lee-sides towards the shore. The strongest currents are westward with another weaker N. N. E. component influencing the ripple trains. The ripple structures are produced by the main westward waves and slightly modified in the breaker zone. The wave lengths and amplitudes are different from those of the Abertay sands, but a more characteristic difference is in the shape of the composite lobes. Structures similar to these linguoid ripples have been described by Van Straaten (1953), Hulsemann (1955), and Nedeco (1959).

Mound Structures

Some of the aerial photographs (Plate 10) show a mound pattern not hitherto reported elsewhere. The mounds are rounded to subrounded depending on the age of the structures as they are seasonal and are best developed in late summer and autumn. The mounds appear in the zones with interference wave patterns, the photographs (Plate 14) shows clearly this pattern in the Buddenness area. The mounds in the Abertay elbow vary in size from few dm to a meter and it is difficult to detect any preferred trend of the mound crests. The height, strength and direction of tidal streams and waves are the main cause of their development.

In the Buddenness and Gaa sands mound structures are best developed, especially in the autumn. The structures are related to the

FIG. 14

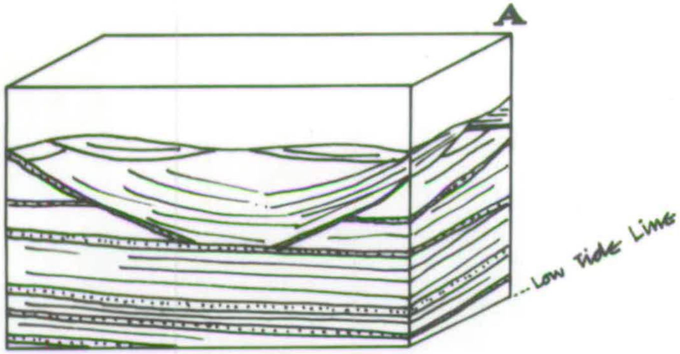

Longitudinal and Transverse cross sections in the 'Mound' structures of Budden Sands. The trough shaped "cut and fill" erosional structures vary in size and shape. There is a fairly good concentration of dark mineral laminations; both regular as well

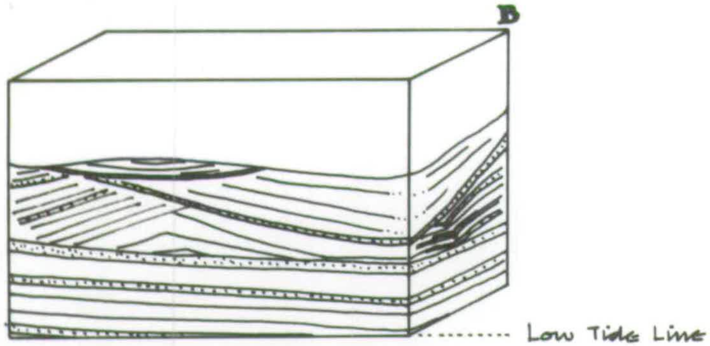

as irregular. The general trend of foreshore lamination is seen in the lower parts of the sections while upper parts show traces of ripple laminations in some sections.

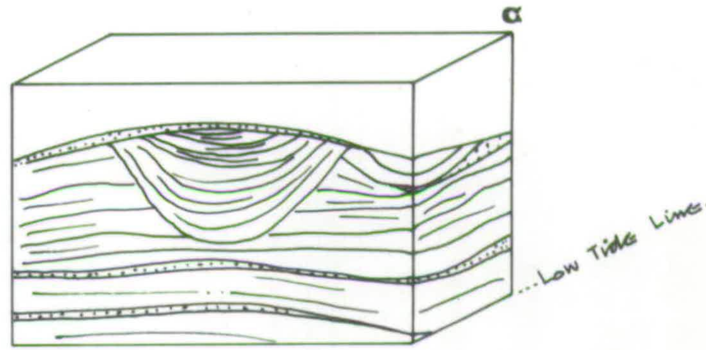

Transverse cross-sections of 'Mound' structures in the Buddenness sands. Sea was away from the observer. Large sets of the cross-stratified trough are seen. The lower boundary surfaces have a concave upward, as do the individual laminae within the fill. The dark bands and

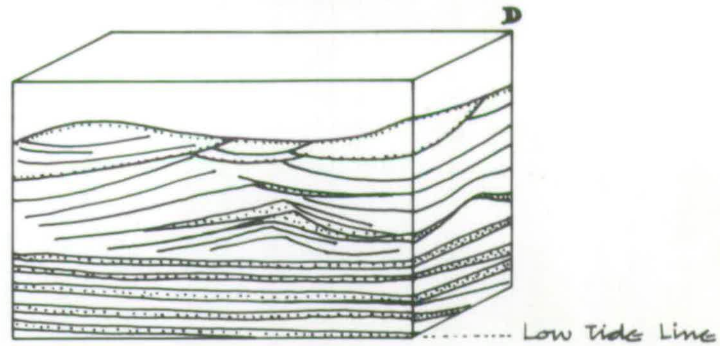

lines are the dark red-brown laminae with many minerals. Both regular as well as irregular laminae are seen. In the lower parts of the sections distinct low angle sea ward dips of the foreshore laminations are recognised.

extensive reworking of the sediment in this part by the interference of two strong wave-sets. In the photographs (Plate 11) the mounds show a rough pattern of crests running in N. W. - S. E. directions. The mounds vary from 1 to 3 meters in width, they are well rounded in shape and have heights up to few dm. They disappear after the high tidal cycle and reappear again after 6 - 9 months. During these months mega-ripples appear in the zone and they are later flattened to give a modulating surface (see Plate 13). In the last two years the mounds have shifted slightly in position, in 1963 they reappeared in the autumn about 30 meters E. N. E. of their position in the previous year.

Sections cut in the mounds show a variable stratification (fig. 14). At the lower part of the section regular foreshore beach laminations are seen with a gentle seaward dip. These regular laminations can be traced from one mound to another for few meters. This regular lamination zone is superposed by another zone with irregular lamination having varying dips. A few "herring bone" type patterns of Kuenen (1957) are also observed in this zone. This type of pattern points to the alternating deposition of sediment by the ebb and flood currents. This set of laminations is relatively poorer in dark mineral laminae than those in the underlying zone. Nearer the surface, troughs of various shapes and sizes bounded by curved erosional surfaces are seen resting on the zone of irregular lamination. Scour and fill structures like these are produced by the erosional cutting and filling by seasonal currents (McKee, 1957; Harms and others, 1963).

Scour patterns would be formed at the storm periods and the same filled up and mounds produced at quieter periods. Under what conditions the mounds actually are formed and the role of the wave interference is not yet clear, but it seems certain that the mounds are distinctive structures appearing because of the superposition of two sets of waves. In the post mound period the mound phase changes and mega-ripples are produced. These mega ripples do not show these trough type scour and fill structures but Allen (1963) has reported similar structures from a few mega-ripples.

2.3.2 Minor ripple structures

Aeolian and aqueous ripple structures with wave lengths less than one meter are included here. All the ripples are asymmetrical with the lee-side on the down current side. The following are the different varieties of minor ripples observed in the area. They are

i Common asymmetrical ripples

ii Superposed ripples

iii Linguoid ripples

iv Flat top ripples

v Rhomboid ripples and

vi Aeolian ripples

Common asymmetrical ripples

The crests of the ripples are straight and parallel to each other with asymmetrical cross-sections. The ~~most of these~~ ripples have regular,

FIG.15

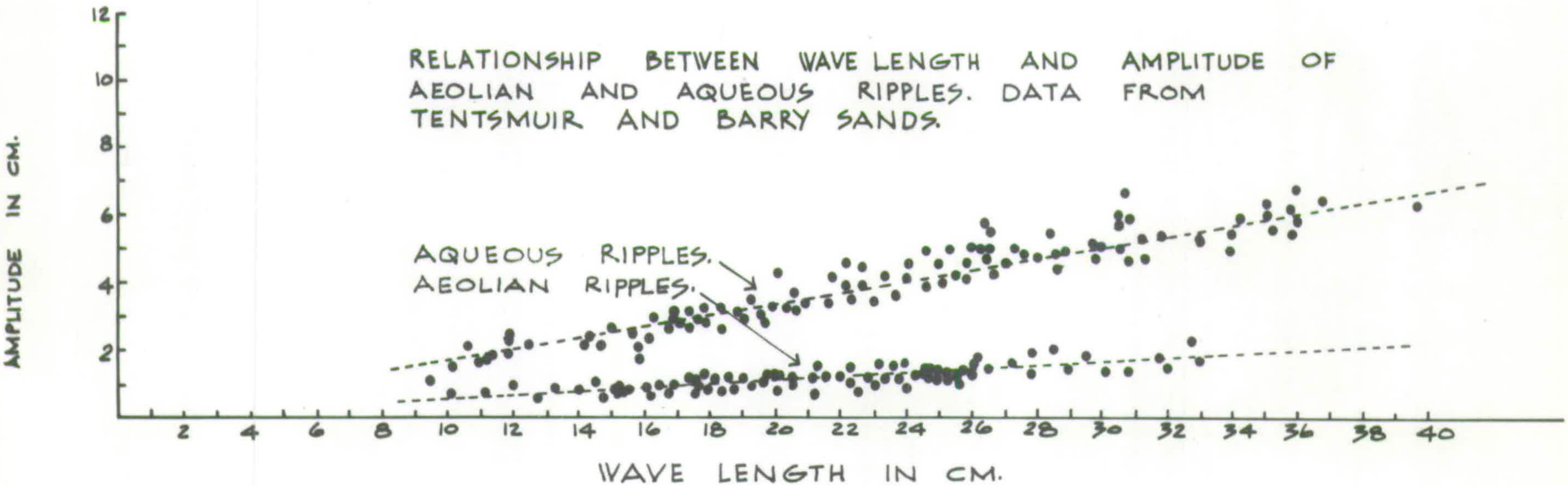
RELATIONSHIP BETWEEN WAVE LENGTH AND AMPLITUDE OF AEOLIAN AND AQUEOUS RIPPLES. DATA FROM TENTSMUIR AND BARRY SANDS.
AQUEOUS RIPPLES.
AEOLIAN RIPPLES.
AMPLITUDE IN CM.
WAVE LENGTH IN CM.
12
10
8
6
4
2
2
4
6
8
10
12
14
16
18
20
22
24
26
28
30
32
34
36
38
40

straight parallel crests with few bifurcations. In a few cases due to excessive bifurcation of the ridges irregular ripple patterns are formed. Most of these ripples are formed by the shoreward currents,thus they have lee-side towards the shore. Some of the ripples have secondary crests developed due to the ebb tides. The ebb tide also leaves some lineation marks along with the secondary crests (see Plate 19). The wave lengths vary from 5 to 25 cm and the ripple index from 3 to 8 (fig. 15).

These ripples are the commonest ripple structures and are best developed in the fore shore parts of the beaches. They are subjected to minor modifications and variations due to reworking more in the shallower parts of the beach than in the deeper waters. The ripples are observed up to 1 meter depth below the mean low tide line and continue in deeper water with better development. In a few cases the normal wave-generated ripples have another set of ripples formed in their troughs.

Superposed ripples

Compound ripple patterns occur frequently in the Buddenness and Barry sands. Three different types of superposed patterns are observed, in the first case the ripple ridges parallel to each other with the development of another ridge on the crest of the primary ripple structure. In the other cases ripple ridges are imposed on the earlier set at a very high angle (almost at right angles). In one type the primary ripple structures are the normal asymmetrical ripples with wave lengths 15 to 30 cm and amplitudes

2 to 5 cm. These are formed by the normal westward waves with the smaller secondary ripples with wave length 8 to 15 cm and 5 to 20 mm amplitude formed by the later ebbing tides. These secondary superposed ripples haveasymmetry towards the low tide line. In a few cases the secondary ripples have formed cusp like projections due to flowage of the saturated sediment. These are best developed in the troughs of the primary ripples. Similar ripples patterns are described by Trefethen and Dow (1960) from the Californian beaches.

In the third cases two sets of ripples were observed being formed by incoming tides. The normal E-W ripples were formed by the inshore waves while, with the incoming tide, another set of smaller ripples at right angles to the earlier set were formed in the troughs of the earlier set. This almost simultaneous formation of the two high angle sets may point to some of the commonly assumed superposed ripples formed almost at the same time with a small time lag between their formation. In this locality in the Barry sands the interesting correlation of the formation was that the inshore waves (northward) were producing one set of ripple train while at the same time the westward entry of tidal waters was producing another set right angles to the earlier set in their troughs from most of the sediment picked up from the earlier ripple trains.

Linguoid ripples

The crest of linguoid ripple is curved and closes in the upcurrent side. The shapes vary from a typical cusp to a tongue-like projection; the lee-side inclines away in a radial fashion from the crest. These ripples are observed in an en echelon pattern as noted by Bucher (1919) or one lobe overlapping the other (see Plate 22). The essential conditions of the formation are variable velocities in stringers without higher flow conditions in shallow water conditions. Some are also formed at late stages of the ebb (see Evans, 1941, 1943). These ripples are common in the various sand banks in the estuary (Plate 23) as well as in the tidal channels on the beaches where high flow conditions are achieved by ebbing tide. The wave length varies between 12 to 20 cm. and amplitudes from 1 to 3 cm., the ripple index is much higher (10 to 17) than the common asymmetrical ripples.

Flat topped ripples

Three types of flat topped ripples are found in the area. In the Barry sands very flat ripples (Plate 20) are developed in the upper foreshore region. The wave length varies between 8 to 18 cm. and amplitude from 5 to 15 mm. These flat ripples are formed on the gentle slope of the beach by the low ebb tides as these ripples have lee sides towards the low tide line. This type of very flat ripples are not found in any other part of the beaches nor have they been reported in the literature.

Flat topped ripples occur in a few channels running across the beaches and also in the shallow tidal pools. These ripples have only the tops of the ripple crests flattened while the original ripple structure is of normal asymmetrical type. The ripples are flattened due to shallow sheets

FIG. 16

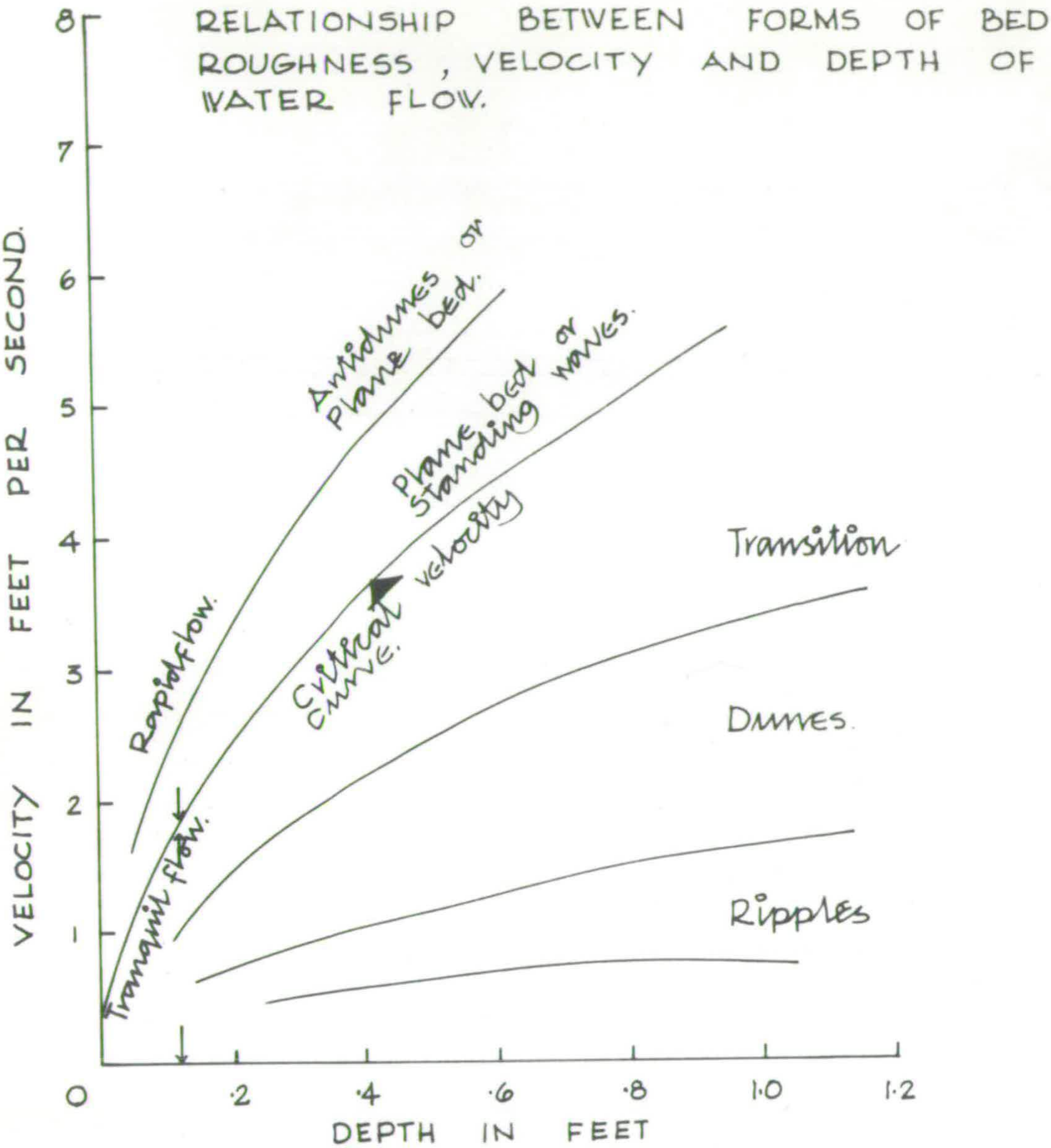

VARIATION OF VELOCITY WITH DEPTH.

Flume studies using medium grade sand.

[from SIMONS, RICHARDSON AND ALBERTSON; 1961].

of water flowing back with the backwash on a falling tide. These types of flat topped ripples have been described elsewhere by Wegner (1932), Shrock (1948), Van Straaten (1953), McKee (1957), and Tanner (1958).

Rhomboid ripples

Rhomboid ripple marks are produced in some of the relatively steeper parts of the upper foreshore beaches. The rhomboidal pattern is produced by the spread of a thin film of water near the swash zone by the backwash. The current direction bisects the acute angle of the rhombs. The marks are produced by the effect on the backwash of obstructing pebbles and shells. The criss-cross rhombic pattern is produced behind. the obstacles by the interference of the flow lines (Plate 18B). A few of the rhombic marks are formed by the interfering swash patterns but these marks are very temporary as they are later destroyed by the backwash. The marks are best developed on a steeper gradient of the beach by the receding tides; they are very common structures on most of the beaches (Kindle, 1917; Johnson, 1919; Kindle & Bucher, 1932; Woodford, 1935; etc.).

Aeolian ripples

Aeolian ripples are always asymmetrical with a gentle windward slope and a steep leeward slope. These wind ripples are quite frequent on the windblown backshore flats and on the coastal dunes. The ripple structures are made up of medium to fine sand and thus come under the sand ripple group of Bagnold (1941). Granule ripples are not present in the area except in a part of the Barry dunes where a rough tendency towards ripple development is seen in the coarse sand and granules. The size of the ripple changes very slightly from one part of the area to another, the wave length range between 3 to 19 cm. and amplitudes from 5 to 15 mm. This gives a much higher value for the ripple index than the aqueous ripples. The mean ripple index for these ripples is about 16 which is much higher than the aqueous ripples index (Fig. 15) but not actually as large as the 4-6 times suggested by Kindle (1917). McKee (1933, 1945), Bagnold (1937, 1941) and Sharp (1963) have shown that an index value below 15 does not always indicate aqueous origin as large variations are quite frequent.

The arrangement of ripple trains and their alignment depend on the wind direction and the place of the ripples on the dunes. Their direction patterns follow the dunes, which ~~themself~~ accord with wind directions. Usually there is a little concentration of heavy minerals near the base of the ripples.

2.4 Cusps and other beach structures

Beach cusps.

Beach cusps project out from the lower foreshore during the cycle of low tides in the Barry sands (Plate 15B); and are composed of medium to medium fine sand. The distance between the individual cusps is not constant and varies between 5 to 20 meters while the heights range from 2 to 7 dm. Sections in the cusps show high angle lower foreshore laminations usually following the general shape and slope of the cusp form. Some cusps have highly rippled tops while in most cases smooth ripple free surfaces are observed. Cuspate projections are eroded by the swash and the backwash deposits the material.

The cusps are formed under conditions of very delicate adjustment of erosion and deposition. Some of the cusps are formed along the beach due to the presence of an obstruction while others are produced by possible selective erosion by the swash (Johnson, 1919). Emery (1960) has described the formation of cusps during the wave cycles of a few hours. In the Barry sands the cusps are formed by the destruction of the beach ridge at the lower foreshore zone and reworking by waves. Evans (1940) has seen a similar process of cusp formation in the Lake Michigan region. In the Barry sands the low beach ridge may be present in one week while the next week it has been gradually destroyed and replaced by the cuspate forms. The definite agencies contributing to the origin of beach cusps are not yet clearly known. In one place one factor may cause the start of the cusp while it fails to produce cusps in another area (Gellert, 1937). In this area only sand cusps are noted and the gravel cusps are absent.

Ridge and trough structures

Ridges and troughs are the systems of large linear elevations and low depressions formed in some sandy foreshore zone of the beaches approximately parallel to the coast line. These structures are also known as fulls and lows, balls and lows (Evans, 1940), ridges and runnels, and surf-megaripples. The large low ridges are produced by the breaker action at the lower part of the beach with a gentle profile. The role of gentle beach profile and abundant supply of sand (Evans, 1940) is of importance in the production of these ridge structures. The ridge may be more than one and they are temporary, always shifting, reworked and destroyed by the breakers. The ridges are very low in shape and breaks at irregular intervals are present. In few cases one of the ridges is better developed after the highest tides to give beach ridge in that part of the beach (Doeglas 1955). The beach ridge in the lower part of the upper foreshore zone is composed of medium to medium fine sand, very loosely packed and devoid of any internal structures (Fig. 7A).

Swash marks

The highest reach of the swash is marked by a thin deposit of sand, flaky minerals, shell fragments, organic debris, etc. This deposit is the swash mark. In some cases due to strong repeated action of the swash by high tides a small ridge is produced and this is termed as swash ridge.

Sand pitting

In the uppermost part of the upper foreshore marks are produced by the imprint of sand grains thrown on the wet sediment. The sand grains are brought by the strong wind and their point of impact on the wet sand forms small pits (Plate 28A). This sand pitting texture is best formed at the time of ebb tides as with the flow tides all pitting marks are destroyed by gradual saturation of that part of the beach.

Crescent marks

These are the scour marks formed by the backwash behind any type of obstacles in its path. These structures are also known as backwash marks and are very common in the upper foreshore beaches. They are best developed in a steeper part of the beach; in most of the cases the obstacles are shells or small pebbles (Plate 26B). The crescent marks are best developed during the ebbing phase of the tides, small in size (5 to 30 mm in size) and have an inverted V or crescent shape behind the obstacle.

Lineations

Primary current lineations are produced under shallow flow conditions; the lineations are mostly formed at the water's edge. With the swash, streaks of mica or other flaky minerals are produced and this gives a type of lineation. Some of the lineations are produced by dragging of sand grains giving fine striations on the beach (Plate 26A) Few lineations are also produced on the ripples by the to and fro motion of the tides (Plate 25B).

Rill marks

Rills are very common structures in the foreshore parts of the beaches. With the receding tides, the saturated sediment starts dewatering, the water drains out and flows towards the slope and forms rills in the sediment (Plate 27). These marks are of varying sizes and have well developed dendritic patterns. The type, shape and branching depend upon the slope and the sediment; well developed rills are produced rather in sands than in the silts. In the silty sands of the estuary rills are thinner and longer which may be due to permeability of the sediment.

Beach chutes

On the steeper gradient of the beach, small channels are formed with the falling tides. The saturated material along with water starts sliding down the slope, breaking ripple trains. The channel with these marks which are produced by the forward creep of the saturated sand in a mass of overlapping lobes and ridges are termed as "beach chutes" by Trefethen and Dow (1960). Craig and Walton (1962) have described similar structures as varieties of their longitudinal ridges.

Marks produced by seaweed.

In the foreshore parts of the beaches there is often some seaweed with attached anchor stones. With the tidal currents and waves, these seaweeds swing from one side to another and drag the attached pebbles on the sand. This dragging of the anchor stone produces a groove. Or the pebble may resist movement while the seaweed is wafted around to produce a series of irregular curved brushing marks around the anchor stone.

FIG. 17

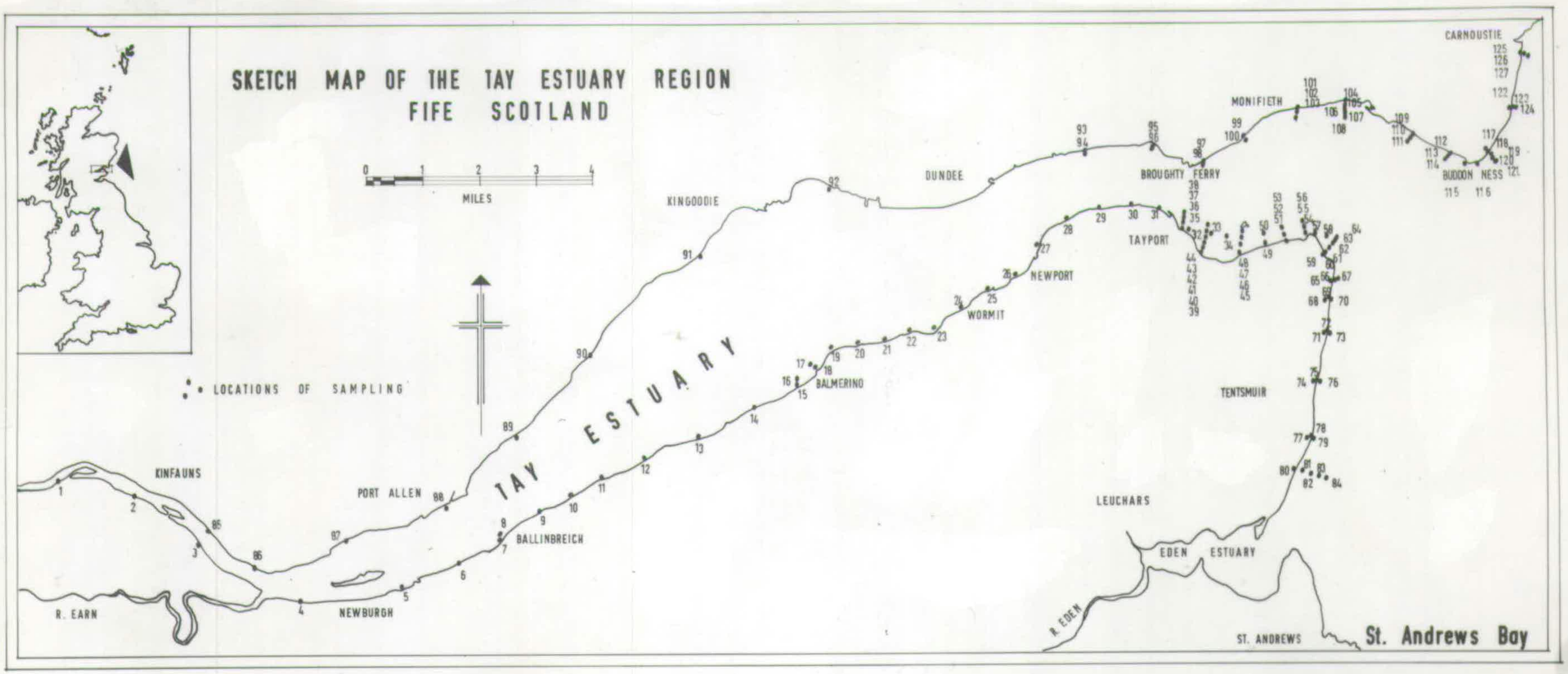
SKETCH MAP OF THE TAY ESTUARY REGION
FIFE SCOTLAND
MILES
LOCATIONS OF SAMPLING
TAY ESTUARY
KINFAUNS
PORT ALLEN
KINGOODIE
DUNDEE
BROUGHTY FERRY
MONIFIETH
CARNOUSTIE
BUDDON NESS
TAYPORT
NEWPORT
WORMIT
BALMERINO
BALLINBREICH
NEWBURGH
R. EARN
TENTSMUIR
LEUCHARS
EDEN ESTUARY
R. EDEN
ST. ANDREWS
St. Andrews Bay

Section 3. GRANULOMETRIC STUDIES

3.1 A series of samples were taken and the sample stations were given location numbers. These constitute a running series and are referred in the text to indicate location; Fig. 17 gives the locations of all sampling stations. The majority of the samples are surface samples but some undisturbed tray samples were taken to study the structures and laminar variations in grain size and mineralogical properties. National kilometer grid squares were used to select the places for samples; for the most part a sample per kilometer square was taken but in a few cases this was changed depending upon the extent of the sandbanks and accessibility. Approximately 200 grams of material was selected at each station and polythene containers were used to store the samples.

In the laboratory samples were dried at a low temperature (30°C) in the oven to remove moisture. Samples with high silt/clay content were not subjected to this treatment as drying tended to harden the whole sample which makes disaggregation of the sample difficult for mechanical analysis. Oven drying was sufficient to disaggregate the grains in most of the samples A rotary type of sample splitter was used and an approximate 20 gram split was obtained for the purpose of mechanical analysis.

Mechanical analysis was carried out by taking about 20 gm. of sample and separating into 16 grades using a set of $\frac{1}{4}$ phi Tyler sieves, shaken on a Ro-Tap Auto Machine for 20 minutes. In most cases, the silt/

FIG. 18

DISTRIBUTION OF FINE GRAIN SEDIMENT (LESS THAN 4 ϕ) OF THE AREA.

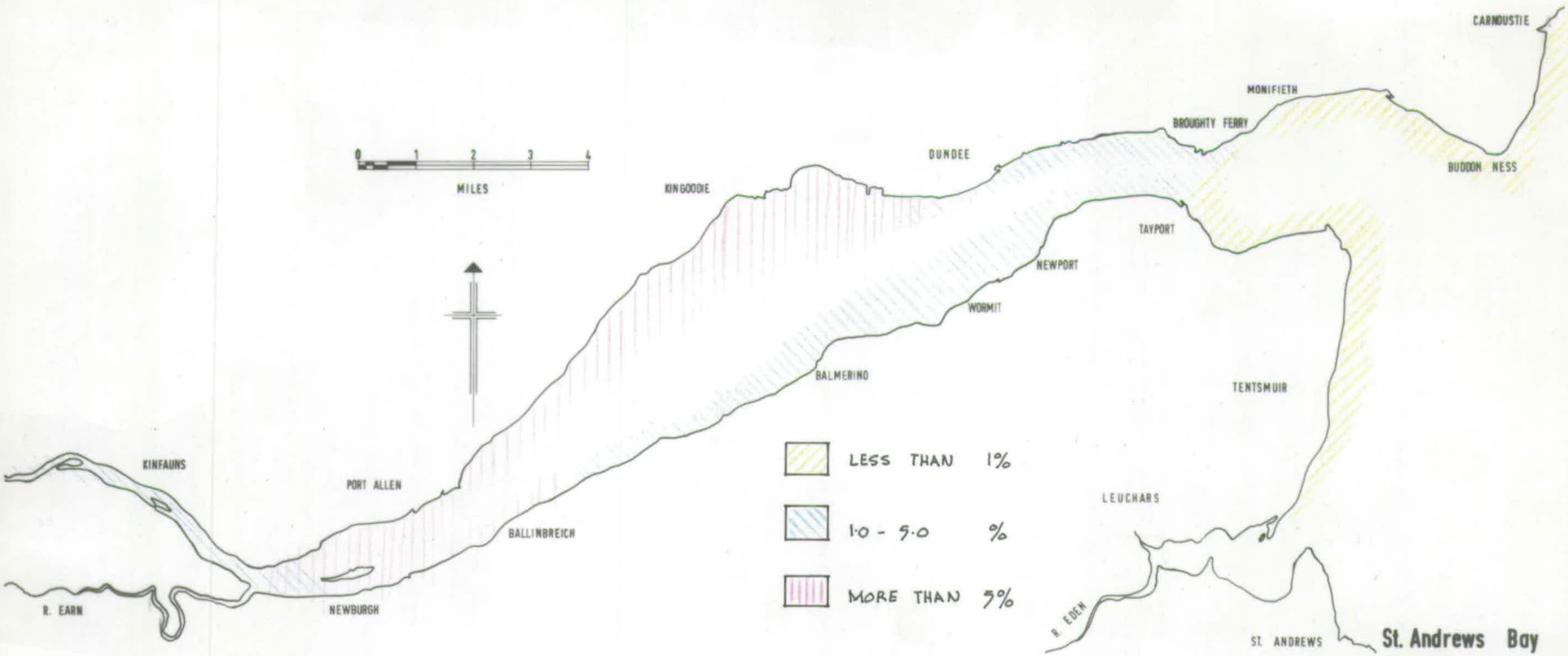

FIG. 19

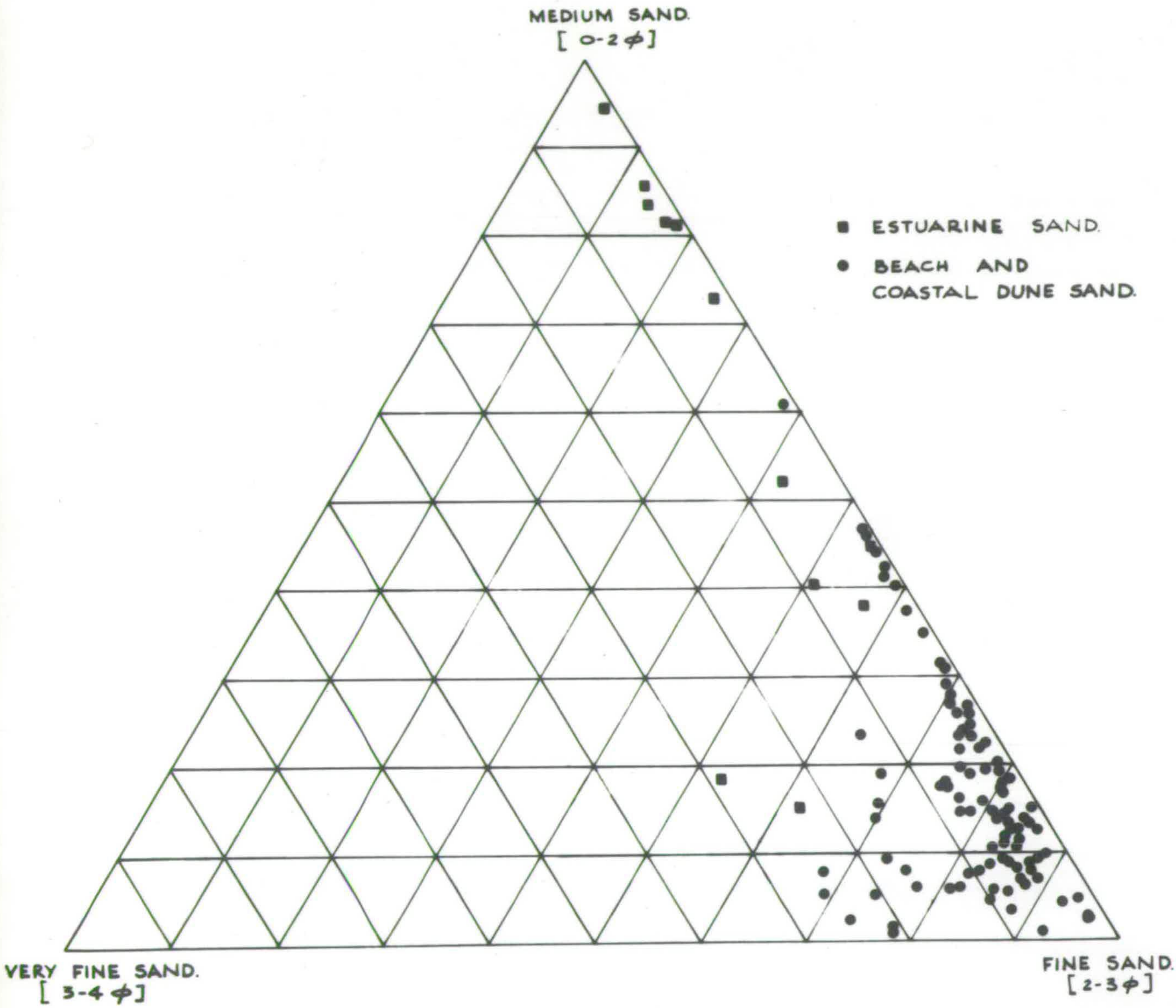

TRIANGLE DIAGRAM OF THE SIZE FREQUENCY DISTRIBUTION OF SANDS OF TAY ESTUARY REGION IN TERMS OF MEDIUM SAND, FINE SAND AND VERY FINE SAND GRADE.

clay grade material (more than 4 ϕ) was less than 10% of the total material; no pipette analyses were carried out. In a few cases the wet seiving method was used for samples with high content of fine material. In this text a combination of Wentworth (1932) and phi scale of classification is used. Phi scale is used as statistical computations are more convenient with the logarithmic scale (Krumbein, 1934).

There is a wide choice in selecting a method for expressing the results of granulometric analysis to help in establishing any regional trend in grain size and distribution and comparing the results from other areas. Roughly, the methods are divided under graphic and statistical groups. Doeglas and Smithuyzen (1941) have shown the advantages of graphical distribution curves, using a probability scale with arithmetic size grade. The advantages of plotting data on this paper are that the normal distributions show up as a straight line while any phenomenon of mixing or differentiation can be distinguished by the change in the shape of the curves. The value of the results obtained by the statistical methods of Trask, Niggli and Krumbein has been questioned by Doeglas (1946). These results do not show much of the actual problem of the environments, distinction between the various environments, direction of transport, etc. Quartiles only refer to the middle part of the frequency curves while the distribution curves suggested by Doeglas (1944, 1946, 1950) give more complete data than the others. Plates 31 to 33 present the characteristic size-frequency distributions of each type, class and their zone diagrams according to Doeglas and Van Andel & Postma (1954).

These classes are based on the shape of the curve and not on its position. Three types of sand distributions and two types of clay distributions were recognised. They are:

B - type .... consists of very ill sorted coarse material

F - type .... is almost a straight line and represents an almost symmetrical distribution with poor sorting

M - type .... is much better sorted than the F type and has a lower and much more sharply defined maximum size than the F-type of the same average size

S - type .... is a clay distribution with up to 50% silts with a well defined maximum size

C - type .... consists of clay with little silt and no pronounced upper size limit.

Some of the mixed curve types are found due to the admixture of two or more curve types. In the present investigation the terms of Van Andel and Postma are used to denote the shape of the distribution curves in order to facilitate

FIG. 20

SIZE FREQUENCY DISTRIBUTION CURVE TYPES IN THE AREA.

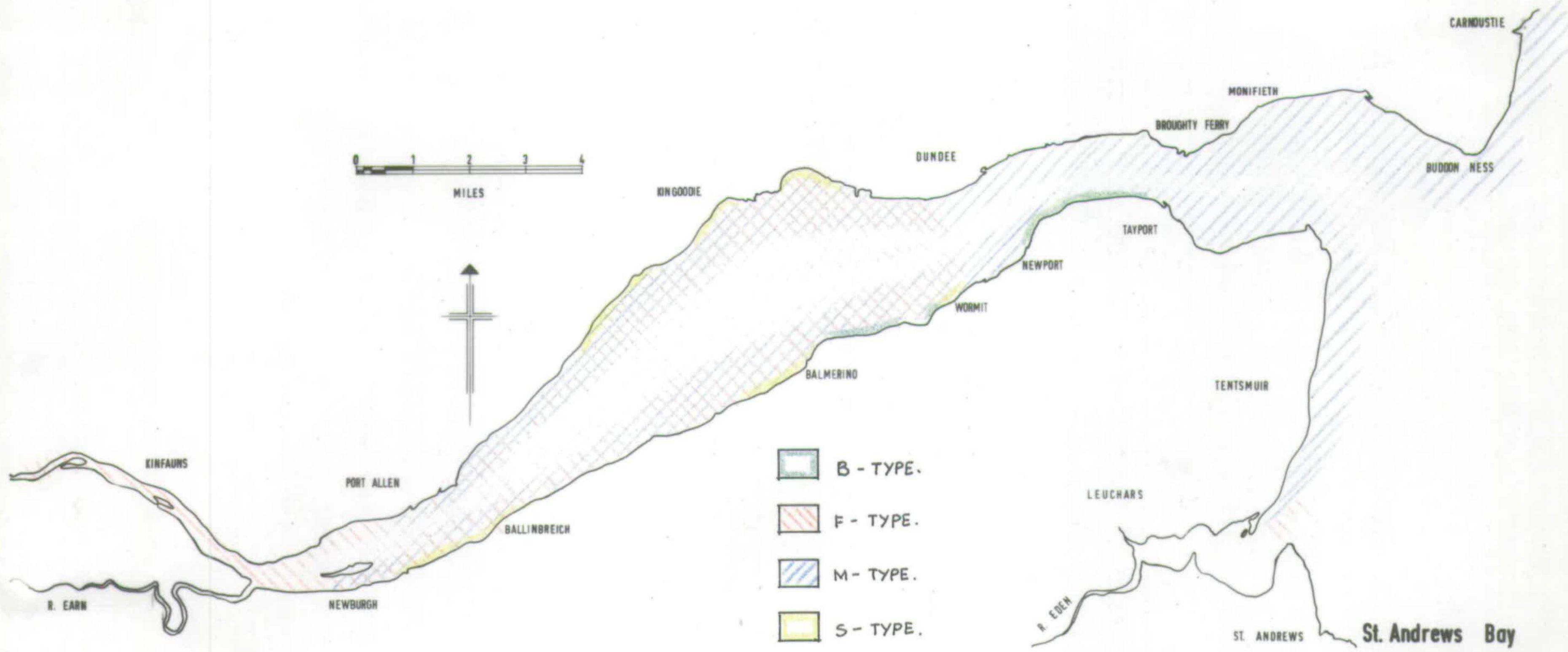

FIG. 21

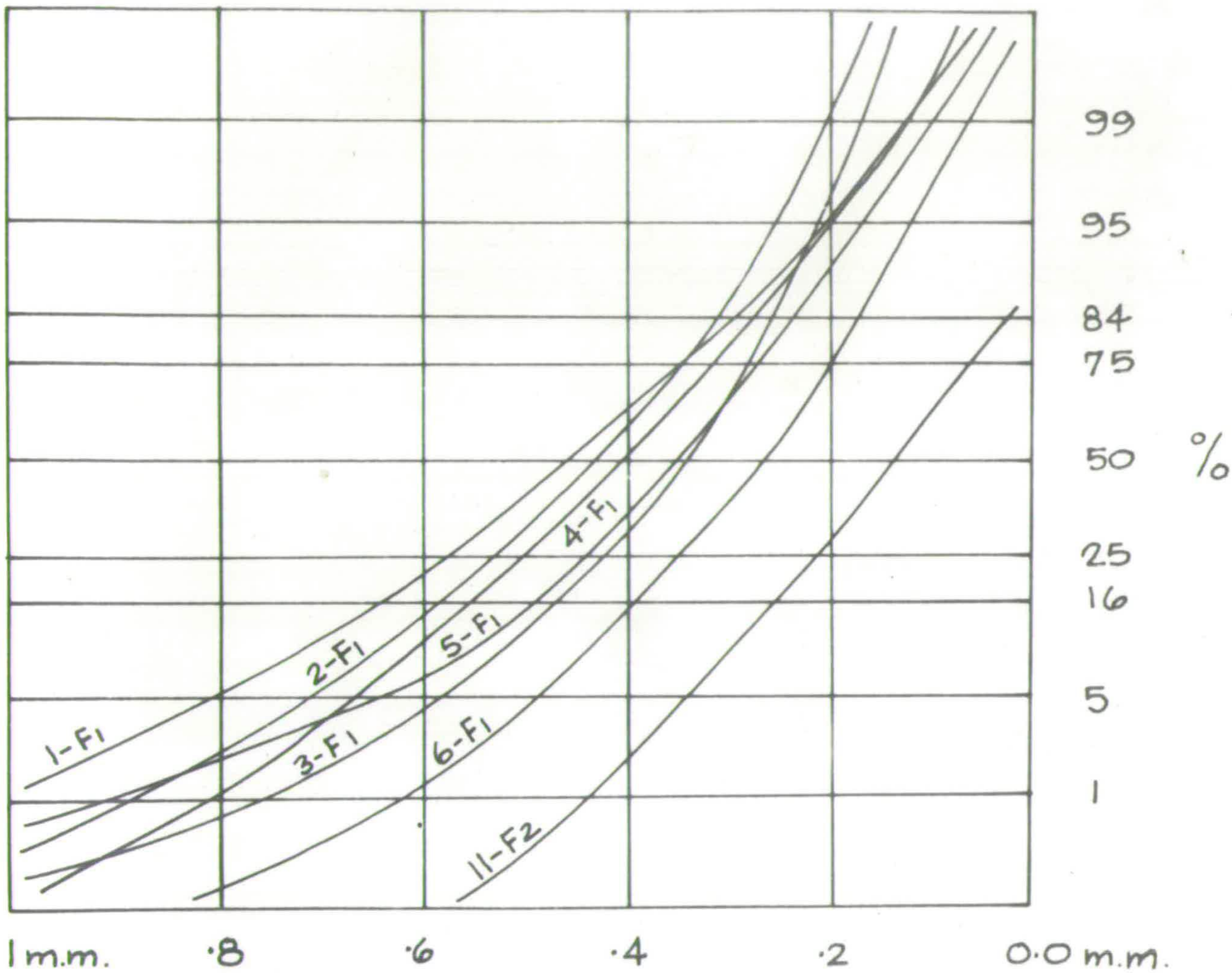

CHARACTERISTIC SIZE FREQUENCY DISTRIBUTION CURVES OF F-TYPE.

FIG. 22

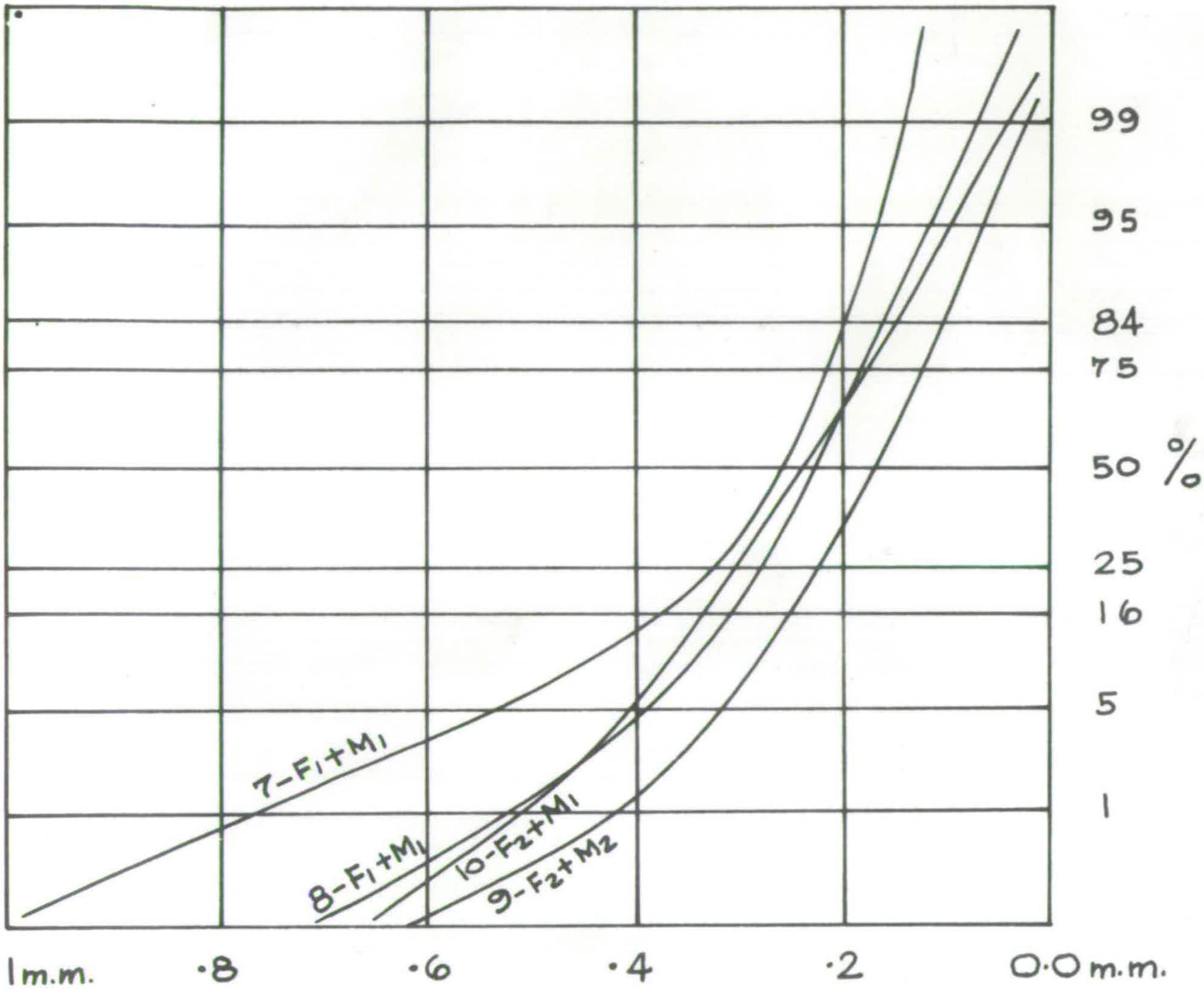

CHARACTERISTIC SIZE FREQUENCY DISTRIBUTION CURVES OF F-M- TYPES.

comparison with the other data. In the upper Tay estuary F - type distribution curves predominate while the lower parts of the estuary shows F + M and M - type curves. The beach sands show the M - type distributions.

3.2 Distribution of Curve Types in the Area

Fig. 20 gives the distribution of various curve types in the area. In the region of Perth the river regime is prominent and F_1 - type curves are found at stations 1, 3, 4, 85, 86, 87, 88 and 89: F_2 - type occur at station 11. The shapes of the distribution curves are similar to those of other rivers (Lugn, 1927; Wentworth, 1932; Russell, 1936; Russell and Taylor, 1937; Doeglas, 1950). Some curves are bent slightly towards left when followed from coarse towards fine end which may be due to winnowing of the fine fractions. Composite sample can give the same type of shape (Doeglas, 1944). A flexure towards the right in the coarse end is produced by the absence of coarse material. This can also happen by the non-availability of a coarse fraction or its removal and deposition in the upper reaches of the river. Doeglas (1950) has found similar distributions in the Lower Rhine and Lek sediments. The grain size decreases gradually downstream and the mixed F M curve types are found in the upper parts of the estuary due to the gradual decrease of the coarse fraction and the influx of medium/fine sand. These mixed F M curves are obtained from the various stations in the estuary. Appendix 1 gives the distribution of curve types at each station and figs. 21 and 22 give the F and F M curve types in the area.

FIG. 23

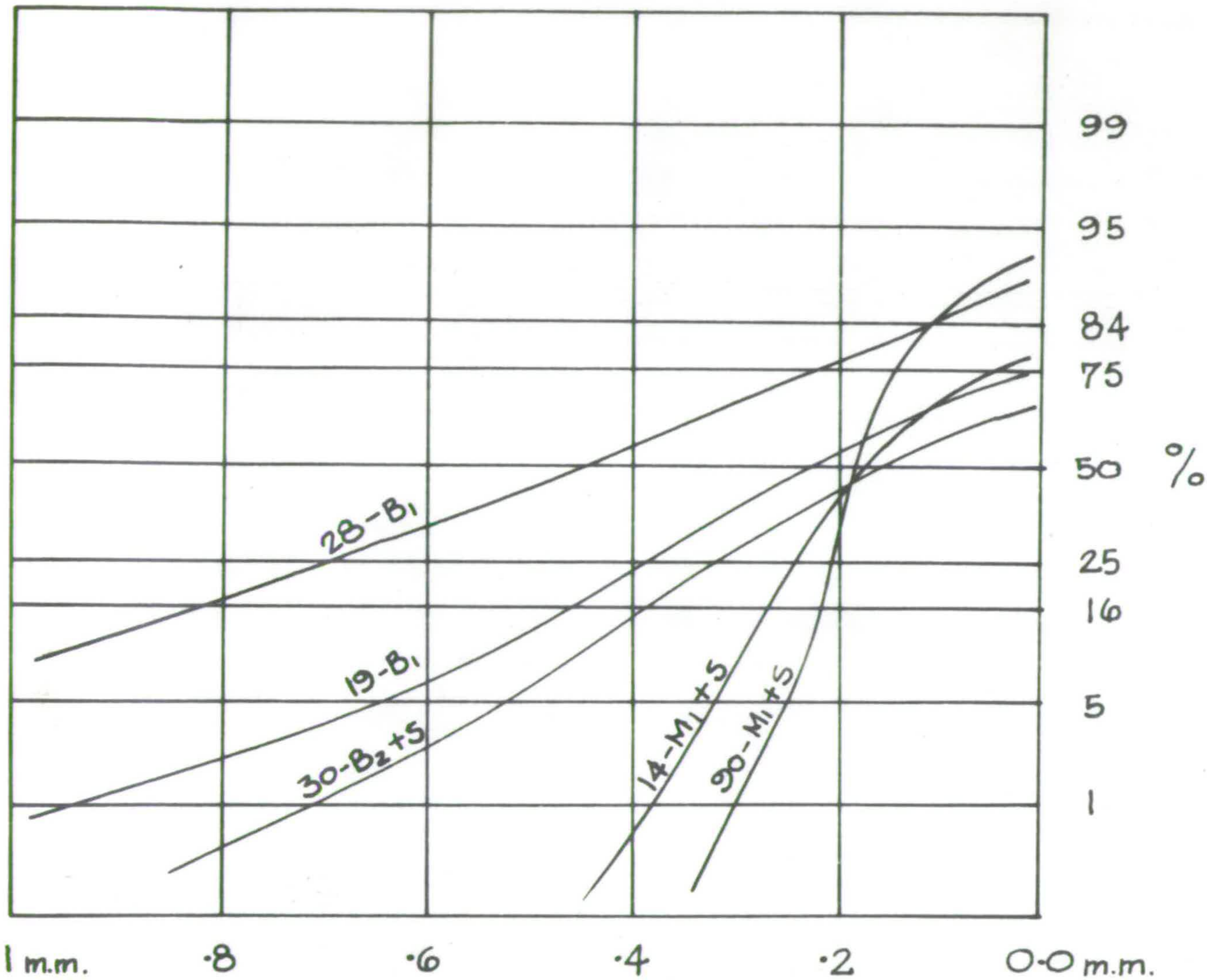

CHARACTERISTIC SIZE FREQUENCY DISTRIBUTION OF M-S- AND B-TYPES.

FIG. 24

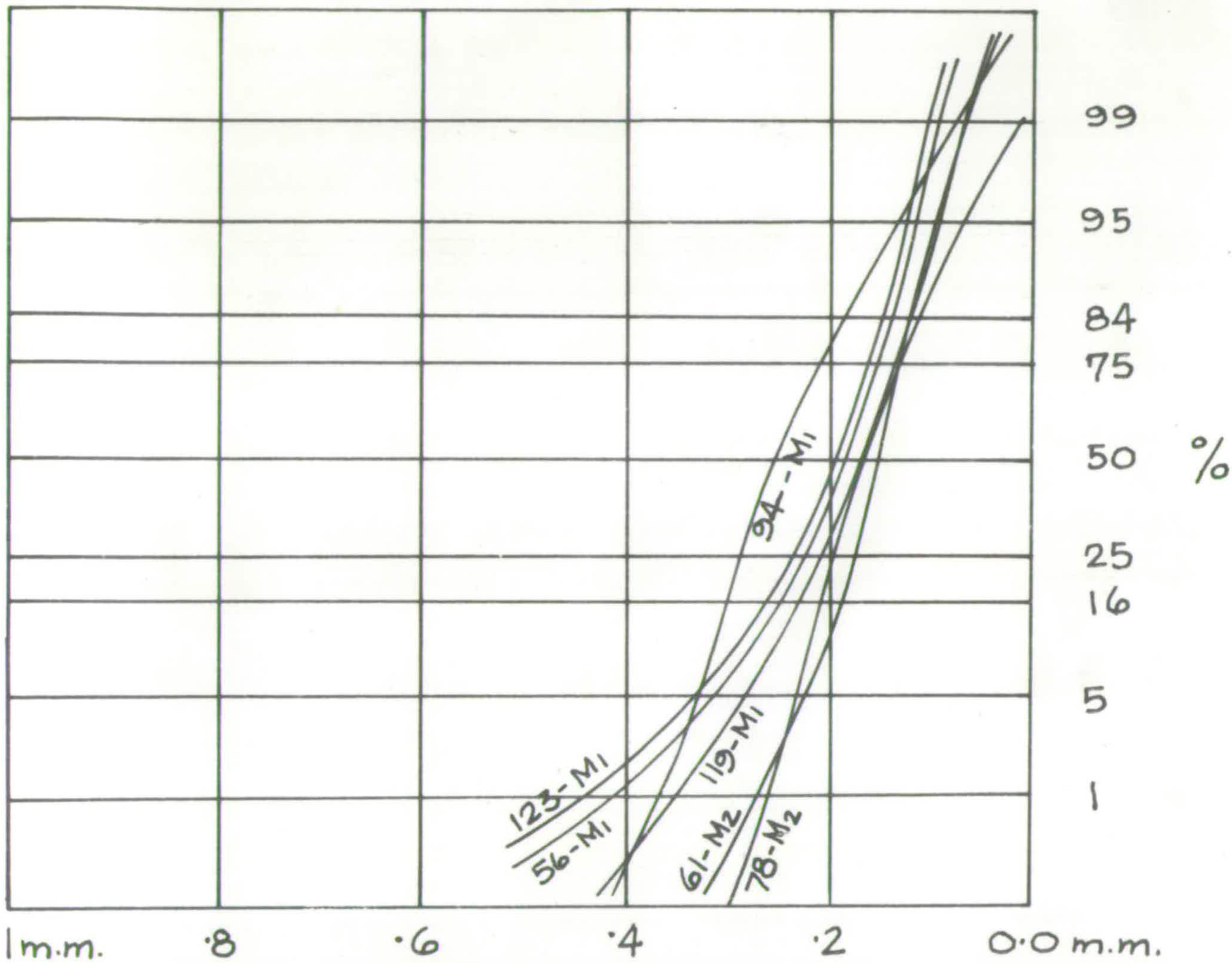

CHARACTERISTIC SIZE FREQUENCY DISTRIBUTION OF M-TYPE CURVES.

In the marsh creeks near Newburgh, Ballinbreich and Errol, poorly sorted material with B S and B M types are found; the most common being B_2 M_2 and B_3 M_2 distributions. B S and M S curves are present near Balmerino and Kingoodie, while near Wormit there is a predominance of B S. Most of the poorly sorted material in this place has come from the cliff falls and its mixing with the river sediments. Many curves from the estuary show steep bends towards the right at the Fine end and this is due to the great influx of fine fraction in the estuary. The mean concentration of solid particles carried in suspension by Tay is of the order of 1 part in 5,000 by weight of water. This amount is small but during the course of time the mud flats have accumulated a substantial amount of material.

The beach sands of Tayport, Tentsmuir, Monifeith and Barry have M_1 and M_2 type curves while in a few cases t_1 - type (Doeglas, 1950) curves are also found (fig. 24). This is due to the presence of more coarse material in the normal M_1 type curves which are equivalent to t_2 curve types. Most of the coarse fraction in the Barry and Tentsmuir sands is composed of calcareous shell debris. Acid treatment modifies the tails of the curves and thus the overall shape of the curve. Kruit, (1955) has found similar changes in shape in the Rhone delta sediments. But the samples of Tay region were not treated with acid as shell debris is taken as an integral part of the sediment.

FIG. 25

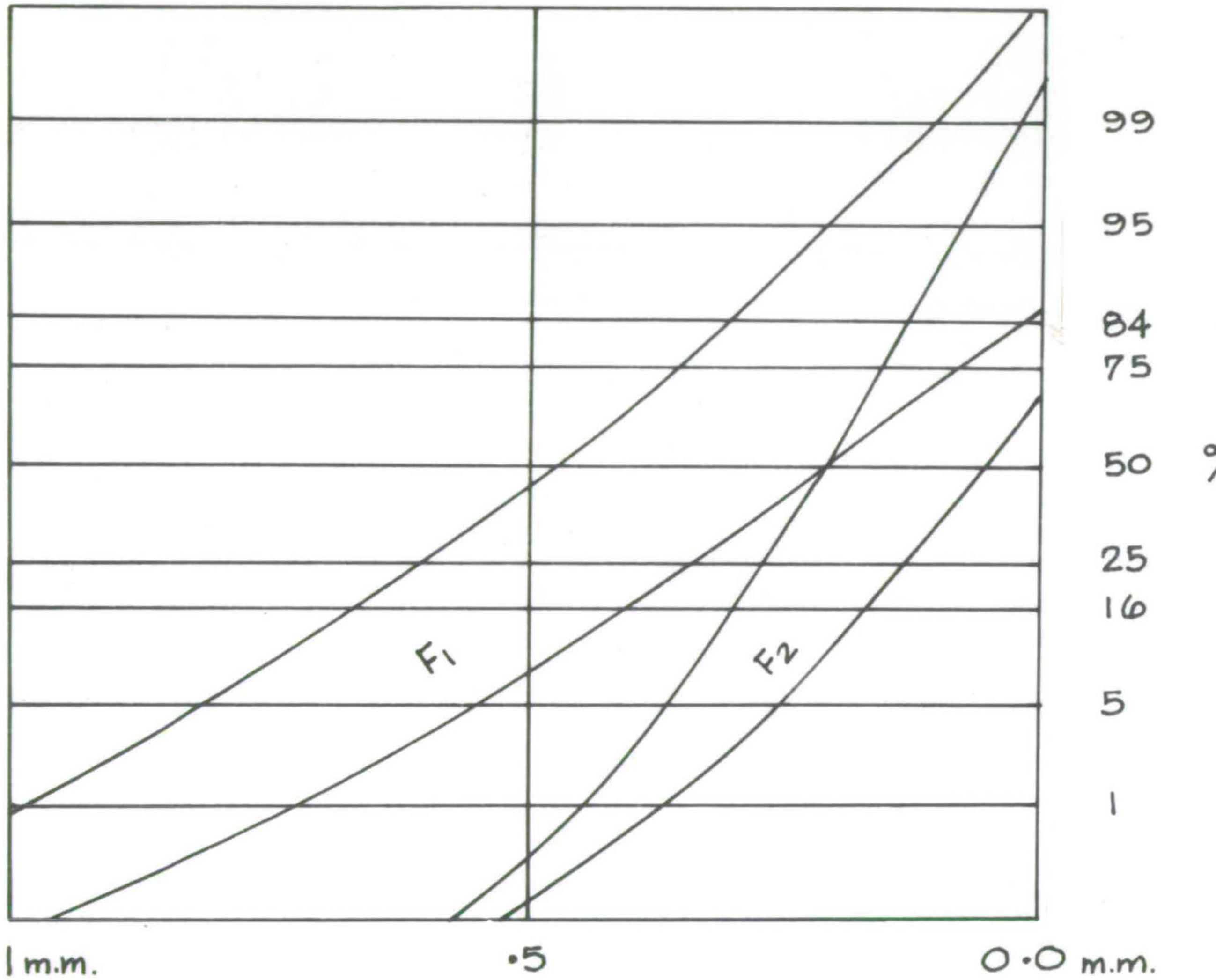

ZONE DIAGRAM OF F-TYPE CURVES.

FIG. 26

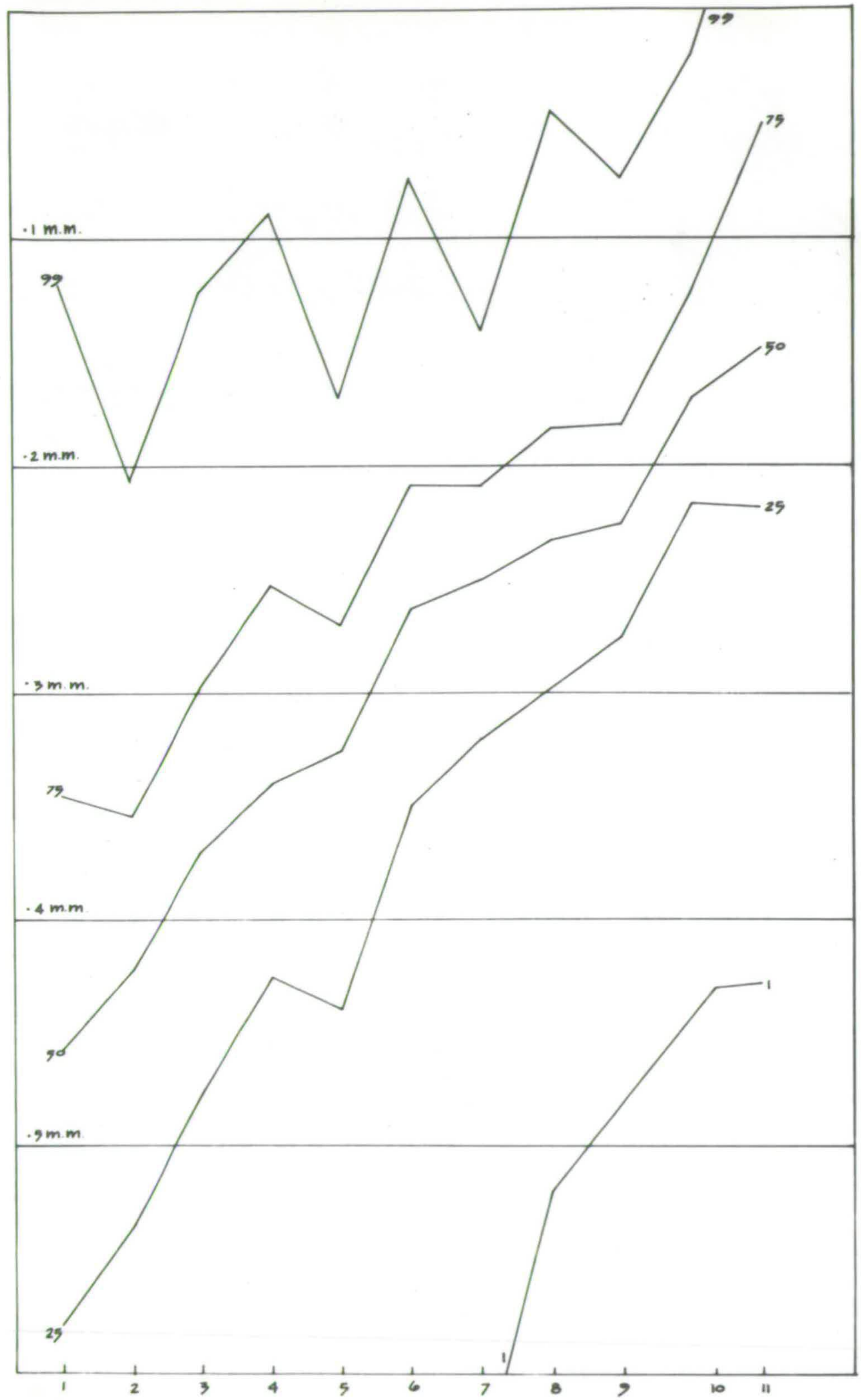

VARIATION OF THE 1ST, 99TH PERCENTILES AND OF THE QUARTILES IN THE TAY ESTUARY.

3.3 Distribution Curves and Environments

The samples from the river Tay and upper part of Tay estuary show characteristic shapes of size frequency distribution curves. The curves (fig. 25) similar to those of the other rivers (Doeglas, 1950) and are mostly the R and F type of Doeglas and Van Andel. In the F M curves of the estuary, the amount of the two components can be calculated from the limit of the horizontal trend. The diagram (figs. 21 and 22) of the F and F M curves show that the coarse material in the tails is being dropped towards downstream; the fine fraction is being mixed in the sediment. Most of the material is carried as the bed load while the fine fractions in suspension are carried into the estuary. This can be inferred from the absence of right angle bend towards the finer end of the tail, and straight nature of the curve. Some step-like shapes in the curves are due to the influx of fine sand with change in the current velocity. The river sediments are poor in the fine fraction which is gradually carried in suspension to the estuary and beyond although the fine fraction is concentrated in some calm, sheltered parts of the river.

The percentile diagram (fig. 26) shows that the first percentile reflects changes in the currents more closely than the 99th; but the overall general trend of the sediments is to be richer in fine sand towards the estuary. This is clearly brought out in the percentile distribution diagram where the decrease in medium size towards the main part of the lower part of the estuary is very distinct.

Estmarine Sediments

FIG. 27

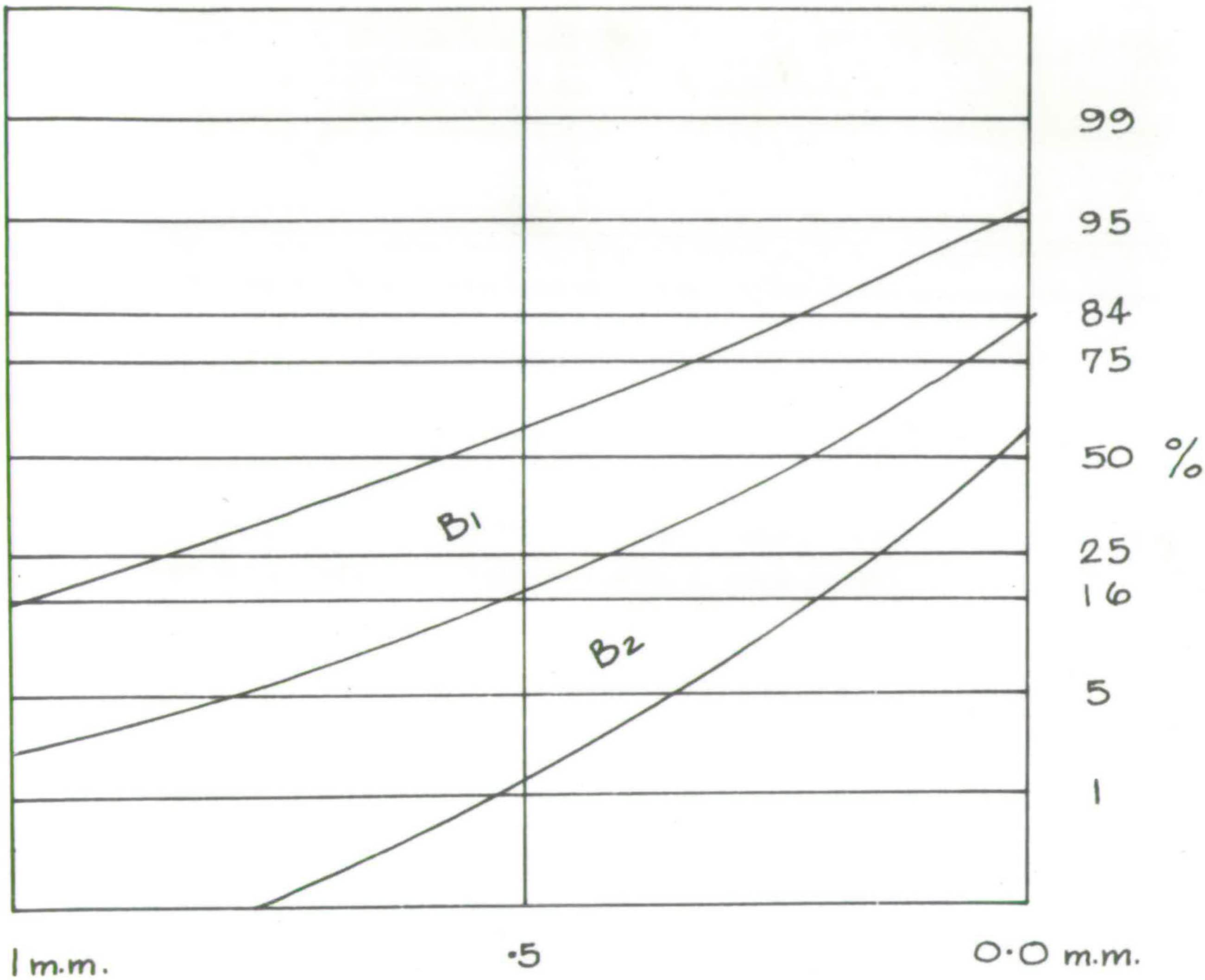

ZONE DIAGRAM OF B- TYPE CURVES.

FIG. 28

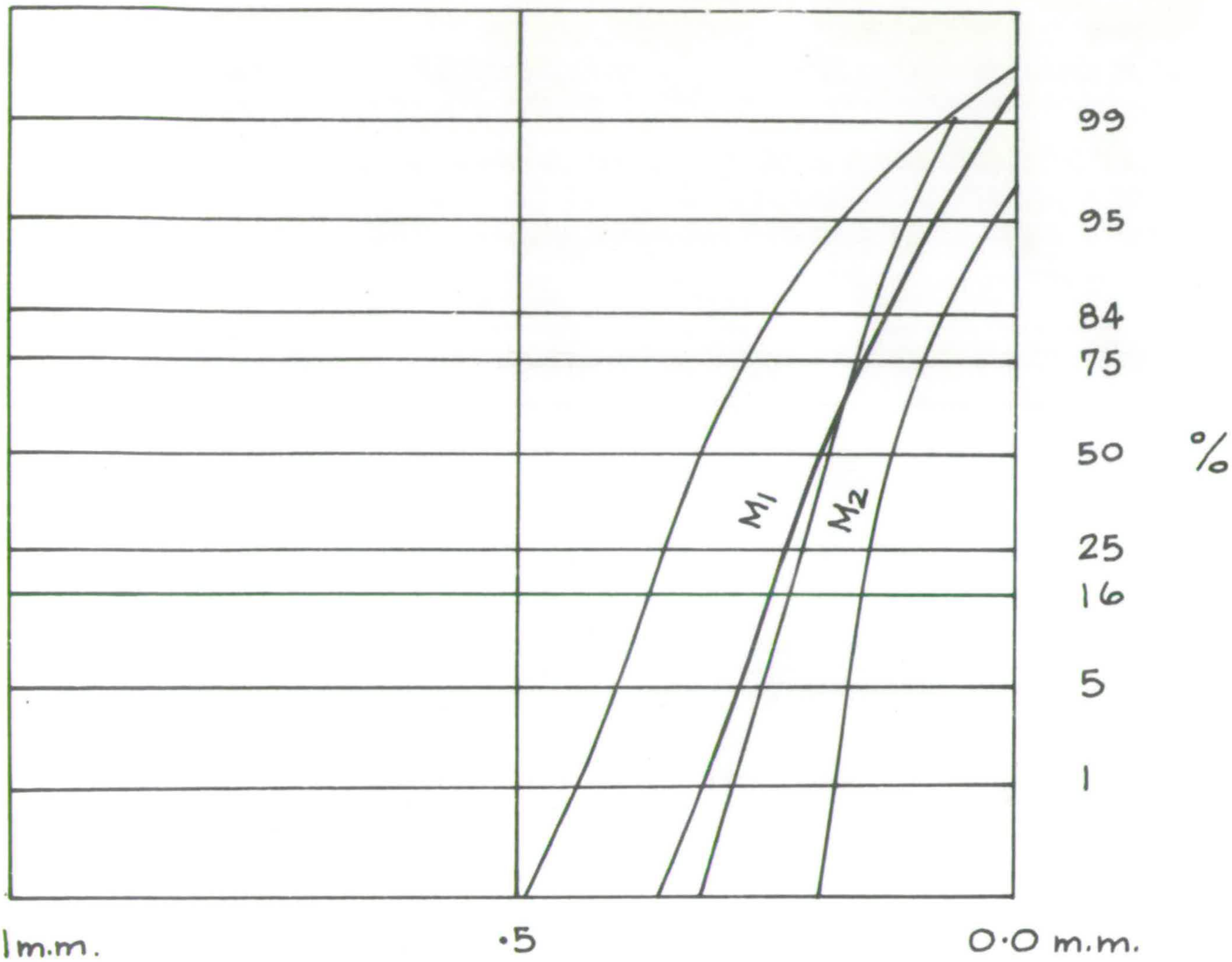

ZONE DIAGRAM OF M-TYPE CURVES.

Estuarine Sediments

The distribution curves from the Tay estuary (fig. 20) are of T and M types of Doeglas and Van Andel. Mixed F M curves are found in the upper reaches of the estuary; the shapes of all the curves are similar though the medium size (position of the curve) varies. There is a general change in the curves from F to F M and then to M towards the lower reaches of the estuary. Similar trends of the changes in the curve types are found in the Dutch estuaries and tidal flats (Doeglas, 1950).

The marsh and marsh-creek sediments give a MS curve shape, the fine fraction brought by the currents in suspension but some of it is also produced by the reworking of underlying boulder-clay deposit. The boulder-clay havei g a M S and M C type mixed curves. The percentage of silt fraction is the highest (max. value 33%) in the estuary, this enrichment of the fine fraction may be due to the 'settling-lag effect' (Van Straaten and Kuenen, 1957).

The percentile distribution diagrams do not show any significant trends; only the 1st and 99 the percentiles tend to fluctuate more than the others, especially in the case of the marsh sediments.

Beach Sediments

The beach sands in the area show t- and M- type curves of Doeglas and Van Andel with coarse tails reaching 15% in a few cases. The size position of the curves vary little with their location in the sub-environments; there is more variation in the coarser end of the curves than in the finer

FIG. 29

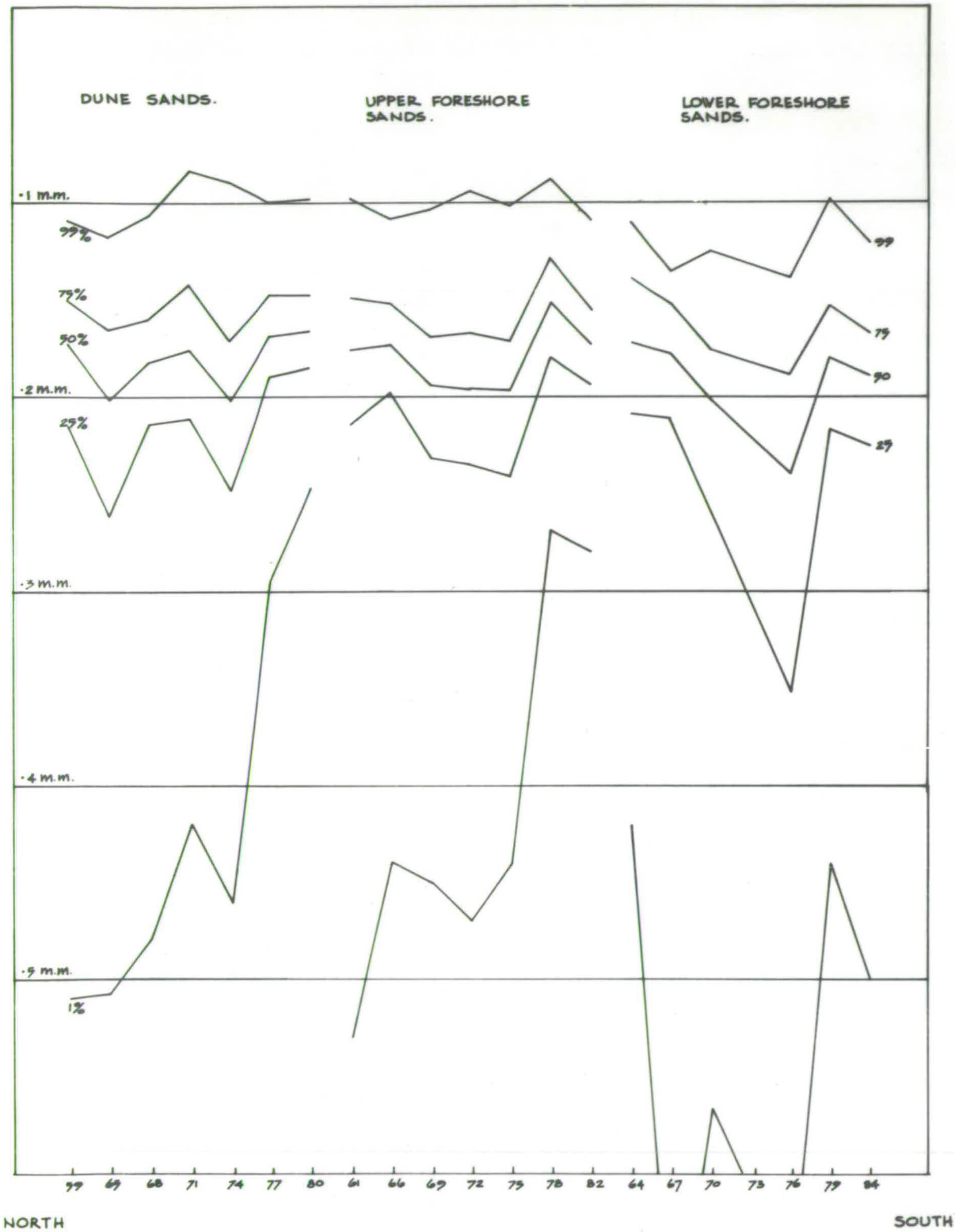

VARIATION OF THE 1ST, 99TH PERCENTILES AND OF THE QUARTILES ALONG TENTSMUIR SANDS.

FIG. 30

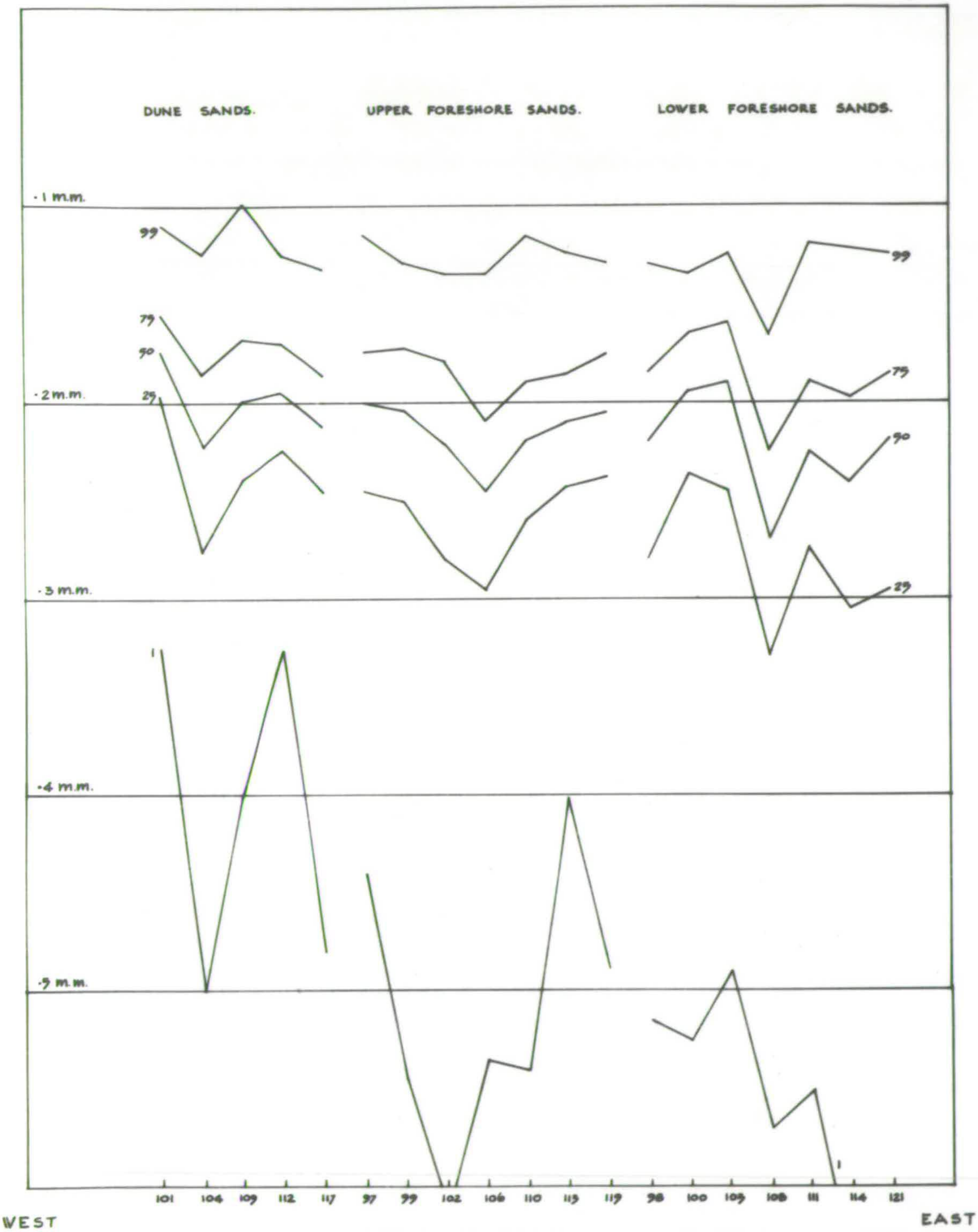

VARIATION OF THE 1ST, 99TH PERCENTILES AND OF THE QUARTILES ALONG THE NORTHERN SANDS.

tail of the curves. Fig 28 gives the zone diagram of the M- type curves in the area.

Percentile distribution diagrams show a significant change in all the percentile values especially in the 1st and 99th percentile from lower foreshore to upper foreshore and backshore sands. The 99th percentile values are fairly constant in the various parts of the beach except in the lower foreshore where the values are usually coarser. The variation is more pronounced in the Tentsmuir sands (fig. 29) than in the Northern (Monifieth and Barry) sands. In the Tentsmuir sands the 1st percentile shows a definite gradual coarsening towards the north which is more marked in the upper foreshore sands than the lower foreshore sands. Northern foreshore sands show a gradual decrease in the grain size towards the west especially in the 1st percentile (fig. 30). This trend is also seen in the coastal dune sands, the trend being contrary to the direction of river flow. This trend is only shown by the 1st percentile, the other percentiles show no significant trend. The minimum size (99th percentile) is constant in most of the samples.

Coastal Dune Sediments

The distribution curves of dune sands vary considerably from one part of a dune to another; these variations are greater in the coarse end than in the fine end (fig. 31). The shape of the curves for the particles less than 200 microns remains practically the same in all the samples.

FIG. 31

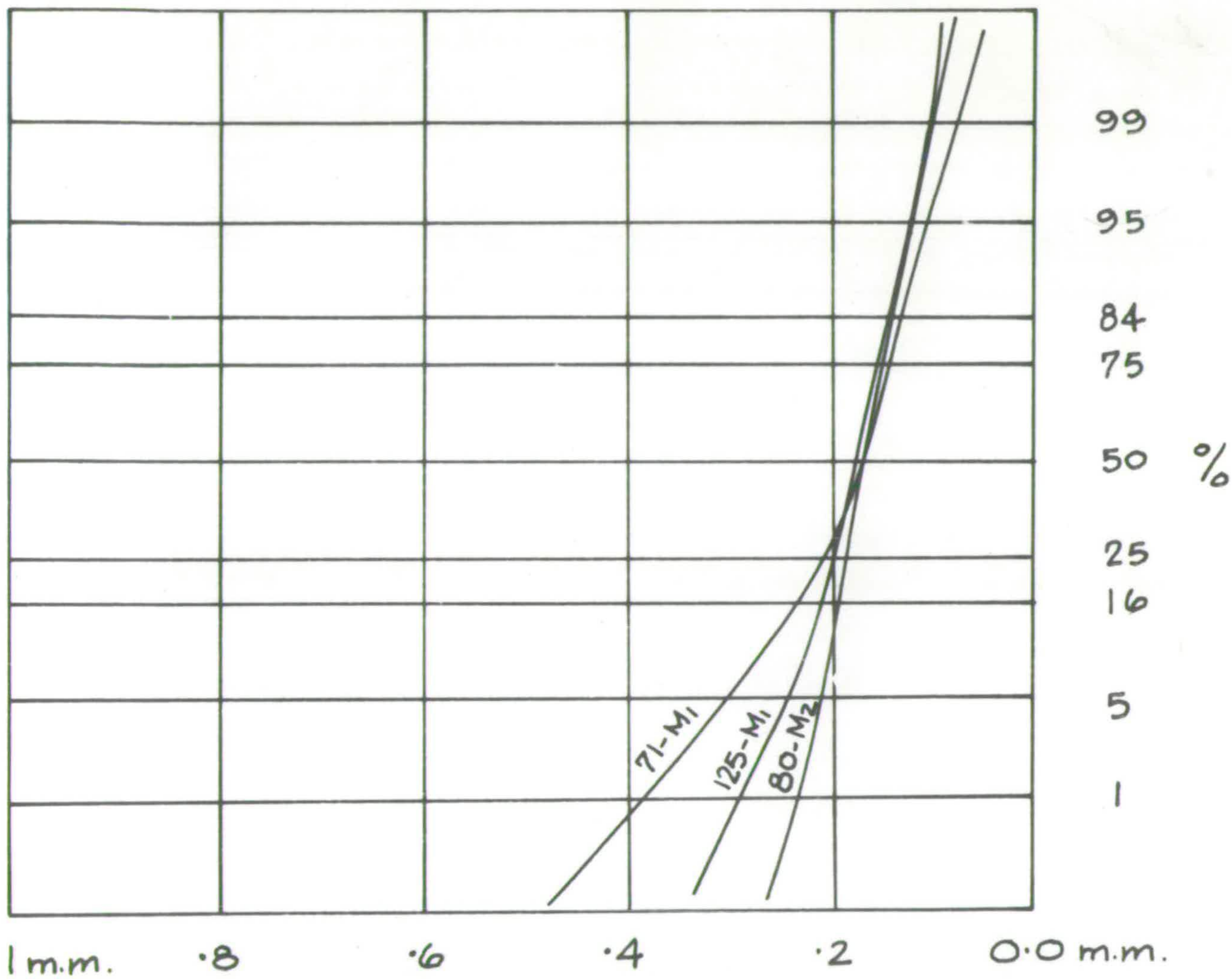

SIZE FREQUENCY DISTRIBUTION CURVES OF DUNE SANDS.

FIG. 32

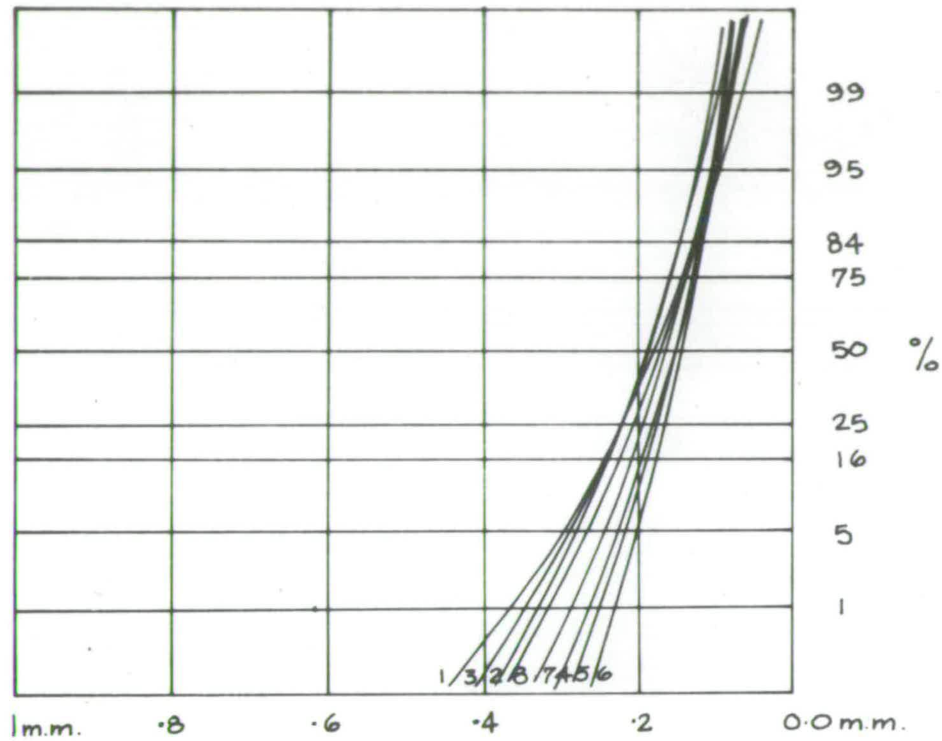

DISTRIBUTION OF SIZE FREQUENCY CURVES OF A BARRY COASTAL DUNE.

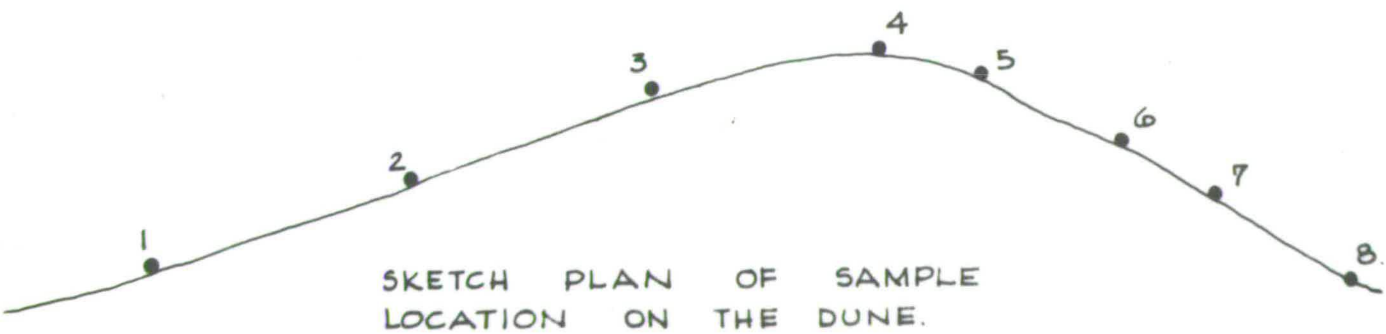

SKETCH PLAN OF SAMPLE LOCATION ON THE DUNE.

Many of the curves have almost symmetrical distribution with minor asymmetry in the tails especially in the zones less than 5% and more than 95%. But Inman (1952) has shown that most of the errors are confined to these zones (Plate 30); thus the most important part of the curve lies between 5th and 95th percentiles.

Distribution curves from the windward side of the dune have coarser tails while more fine material is found in the samples near the top and from the leeward side of the dunes. All these conditions can easily be attributed to the sorting action of the wind and its competency. The diagram (fig. 31) of dune sands shows the particles less than 170 microns have a very steep curve with a limited spread. This steep zone seems to be characteristic of dune sands and can be easily distinguished from the same zones of other environments. The dune sands have low content of fine material which must have been deposited when the wind velocity dropped to a calm. Most of the fine material is removed by the winnowing effect of the wind, which makes that end of the curve asymmetrical. This is one of the main reasons why most of the dune-sands have positive skewness values. The size range in the narrow zone less than 170 micron may be due to the limited competency of wind transportation.

In the Tentsmuir sands the minimum size (99th percentile) is

FIG. 33

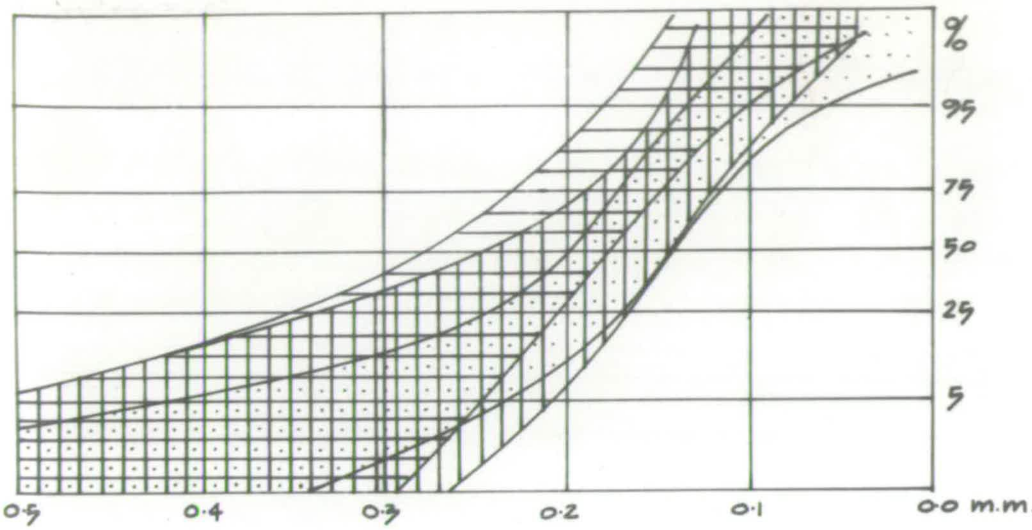

ZONE DIAGRAM SHOWING RELATIONSHIP BETWEEN TAYPORT, TENTSMUIR AND NORTHERN SANDS.

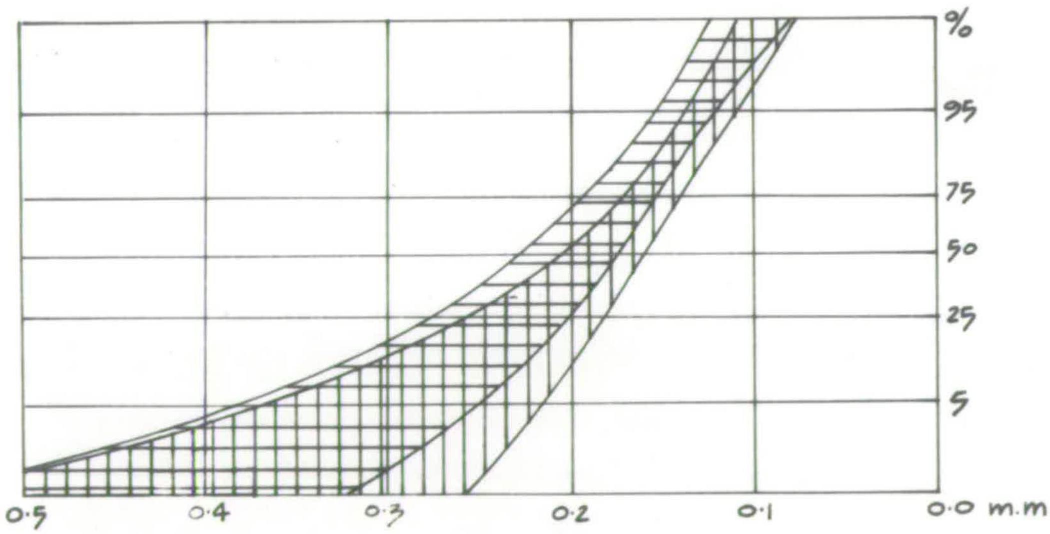

DUNE SANDS.

NORTHERN SANDS. TAYPORT SANDS. TENTSMUIR SANDS.

constant while the 1st percentile varies considerably, decreasing in the size from north to south. Northern dunes show similar considerable variations in the 1st percentile while slight variations are also seen in all other percentiles (fig. 30). Most of the percentiles show a decrease from east to west. The graphic and percentile diagrams show Tentsmuir sands finer than the Northern dune sands.

3.4 Statistical Analysis

It is convenient to have quantitative data for the evaluation and comparison of a large number of grain-size distributions. There are various statistical methods, used to describe size frequency distribution curves, but these fall into two main methods. One is of graphic parameters, plotting the size distribution curves and reading the size diameter against various percentages; the other method of moment measures involves elaborate calculations. The results obtained from these two methods are described and their significance assessed.

3.41 Graphic Parameters

In the present investigation the parameters suggested by Inman (1952) are used. These are probably the best set of parameters available at present. Recently Van Andel and Postma (1954) have shown the disadvantages of these parameters in bimodal distributions; but they are the best set of parameters for unimodal distributions with low and moderate skewness where they approximate to the statistical moment measures.

FIG. 34

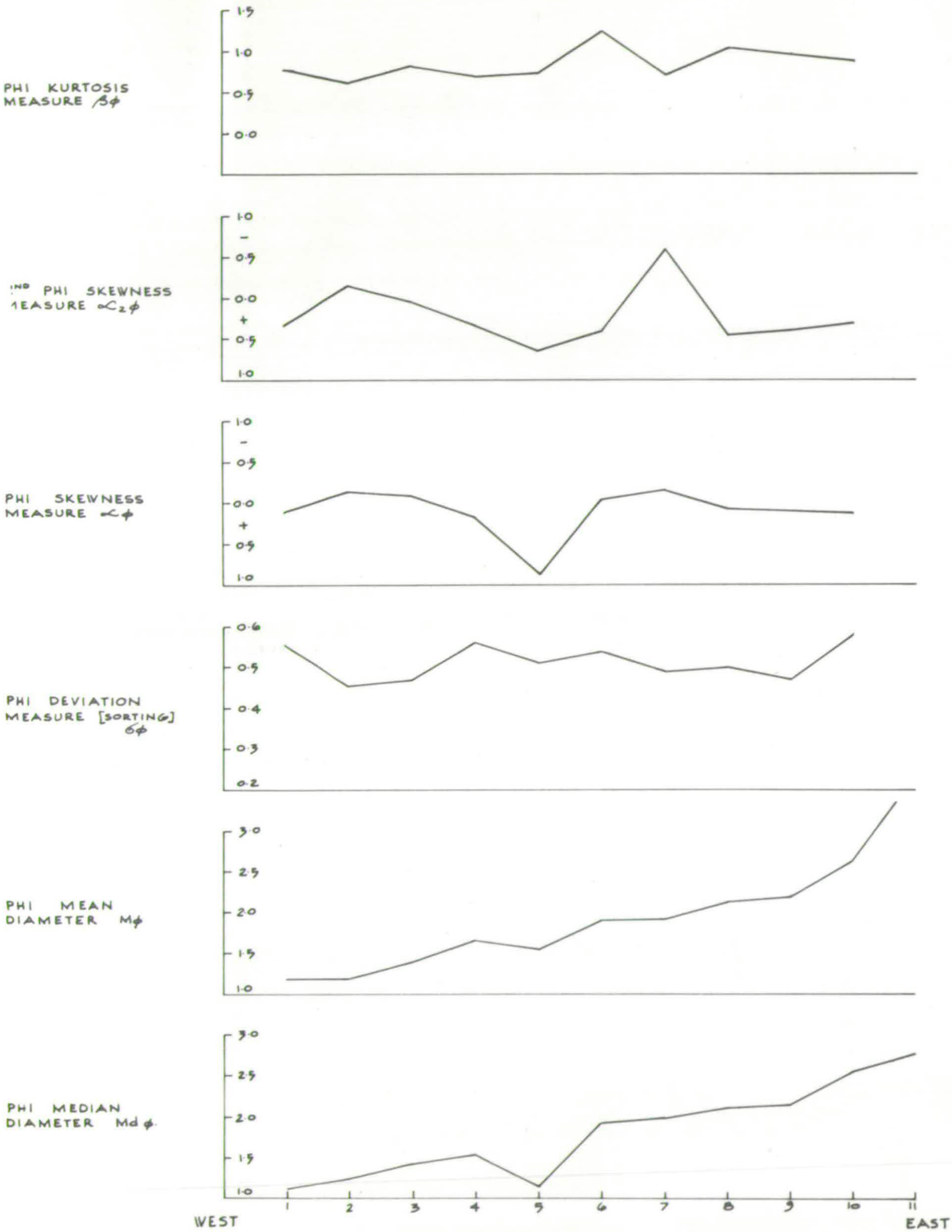

VARIATIONS OF GRAPHIC PARAMETERS ALONG RIVER AND ESTUARINE SANDS.

The Inman parameters are based on five percentile diameters obtained from the size frequency curve (plotted on the arithmetic-probability paper). The five percentile diameters used are 5, 16, 50, 84 and 95 and the parameters used are median diameter, mean diameter, sorting, kurtosis and the two measures of skewness, one of which is more sensitive to the skewed properties of the 'tails'.

Phi Median Diameter (Mdϕ)

This is the easiest measure to determine and corresponds to the 50th percentile in phi scale; half the particles by weight are coarser than the median, and the other half finer. The median is less affected by the extreme values of skewness as it is closer to the modal diameter. The disadvantage is that it does not reflect the overall size of the sediment especially in the skewed curves. It is almost useless for the bimodal distributions.

Phi Mean Diameter (Mϕ)

The phi mean diameter is the average of the 16th and 84th percentile diameters in phi units. The graphic mean is a good approximation to the mean moment measure for a large varieties of distributions. It is a better parameter of central tendency than the median as it covers a larger part of the curve and gives a better overall picture. The mean is more sensitive to the skew properties of the curve than the median and gives a better mean value (arithimetic mean) when the average of a group

FIG. 35

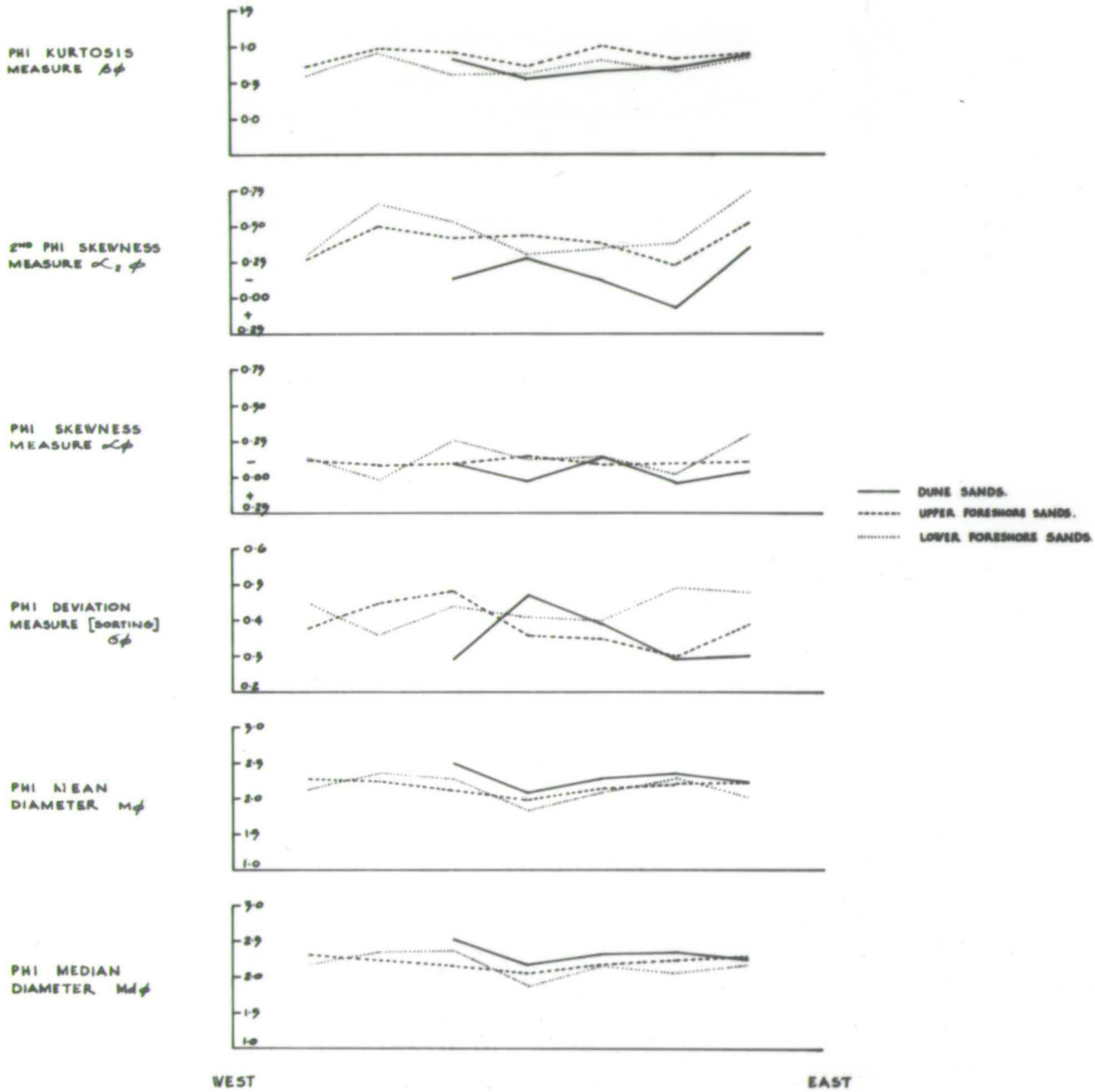

VARIATIONS OF THE GRAPHIC PARAMETERS ALONG NORTHERN SANDS.

of sample is taken; this is also true when a sample composed of several laminae of different grain sizes is analysed. For such a sample, the mean grain size of the total composite sample is equal to the average of the means of the individual laminae.

Phi Deviation Measure ($\sigma\phi$)

This is the measure (in phi units) of the uniformity or sorting of the sediments. It is also known as the graphic standard deviation (Folk, 1961) and it is defined as half the difference between ~~the arithimetic means of the~~ 16th and 84th percentile diameters (84 - 16) / 2. The measure is very close to the well known standard deviation but the two measures diverge with the increase in skewness.

Phi Skewness Measure

Size frequency curves may have the same mean and sorting but differ in their asymmetry. The phi skewness measure is defined as

$$\alpha\phi = \frac{1/2\,(\phi 16 + \phi 84) - Md\phi}{\sigma\phi} = \frac{M\phi - Md\phi}{\sigma\phi}$$

Skewness measures the departure of median from the mean, expressed as a fraction of the phi deviation measure. It measures the degree of asymmetry as well as the 'sign'; i. e., whether a curve has an asymmetrical tail towards fines (+ve value) or is skewed towards the coarse end (-ve value).

A secondary skewness measure is also used which is based on the 5th and 95th percentile diameter instead of 16th and 84th diameters as in

FIG. 36

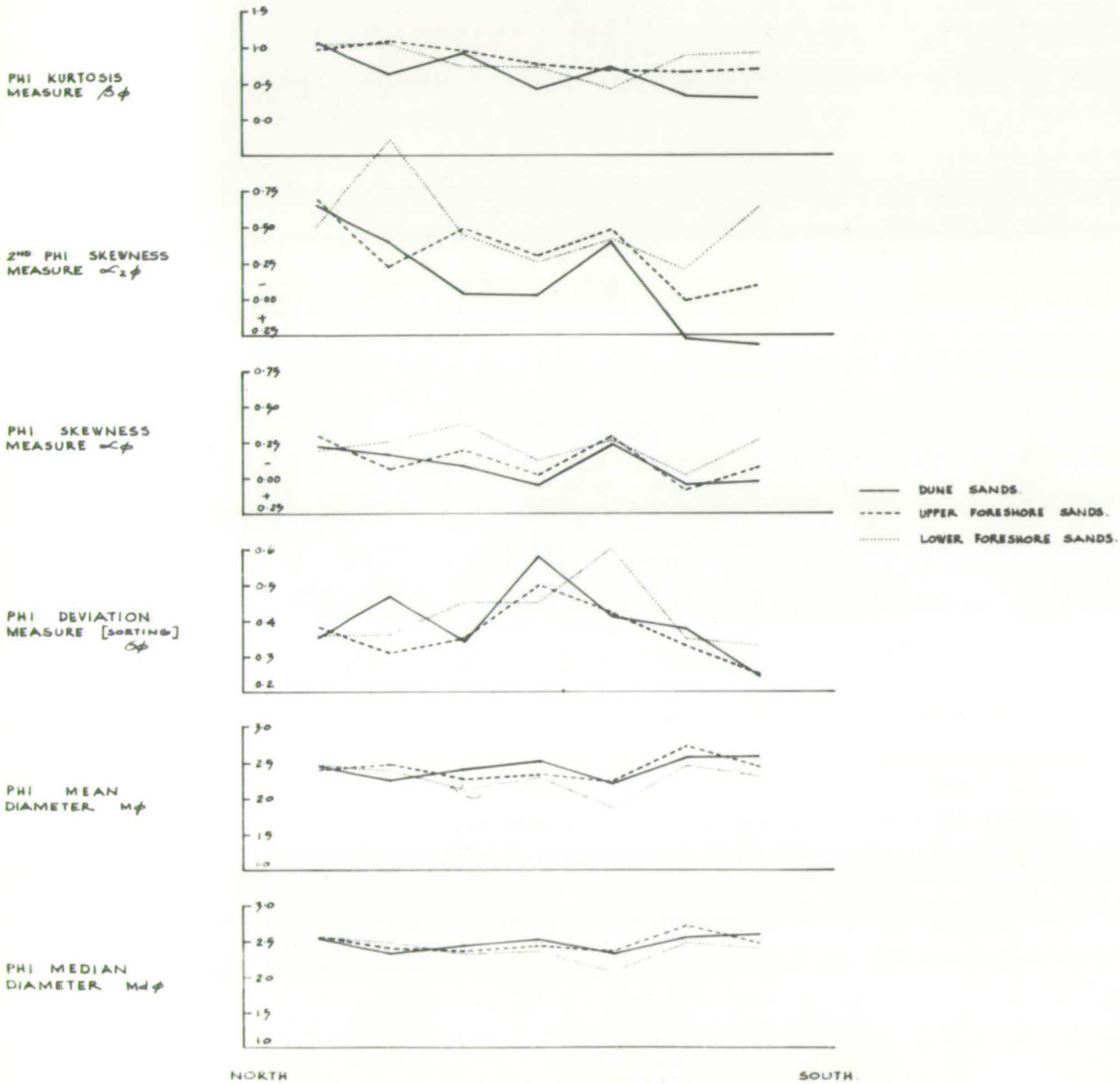

VARIATIONS OF THE GRAPHIC PARAMETERS ALONG TENTSMUIR SANDS

FIG. 37

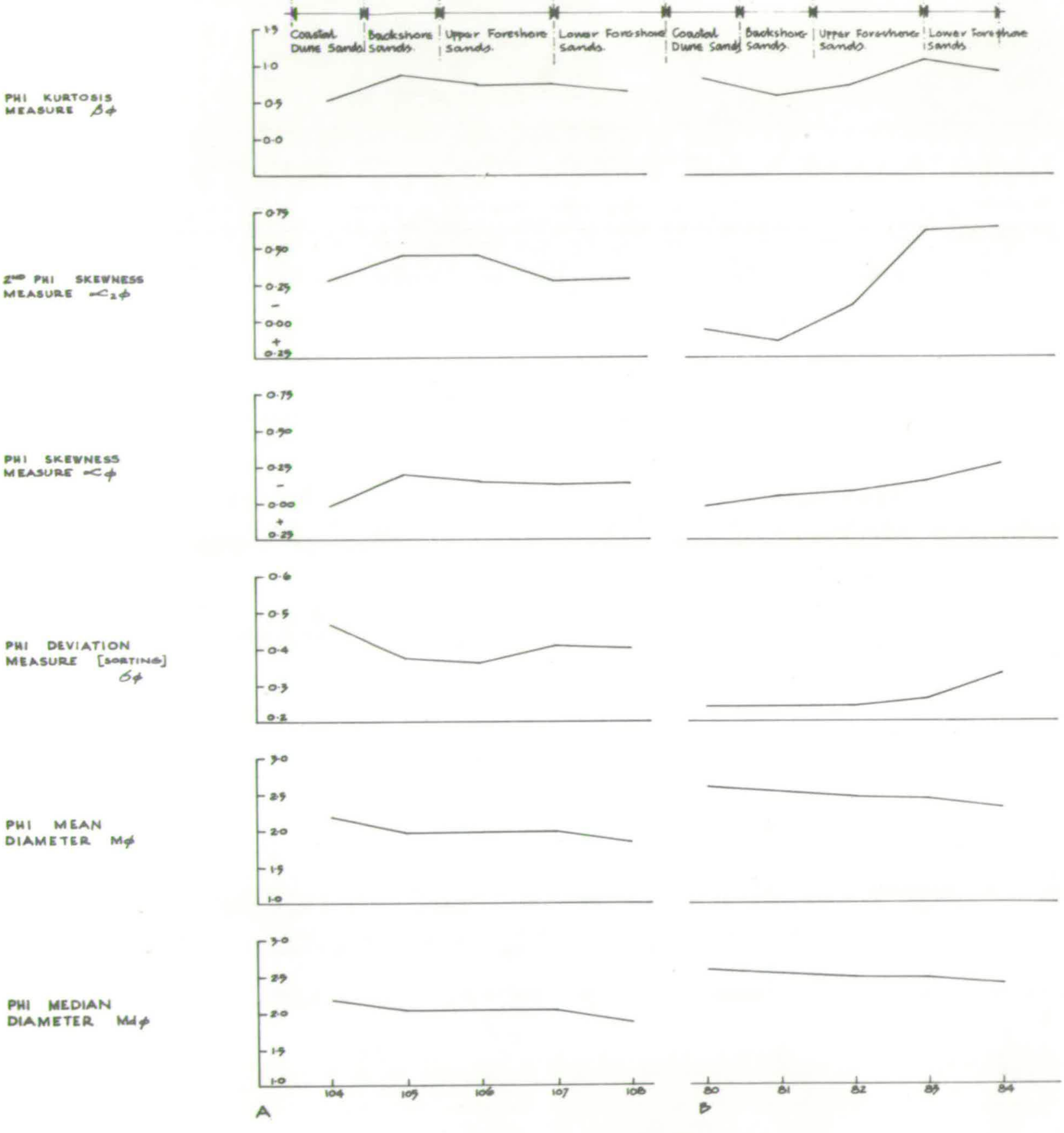

VARIATIONS OF GRAPHIC PARAMETERS FROM COASTAL DUNES TO LOWER FORESHORE SANDS. ILLUSTRATED FROM TWO TRAVERSES
A - NORTHERN SANDS. B - TENTSMUIR SANDS.

the primary phi skewness measure. This measure is more sensitive to the skewed properties of the 'tails' and covers a wider part of the distribution curve. Thus this measure is more useful where the skewed properties of tails are studied, while the primary skewness measure gives the skewed properties of the central 68% of the curve. Inman (1952) has shown the approximate relationship between the moment measure and the phi skewness measure where $\alpha_3 = 6\alpha\phi$.

Phi Kurtosis Measure

Kurtosis is a measure of peakedness and is related to the fourth moment of statistics. It measures the ratio between the sorting in the 'tails' of the curve and sorting in the central part of the curve. If the central part ($\phi 84$ to $\phi 16$) is better sorted than the tails, the curve is excessively peaked or 'leptokurtic'; while if the tails are better sorted than the central part, the curve is flat peaked or 'platykurtic'. Highly platykurtic curves are often bimodal. Phi Kurtosis value for a normal distribution is 0.65 (Inman, 1952). If the distribution is less peaked than the normal then the tails have a larger distribution and $\beta\phi$ is greater than 0.65. Similarly, values of less than 0.65 indicate that the distribution is more peaked than the normal.

3.42 Moment Measures

These are statistical measures in which computation is used and a truer picture of the grain size distribution is obtained. The first moment measure (mean), second moment measure (standard deviation), third moment measure (skewness) and the fourth moment measure (Kurtosis) of the grain size distribution were computed on the Atlas Computer for each of the samples. The computer program is based on the Atlas Autocode (Brooker and Rohl, 1963) and the programs are given in the Appendix VIII and IX.

Table 1 Showing the definitions of various moment measures

Statistical Name	Common Name	Equation
First moment measure	Mean (α_1)	$\bar{x}\phi = 1/100 \sum f m \phi$
Second moment measure	Standard deviation (α_2)	$[\sum f (m\phi - \bar{x}\phi)^2/100]^{1/2}$
Third moment measure	Skewness (α_3)	$(1/100)\alpha_2^{-3} \sum f (m\phi - \bar{x}\phi)^3$
Fourth moment	Kurtosis (α_4)	$(1/100)\alpha_2^{-4} \sum f (m\phi - \bar{x}\phi)^4$

where $\bar{x}$ = mean grain size in ϕ units

f = frequency of different grain size grades present as a percentage

and m = midpoint of each grain size grade in phi units

The results of the moment measure computation are given in Appendix II in a tabulated form.

3.43 Variance Analysis

Variance analysis was carried out on the size-distribution data from the area using the Atlas Computer (Appendix XI). This method was preferred to the 't' and 'chi-square' test because of its greater sensitivity. The variance ratio tests allowed for an estimate of significance of variance for the source, geographical locations and environments. Two levels of significance are used, based on Snedecor's tables (Fisher, 1948); first 5% level giving a significant difference ($P = 0.05$) and a second 1% level of significance ($P = 0.01$) giving very significant difference.

The first moment measure α_1 (mean) varies considerably (1.065ϕ - 3.245ϕ) over the area. The variance analysis has shown that the first moment measure does not show any significant variation due to possible direction of sediment transport. but shows a very significant variation due to geographical location and the environments. The variance is much higher between environments ($f = 4.898$) than within environments. The river sands have an average mean value 1.228 which shows a very significant ($P = 0.01$) difference from all the other environments. The estuarine sediments have a mean value of 2.739 Northern beach sands 2.117ϕ, Tayport sands 2.499ϕ and the Tentsmuir beach sands $2.372\ \phi$. Thus all these beach sands show significant variations ($P = 0.05$) from one another. All beach sands show significant variation from the dune sands; the dune sands have a much higher value of first moment measure (mean 2.364ϕ) than the beach sands (mean 2.324). In the beach sands there is a very significant decrease in the mean grain size towards the lower foreshore zone. The Northern sands are coarser than the Southern sands and show significant difference for both the beach and dune environments.

The distribution of second movement measure α_2 (standard deviation) does not show any significant variation due to direction of sediment transport as well as for the geographical locations. But the second moment measure shows a very significant (P = 0.01) difference between the environments. The dune sands are best sorted and have an average mean value of α_2 = 0.418 ϕ while the value for standard deviation decreases significantly towards the lower foreshore zone. The upper foreshore beach sands have an average standard deviation 0.427 ϕ and the lower foreshore beach sands an average value of 0.453 ϕ. The estuarine sediments have an average value of 0.542 ϕ while the river sediments have 0.836 ϕ, the highest mean value between all these categories. In a normal distribution of Pearson type III curves (Inman, 1952; Fig. 7) the standard deviation is 0.50 ϕ and so in the present discussion, standard deviation value 0.50 will be taken to denote a near symmetrical/symmetrical distribution.

There is a considerable variation in the values of third moment measure α_3 (Skewness) in the area (see Appendix II). The variance analysis shows no significant variation due to possible direction of transport but shows very significant (P = 0.01) variations due to geographical locations and environments. The river sands have a mean value of

FIG. 38

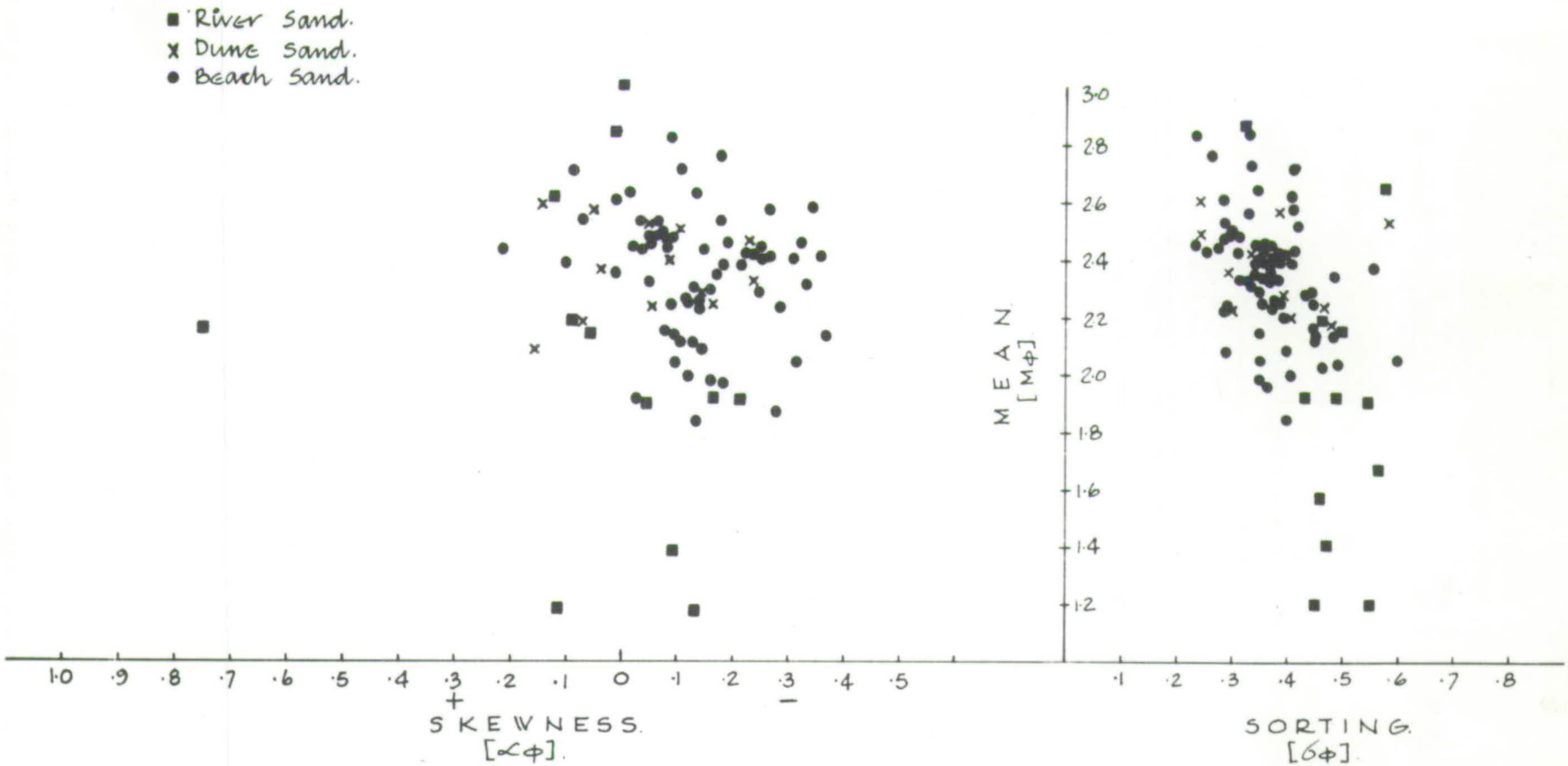

COMPARISON OF MEAN [Mφ], SKEWNESS [αφ] AND SORTING [σφ] OF INDIVIDUAL SAMPLES OF RIVER, DUNE AND BEACH SANDS.

+0.421 while the estuarine sands show the lowest -ve value of -0.061 for the mixed curve types and an average of -0.562 for all the samples. The dune sands have near symmetrical distributions (-0.146) and the beach sands -0.518. Usually there is a gradual increase in negative skewness towards the low tidal zones.

The moment coefficient of Kurtosis (α_4) does not show any significant difference due to any of the factors involved in the variance analysis. For the normal distribution the moment coefficient of kurtosis value is 3; the values more than 3 denotes leptokurtic distributions and the values less than 3 denotes platykurtic distribution. Appendix II shows that a great majority of samples show leptokurtic distributions.

The average value of phi mean diameter ($M\phi$) of all the samples in the area is 2.482 ϕ. River, estuarine, beach and coastal dune sands all differ from each other very significantly (P = 0.01) with mean value of 1.391ϕ, 2.718 ϕ, 2.356ϕ and 2.408 respectively. The variance of the mean due to location of the samples from one another is also significant (P = 0.5), while no significant variation exists due to possible direction of sediment source. There is a gradual increase in the mean size towards the low tide region; the upper foreshore has an average $M\phi$ of 2.412 and the lower foreshore 2.389ϕ.

There is a considerable variation in the phi median diameter ($Md\phi$) value in the area, the mean value being 2.427ϕ. River, estuarine, beach and coastal dune sands all show very significant (P = 0.01) difference

FIG. 39

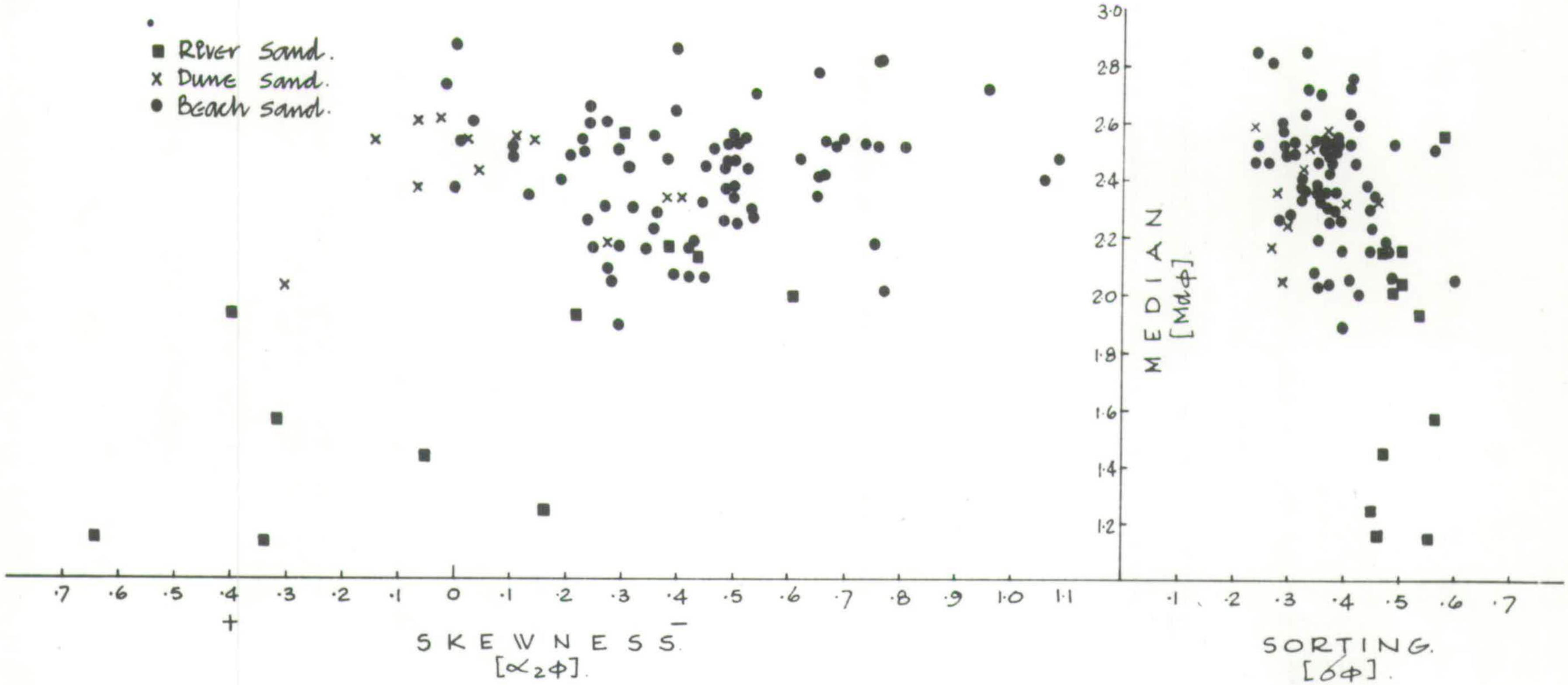

COMPARISON OF MEDIAN [MdΦ], SECOND SKEWNESS MEASURE [$\alpha_2\Phi$] AND SORTING [σΦ] OF INDIVIDUAL SAMPLES OF RIVER, DUNE AND BEACH SANDS.

FIG. 40

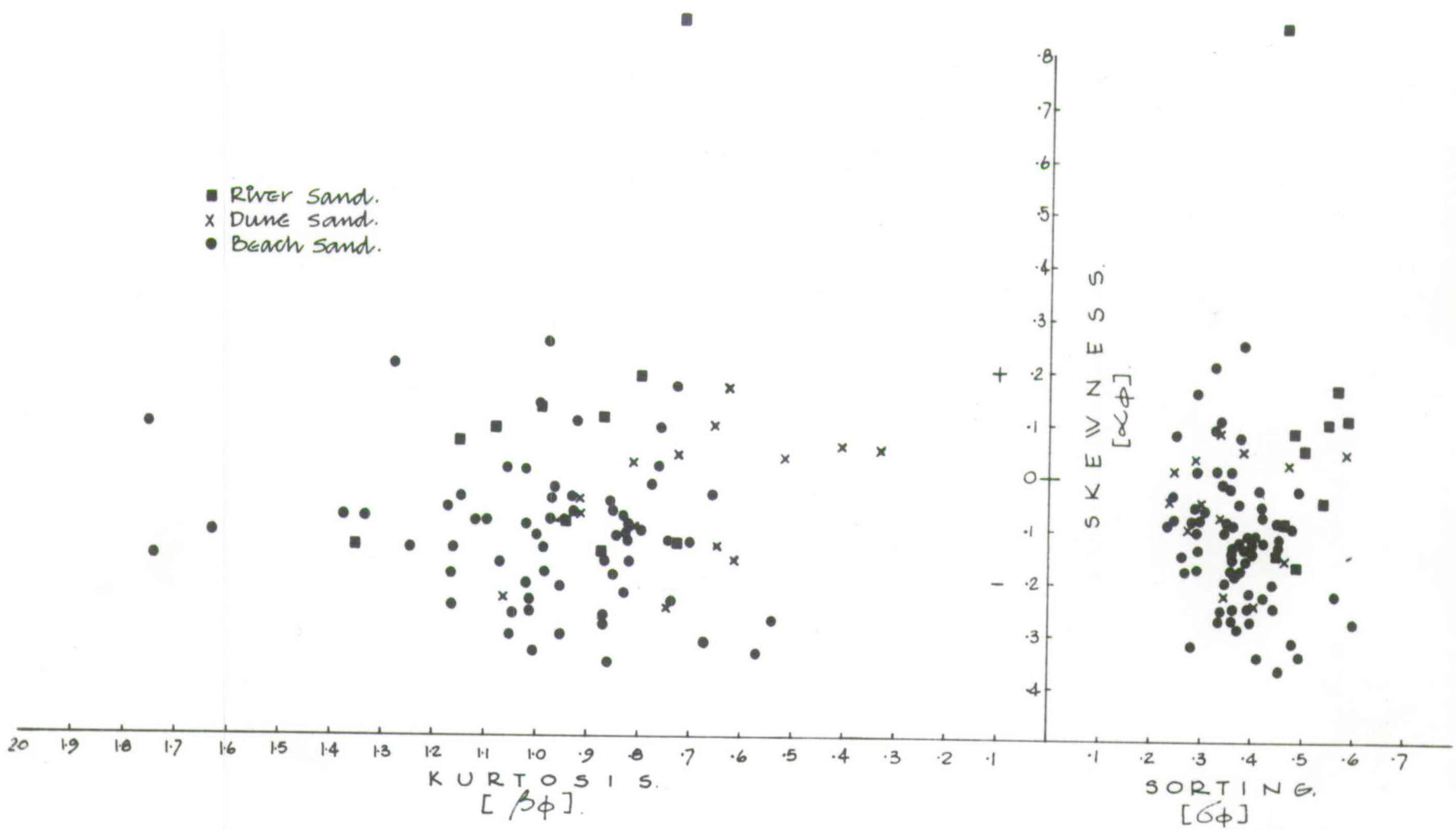

COMPARISON OF SKEWNESS [∝ϕ], KURTOSIS [βϕ] AND SORTING [σϕ] OF INDIVIDUAL SAMPLES OF RIVER, DUNE AND BEACH SANDS.

with Mdϕ values of 1.321, 2.630, 2.346 and 2.385 respectively. The variance of Mdϕ due to location of the samples is also significant ($P = 0.05$) while no significant difference exists due to the source of sediment transport. The upper foreshore beach sands (mean Mdϕ 2.369) differ significantly from the lower foreshore sands (mean Mdϕ 2.333) as the medium grain size decreases towards the low tide zone.

Phi sorting ($\sigma\phi$) shows very significant variations due to environments and significant variations due to geographical location in few cases. The distribution pattern of various graphic parameters are given in the Figs. 34 to 37 for the various sub-areas.

The variance analysis of the skewness and phi kurtosis does not show any significant variations due to any of the three major factors used in the analysis. The following table shows the summary of statistical parameters and the results of variance analysis on various level of significance.

Table 2

Table showing Relationship between Statistical Parameter and Significance of Variance due to :-

1. Direction of Transport
2. Geographical location and
3. Environments

Statistical Parameters	Variance due to	Level of Significance		
		Very Significant (P=0.01)	Significant (P=0.05)	Not Significant
First Moment Measure	1			X
	2	X		
	3	X		
Second Moment Measure	1			X
	2			X
	3	X		
Third Moment Measure	1			X
	2	X		
	3	X		
Fourth Moment Measure	1			X
	2			X
	3			X
Phi Means Diameter	1			X
	2	X		
	3	X		
Phi Median Diameter	1			X
	2		X	
	3	X		
Phi Deviation Measure	1			X
	2		X	
	3	X		
Phi Skewness Measure	1			X
	2			X
	3		X	

Statistical Parameters	Variance due to	Level of Significance: Very Significant (P=0.01)	Significant (P=0.05)	Not Significant
Phi Secondary Skewness Measure	1			X
	2			X
	3		X	
Phi Kurtosis	1			X
	2			X
	3			X

3.5 <u>Distribution Curves and Graphic Parameters</u>

The F-type distribution curves have the median ranging between 1.13ϕ - 1.56ϕ with a gradual increase in the median value towards the estuary. The value of mean ($M\phi$) differs from 1.18ϕ to 1.66ϕ while the sorting varies between 0.45 to 0.98. The skewness ($\alpha\phi$) varies considerably from +0.85 to -0.13 thus showing the sensitiveness of the measure; the 'tails' of the distribution do not show any significant difference ($\alpha\phi_2$ varies from +0.64 to -0.16) from the central parts of the curves. The F- curves are mesokurtic (0.62 - 0.84) and show near symmetrical distribution. Most of the curves have lost the fine material by removal in suspension and thus most of sediments showing F- type curves are probably derived from the bottom load of the river.

The M- type distribution curves are usually of M_1- and M_2- type with predominance of the former type. The phi- median shows a considerable variation from 1.89ϕ to 2.82ϕ and the mean from 1.84ϕ to 2.77ϕ.

These M- type distribution curves are mostly from the beach sands and show a significant increase in mean/median towards the upper foreshores. These curve types are better sorted than the F-types with the same average size. Sorting varies between 0.24 to 0.58 and shows better sorting with the increase in the median-value. The sorting decreases with the increase in the silt/clay fraction as inside the estuary. Due to the turbulent action of the breaking waves on a beach, the sorting is improved by repeated reworking (local sorting). With depth, the turbulence decreases, material of many grades can be deposited and sorting decreases (see also Inman, 1949, 1952; Shepard, 1964). M- type curves from the dunes show very well sorted distribution while the curves from the estuary show moderate sorting values. There is a considerable variation in the skewness; values from +0.25 to -0.37 are quite common. The 'tails' of the curves are far more skewed than the central parts of the curves, thus giving leptokurtic values. Most of the dune curves are positively skewed where the fines less than 0.125 mm (3 ϕ) are removed by the prevailing winds. In the lower foreshore sands, the curves give considerable negative skewness values due to the influx of coarse materials by the seasonal high tides; this influx has slightly modified the symmetrical shape of the curves towards the coarse end. Highly negatively skewed curves of M - type have been described by Muir (1958) as B M - type; the prefix B indicating presence of coarse material. In most of the samples this coarse fraction consists of shell debris which can be easily transported to higher parts of the beach due to its smaller specific gravity.

Mixed distribution curves (FM) are quite frequent in the estuarine environment. The median varies from 1.92 ϕ to 3.38 ϕ and the mean 1.90 ϕ to 4.08 ϕ. This considerable variation in the size of the central tendency is due to the mixing of the two components F. and M. in various proportions. This is a common phenomenon and has been dealt with in great details by Doeglas (1941, 1944, 1950). The sorting also varies considerably (0.47 ϕ - 2.08 ϕ) due to variations in depth, currents, sediment types and higher proportion of silt fraction. Usually with the higher content of particles of more than 4 ϕ, there is a decrease in the sorting (Van Andel and Postma, 1954). Both phi skewness measures vary considerably, $\alpha\phi$ (+0.64 - -0.16) and $\alpha\phi_2$ (+0.43 - -0.60). This may be due to a greater difference of grain size and this also gives higher values of kurtosis (0.72 - 1.25), most of the curves being leptokurtic.

The MS - type of distribution curves shows trends similar to those of the other mixed type (FM). They have higher median values (2.51 - 3.50) and mean from 2.35 ϕ to 3.15 ϕ. The maximum amount of fraction greater than 4 ϕ is 33% while the average value is 16%. The sorting range from σ 0.49 to 0.84 and a few samples have a much higher value but could not be computed precisely due to excess of fines. Most of the curves are leptokurtic with a few platykurtic (bimodal) distributions. The skewness $\alpha\phi$ varies between +0.02 - -0.34 and $\alpha\phi_2$ 0.0 to -0.77. The MS- type sands are deposited in the quieter parts of the estuary, especially in the marshes. The Fine fraction is concentrated due to the absence of strong wave action and reworking currents.

The distribution curve types F, M, and their mixtures FM and MS represent the river, beach and estuarine environments in the area. The river sands may be recognised by their curves associated with low values of mean, median, moderate to poor sorting, near symmetrical to positive skewness and meso - to leptokurtic distributions. The estuarine sediments show an assemblage of FM, FS and M- type distribution curves with fairly high to moderate value of mean and median, moderate to poor value of sorting, leptokurtic to very leptokurtic curves. The amount of silt/clay fraction is more than the average M curve. The beach sands have more or less symmetrical M distribution curves with medium to medium fine sand grades, moderate value of mean and median and well sorted to moderately sorted sands. They have negative skewness and mesokurtic to leptokurtic distribution. In the coastal dune environment the distribution curves have M- type shape with mostly positively skewed tail. The curves are very straight from 2 ϕ towards the fine end. These different environments can be distinguished to certain degree by using the distribution curves and graphic parameters (see scatter plots Figs. 38-40).

FIG. 41

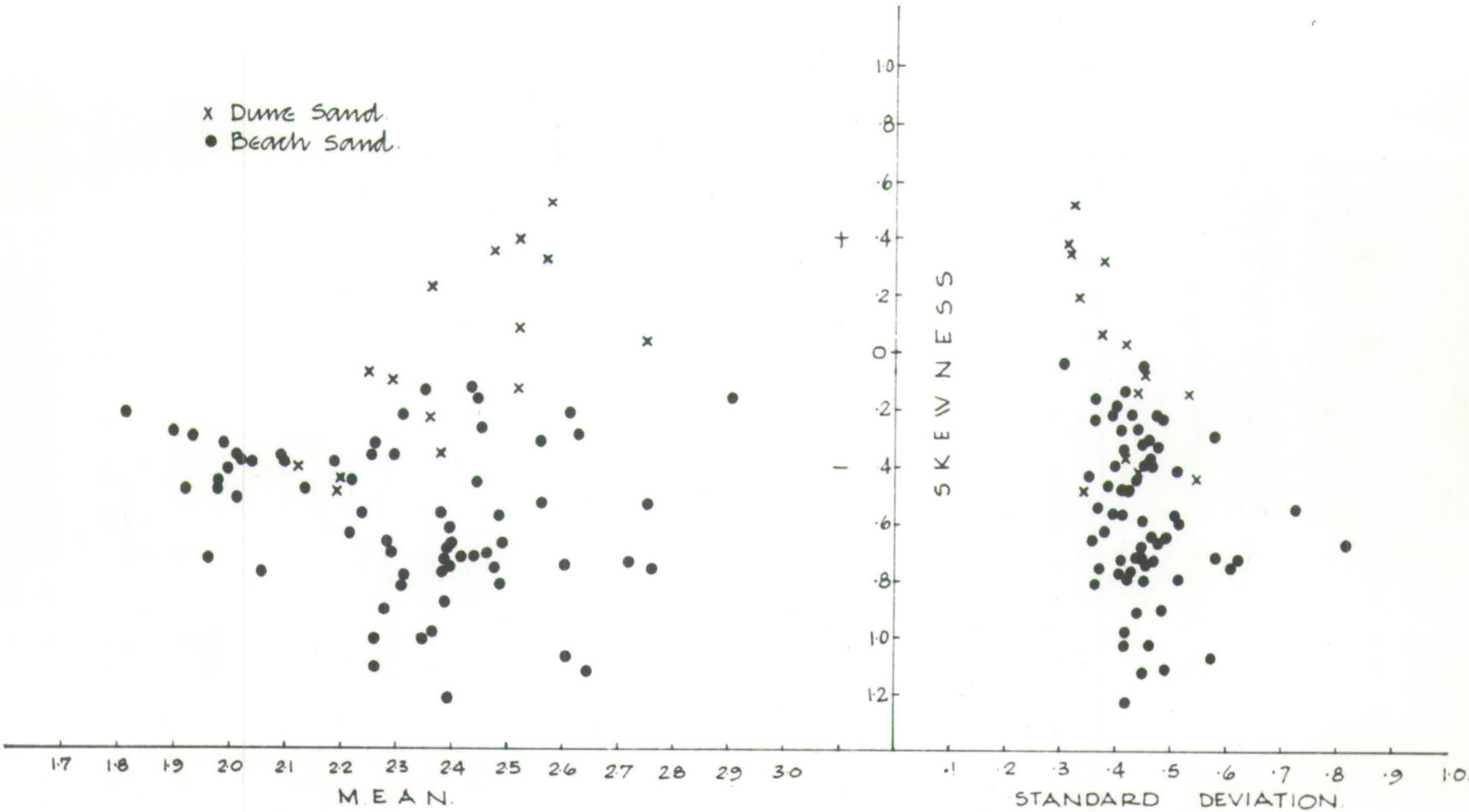

PLOT OF FIRST MOMENT [MEAN], SECOND MOMENT [STANDARD DEVIATION], AND THIRD MOMENT [SKEWNESS], FOR BEACH AND DUNE SANDS. IN PHI SCALE.

3.6 Moment Measures and the Environments

The moment measures are plotted against each other on scatter plots to distinguish their relationship with the various environments (Figs. 41-43).

In the Fig. 41 the first moment measure (mean) is plotted against the third moment measure (skewness) for the data in phi scale. There is nearly a complete separation between the dune and beach sands. The dunes being mostly positively skewed or with near symmetrical distribution and the beach sands are generally negatively skewed. A few of the beach sands have positive skewness which may be due to the possible "inherited" property of the original positive skewed river sands which have not yet reached equilibrium in the new environment. Similar separated scatter zones were observed by Friedman (1961) in his textu-ural studies on different environments.

The Fourth moment measure (Kurtosis) does show little sensitiveness towards the environments (Fig. 42). Both dune and beach environments can be separated to a certain extent, with a wider spread, then a scatter plot of the skewness against mean. Both river and dune sands are mostly positively skewed and with a few exceptions shows sensitivity of skewness.

In Fig. 41 the second and the third moment measures are plotted for the beach and dune sands; both the environments can not be separated as there is quite a lot of overlap in the scatter plots.

FIG. 42

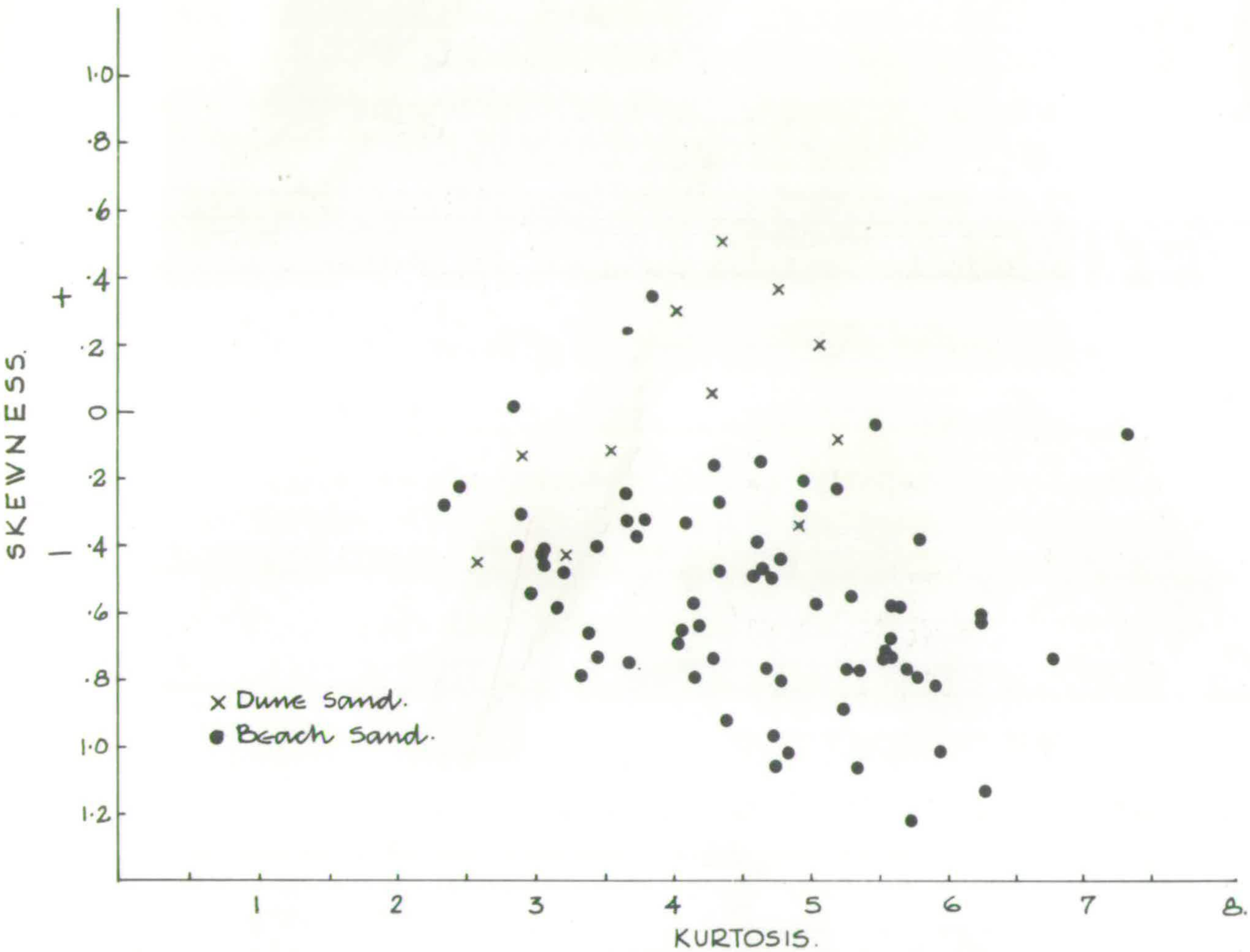

SCATTER PLOT OF THIRD MOMENT [SKEWNESS] AND FOURTH MOMENT [KURTOSIS], USING PHI SCALE.

Similar trend for these two environments is observed in the plot of first moment measure (mean) and the second moment measure (standard deviation). On the other hand this plot can separate river sands from the beach and dune sands (Fig. 43).

The moment measures reflect the mode of transporting medium and the energy distribution in the medium. The size limits of the particle size carried in suspension or by saltation are governed by the competency of the medium. Aeolian and fluvial transportation is due to the uni-directional flow and is one of the major factors in causing the positive skewness in these two environments. On the beaches, the material is subjected to swash and backwash currents which winnow out fine material and the material from any normal distribution becomes negatively skewed.

The following conclusions can be made from the study of moment measures of the Tay sediments:

i) The dune and beach sands can be distinguished on the basis of plots of first and the third moments.

ii) The river sands may be separated from the beach and dune sands by the first and second moment plots

iii) The river and dune sands may be separated from the beach sands by the second and third moments plots.

iv) The fourth moment is not very sensitive to environment and can only separate dune and river sands from the beach sands.

FIG. 43

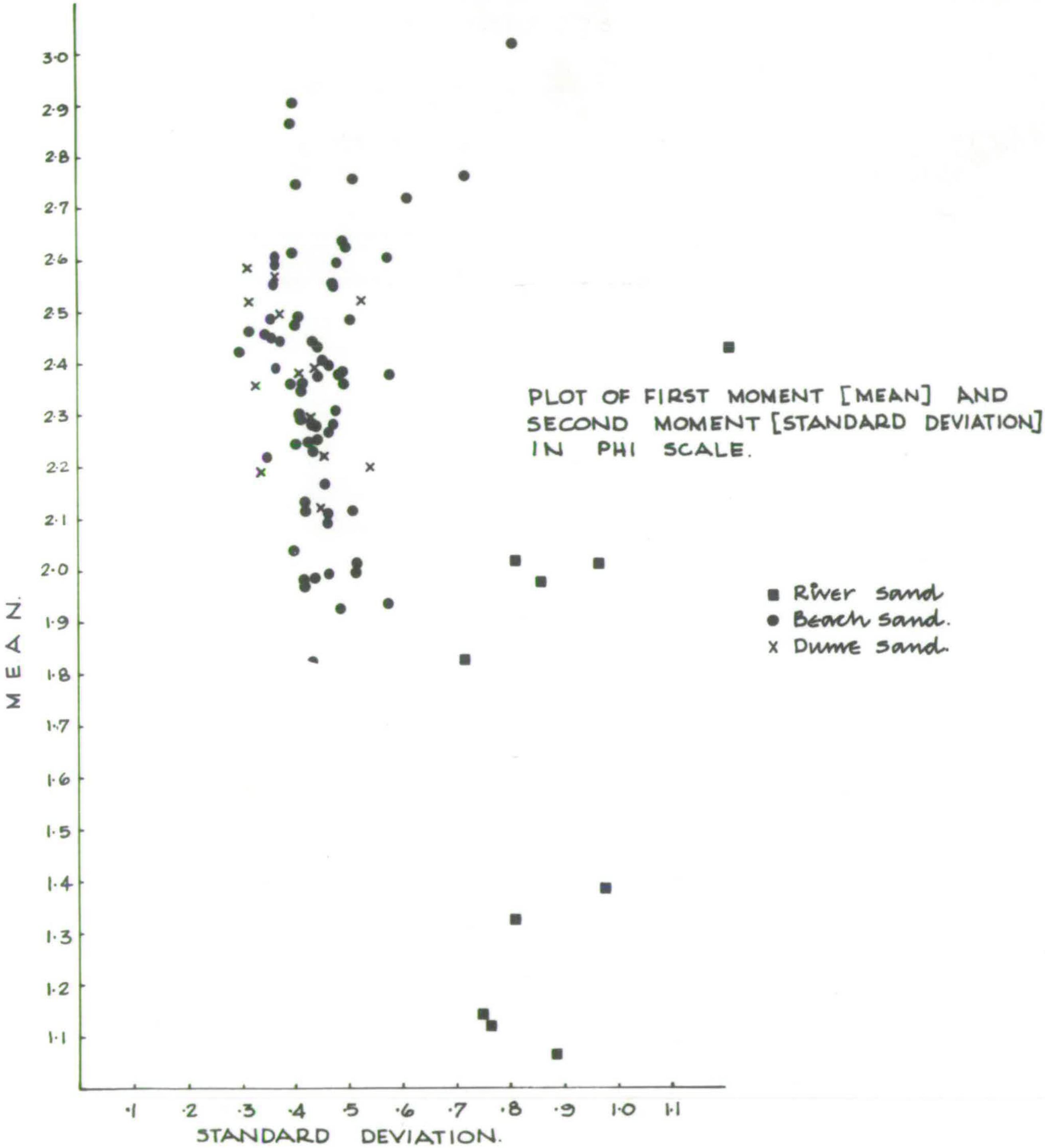

3·0
2·9
2·8
2·7
2·6
2·5
2·4
2·3
2·2
2·1
2·0
1·9
1·8
1·7
1·6
1·5
1·4
1·3
1·2
1·1
MEAN.
·1
·2
·3
·4
·5
·6
·7
·8
·9
1·0
1·1
STANDARD DEVIATION.
PLOT OF FIRST MOMENT [MEAN] AND SECOND MOMENT [STANDARD DEVIATION] IN PHI SCALE.
■ River sand
● Beach sand.
x Dune sand.

v) Dune sands are relatively better sorted than the beach sands. In the beach sands the sorting decreases towards the low water mark i.e. depth of water.

vi) Dune and river sands cannot be distinguished clearly from each other on the basis of moment measures alone. Both show positive skewed value but relatively the dune sands are finer than the river sand in the grain size. Additional data help to distinguish between the two i.e., heavy mineral content, shape of distribution curves, etc.

vii) Estuarine sands with mixed curve types are difficult to separate by scatter plots only. They require additional data about the shape of the distribution curve to separate them from the other.

viii) In the open-ended distributions, the moment measures are of no significance. In this case better results are obtained by the use of graphic parameters which give better approximation of the statistical parameters.

3.7 Moment measures and Graphic Parameters.

The moment measures of a size frequency distribution gives the most accurate data on the behaviour of the distribution (except in the open ended distribution). These moment measures are not commonly favoured as they take considerable time and are difficult to compute. Due to these two main objections against the moment measures, various graphic measures are used.

McCammon (1962) has shown the efficiencies of various graphic measures as more percentile data are used for the computation of any particular graphic measures. The statistical efficiency of a graphic measure is the ratio of the variance of the distribution of the corresponding efficient estimate and the variance of the limiting distribution of the graphic measure. The more percentile data are used in a graphic measure, ~~the higher~~ it will be nearer to the statistical moment measure (Mosteller, 1946; Wilks, 1948; Blom, 1958; Sahu, 1964). Graphic measures are nearest to the moment measures in a symmetrical distribution but normally they do show significant difference (P=0.05). McCammon (1962) has shown that the efficiency of the Inman graphic measures is, for the phi mean diameter 74% and 54% for the phi deviation measure (sorting). The mean diameter ($M\phi$) is always significantly higher than the first moment measure (α_1) for the same distribution (see Appendix I and II). Similarly, other graphic measures used in the text show considerable variations from the corresponding moment measures. A better approximation is obtained only in a few cases with near symmetrical distribution (α_3 between +0.2 and -0.2).

The Inman graphic measures used in the present investigation are of little help in distinguishing the sediments from various environments in the Tay region. The scatter plots (Figs. 38-40) show too much overlap between the various environments except perhaps the positive values of skewness shown by most of the dune and river sands. Moment measures give a far better result for the environmental studies and variance analysis. Thus usually the graphic measure may only be useful for giving a general approximate trend of the size distribution and areal variations.

Sediments in the different environments may be recognised by the following size distribution characteristics:

1. River sediments can be recognised by their F- type distribution curves with common positive skewness. They can be separated from the beach sands by the skewness - mean scatter plots. River sands can be distinguished from the dune sands on the basis of their shape of the distribution curves.

2. The estuarine sediments may be recognised by the presence of mixed curve types and higher than average content of silt/clay fraction. They can also be separated from the beach and dune sands from the triangular plot of proportion of medium, fine and very fine sand fraction. The statistical measures in most of the cases and distribution curves in a few cases are of little use for thisenvironment due to considerable overlapping of the river and marine sediment types.

3. Dune sands can be recognised easily from the river sediments on the basis of the shape of the curve and from the beach sands by mean - skewness plots of moment measures.

4. Beach sands may be separated from the river sands by the shape of the distribution curves and the skewness - standard deviation plots. Scatter diagrams of the skewness and the mean can separate the beach and dune sands.

3.8 Relationship between roundness of grains and environments.

There is a large amount of literature available for determining roundness. In the present investigation the visual estimation method of Shepard and Young (1961) was used. In all the cases 2 ϕ to 4 ϕ fraction was used as this fraction constitutes a large proportion of the dune sands. Beach sands were compared with the adjacent dune sands. A count of 100 grains was made,based on the six classes of roundness (Plate 34); by the point counting method commonly used in the heavy mineral analysis. The chi- square tests does not show any significant difference between the adjacent beach and dune sands. This may be due to prevailing off-shore winds in the area. Both the environments have sub-angular to sub-rounded grains. The estuarine and river sands have angular to sub-angular grains and these show significant difference (P = 0.02 - 0.05) from the beach and dune sands.

Section 4. HEAVY MINERAL STUDIES

4.1 Laboratory technique

Study of the sample fraction retained on the 0.5mm sieve by bionocular microscope revealed the absence of any appreciable number of heavy mineral grains. So the material retained on the 0.5mm sieve was rejected and the rest of the sample was split by a rotary splitter. It was found that approximately 10 grams of sample gave the most consistent results and this amount was used for each sample analysed.

There was no necessity for the disaggregation and clarification of grains. The heavy minerals were separated by introducing approximately 10 grams of sample into 150 ml. of bromoform in a 250 ml. pear-shaped separating funnel and stirring at five-minute intervals over a period of one hour. The heavy minerals were collected, washed with water to remove bromoform and oven dried. The bromoform was collected by filtration under reduced pressure; the water being immiscible with bromoform is readily separated by the use of another funnel. The specific gravity of the bromoform was repeatedly checked by a Blake type bromoform hydrometer. Complete separation of water from the bromoform can be achieved by filtering the bromoform through a thick pad of filter papers under reduced pressure. This operation takes very little time and about 98% of the bromoform can be recovered.

In the case of silty sands, the separation was carried out with the use of a centrifuge which accelerates separation of the heavy minerals.

The centrifuge method gives a rapid and efficient separation of grains smaller than 0.125 mm and was very useful for the fractional mineral analysis. When a separation failed to yield a mineral crop of more than 300 non-opaque grains; it was rejected. Normally the entire mineral crop was mounted except when it was too large. Large crops of heavy minerals obtained were split by a Otto (1937) type microsplit and approximately 1000 grains were mounted in Canada balsam. To test the satisfactory work of the microsplit, a series of counts of splits from an original sample was taken. The values obtained by various splits remained within the 2% limit of counting error.

The heavy minerals were identified and counted by means of a mechanical stage and point counter. The line-counting method was used as it has many advantages over the other methods in which all the grains in a number of fields of view are counted (Doeglas, 1940; Van Andel, 1950). In the slides 300 grains were identified; the alterites (Edelman, 1933) were noted but not included in the count of 300. The proportion of alterites was expressed as a percentage of heavy mineral counts. The accuracy of a count can be calculated statistically (Dryden, 1931; Muller, 1943). Three hundred grains were identified and counted, as Dryden (1931) has shown that the accuracy increases rapidly with more grains counted till a number of 300 is reached. Counting more grains gives a relatively small increase in accuracy. In the Appendix VI the results of the counts respectively of various numbers are given. The variation is large for the minerals with higher percentages, but rarely exceeds 3%. In most of the cases, the count of 100 grains itself gives results slightly different from that obtained from 300 grain counts with an error of 5%. In practice, an absolute error of 5% for the higher percentage is perfectly admissible (Van Andel, 1950), but for the sake of consistency 300 grains were counted.

4.2 Mineral variations

The mineralogical composition of a single association may vary considerably due to true variations within the association and operator variance (of sampling and analysing). To a certain extent these variations and the significance of variance can be tested by statistical methods. In the present investigation, statistical methods have given useful results (cf. Rittenhouse, 1943). The variance in mineral species can easily be ascribed to three main factors; source material, the transporting medium and the conditions at the place of deposition. The last two factors can effectively segregate minerals of different shape, size and specific gravity, but rarely produce any large scale variations. A minor change in the source may not be detected but it is unlikely that any major change will not show in the proportion of mineral species, especially the different varieties of some minerals, i.e., zircon, rutile, tourmaline, hornblende, etc. The relative influence of size and specific gravity is not yet agreed; Rubey (1933) took specific gravity to be the main

FIG. 44

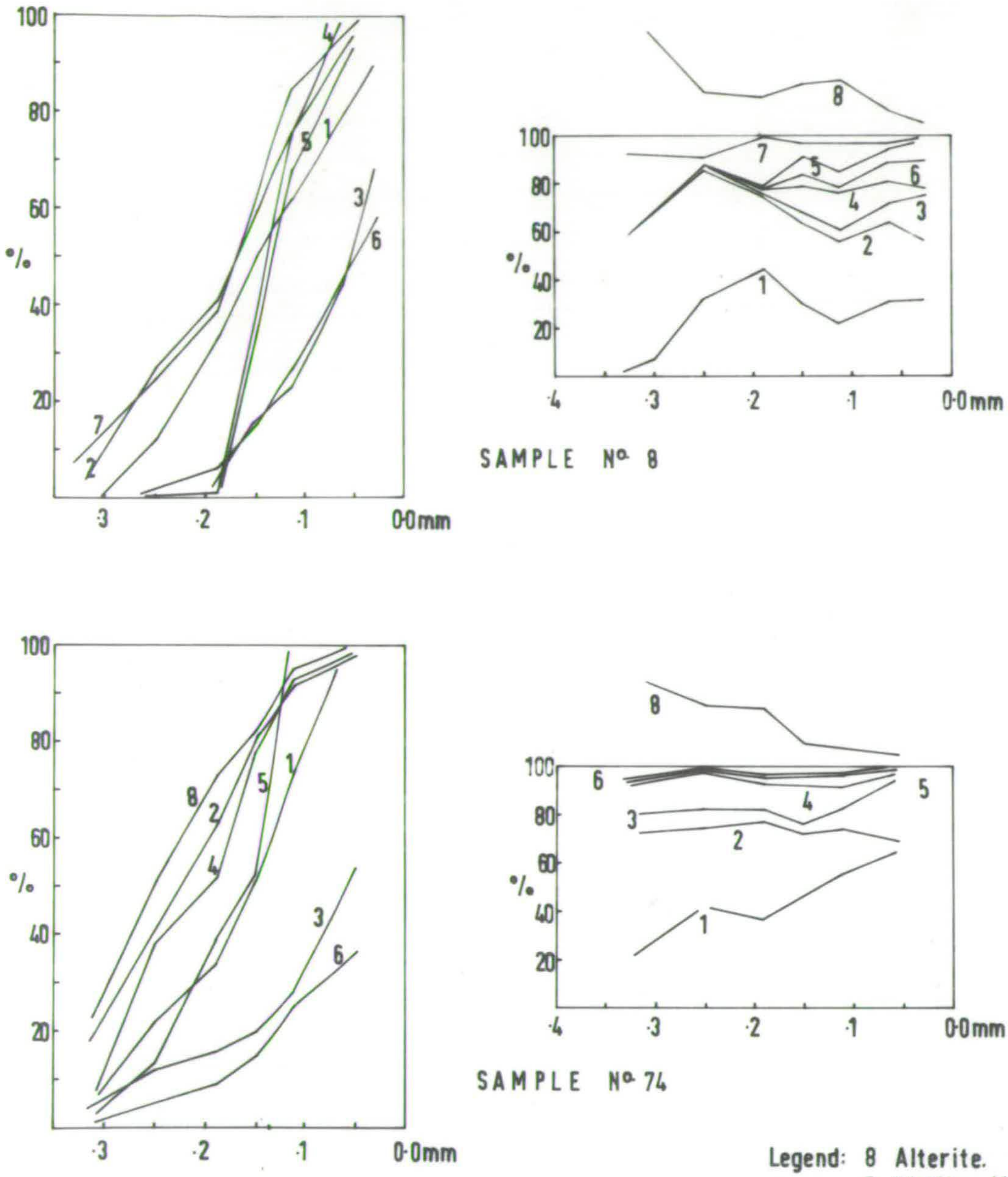

MINERALOGICAL FRACTION ANALYSES.
HORIZ.: SIZE GRADE; VERTIC.: CUMULATIVE
MINERAL NUMBER PERCENTAGES.

Legend:
8 Alterite.
7 Biotite-Muscovite.
6 Zircon-Rutile.
5 Hypersthene.
4 Epidote.
3 Magnetite-Ilmenite.
2 Hornblende.
1 Garnet.

FIG. 45

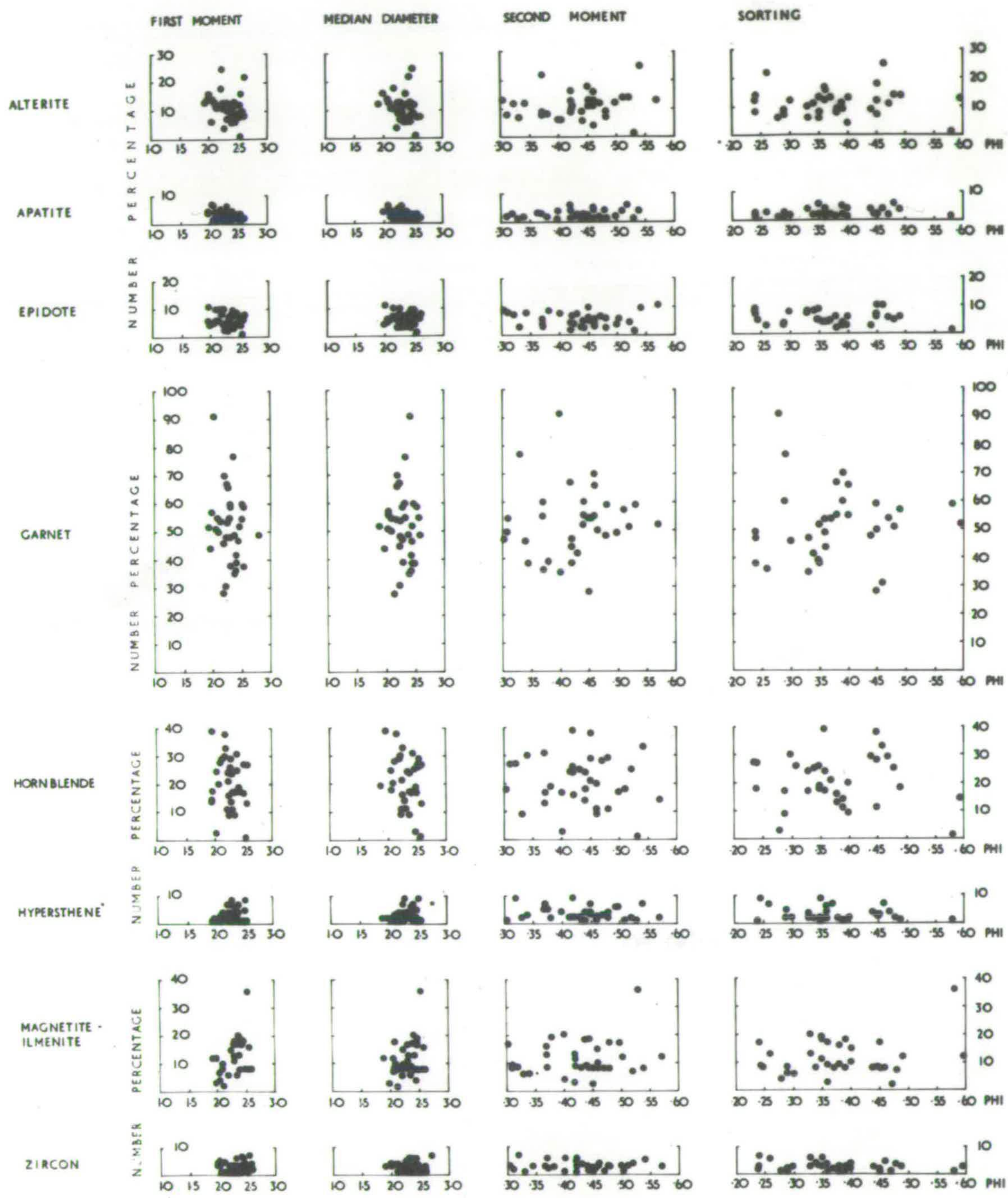

RELATION BETWEEN A FEW FREQUENT HEAVY MINERALS AND FIRST MOMENT [MEAN] MEDIAN DIAMETER [Mdϕ] SECOND MOMENT [STANDARD DEVIATION] AND SORTING [$\sigma\phi$].

factor, while Zonneveld (1946) suggested differences in original size have a larger influence.

4.2.1 Mineralogical composition of different size grade

The mineralogical composition of different size grades of a few samples has been studied. This gives a better picture of the behaviour of mineral species and the size-frequency distribution curves. Fig. 44 shows considerable variation between the grades. Garnet shows a sharp increase in amount between 300 - 100 micron grade, while magnetite-ilmenite, zircon and hypersthene show increase towards the finest grade. Alterites and hornblende show a significant decrease with the grain size (Appendix VII). Different assemblages occur in different grades; in sample 74 the finest grades have a garnet-magnetite-ilmenite assemblage, where as the coarser grades have a hornblende-garnet-epidote assemblage.. This clearly illustrates the misconstructions which could arise from the study of a single grade (Sindowsky, 1949) or of selected grades as suggested by Rubey (1933) and Russell (1936). The total mineral crop should be studied.

4.2.2 Relation between grain size parameters and heavy minerals

The number-percentage of some important heavy minerals have been compared with the grain size parameters (First moment, mean, median diameter, standard deviation, and sorting). No close relationship exists between the parameters and the number percentages of the eight

FIG.47

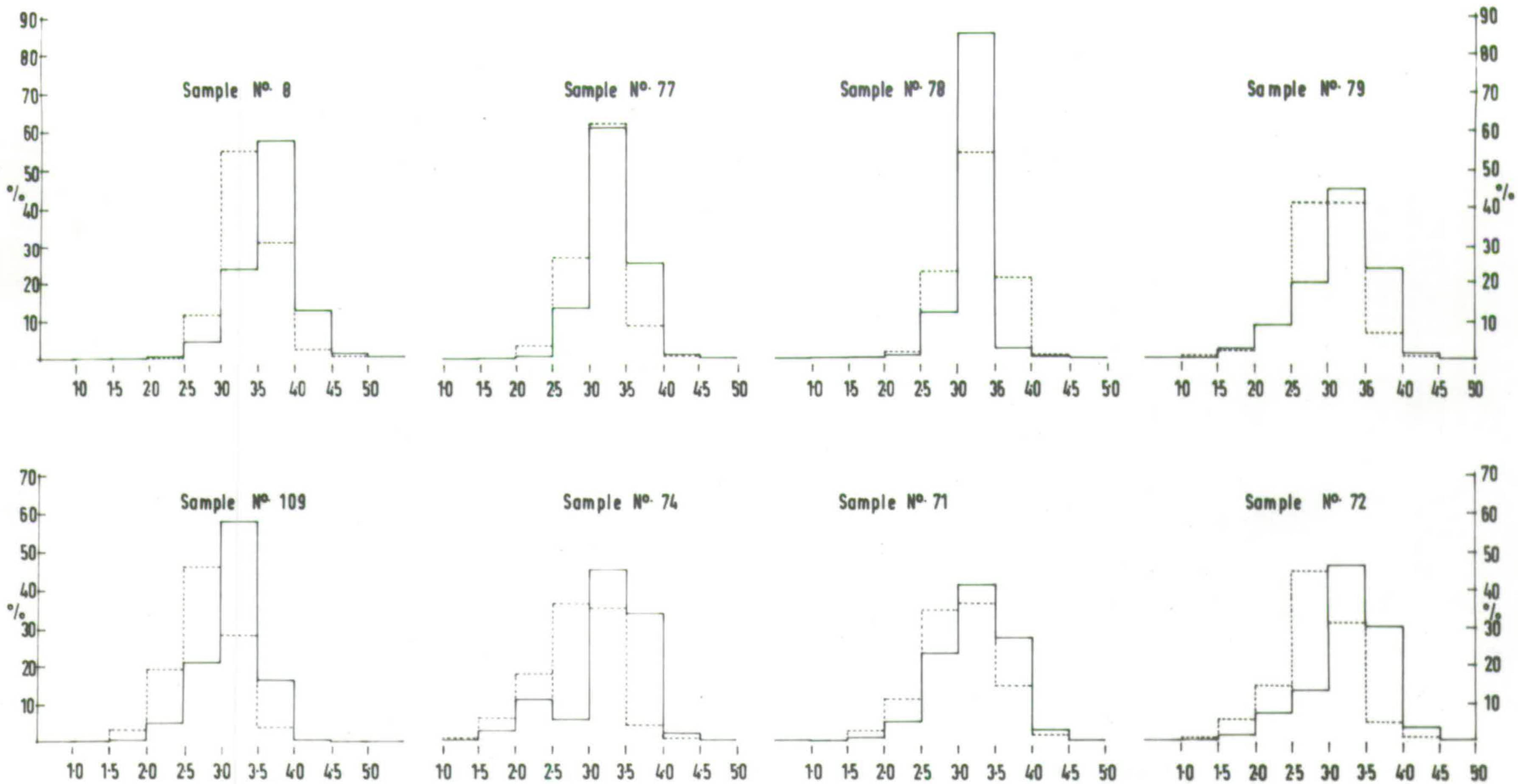

HISTOGRAMS SHOWING RELATION BETWEEN SIZE FREQUENCY DISTRIBUTION OF HEAVY MINERALS AND THE TOTAL AMOUNT OF MATERIAL IN THE SAME SAMPLE.
HORIZ: SIZE GRADE (in PHI units); VERTIC.: WEIGHT PERCENTAGES.

Legend: ——— Heavy Mineral Distribution.
------ Total Sediment Distribution.

FIG. 46

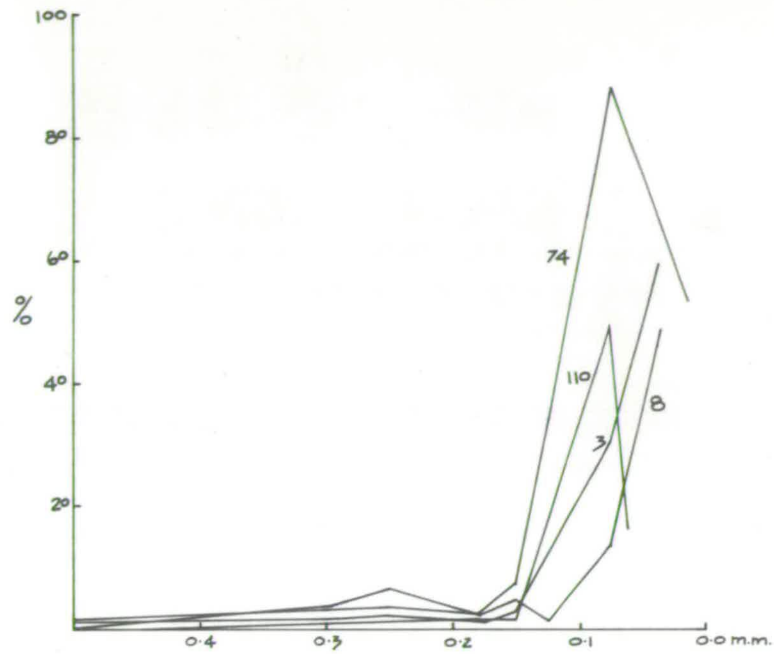

RELATION BETWEEN SIZE GRADE AND HEAVY MINERAL CONTENT IN PERCENTS OF TOTAL AMOUNT OF SEDIMENT IN THE SAME GRADE.

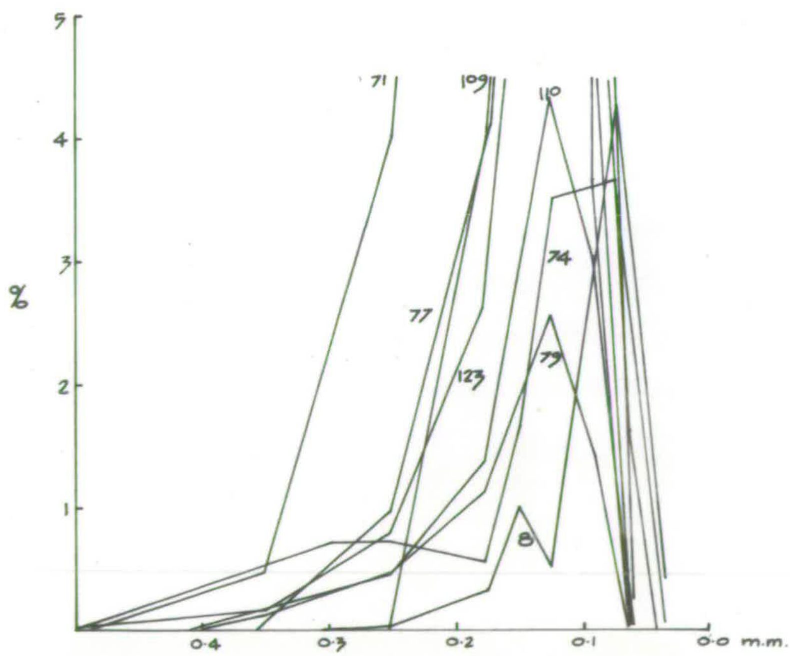

RELATION BETWEEN SIZE GRADE AND HEAVY MINERAL CONTENT IN PERCENTS OF THE TOTAL AMOUNT OF SEDIMENT IN THE WHOLE SAMPLE.

major heavy mineral species. Perhaps there is a slight tendency to increase with increase in grain size of alternites and apatite while magnetite-ilmenite and zircon show an inverse relationship with grain-size parameters (fig. 45).

4.2.3 Conclusions on mineral variations

The size-frequency distribution of the heavy mineral species is apparently based on the original size of the grains and the mineral specific gravity. No significant relationship has been established between the heavy minerals and the grain size parameters. Most of the heavy mineral crop is derived from the fine to very fine fractions of the samples (fig. 46), thus a variation in the amount of this grade can influence the amount of heavy minerals. The normal variations found can be primarily due to the supply of material of varying composition. The fractional analyses are less influenced by the granular variations than the normal whole sample analyses; the fluctuations are more frequent in the finest grades only. Relatively useful results can be obtained from the normal whole sample analyses while the fractional analyses are time consuming.

4.3 Heavy Minerals and their Areal Distribution

In addition to the alterites some 23 species of heavy minerals have been identified and they are arranged in an alphabetical order below.

Anatase	Corundum	Monazite
Andalusite	Epidote	Rutile
Apatite	Garnet	Sillimanite
Augite	Hornblende	Spinel
Biotite	Hypersthene	Staurolite
Brookite	Kyanite	Topaz
Chlorite	Magnetile-Ilmenite	Tourmaline
	Muscovite	Zircon

Minerals and their varieties are for convenience grouped together in percentage calculations. Varieties have only been used when they appear to have regional and/or genetic significance. Some minerals, which have been found only once and therefore have no significant diagnostic importance, are not described here. Micas are usually not used in heavy mineral studies as their specific gravity fluctuates around 2.90, but in the present study they are significantly present in one association and repeated separations and specific gravity tests have shown reliable separations. The results of heavy mineral analyses have been tabulated in the Appendix III - V.

The variations in each of the commonly occurring heavy mineral species has been described separately.

Alterites

Alterites are fine to coarse grained minerals or mineral aggregates of uncertain composition originating from the alteration of of various species. Throughout the area the alterite percentage varies between 1 to 25 percent; in the river and estuarine sands there is a significant decrease in alterite content downstream (fig. 48). The estuarine and river sands have the highest alterite content (from 10 to 25 percent) and the alterite appears to be of schist and mica aggregates, hornblende alterites, augite-alterites and epidote-alterites. Of these varieties, the hornblende and augite alterites are by far the most common. Fractional analyses shows a significant increase in the alterite content with the increase in the grain size. This is reflected in the increase in alterites towards the low tide zone in the beach sands. There is a significant (P = 0.05) difference in the higher content of alterites in the estuarine sands from the beach sands while no significant difference exists between the alterite content of the Northern, Tayport and Tentsmuir sands. Significant differences in the mineral percentages only occur in different environments (fig. 49). The coastal dunes have the least amount of alterites, the amount increases towards the lower-foreshore zone and both the Northern and Tentsmuir sands give this pattern. Both the Northern and Tentsmuir sands have similar hornblende and epidote-alterite varieties.

Garnet

Garnet is one of the major heavy detritals in the area. The grains are colourless to light pink variety and vary from 21 to 91 percent from one part of the region to another. Garnet percentages are the lowest in the river and estuarine sand. They vary from 21 to 38 percent with a slight tendency to increase downstream. The Northern sands have a significantly (P = 0.07) higher content of garnet than the southern Tayport and Tentsmuir sands but both Northern and Southern sands show an increase towards the coastal dunes. In the Buddenness sands the dark-coloured heavy-mineral laminae have a very high garnet content (up to 91%).

Hornblende

Hornblende is a very common mineral and is of two main types; one is the common brown-green basaltic hornblende and the other a green-blue variety which is found only in the Tentsmuir sands. The river and estuarine sands have the highest content (26 - 55%) while in the beach sands higher concentrations are found in the lower foreshore sands. Normally the dune sands have a lower content of hornblende than the beach sands, but in a few cases in the Tentsmuir and Buddenness much higher (33%) values are obtained. The Tentsmuir sands have a significantly higher content of hornblende than the Northern sands. In the Tentsmuir sands there is a decrease in the hornblende content (see fig. 50) in the middle part of the area. Northern sands also show a gradual increase in the percentage towards Buddenness, Fractional analyses shows that the percentage of hornblende increases with the increase in the grain size (fig. 44). This may be one of the main causes in the increase in its content in the lower foreshore sands.

Magnetite Ilmenite

There is a gradual increase in magnetite-ilmenite eastward in the estuary with a mean value of 12 percent (fig. 48). Usually dune sands have a higher content of these minerals but in a few cases there is a slight increase towards the lower foreshore sands, as in the southern parts of Tentsmuir sands. Tentsmuir sands are richer in these iron ores than the Northern sands. Fractional analysis shows that they increase in amount with the decrease in grain size and up to 60% content is found in the fraction 63 - 33 microns, in the dune sands. Beach sands also show this correlation with grain size, but the increase is not so high as in the dune sands.

Epidote

Epidote is present overall in the area varying from 3 to 10 percent. Three types of epidotes are found; a distinctly pleochroic pale yellow-green variety in the river and estuarine sands, yellow and colourless varieties in the Northern and Tentsmuir sands. Northern sands rarely have more than 8% content, while the estuarine and the Tentsmuir sands occasionally have higher values (fig. 49). There is a slight tendency towards increase in epidote with the increase in the grain size.

Hypersthene

The amount of hypersthene varies from 0 to 9%; the Tentsmuir sands have a much higher content than the other areas. Normally the dune sands have a relatively lower content than the adjacent beach sands.

Estuarine sands have 0 - 3% hypersthene - a relatively lower content than the Northern and Tentsmuir sands.

Zircon

Zircon is a minor constituent in the area with values rarely more than 9%, the mean value being 3%. In the river and estuarine sands low values of zircon (1 - 2%) are obtained while a significantly higher content is found in the Northern and Tentsmuir sands. There are two varieties of zircon; the common colourless variety and the rare purple-brown variety. Fractional analyses shows an increase in the zircon content with the decrease in grain size (fig. 44). The purple -brown variety forms less than 10% of the total zircon content and its ratio with the colourless variety changes little in the Tentsmuir sands. The coloured variety is absent in the river and estuarine sands. There is no significant difference in the proportions of coloured zircon between the Tentsmuir and Northern sands.

Tourmaline

Tourmaline is seldom in amounts more than 2%, and is less than 1% in many of the Northern sands. Three varieties of tourmaline are present: light brown, blue and green. The blue type is found in the Tentsmuir sands, while the other two varieties occur in the other areas. Proportions of tourmaline are too small to give any significant ratio between the different varieties but the brown variety

FIG. 48

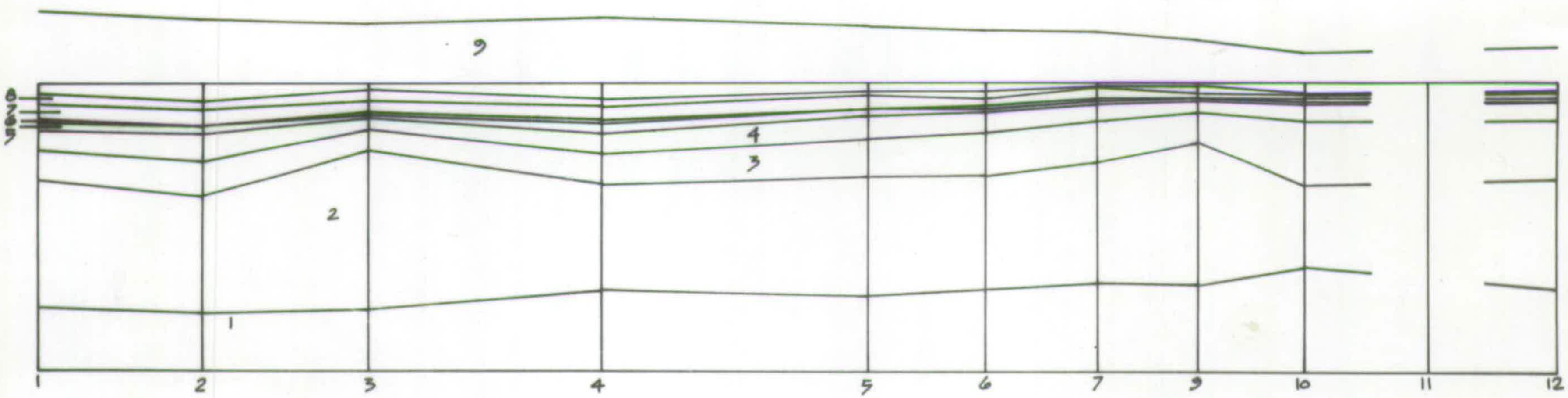

LONGITUDINAL MINERAL PROFILE FROM PERTH TOWARDS BALMERINO IN THE TAY ESTUARY
VERTIC.: CUMULATIVE MINERAL PERCENTAGES.
HORIZ.: SAMPLE LOCATIONS; DISTANCES ARE ROUGHLY PROPORTIONAL TO ACTUAL DISTANCES.

Legend:

9. - Alterite. 8. - Chlorite. 7. - Biotite - Muscovite. 6. - Zircon - Rutile.
5. - Hypersthene. 4. - Epidote. 3. - Magnetite - Ilmenite. 2. - Hornblende.
1. - Garnet.

is the most common in the whole area.

Biotite-Muscovite

Biotite and muscovite micas are present in amounts up to 6% in the river and estuarine sands but virtually absent in the other sands. The proportion increases with the grain size and there is a gradual decrease downstream.

The distribution of minor constituents of heavy mineral suite is given in the appendix.

4.4 Heavy Mineral Association

The mineral association is that combination of minerals which characterises a sediment that belong to the same source-rock province. The standard composition of an association can be defined by investigating the percentages of various heavy mineral species and the number of samples in which each percentage occurs (fig. 51). Variation studies reveal the existence of 3 major types of heavy minerals associations; their characteristics are given in the table 3 and the distribution in Fig. 53.

4.4.1 N-Hornblende Association

The N (= Newburgh) hornblende association consists of hornblende (26 - 55%) garnet (20 - 38%), iron ores, epidote, micas and lesser amounts of chlorite, angite, staurolite and zircon. This association covers the greater part of the estuary from Perth to Dundee.

The mineral profile diagram (fig. 48) shows a high hornblende/garnet ratio which gradually decreases towards east. The hornblende varieties are the common brown-green type and the dark-brown basaltic variety, the former being the more frequent. Garnet is of the light pink and colourless variety and does not show any significant difference in variety from those of the other associations. The micas are biotile and muscovite with a higher proportion of the latter. Epidotes are of the yellowish-green type, together with a few colourless grains. The yellow-green epidotes are in higher proportion than in the T- and M-Garnet associations further downstream. Tourmaline is of the brown and green type; while zircon consists of anhedral to subhedral grains of the colourless variety. The alterite percentages are much higher (10-25:) than those of the Northern sands and the grains are of hornblende-alterites, angite alterites and epidote-alterite.

TABLE 3 Table showing distribution of some characteristic heavy-minerals in the heavy-mineral associations of the Tay estuary region.

Heavy Mineral Species	N- Hornblende Association	M- Garnet Association	T- Garnet Association
Alterites	10 - 25%	7 - 16%	4 - 25%
Andalusite	0 - 1%		
Augite	0 - 2%		
Biotite-Muscovite	1 - 6%		
Brookite	0 - 1%		
Chlorite	1 - 4%	0 - 1%	0 - 1%
Corundum			0 - 1%
Epidote	4 - 10%	2 - 6%	1 - 10%
Garnet	20 - 38%	44 - 91%	28 - 66%
Hornblende	26 - 55%	10 - 39%	1 - 38%
Hypersthene	1 - 3%	1 - 5%	0 - 9%
Magnetile-Ilmenite	7 - 22%	2 - 17%	8 - 26%
Monazite			0 - 1%
Rutile		0 - 1%	0 - 1%
Spinel	0 - 1%		
Zircon	0 - 1%	2 - 6%	1 - 9%

4.4.2 M- Garnet Association

The M (= Monifeith) garnet association has a very high proportion of garnet (44 - 91%) hornblende (10 - 39%) iron ores (2 - 17%) and lesser percentages of epidote, hypersthene, rutile and zircon. The alterite percentage vary from 7 to 16%, and the alterites are mostly of hornblende-alterite and epidote-alterite variety. Garnets are of the common colourless and very light-pink varieties while the hornblende is of common brown-green variety. Tourmaline is made up of the brown and green varieties; most of the zircons are mostly colourless with a small number of purple-brown grains in a few samples. The M- Garnet association is very similar to the T (= Tentsmuir) garnet association but contains much more garnet and a few grains of purple-brown zircon (see Table). The chi-square test does not show any significant (P = 0.03) variation between these two garnet association. But normal mineral studies show that this association can be separated from the T- garnet association by the absence of monazite and corundum. Both garnet associations can be distinguished from the N- hornblende association on the basis of hornblende/garnet ratio, higher zircon content, lower percentage of chlorite, and the absence of andalusite, angite, micas and rutile.

The M- garnet association is found in the Northern sands where it shows considerable variation in the percentage of various mineral species over the area (fig. 52). The garnet/hornblende ratio

FIG. 49

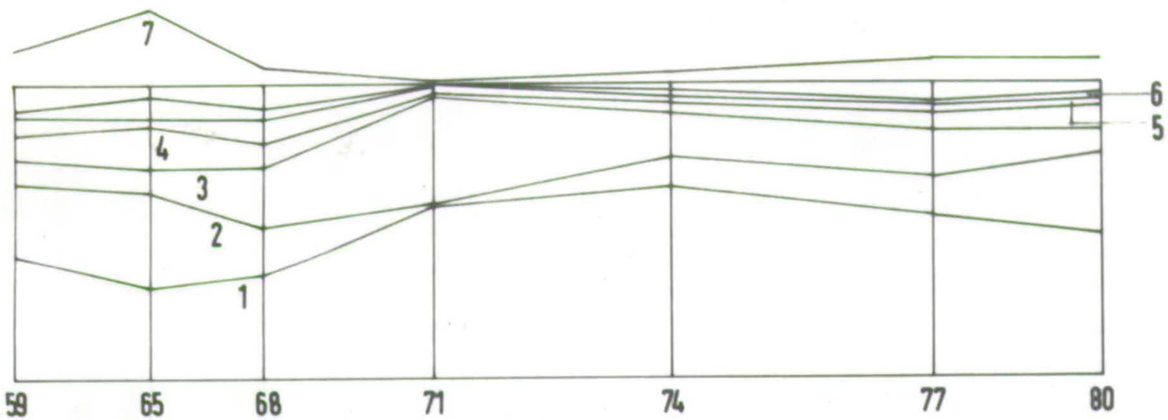

Coastal Dune Sands.

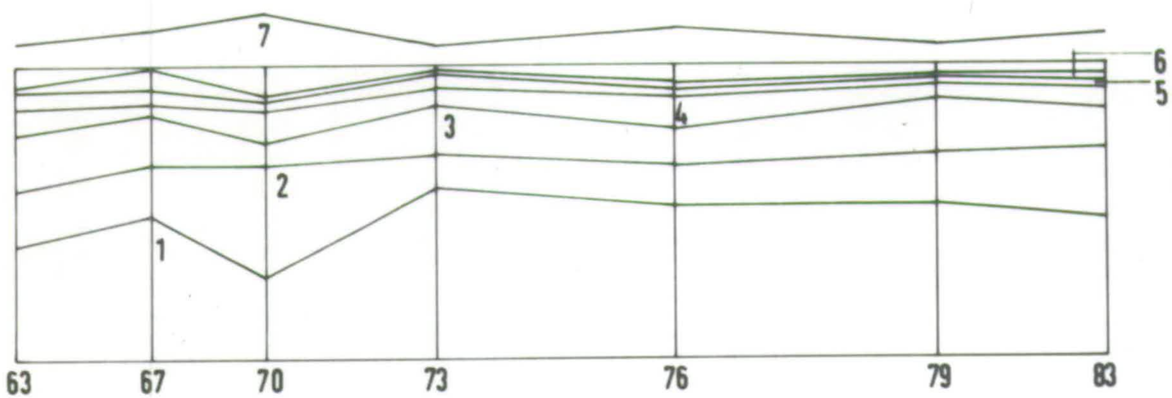

Lower Foreshore Sands.

Legend:

7 Alterite.
6 Zircon - Rutile.
5 Hypersthene.
4 Epidote.
3 Magnetite - Ilmenite.
2 Hornblende.
1 Garnet.

LONGITUDINAL MINERAL PROFILES OF THE TENTSMUIR SANDS.
VERTIC.: CUMULATIVE MINERAL PERCENTAGES;
HORIZ. : SAMPLE LOCATIONS; DISTANCES ARE ROUGHLY PROPORTIONAL TO ACTUAL DISTANCES.

varies especially near the central region with increase in garnet content towards the coastal dunes. This garnet/hornblende relationship is frequent in both T - and M- associations. In the Northern lower foreshore sands garnet and alterites increase gradually towards east. All other mineral species show no significant variation in this Northern sand area except slight variations in epidote, hypersthene and iron ores. In the Budden ness very high concentration of garnet (up to 91%) are found in the sands near the foot of coastal dunes. These high grade garnet deposits are formed by reworking of the coast dunes by wave action. Coastal erosion is very marked in this region and study of old maps shows that in last 100 years approximately 30 acres of Barry sand dunes have been eroded away.

4.4.3 T- garnet Association

The T (= Tentsmuir) garnet association is very similar to the M- garnet association, but contains a lesser amount of garnet and a much greater percentage of zircon, epidote, hypersthene and alterites. Monazite and corundum occur in small amounts; they are absent in the other two associations (fig. 51). The association has high percentages of garnet (28 - 66%), hornblende (1 - 38%), iron ores (8 - 36%), epidote (1 - 10%), hypersthene (0 - 9%), zircon (1 - 9%), and smaller percentages of corundum, monazite, chlorite and rutile. The alterites range between 4 - 25% and are of hornblende - and epidote - alterite varieties. Most

FIG. 50

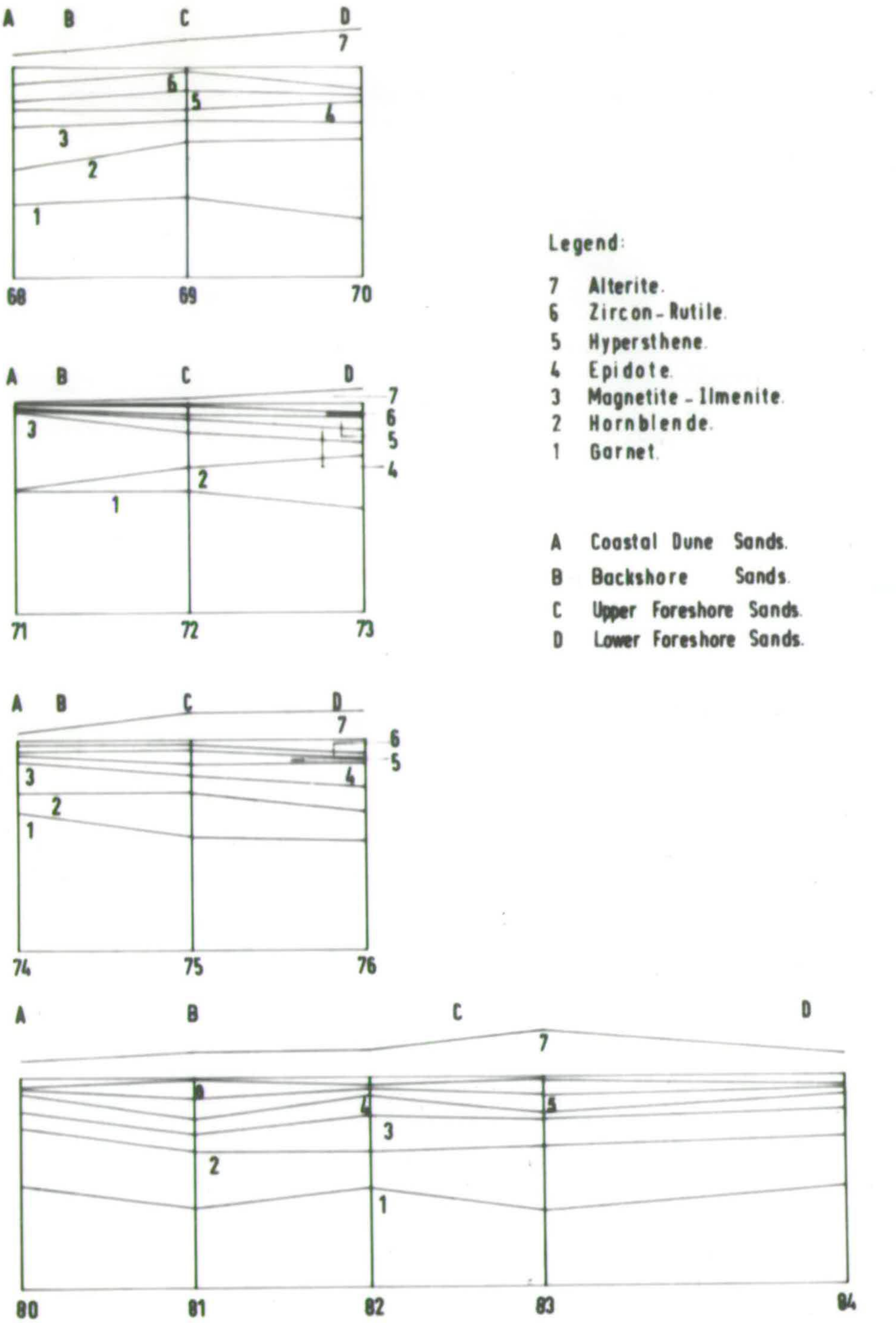

LONGITUDINAL PROFILES SHOWING VARIATIONS IN MINERALS FROM COASTAL DUNE SANDS TO LOWER FORESHORE SANDS.
VERTIC.: CUMULATIVE MINERAL PERCENTAGES;
HORIZ.: SAMPLE LOCATIONS; DISTANCES ARE ROUGHLY PROPORTIONAL TO ACTUAL DISTANCES.

of the garnets are of the light-pink variety with a few colourless grains. Two types of hornblende are found, the common brown-green variety and green-blue variety 1 - 2% of the total percentage of hornblende. Epidotes are the light yellow and colourless varieties similar to those of the M- garnet association. Three varieties of tourmaline are found; brown, green and blue. The last (blue) variety is only found in this association, In the T- garnet association considerable variation in the mineral percentages of various species is observed (see figs. 49 and 50). Alterite percentage decreases gradually towards the south especially in the dune sands. Normally a gradual decrease occurs in the alterite content when followed (on the mineral profile diagram fig. 50) along the beach from lower foreshore towards the coastal dune sands, except near the northern edge of the Tentsmuir sands. Garnet increases towards the central part of the Tentsmuir sands; a similar trend is also exhibited by magnetile-ilmenite grains which are more abundant in the dune sands. Minimum percentages of hornblende are observed in the central part of the Tentsmuir sands. This gives variable garnet/hornblende ratios which increase towards the central Tentsmuir sands. This antipathetic relationship with garnet also exists for hypersthene and epidote.

FIG. 51

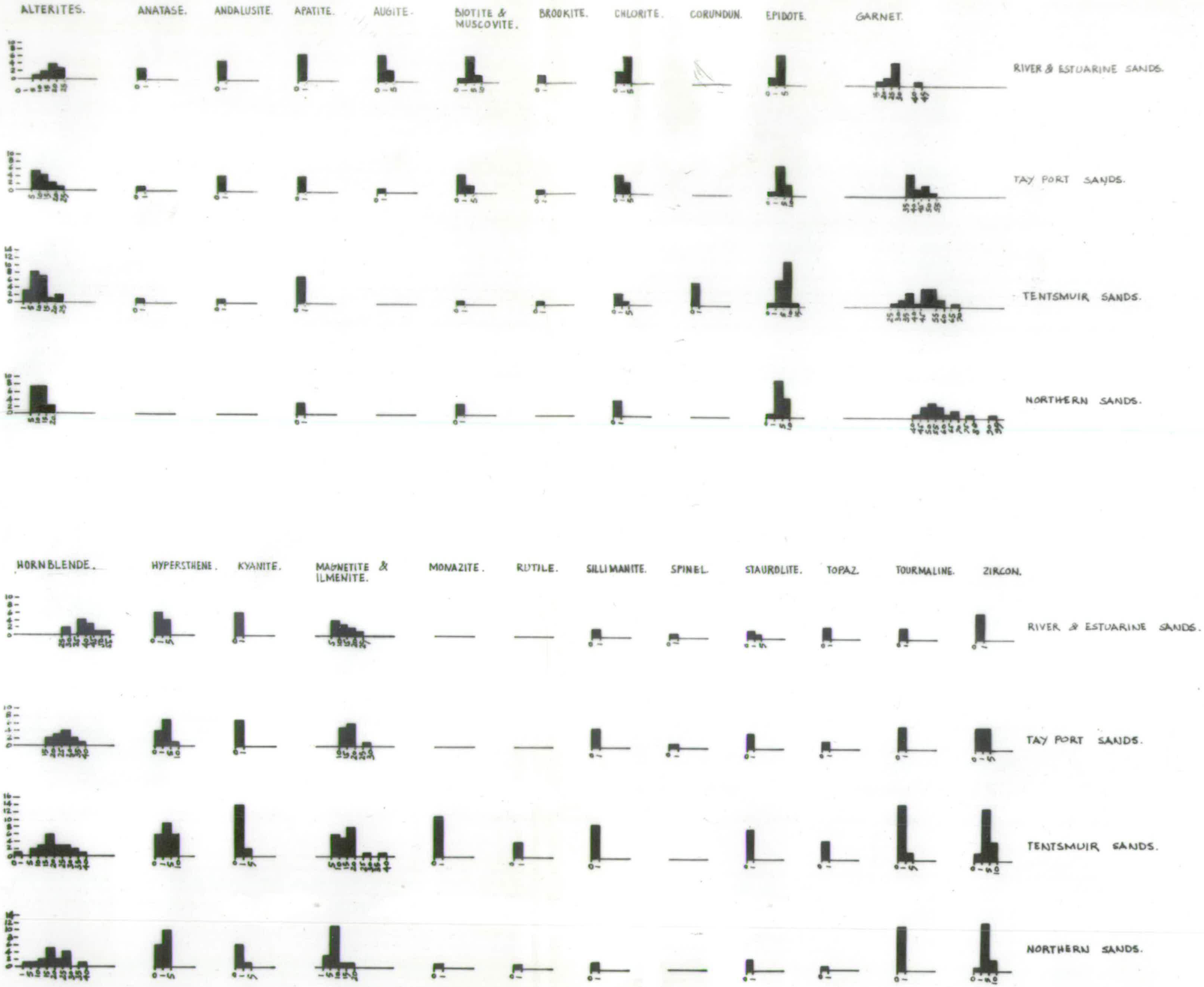

RELATION BETWEEN PERCENTAGES OF DIFFERENT HEAVY MINERALS AND NUMBER OF SAMPLES THAT CONTAIN THESE PERCENTAGES IN THE VARIOUS PARTS OF THE AREA

VERIC. : NUMBER OF SAMPLES,
HORIZ. : MINERAL PERCENTAGES.

TABLE 4 Mineral associations and the distribution of different varieties of heavy minerals

Mineral	N- Hornblende Association	M- Garnet Association	T- Garnet Association
Alterite	Hornblende- Epidote - Augite and others	Hornblende - Epidote- and others	Hornblende- Epidote- and others
Garnet	Light pink and Colourless	Light pink and Colourless	Light pink and Colourless
Hornblende	Brown-green Red-brown	Brown-green -	Brown-green Green-blue
Epidote	Yellowish-green	Yellow and Colourless	Yellow and Colourless
Zircon	Colourless -	Colourless -	Colourless and Purple-red variety
Tourmaline	Brown Green -	Brown Green -	Brown Green Blue

The Tayport sands shows T- garnet association distribution and does not show any significant (P = 0.17) variation from the T- garnet association of Tentsmuir sands. In the Tayport sands slightly higher values of hornblende are obtained with some biotite-muscovite which probably are from the N- hornblende association upstream. A study of several heavy mineral samples from the same T- garnet association

FIG. 52

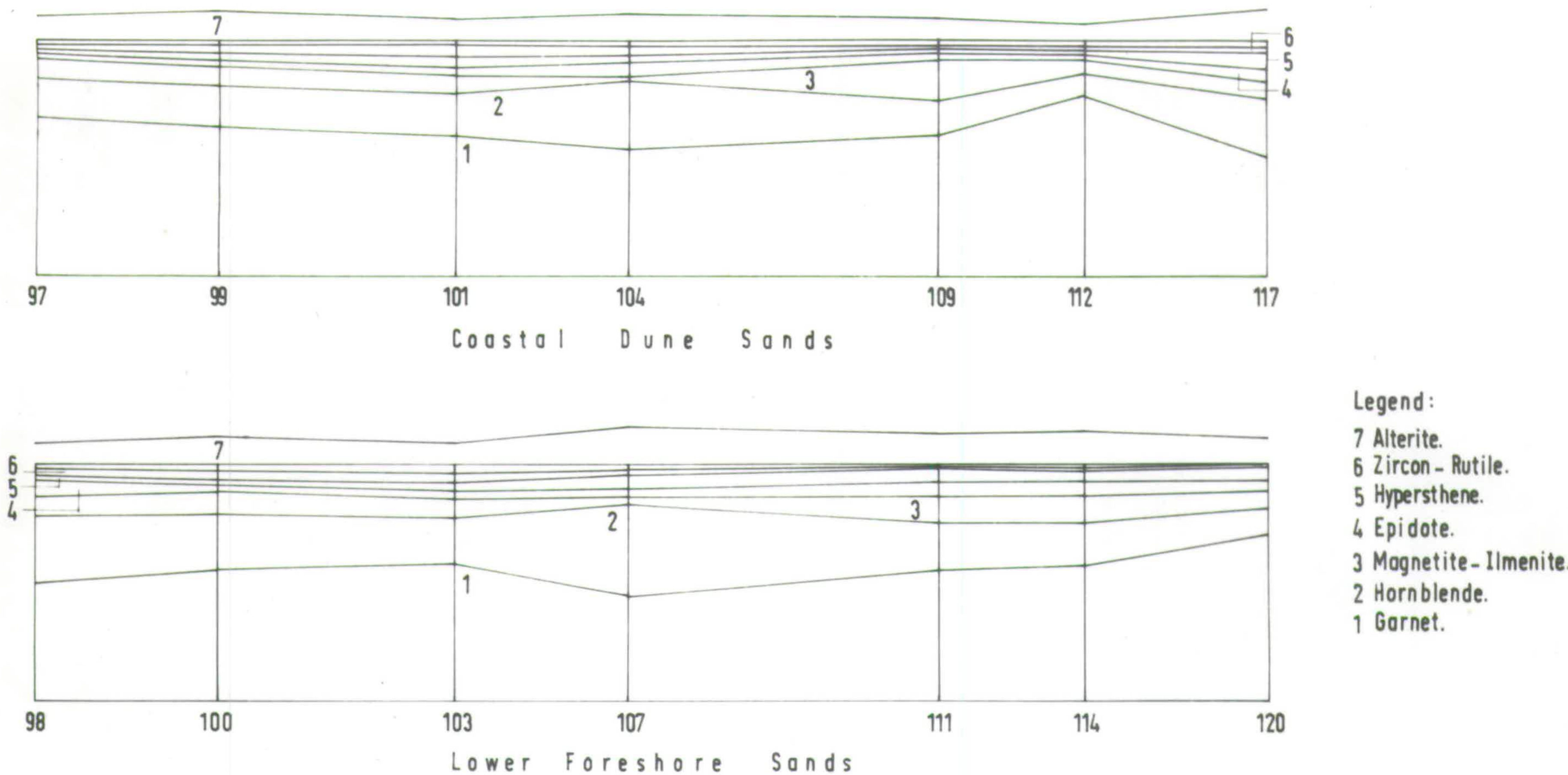

LONGITUDINAL MINERAL PROFILES OF THE NORTHERN SANDS.
VERTIC.: CUMULATIVE MINERAL PERCENTAGES;
HORIZ.: SAMPLE LOCATIONS; DISTANCES ARE ROUGHLY PROPORTIONAL TO ACTUAL DISTANCES.

FIG.53

DISTRIBUTION OF VARIOUS HEAVY MINERAL ASSOCIATION.

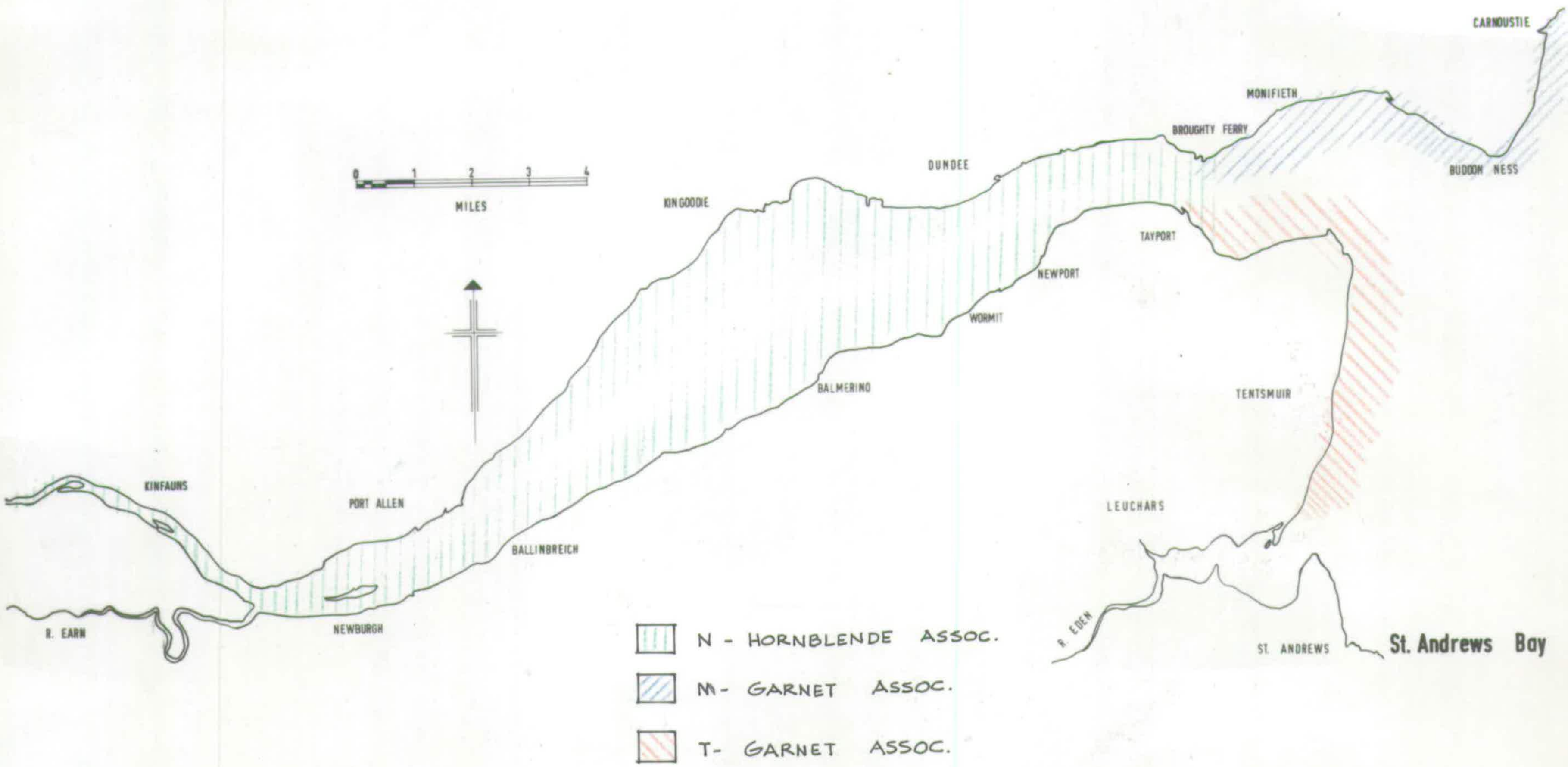

showed that no significant relationship exists between the mean size of the heavy minerals and the mean size of the sediments. Similar results are obtained for sorting and heavy-mineral size. These observations are in accordance with previous results of Van Andel (1950), Van Andel and Postma (1954), Muir (1958). Thus the size-frequency distribution of a heavy mineral assemblage is mainly a function of the source material and their limited size ranges are insufficiently sensitive to sorting.

4.5 Provenance of the heavy minerals

Various heavy minerals and their varieties are considered with the relation to the information regarding their possible source rock types. Only those minerals are discussed in details which help in provenance reconstruction. Direct information is obtained by consideration of the extent of the Tay drainage basin and other streams affecting the estuary. Fig. 54 illustrates this drainage system extending across Moine and Dalradian rocks, igneous rocks associated with the Dalradian metamorphics, Highland Border Series, Basaltic and andesitic lavas of the Middle Old Red Sandstone. Old Red Sandstones and the Carboniferous formations of Fife.

In the Grampian Highlands, the Moine series have abundant mica in the muscovite-biotite gneiss, abundant garnet in the pelitic semi-pelitic gneisses and zoisite-granulites. Hornblende is widespread

FIG. 54

GEOLOGICAL SKETCH MAP OF THE TAY DRAINAGE REGION.
(Based on Geological Survey 'TEN MILE' map of Gt. Britain)

Legend.

- Carboniferous limestone series. } Sedimentary formations.
- Calciferous sandstone series.
- Upper old red sandstone series.
- Lower old red sandstone series.
- Dalradian. } metamorphic rocks.
- Moine.
- Tuffs. } igneous rocks.
- Andesite and Basaltic lavas.
- Granite, syenite, etc.
- Basalt, Dolerite, Camptonite etc.

All superficial deposits omitted.

in the hornblende and other schists. The Dalradian series have various mica- schists, gneisses and green-beds with abundant chlorite, epidote and hornblende. The intrusive igneous rocks are the granites of the Central Highland, felsites, quartz-porphyry, with the main heavy mineral constituents as apatite, biotite, hornblende, monazite, muscovite, zircon etc. Mackie (1923) has studied the heavy minerals in the Old Red Sandstone formations. The Heavy mineral suite of Middle Old Red Sandstone consists of dominant garnet with abundant iron ore, rutile, monazite, staurolite, etc., but rare tourmaline and zircon. The upper Old Red Sandstone formations have zircon as the main heavy mineral with abundant tourmaline rutile, anatase, monazite, etc. but garnet is rare or absent. The main minerals of igneous rocks of the lower Old Red Sandstone series are biotite, apatite, zircon, tourmaline, hornblende, iron ores and augite.

Hornblende

Three varieties are found in the Tay sands the common hornblende (brown-green) basaltic hornblende (red-brown) and metamorphic hornblende (blue-green). The metamorphic variety has probably been derived from the Moine and Dalradian series while the basaltic variety could have originated in the basaltic and andesitic lavas in the Lower Old Red Sandstones. The common variety of hornblende is a major constituent of most of the rock types found in the area.

4.5

Tourmaline

Three varieties of tourmaline are recorded in the associations. The well-rounded grains of blue tourmaline (type 2 of Krynine's (1946) classification) are probably of pegmatitic origin. Brown tourmaline (type 3b, Krynine 1946) are derived from slates phyllites or basic schists. Green tourmalines (type 1. Krynine 1946) are derived from granites and pegmatites. Only 6% of the newer granites of the Highlands contain tourmaline (Mackie 1932). Higher percentages of brown tourmaline and green varieties are reported from the older foliated granites (40%) and 20% of the pegmatites contain blue and brown varieties. Minute amounts of tourmaline are found in the Dalradian (Barrow 1893); green grains are present in the garnet-schists and the blue variety in limestones and staurolite-schists. Lesser amount of green and red-brown varieties are reported from the Moine gneiss. In all the associations brown and green varieties are present while a few grains of the blue variety are obtained in the T-garnet association. Most of the tourmaline in the area is derived from the Moine and Dalradian formations of the Highlands.

Zircon

This mineral is one of the most ubiquitous of heavy minerals, thus its presence does not indicate the provenance with any precision. Some attention has been paid to study the varietal properties in different rock types by numerous investigators (e.g. Tyler and Marsden 1937,

FIG. 55

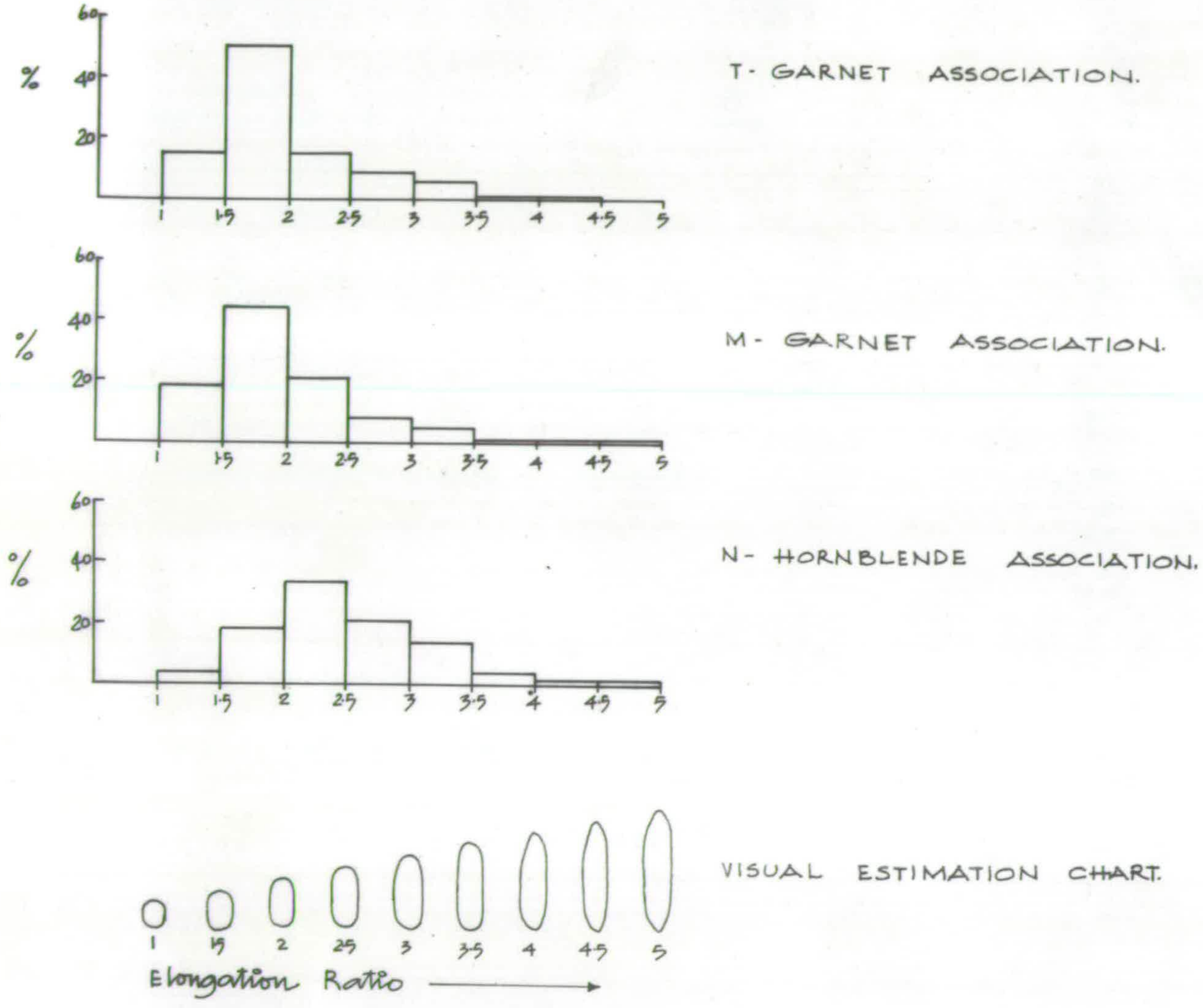

ZIRCON ELONGATION RATIO IN DIFFERENT MINERAL ASSOCIATIONS.

4.5

Tyler, 1940, Slaviic, 1952; Poldervaart, 1955, 1956; Muir 1958 etc.)

The zircon elongation (length-breadth ratio) was determined for each association and the percentage computation was carried out on the basis of a visual chart (fig. 55). In the N- hornblende association the zircons are quite long. 21% have elongations over 3.0 (16% in 3.0 - 3.5 class and 5% in 3.5 - 4.0 class) Most of the zircons are euhedral and have well developed faces. Such zircons have probably come from granites, pegmatites and possibly foliated granites of the Highlands (Mackie, 1932; Wyatt, 1954; Muir, 1958; Dalziel, 1963). In the 2.0 - 3.0 class there are 56% zircons; these are mostly derived from the contaminated granites, aplites and granodiorites. Some of the Moine and Dalradian schists could have contributed to this class. Most of the 32% zircons of the 1.0 - 2.0 class have probably been derived from the reworked sediments of Moine and Dalradian series.

The zircon elongation studies reveal no significant difference between the M- and T- garnet associations. Most of the zircons belong to 1.0 - 2.0 class, therefore it is apparent that most of the zircons in these two associations are derived mainly from garnetiferous schists, gneisses, quartzites and partly from the granites, pegmatites and other acid igneous rocks. This suggests that most of the sediment in these two garnet associations consists of reworked material from the Moine and Dalradian rocks.

4.6 Distribution and Possible Horizon of Source Rocks

Three heavy mineral associations have been shown to exist in the recent sediment of the Tay estuary region and it could be visualized that three different types of source area are involved. But a closer study of the three mineral associations and the provenance of the different heavy mineral species gives a different picture. All the three mineral associations have detrital mineral suites characteristic of a metamorphic region (andalusite, garnet, hornblende, kyanite, sillimanite, staurolite, etc.) with acid igneous rocks (anatase, augite, brookite, hypersthene, magnetite-ilmenite, rutile) and pegmatites (topaz, tourmaline, zircon). The mineral assemblages show similarities with those of the Middle Old Red Sandstone in the dominance of garnet with abundant iron ores with rare tourmaline and zircon (Mackie, 1923)

It is apparent that all the three mineral associations have been derived from the same mineral province in which metamorphic rocks predominate. Most of the material has been derived from the Grampian Highlands and the Old Red Sandstone of the Midland Valley south of the Highland Boundary fault. Differences in the three associations are due to the later processes of reworking and influx of fresh material. In the N- hornblende association there is a greater amount of basaltic hornblende which is mostly derived from the basaltic and andesite lavas

FIG. 56

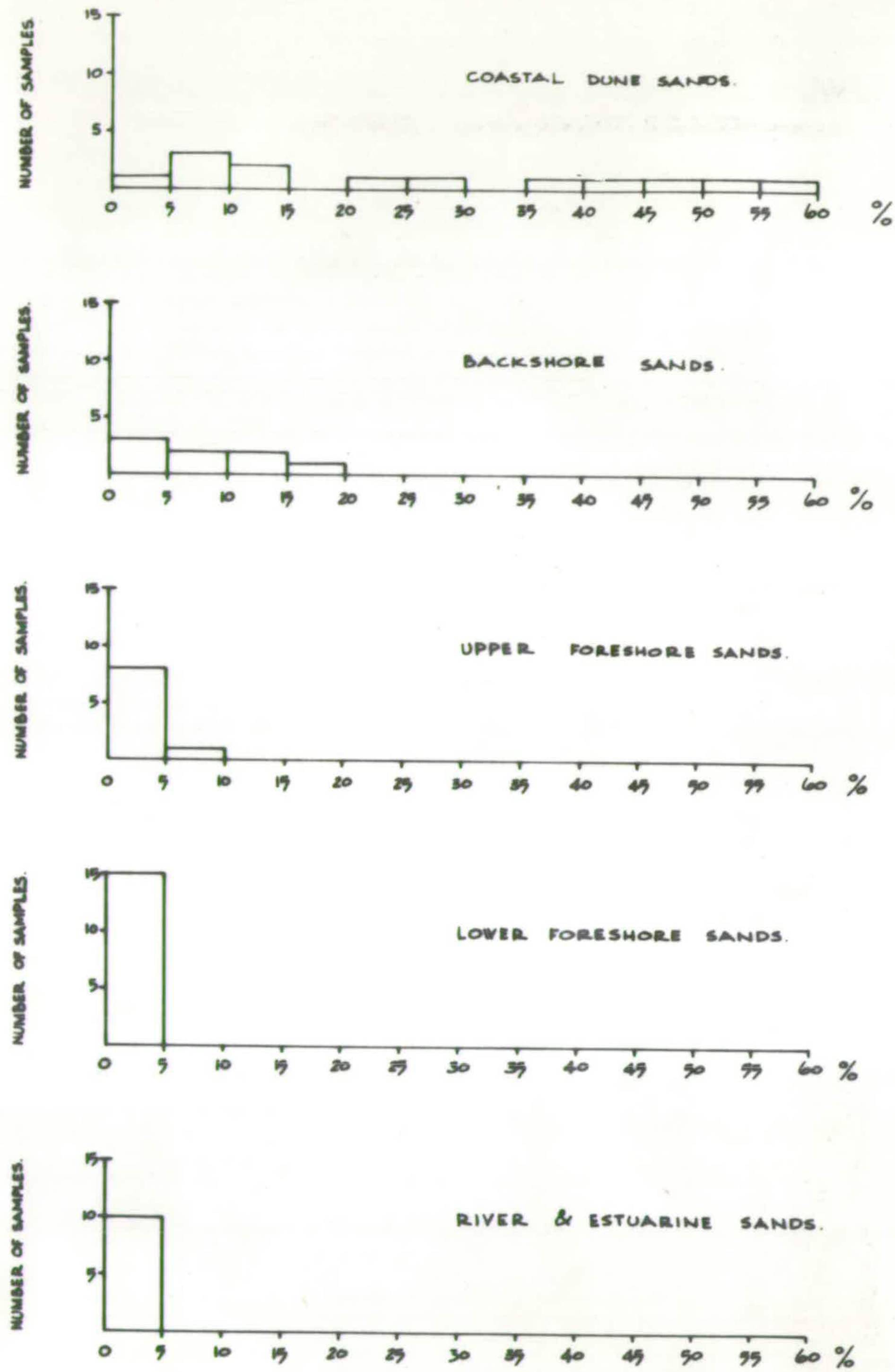

RELATION BETWEEN PERCENTAGES OF HEAVY MINERALS AND NUMBER OF SAMPLES THAT CONTAIN THESE PERCENTAGES IN THE VARIOUS ENVIRONMENTS AND SUB-ENVIRONMENTS.

of the Lower Old Red Sandstone. Biotite and muscovite are only present in this association as the area occupied by this association is nearest to the Highland drainage. These micas are not present in the other associations as these minerals are unstable and are not preserved in the more rigorous conditions under which the garnet-associations have formed. The presence of augite is due to local contributions from the lavas(of Lower Old Red Sandstone) to the original parent Highland assemblage. The high garnet content in the M and T garnet associations is due to the enrichment of garnet sands in the coastal dunes. Normally dune sands have the highest content of heavy minerals(fig. 56). In the M garnet association of the Northern sands very high garnet percentages are obtained from wave reworking of dunes as well as some from the sediment brought down by the river. In the T garnet association fairly high garnet values are due to spread of dune sands on the beach by the strong cycle of offshore winds. Zircon elongation study shows no significant difference in the sources of M and T garnet associations. The presence or absence of other minor heavy minerals may be due to chance variations as these variations are seldom more than 1% (i.e. corandum, monazite, blue-green tourmaline, etc.). Contributions from the local calciferous sandstones could also be the cause of minor variations in the distribution of epidote and tourmaline.

Section 5 SUMMARY AND CONCLUSIONS

The Tay area has been divided on the basis of various environments present and emphasis has been placed on the characters which differentiate the sediment in various environments.

The sediments show various types of sublenticular laminations. Marsh laminations are characterised by undulating nodular laminae mostly composed of silty sands and sandy silts with abundant rootlets. Rippled laminae are absent. The tidal flats have more regular laminae composed of fine to medium sand and silty sands. Rippled laminae are observed and heavy mineral laminae are absent. Three types of laminations are found in the beach environments. The backshore sands have low landward dips while the upper foreshore laminae have low seaward directions of dip. Both types of laminations are characterised by well sorted fine to medium fine sands with well developed heavy mineral laminae. Rippled laminae are frequent and there is a noticeable absence of silt and clay. The lower foreshore sands have coarser sands than the other two and the irregular laminae have high values of seaward dip. Heavy mineral laminae are not so well developed as in the other parts of the shore. Coastal dunes have an abundance of cross-laminations with varying orientations and amounts of dip; laminae are very thin and consists of fine to very fine sand with streaks of heavy minerals. Various ripple and rill structures are studied; a very flat ripple variety occurs in the Barry sands. One mega structure - the mound structure-is found in the Budden ness and Gaa sands, which has not been previously reported. Other types of mega structure are found in the sandy parts of the estuary and on sand banks and spits.

The grain-size distribution reveal three major types of distribution curves and it is possible to distinguish sediments of various environments from each other. Statistical studies show that the moment measures are the best statistical parameters for environmental studies. These measures are not applicable in the case of open-ended distributions; in these cases graphic parameters may be used. Inman's graphic parameters are of little value in the environmental studies. Thus a combination of distribution curves and moment measures should be used to describe the size-frequency distribution of sediments. The results of the study of the roundness of grains from various environments does not show any significant differences between beach and dune sands. This is mostly due to offshore winds mixing up the grains of the two environments. River and estuarine sands are more angular than the beach and dune sands.

Heavy mineral studies reveal no significant relationship between the mineralogical composition of a sample and its grain-size distribution. The mineralogical composition of a sample depends on the mineral content of different size grades in which the role of the original size of the minerals is important; most of the minerals are derived from the fine sand fractions. Dune sands have the highest percentage content in the fine sand/coarse silt grade than in any other type sands. Three types of mineral associations are found and all are derived from the same source area which consists of the metamorphic Moine and Dalradian rocks with associated igneous masses together with old Red Sandstone sediments and lavas and, locally, carboniferous sediments.

ADMIRALTY (British) 1959 North Sea Pilot, Vol. II
Northern and Eastern Coasts of Scotland.
11th Ed., H.M.S.O., London.

1960 Charts 149 and 1481.
H.M.S.O., London.

ALLEN, J.R.L. 1962 Asymmetrical ripple marks and the origin of cross-stratification.
Nature, Lond., 194, 167.

1963 Asymmetrical ripple marks and the origin of water-laid cosets of cross strata.
Lpool. Manchr. geol. J., 3, 187 - 236.

1963 Henry Clifton Sorby and the sedimentary structures of sands and sandstones in relation to flow conditions.
Geol. en Mijnb., 42, 223 - 228.

ANDEL, Tj. H. van 1950 Provenance, transport, and deposition of Rhine sediments.
Wageningen.

ANDEL, Tj. H. van & POSTMA, H. 1954 Recent sediments of the Gulf of Paria: Reports of the Orinoco shelf expedition, vol. 1.
Verh. Akad. Wet. Amst., 20, 1 - 244.

ANDEL, Tj. H. van 1955 Sediments of Rhone delta, II. Source and deposition of heavy minerals.
Verh. geol. - mijnb. Genoot. Ned. Kolon., 15, 515 - 556.

BAGNOLD, R. A. — 1937 The transport of sand by wind. Geogr. J. 89, 409 - 438.

1937 The size grading of sand by wind. Proc. roy. Soc. A., 163, 250 - 264.

1941 The physics of blown sand and desert dunes. Methuen & Co. London.

1956 The flow of cohesionless grains in fluid. Proc. roy. Soc. A., 249, 235 - 297.

BARROW, W. — 1893 On the intrusion of muscovite-biotite gneiss in the south-eastern Highlands of Scotland and its accompanying metamorphism. Quart. J. geol. Soc. Lond., 49, 330.

BLOM, G. — 1958 Statistical estimates and transformed beta-variables. John Wiley & Sons. Inc. New York.

BOSWORTH, T. O. — 1913 The heavy minerals in the sandstones of the Scottish carboniferous rocks. Proc. Geol. Ass. Lond., 24, 37.

BREMNER, A. — 1916 Problems in the glacial geology of the north east Scotland. Trans. Edinb. geol. Soc., 10, 344.

1939 The late glacial geology of the Tay basin from Pass of Birnan to Grandtully and Pitlochry. Trans. Edinb. geol. Soc., 13, 473.

BROOKER, R. A. & ROHL, J. S. — 1963 Atlas Autocode Manual. Computing Machine Laboratory, Manchr. University.

BUCHER, W.H. 1919 On ripples and related sedimentary surface forms and their paleographic interpretation. Amer. J. Sci., 47, 149 - 210.

CALLENDER, J.G. 1929 Land movement in Scotland in prehistoric and recent times. Proc. Soc. Antiq. Scot., 63, 314 - 322.

CLOET, R.L. 1954 Sand waves in the southern North sea and in the Persian Gulf. J. Inst. Navig., 7, 272 - 279.

CRAIG, G.Y. & WALTON, E.K. 1962 Sedimentary structures and paleocurrent direction from the Silurian rocks of Kirkcudbrightshire. Trans. Edinb. geol. Soc., 19, 100 - 119.

DALZIEL, I.W.D. 1963 Zircons from the granite gneiss of Western Ardgour, Argyll: The bearing on its origin. Trans. Edinb. geol. Soc., 19, 363 - 425.

DAVIDSON, C.F. 1937 Note on the occurence of garnet sands in the Tay estuary. Trans. Perthsh. Soc. nat. Sci., 9, 1937.

DOEGLAS, D.J. 1940 The importance of heavy mineral analysis for regional sedimentary petrography. Nat. Res. Coun., Comm. on Sedim., Rep. 1939 - 1940, 102 - 121.

DOEGLAS, D.J. & SMITHUYZEN, W.C.B. 1941 De interpretatie van de resultaten van korrelgrootle-analysen. Geol. en Mijnb., 8, 273 - 296.

DOEGLAS, D.J. 1944 De interpretatie van korrelgrootle-analysen. Lek. Verh. geol. -mijnb. Genoot. Ned. Kolon. Geol. Serie, deel 15, 2e stuk.

1946 Interpretation of the results of mechanical analysis. J. Sediment. Petrol., 16, 19 - 40.

1950 De interpretatie van korrelgrootle-analysen. Verh. geol. -mijnb. Genoot. Ned. Kolon. 15, 247 - 328.

1955 The origin and destruction of beach ridges. Leid. geol., Meded. 20, 34 - 37.

DRYDEN, A.L. 1931 Accuracy in percentage representation of heavy mineral frequencies. Proc. nat. Acad. Sci. Wash., 17, 233 - 238.

EDELMAN, C.H. 1933 Petrologische provincies in het Nederlandse Kwartair. Amsterdam.

EMERY, K.O. 1960 The sea off Southern California : A modern habitat of petroleum. John Wiley & Sons. Inc. New York.

ESCHER, B.G. 1948 Grondslagen der algemene geologie. Wereldbibliothick, Amsterdam.

EVANS, O.F. 1940 The low and ball of the eastern shore of Lake Michigan. J. Geol., 48, 476 - 511.

1941 The classification of wave formed ripples. J. Sediment. Petrol., 11, 37 - 41.

1943 Effect of change of wave size on the size and shape of ripple marks. J. Sediment. Petrol., 13, 35 - 39.

1949 Ripple marks as an aid in determining depositional environment and rock sequence. J. Sediment. Petrol., 19, 82 - 86.

FISHER, R. A. 1948 Statistical methods for research workers. Oliver & Boyd, Edinburgh.

FOLK, R. L. 1961 Petrology of sedimentary rocks. Hemphill"s Pub. Co., Austin, Texas.

1962 Discussions of skewness and sands. J. Sediment. Petrol., 32, 145 - 146.

FRIEDMAN, G. M. 1961 Distinction between dune, beach and river sands from their textural characteristics. J. Sediment. Petrol., 31, 514 - 529.

GILBERT, G.K. 1899 Ripple marks and cross bedding. Bull. geol. Soc. Amer., 10, 135 - 140.

GREGORY, J. W. 1926 The Scottish kames and their evidence on the glaciation of Scotland. Trans. roy. Soc. Edinb., 54, 395 - 432.

HACK, J. T. 1941 Dunes of Western Navajo Country. Geol. Rev., 31, 240 - 260.

HAMBLIN, W. K. 1962 X-ray radiography in the study of structures in homogeneous sediments. J. Sediment. Petrol., 32, 201 - 210.

HANTZSCHEL, W. 1936 Die Schichtungs-Formen rezenter Flachmeer-Ablagerunggen im Jade-Gebiet. Senckenbergiana, 18, 316 - 356.

	1938	Bau und Bildung von Gross-Rippeln im Wattenmeer. Senckenbergiana, 20, 1 - 42.
	1939	Tidal flat deposits. In : Recent Marine Sediments, 195 - 206 (Ed. Trask)
HARMS, J. C. & OTHERS	1963	Stratification in modern sands of the Red river, Louisiana. J. Geol., 71, 566 - 580.
HARRIS, S.A.	1958	Probability curves and the recognition of adjustment to depositional environments. J. Sediment. Petrol., 28, 151 - 163.
HULSEMANN, J.	1955	Gross-Rippeln und Schragschichtungs-Gefuge im Nordsee-Watt und in der Molasse. Senckenbergiana, 36, 359 - 388.
INMAN, D.L.	1949	Sorting of sediments in the light of fluid mechanics. J. Sediment. Petrol., 19, 51 - 70.
	1952	Measures for describing the size distribution of sediments. J. Sediment. Petrol., 22, 125 - 145.
	1957	Wave generated ripples in nearshore sands. Tech. Mem. Beach Erosion Board, 100, 1 - 41 ; and A1 - A23.
JAMIESON, T.F.	1865	On the history of the last geological changes in Scotland. Quart. J. geol. Soc. Lond., 16, 347.
JOHNSON, D.W.	1919	Shore processes and shoreline development. New York.

KINDLE, E.M. 1917 Recent and fossil ripple marks. Geol. Surv. Can. Mus. Bull., 25, 121.

KINDLE, E.M. & BUCHER, W.H. 1932 Ripple marks and its interpretation. In : Treatise on sedimentation. 2nd Ed., 632 - 668. Williams & Wilkins, Baltimore.

KRUIT, C. 1955 Sediments of Rhone Delta. I. Grain size and micro-fauna. Ver. geol. -mijnb. Genoot. Ned. Kolon., 15, 357 - 462.

KRUMBEIN, W.C. 1934 Size frequency distribution of sediments. J. Sediment. Petrol., 7, 65 - 77.

1934 The probable error of sampling sediments for mechanical analysis. Amer. J. Sci., 27, 204 - 214.

KRUMBEIN, W.C. & PETTIJOHN, F.J. 1936 Manual of sedimentary petrology.

1938 D. Appleton. Centuary Co. Ltd., Inc. New York.

KRYNINE, P.D. 1946 The tourmaline group in sediments. J. Geol., 54, 65 - 87.

LANDSBERG, S.Y. 1956 The orientation of dunes in Britain and Denmark in relation to wind. Geogr. J., 122, 176 - 189.

LUDERS, K. 1929 Entstehung und Aufbau von Groszrucken mit Scillbedeckung in Flut-bezw. Ebbetrichten der Auszenjade. Senckenbergiana, 11, 123 - 142.

1930 Entstehung der Gezeitenschichtung auf den Walten im Jadebusen. Senckenbergiana, 12, 229 - 254.

LUGN, A. L. 1927 Sedimentation in the Mississippi river between Davonport, Iowa and Cairo, Illinois. Augustana Libr. Publ. Nr. 11, 1927.

MACGREGOR, M. & MACGREGOR, A. G. 1948 Midland Valley of Scotland. British Regional Geology. 2nd Ed. Geol. Surv. Pub., H.M.S.O. Edinburgh.

MACKIE, W. 1923 The principles that regulate the distribution of particles of heavy minerals in Sedimentary Rocks. Trans. Edinb. geol. Soc., 11, 138.

1932 The heavier accessory minerals in the granites of Scotland. Trans. Edinb. geol. Soc., 12, 22 - 40.

MARTINS, J. H. C. 1939 / 1959 Beaches. In : Recent Marine Sediments. (Ed. Trask). 207 - 218. Murby, London.

MASON, C. C. & FOLK, R. L. 1958 Differentiation of beach, dune and aeolian flat environments by size analysis, Mustang Island, Texas. J. Sediment. Petrol., 28, 211 - 226.

McCAMMON, R. B. 1962 Moment measures and the shape of size frequency distributions. J. Geol., 70, 89 - 92.

1962 Efficiencies of percentile measures for describing the mean size and sorting of sedimentary particles. J. Geol., 70, 453 - 465.

MCKEE, E. D. 1933 The Coconino sandstone - its history and origin. Carnegie Inst. of Wash., 440, 78 - 115.

	1945	Small scale structures in the Coconino Sandstone in Northern Arizona. J. Geol., 53, 313 - 325.
MCKEE, E.D. & WEIR, G.W.	1953	Terminology for stratification and cross-stratification in sedimentary rocks. Bull. geol. Soc. Amer., 64, 381 - 390
MCKEE, E.D.	1957	Flume experiments on the production of stratification and cross-stratification. J. Sediment. Petrol., 27, 129-134.
	1957	Primary structures in some recent sediments. Bull. Amer. Ass. Petrol. Geol., 41 1704 - 1747.
MCKEE, E.D. & STERRET, T.S.	1960	Laboratory experiments on form and structure of longshore bars and beaches. In: Geometry of Sandstone Bodies (Ed. Peterson & Osmond). Amer. Ass. Petrol. Geol. Tulsa, 13 - 28.
McMULLEN, R.M. & ALLEN, J.R.L.	1964	Preservation of sedimentary structures in wet unconsolidated sands using polyester resins. Marine Geol., 1, 88 - 97.
MOORE, D.G. & SCRUTTON, P.C.	1957	Minor internal structures of some recent unconsolidated sediments. Bull. Amer. Ass. Petrol. Geol., 41 2723 - 2751.
MOSTELLER, F.	1946	On some useful 'inefficient' statistics. Ann. math. Statist., 17, 377 - 408.
MUIR, R.O.	1958	Scottish Millstone Grit. Unpub. Ph.D. Thesis, University of Edinburgh.
	1963	Petrology and provenance of the Mill-

		stone Grit of Central Scotland. Trans. Edinb. geol. Soc. 19, 439-485
MULLER, A.	1938	Die mechanische und mineralogische konstituion der Saanesande. Ber. schwyznaturf. Ges. H.2., 7-78
MULLER, J.E.	1941	Experimenten over het ontstaan van stroom ribbels. Geol. en Mijnb., Jrg. 3, 18-23
	1943	Sedimentpetrologie van het dekgebergte in himburg. Meded. Rijks. geol. Dienst. (Sticht) Ser. CII - 2, No. 2
NATIONAL PHYSICAL LABORATORY	1962	Modern computing methods. H.M.S.O. (S.O. Code No. 48-120-16 - 61).
NOTA, D.J.G.	1958	Sediments of the Western Guiana Shelf H. Veenman & Zonen, Wageningen.
OTTO, G.H.	1937	The use of statistical methods in effecting improvements on a Jones sampling splitter. J. Sediment. Petrol., 7, 110-132.
PAYNE, T.G.	1942	Stratigraphic analysis and environmental reconstruction. Bull. Amer. Ass. Petrol. Geol., 26, 1697 - 1770
PETTIJOHN, F.J.	1949	Sedimentary rocks. 2nd. Ed. Harper & Brothers. New York.
POLDERVAART, A.	1955	Zircon in rocks. I. Sedimentary rocks. Amer. J. Sci., 253, 433 - 461
	1956	Zircon in rocks. II. Igneous rocks. Amer. J. Sci., 253, 433-461
POSTMA, H.	1957	Size frequency distribution of sands in the Dutch Wadden Sea. Arch. n'eerl. Zool. 12, 319 - 349

RAO, C.R. 1952 Advanced statistical methods in Biometric research. John Wiley & Sons, Inc. New York.

READ, H. H. 1952 The Grampian Highlands. British Regional Geology. Rev. 2nd. Ed., H.M.S.O. Edinburgh.

RITTENHOUSE, G. 1943 The transportation and deposition of heavy minerals. Bull. geol. Soc. Amer., 54, 1725-1780

RUBEY, W.W. 1933 The size distribution of heavy minerals within a water-laid sandstone. J. Sediment. Petrol., 3, 3 - 29.

RUSSELL, R.D. 1936 The size distribution of minerals in Mississippi river sands. J. Sediment. Petrol., 6, 125 - 142.

RUSSELL, R.D. & TAYLER, R.E. 1937 Roundness and shape of Mississippi river sands. J. Geol., 45, 225 - 267.

SAHU, B.K. 1964 Depositional mechanisms from the size analysis of clastic sediments. J. Sediment Petrol., 34, 73 - 83.

SHARP, R.P. 1963 Wind ripples. J. Geol., 71, 617 - 636.

SHEPARD, F.P. & YOUNG R. 1961 Distinguishing between beach and dune sands. J. Sediment. Petrol., 31, 196 - 214.

SHEPARD, F. P. 1964 Criteria in modern sediments useful in recognizing ancient sedimentary environments. In: Developments in Sedimentology, Vol. I., 1 - 25. (Ed. Van Straaten). Elsevier Pub. Co., Amsterdam.

SHROCK, R.R. 1948 Sequence in layered rocks. McGraw-Hill, New York.

SIMPSON, J.B. 1933 The late-glacial readvance moraine of the Highland Border West of Tay. Trans. Roy.Soc. Edinb., 67, 633-646

and Others 1940 Discussion on the raised beaches of the Forth and Tay Advance Sci. Lond. (Rep.Brit. Assoc.), 1, 254-256.

SIMONS, D.B. & RICHARDSON, E.V. 1961 Forms of bed roughness in alluvial channels. Proc.Amer.Soc.civ. Engrs. No.HY3, Paper 2816, 87-105.

and Others 1961 Flume studies using medium sand (0.45mm). U.S.Geol.Surv.Water-Supply Paper 1498-A.

SINDOWSKI, F.K.H. 1949 Results and problems of heavy mineral analysis in Germany. A review of sedimentary petrological papers 1936-1948. J.Sediment. Petrol, 19, 3 - 25.

SLAVIIC, J. 1952 Heavy minerals from the weathered material of the eastern part of the pluton of Central Bohemia. Abstract Miner. Mag., 12, 263.

STRAATEN, L.M.J.U. van 1950 Giant ripples in tidal channels. Tijdschr. ned. aardijksk. Genoot., 67, 76-81. and 336-341.

1950 Periodic patterns of rippled and smooth areas on water surfaces induced by wind action. Proc.Kon.Ned.Akad.Wetensch., 51, 1217-1227.

STRAATEN, L.K.J.U. van — 1951 — Longitudinal ripples in mud and sand. J. Sediment. Petrol., 21, 47-54.

1953 — Mega ripples in the Dutch Wadden Sea and the Basin of Arcachan (France). Geol. en Mijnb., 15, 1 - 15.

1953 — Rhythmic patterns on Dutch North Sea beaches. Geol. en Mijnb., 15, 31-43.

1954 — Composition and structure of recent marine sediments in the Netherlands. Leid. geol. Meded., 19, 1-110.

& KUENEN, Ph. H. — 1957 — Accumulation of fine grained sediments in the Dutch Wedden Sea. Geol. en Mijnb., 19, 329-354.

STRAATEN, L.M.J.U. van — 1959 — Minor structures of some recent littoral and neritic sediments. Geol. en Mijnb., 21, 197-216.

STRIDE, A.H. — 1963 — Current-swept sea floors near the southern half of Great Britain. Quart. J. geol. Soc. Lond., 119, 175-199.

TANNER, W.F. — 1958 — An occurrence of flat-topped ripple marks. J. Sediment. Petrol., 28, 95-96.

1960 — Shallow water ripple mark varieties. J. Sediment. Petrol., 30, 481-485.

TEN HAAF, E. — 1956 — Significance of convolute laminations. Geol. en Mijnb., 18, 188-195.

THOMPSON, W.O. 1937 Original structures of beaches, bars and dunes.
Bull. geol. Soc. Amer., 48, 723-752.

TRASK, P.D. (Editor) 1939 Recent Marine Sediments. A Symposium.
Amer. Ass. Petrol. Geol., Tulsa.

TREFETHEN, J.M. & DOW, R.L. 1960 Some features of modern beach sediments.
J. Sediment. Petrol., 29, 564-574.

TYLER, S.A. & MARSDEN, R.W. 1937 A discussion of some errors introduced in accessory mineral separation.
Nat. Res. Counc. Ann. Rep., 3-9.

TYLER, S.A. 1940 Zircon studies in the New Jersey Highlands.
Amer. J. Sci., 238, 260-271.

TWENHOFEL, W.H. 1950 Principles of Sedimentation. 2nd Ed.
McGraw Hill, New York.

VANONI, V.A. 1941 Some experiments on the transportation of suspended load.
Trans. Amer. geophys. Un., 19, 608-621.

1946 Transportation of suspended sediment by water.
Trans. Amer. Soc. civ. Engrs., 111, 67-102

VEEN, J. van 1936 Onderzoekingen in de Hoofden.
s' - Gravenhage.

1938 Die unterseeische sandwuste in der Nordsee.
Geol. Meere, 2, 62-86.

VRIES, V. de 1949 Over de Granaat-Erts verhouding in garanaat-zandmonsters verzameld lange de Nederlandse Kust.
Natuurwet. Tijdschr., (Gent), 31, 195-200.

WEGNER, Th. 1932 Unter Gezeiteneinwirkung entstandene Wellenfurchen.
Zbl. Miner Geol. Palaont., Abt. B., 31-34.

WENTWORTH, C.K.	1932	A scale of grade and class terms for clastic sediments. J.Geol., 30, 377-392.
WILKS, S.S.	1948	Order statistics. Bull.Amer.math.Soc., 54, 6-50.
WOODFORD, A.O.	1935	Rhomboidal ripple mark. Amer.J.Sci., 29, 518-525.
WYATT, M.	1954	Zircons as provenance indicators. Amer.Min., 39, 983-990.
YULE, G.U. & KENDALL, M.G.	1958	An introduction to the theory of statistics. Griffin & Co.Ltd., London.
ZONNEVELD, J.I.S.	1946	Beschouwingen naar aanleiding van de korrelgrootte der zware mineralen in zandige sedimenten . Geol. en Mijnb., 8, 83-90.

APPENDIX I

Grain Size Parameters and Type of Grain Size Frequency Distributions.

Station	$Md\phi$	$M\phi$	$\sigma\phi$	$\alpha\phi$	$\alpha\phi 2$	$\beta\phi$	Remarks
1	1.13	1.19	0.55	+0.11	+0.34	0.77	F-
2	1.24	1,18	0.45	-0.13	-0.16	0.62	F M
3	1.43	1.39	0.47	-0.09	+0.05	0.84	F
4	1.56	1.66	0.56	+0.18	+0.32	0.70	F
5	1.16	1.55	0.46	+0.85	+0.64	0.73	F M
6	1.92	1.90	0.54	-0.04	+0.40	1.25	F M
7	2.00	1.92	0.49	-0.16	-0.60	0.72	F M
8	2.11	2.14	0.50	+0.06	+0.43	1.05	F M
9	2.15	2.19	0.47	+0.09	+0.38	0.98	F M
10	2.56	2.63	0.58	+0.12	+0.30	0.89	F M
11	2.76	4.08	2.08	+0.64	...	...	F
12	2.56	2.83	1.09	+0.58	.	.	F M
13	2.32	2.41	0.56	+0.04	+0.23	0.69	F M
14	2.37	2.46	0.44	+0.07	+0.17	0.88	M + pebbles
15	2.72	2.68	0.41	+0.14	+0.36	0.93	M
16	2.29	2.15	0.70	+0.54	+0.76	0.63	M C
17	3.16	3.47	1.43	+0.76	+0.53	0.84	M S
18	2.77	3.25	2.21	-0.34	-0.02	1.32	F M + pebbles

Station	$Md\phi$	$M\phi$	$\sigma\phi$	$\alpha\phi$	$\alpha\phi 2$	$\beta\phi$	Remarks
19	1.21	.	.	.	.	.	B M + pebbles
20	1.89	1.94	0.47	-0.32	-0.53	0.86	M
21	0.96	.	.	.	.	.	B S + pebbles
22	1.73	.	.	..	.	.	B M + Pebbles
23	1.23	.	.	.	.	.	B M + granule
24	2.32	.	.	.	.	.	B S + granule
25	4.32	.	.	.	.	.	B S + pebbles
26	2.97	.	.	.	.	.	M S
27	3.23	.	.	.	.	.	B S + granule
28	4.03	.	.	.	.	.	M S
29	2.75	.	.	.	.	.	B M + granule
30	3.84	.	.	.	.	.	B S
31	2.98	2.74	0.67	+0.07	+0.21	0.68	M S + granule
32	2.70	2.65	0.36	-0.14	-0.54	0.88	M
33	2.39	2.36	0.36	-0.09	-0.19	0.92	M
34	2.53	2.56	0.38	+0.08	-0.01	1.63	M + pebbles
35	2.76	2.72	0.41	-0.11	-0.65	1.53	M
36	2.82	2.77	0.27	-0.18	-0.76	2.05	M
37	2.73	2.59	0.41	-0.34	-0.94	0.44	M + pebbles
38	2.51	2.39	0.56	-0.22	-0.46	0.85	M
39	2.39	2.46	0.32	+0.21	+0.50	1.16	M
40	2.50	2.42	0.39	-0.22	-0.49	0.84	M
41	2.26	2.22	0.29	-0.14	-0.48	1.14	M

Station	$Md\phi$	$M\phi$	$\sigma\phi$	$\alpha\phi$	$\alpha\phi_2$	$\beta\phi$	Remarks
42	2.60	2.61	0.29	+0.01	-0.03	0.95	M
43	2.64	2.58	0.33	-0.26	-0.24	0.91	M
44	2.60	2.52	0.42	-0.06	-0.24	0.76	M
45	2.30	2.25	0.37	-0.13	-0.31	0.80	M
46	2.51	2.48	0.30	-0.08	-0.49	1.27	M
47	2.52	2.50	0.30	-0.08	-0.23	0.87	M
48	2.49	2.48	0.30	-0.05	-0.30	0.83	M
49	2.64	2.63	0.41	+0.02	-0.39	0.34	M
50	2.59	2.54	0.29	-0.17	-0.27	0.97	M
51	2.54	2.43	0.36	-0.03	-0.53	0.86	M
52	2.53	2.43	0.42	-0.23	-0.50	0.73	M
53	2.44	2.41	0.42	-0.07	-0.31	0.75	M
54	2.46	2.39	0.37	-0.18	-0.48	0.75	M
55	2.42	2.36	0.38	-0.17	-0.45	0.76	M
56	2.36	2.30	0.39	-0.16	-0.42	0.78	M
57	2.27	2.36	0.38	+0.25	-0.36	0.36	M
58	2.30	2.23	0.42	-0.21	-0.36	0.48	M
59	2.54	2.46	0.35	-0.23	-0.66	1.06	M
60	2.53	2.43	0.39	-0.25	-0.70	0.91	M
61	2.53	2.41	0.38	-0.31	-0.69	0.96	M
62	2.52	2.41	0.40	-0.27	-0.74	0.76	M
63	2.51	2.41	0.36	-0.27	-0.80	0.94	M
64	2.54	2.47	0.36	-0.19	-0.50	1.06	M

Station	Mdϕ	Mϕ	$\sigma\phi$	$\alpha\phi$	$\alpha\phi_2$	$\beta\phi$	Remarks
65	2.32	2.25	0.47	-0.16	-0.39	0.62	M
66	2.50	2.48	0.31	-0.06	-0.23	1.07	M
67	2.49	2.40	0.36	-0.25	-1.09	1.06	M
68	2.44	2.41	0.36	-0.08	-0.04	0.92	M
69	2.36	2.29	0.35	-0.20	-0.50	0.92	M
70	2.31	2.14	0.45	-0.37	-0.44	0.75	M
71	2.51	2.54	0.58	+0.05	-0.02	0.41	M
72	2.48	2.41	0.52	+0.01	-0.00	0.54	M
73	2.36	2.30	0.45	-0.13	-0.25	0.72	M
74	2.32	2.22	0.41	-0.24	-0.40	0.74	M
75	2.36	2.25	0.37	-0.29	-0.49	0.77	M
76	2.06	1.89	0.60	-0.28	-0.42	0.44	M
77	2.56	2.58	0.38	+0.05	+0.03	0.34	M
78	2.72	2.73	0.33	+0.09	+0.01	0.66	M
79	2.47	2.46	0.35	-0.02	-0.21	0.89	M
80	2.59	2.60	0.24	+0.02	+0.06	0.81	M
81	2.53	2.52	0.24	-0.04	+0.14	0.56	M
82	2.47	2.45	0.24	-0.08	-0.10	0.73	M
83	2.47	2.43	0.26	-0.15	-0.62	1.06	F M
84	2.40	2.31	0.33	-0.27	-0.65	0.94	F M
85	1.75	1.39	0.98	+0.32	+0.58	0.87	F

Station	$Md\phi$	$M\phi$	$\sigma\phi$	$\alpha\phi$	$\alpha\phi_2$	$\beta\phi$	Remarks
86	1.38	1.21	0.76	+0.28	+0.18	0.64	F
87	1.32	1.10	1.06	+0.08	+0.38	0.59	F +Granule
88	1.50	1.26	0.64	+0.21	+0.63	0.62	F
89	1.28	1.26	0.55	+0.07	+0.26	0.69	F + granule
90	2.03	2.58	0.58	+0.18	+0.37	0.86	F M
91	2.00	1.91	0.43	-0.21	-0.77	0.94	F M
92	3.38	3.15	0.84	-0.28	-0.10	0.93	M S
93	2.51	2.35	0.49	-0.34	-0.76	0.90	M + pebbles
94	2.85	2.86	0.33	+0.02	0.00	0.66	F M
95	2.85	2.83	0.24	-0.08	-0.40	1.23	M S
96	2.43	2.04	0.36	-0.37	-0.54	0.87	M
97	2.30	2.26	0.38	-0.12	-0.27	0.71	M
98	2.17	2.11	0.45	-0.13	-0.29	0.60	M
99	2.24	2.25	0.45	-0.09	-0.50	0.99	M
100	2.35	2.36	0.36	+0.01	-0.65	0.92	M
101	2.53	2.50	0.29	-0.10	-0.14	0.83	M
102	2.17	2.13	0.48	-0.10	-0.43	0.72	M
103	2.39	2.28	0.44	-0.25	-0.53	0.63	M
104	2.17	2.19	0.47	+0.03	-0.27	0.52	M
105	2.04	1.97	0.37	-0.19	-0.45	0.88	M
106	2.04	1.99	0.36	-0.16	-0.45	0.72	M

Station	Md_ϕ	M_ϕ	σ_ϕ	α_ϕ	$\alpha_{\phi 2}$	β_ϕ	Remarks
107	2.05	2.00	0.41	-0.12	-0.28	0.74	M
108	1.89	1.84	0.40	-0.13	-0.29	0.64	M
109	2.33	2.28	0.39	-0.14	-0.12	0.65	M
110	2.18	2.15	0.35	-0.09	-0.39	1.01	M
111	2.15	2.10	0.40	-0.14	-0.35	0.82	M
112	2.35	2.36	0.29	+0.04	+0.07	0.72	M
113	2.25	2.22	0.29	-0.10	-0.24	0.83	M
114	2.06	2.05	0.49	-0.03	-0.39	0.67	M
115	2.36	2.40	0.34	+0.10	0.00	0.82	M
116	2.08	2.05	0.35	-0.10	-0.28	0.70	M
117	2.24	2.23	0.30	-0.05	-0.36	0.92	M
118	2.03	2.08	0.29	+0.16	+0.30	0.63	M
119	2.27	2.22	0.39	-0.13	-0.54	0.90	M
120	2.48	2.46	0.37	-0.05	-0.38	1.05	M
121	2.18	2.04	0.48	-0.31	-0.75	0.85	M
122	2.60	2.61	0.25	+0.03	+0.08	0.89	M
123	2.55	2.46	0.28	-0.32	-0.36	0.57	M
124	2.34	2.32	0.32	-0.05	-0.13	0.87	M
125	2.51	2.50	0.30	-0.08	-0.12	0.84	M
126	2.53	2.49	0.37	-0.21	-0.53	0.96	M
127	2.06	2.02	0.36	-0.12	-0.31	0.75	M

APPENDIX 11

Moment Measures and Grain Size Frequency Distribution

Station	Mean	Standard Deviation	Skewness	Kurtosis	Remarks
1	1.0652	0.8923	+0.6621	4.6174	F
2	1.1341	0.7512	-0.7636	5.3881	F M
3	1.3237	0.8241	-0.5426	3.0996	F
4	1.9389	0.9873	+1.1426	3.6621	F
5	1.0113	0.7634	+1.5021	4.3428	F M
6	1.8274	0.7230	-0.1629	5.0887	F M
7	2.0975	0.8613	-0.9621	4.2981	F M
8	2.2120	0.5612	+0.3638	3.9974	F M
9	2.0293	0.9723	+0.5454	4.6753	F M
10	2.8832	1.2201	+0.7284	5.6670	F M
32	2.6394	0.4509	-1.1352	6.2767	M
33	2.3548	0.4181	-0.1380	4.6692	M
34	2.5887	0.4855	+1.0674	5.4870	M
35	2.7207	0.6161	-0.7640	4.6690	M
36	2.7639	1.5194	-0.7745	5.3681	M
37	2.6072	0.5797	-1.0703	4.7579	M
38	2.7589	0.7332	-0.5402	2.9699	M

Station	Mean	Standard Deviation	Skewness	Kurtosis	Remarks
39	2.4467	0.3592	-0.1689	4.3137	M
40	2.4170	0.4546	-0.7428	3.6957	M
41	2.2298	0.4439	-0.0587	7.3405	M
42	2.6141	0.3705	-0.2255	5.2198	M
43	2.6211	0.4063	-0.2793	4.9563	M
44	2.5638	0.4825	-0.3216	3.8182	M
45	2.2400	0.4127	-0.5694	4.1961	M
46	2.4854	0.3606	-0.8154	5.9276	M
47	2.4931	0.3600	-0.6639	5.6239	M
48	2.4637	0.3533	-0.7204	5.5918	M
49	2.5995	0.3665	-0.7449	6.7666	M
50	2.5619	0.3734	-0.5441	5.2929	M
51	2.4796	0.4101	-0.7756	5.2946	M
52	2.4367	0.4545	-0.7258	4.2994	M
53	2.4027	0.4479	-0.6836	4.0529	M
54	2.3064	0.4195	-0.7939	4.1879	M
55	2.3593	0.4192	-0.9751	4.7741	M
56	2.3888	0.4181	-1.2326	5.7646	M
57	2.2684	0.4654	-1.0115	5.3616	M
58	2.3247	0.4453	-0.9867	5.7620	M
59	2.3902	0.4366	-0.7941	5.8493	M

Station	Mean	Standard Deviation	Skewness	Kurtosis	Remarks
60	2.3798	0.4503	-0.5885	5.6517	M
61	2.3979	0.4724	-0.7279	5.6174	M
62	2.3761	0.4930	-0.8977	5.2256	M
63	2.3524	0.4198	-1.0305	5.9526	M
64	2.3907	0.3808	-0.6329	6.2482	M
65	2.2034	0.5454	-0.4571	2.5286	M
66	2.4418	0.3794	-0.4716	4.6113	M
67	2.3624	0.4994	-1.1192	4.8878	M
68	2.3834	0.4069	-0.3579	4.4313	M
69	2.2924	0.4231	-0.3692	5.8521	M
70	2.1717	0.4590	-0.3978	2.8879	M
71	2.5154	0.5344	-0.1350	2.8981	M
72	2.4292	0.5238	-0.1101	3.1812	M
73	2.3098	0.4840	-0.2363	3.6960	M
74	2.2470	0.4633	-0.0883	5.2093	M
75	2.2569	0.4537	-0.3195	3.6876	M
76	1.9354	0.5759	-0.2780	2.3587	M
77	2.5696	0.3731	+0.3101	4.0132	M
78	2.7513	0.4138	+0.0290	2.8264	M
79	2.4451	0.4408	-0.2635	4.3531	M
80	2.5844	0.3172	+0.5179	4.3625	M

Station	Mean	Standard Deviation	Skewness	Kurtosis	Remarks
81	2.5150	0.3206	+0.3818	4.7785	M
82	2.4275	0.3014	-0.0311	5.4996	M
83	2.3950	0.3711	-0.7605	5.7197	F M
84	2.3066	0.4268	-0.8160	4.7793	F M
85	1.0052	0.9897	+0.0634	6.4208	F
91	2.3900	0.5852	-0.7141	3.7178	F M
92	2.8695	0.4023	-0.5717	5.0596	M S
93	1.9279	0.4902	-0.6543	4.0703	M
94	2.9099	0.4051	-0.1922	3.4153	F M
95	3.2447	0.8253	-0.6755	2.5051	M S
97	2.2467	0.4265	-0.3306	4.1024	M
98	2.1096	0.4713	-0.3962	3.0960	M
99	2.0007	0.4653	-0.4329	4.0217	M
100	2.2816	0.4441	-0.9208	4.4055	M
101	2.5054	0.3675	+0.0603	4.2693	M
102	2.1160	0.5107	-0.5870	3.1653	M
103	2.2888	0.4783	-0.6603	3.4464	M
104	2.1258	0.4546	-0.4230	3.2161	M
105	1.9652	0.4179	-0.7304	3.4527	M
106	1.9708	0.4199	-0.4830	3.2188	M

Station	Mean	Standard deviation	Skewness	Kurtosis	Remarks
107	1.9929	0.4656	-0.3007	2.9039	M
108	1.8232	0.4329	-0.2251	2.0090	M
109	2.2900	0.4442	-0.1064	3.5791	M
110	2.1378	0.4269	-0.4706	4.3687	M
111	2.0998	0.4688	-0.3716	3.7471	M
112	2.3645	0.3316	+0.2082	5.0874	M
113	2.2194	0.3479	-0.4444	4.7901	M
114	1.9858	0.5154	-0.4062	3.0165	M
115	2.4651	0.3184	+0.3582	3.8428	M
116	2.2897	0.4420	-0.7232	5.6227	M
117	2.1993	0.3440	-0.4823	4.6075	M
118	1.9806	0.4381	-0.4460	3.0846	M
119	2.2104	0.4671	-0.6428	4.2131	M
120	2.4885	0.5142	-0.5810	5.6331	M
121	2.0493	0.5231	-0.7893	3.3643	M
122	2.3015	0.4145	-0.2688	4.1753	M
123	2.3578	0.4001	-0.2129	4.9946	M
124	2.0385	0.4032	-0.3893	3.4982	M
125	2.3500	0.4269	-0.0030	4.9809	M
126	2.3863	0.4320	-0.4238	4.5320	M
127	1.9899	0.5007	-0.2594	3.6539	M

APPENDIX III

Heavy Mineral Analyses
(percentage by number, alterite in % of other mineral grains).

N-Hornblende Association

Mineral	Sample Stations									
	1	2	3	4	5	6	7	9	10	12
Alterites	25	22	20	23	19	17	16	14	10	12
Anatase	.	.	.	1	.	.	.	.	.	1
Andalusite	.	1	.	.	1	.	.	.	.	1
Apatite	1	1	1	1	.	.	.	.	1	1
Augite	2	2	.	2	.	1	1	.	1	.
Biotite & Muscovite	5	6	4	5	6	3	4	2	1	2
Brookite	.	.	.	.	.	1	.	.	.	.
Chlorite	4	3	4	3	2	3	1	3	1	1
Corundum	.	.	.	.	.	.	.	.	.	.
Epidote	7	10	4	8	8	7	6	4	6	7
Garnet	22	20	21	28	26	28	30	30	36	28
Hornblende	44	40	55	36	41	39	41	49	28	38
Hypersthene	3	2	1	3	1	1	1	1	1	1
Kyanite	.	1	.	.	1	1	.	.	1	.
Magnetite & Ilmenite	10	12	7	10	13	15	15	10	22	20

Mineral	Sample	Stations								
	1	2	3	4	5	6	7	9	10	12
Monazite	.	.	.	.	.	.	.	.	.	.
Rutile	.	.	.	.	.	.	.	.	.	.
Sillimanite	.	1	.	1	.	.	.	.	.	.
Spinel	.	.	.	.	.	.	.	1	.	.
Staurolite	.	.	2	.	.	1	.	.	.	.
Topaz	.	1	.	1	.	.	.	.	.	.
Tourmaline	1	.	.	.	.	.	.	.	1	.
Zircon	1	.	1	1	1	.	1	.	1	.

APPENDIX IV

Heavy Mineral Analyses
(percentage by number, alterite in % of other mineral grains).

M-Garnet Association

Minerals	Sample Stations															
	97	98	99	100	101	103	104	106	109	111	112	113	114	117	119	121
Alterite	9	12	9	16	9	9	11	16	9	13	7	6	14	12	11	14
Anatase	.	.	.	.	.	.	.	.	.	.	.	.	.	.	.	.
Andalusite	.	.	.	.	.	.	.	.	.	.	.	.	.	.	.	.
Apatite	.	.	.	.	1	.	.	1	.	.	.	.	1	.	.	1
Augite	.	.	.	.	1	1	.	.	.	.	.	.	.	.	.	.
Biotite - Muscovite	.	1	.	1	.	.	1	.	.	.	.	.	.	.	.	.
Brookite	.	.	.	.	.	.	.	.	.	.	.	.	.	.	.	.
Chlorite	.	1	.	.	.	1	.	1	..	.	.	.	.	.	.	1
Corundum	.	.	.	.	.	.	.	.	.	.	.	.	.	.	.	.
Epidote	2	7	5	3	4	3	6	4	3	6	3	.	6	8	4	5
Garnet	67	50	63	55	60	48	54	44	60	55	77	91	57	46	70	51
Hornblende	16	28	19	24	17	29	29	39	14	20	9	3	18	30	11	25
Hypersthene	2	3	2	4	5	4	4	2	1	1	2	.	1	3	1	1
Kyanite	1	.	.	1	.	1	.	.	.	.	1	.	1	1	.	2
Magnetite-Ilmenite	9	8	7	9	8	8	2	3	18	10	6	4	12	6	8	7

Minerals	Sample Stations															
	97	98	99	100	101	103	104	106	109	111	112	113	114	117	119	121
Monazite	.	.	.	.	.	.	.	.	.	.	.	.	.	.	.	.
Rutile	.	.	.	.	.	.	.	.	.	.	.	.	.	.	.	.
Sillimanite	.	.	.	.	..	.	.	.	1	1	.	.	.	.	.	.
Spinel	.	.	.	.	.	.	.	.	.	.	.	.	.	.	.	.
Staurolite	.	.	.	.	.	.	.	.	.	1	1	.	.	.	.	.
Topaz	.	.	.	.	.	.	.	.	.	.	.	.	.	.	.	.
Tourmaline	1	.	1	1	1	1	1	1	1	.	.	.	.	1	.	1
Zircon	2	2	3	2	3	4	3	5	2	6	1	2	4	5	6	6

APPENDIX V

Heavy Mineral Analyses
(percentage by number, alterite in % of other mineral grains).

T-Garnet Association

Minerals	Sample Stations															
	35	38	39	44	45	48	49	50	51	52	54	56	59	64	65	67
Alterite	19	23	10	14	9	12	6	8	7	15	11	17	11	8	25	12
Anatase	1	.	.	.	.	.	.	.	.	.	.	.	.	.	.	.
Andalusite	.	1	.	.	.	.	.	.	.	.	.	.	.	.	.	.
Apatite	.	1	1	1	.	1	.	.	.	.	.	.	1	1	1	1
Augite	.	1	.	1	.	.	.	.	.	.	.	.	.	.	.	.
Biotite-Muscovite	.	2	1	2	.	1	.	1	.	.	.	.	.	.	.	.
Brookite	.	.	.	.	.	.	.	.	.	.	.	.	.	.	.	.
Chlorite	1	2	1	2	.	2	.	1	.	1	.	.	1	1	.	.
Corundum	.	.	.	.	.	.	.	.	.	.	.	.	.	.	.	.
Epidote	7	9	2	6	3	5	2	3	1	2	3	4	8	9	10	4
Garnet	38	44	48	39	49	39	48	37	51	43	49	37	42	39	31	46
Hornblende	18	19	23	25	24	28	27	29	31	33	27	39	25	19	33	17
Hypersthene	2	4	1	2	1	3	1	6	1	5	2	4	3	2	7	6
Kyanite	.	1	1	1	1	1	.	.	1	.	.	1	2	2	1	.
Magnetite-Ilmenite	29	13	20	17	18	16	20	19	13	14	15	12	8	19	8	17

Minerals	Sample Stations															
	35	38	39	44	45	48	49	50	51	52	54	56	59	64	65	67
Monazite	.	.	.	.	.	.	.	.	.	.	.	.	1	1	.	1
Rutile	.	.	.	.	.	.	.	.	.	.	.	.	.	.	.	.
Sillimanite	.	.	.	1	.	.	1	1	.	.	1	.	1	.	1	1
Spinel	.	.	.	.	.	1	.	.	.	.	.	.	.	.	.	.
Staurolite	.	.	.	1	1	1	.	.	.	.	.	1	.	1	.	.
Topaz	.	.	.	.	.	.	.	1	.	.	.	1	1	.	.	1
Tourmaline	1	1	.	1	.	1	.	1	.	1	.	.	1	1	2	1
Zircon	3	2	2	1	3	1	1	1	2	1	3	1	6	5	6	5

Minerals	Sample Stations																
	68	69	70	71	72	73	74	75	76	77	78	79	80	81	82	83	84
Alterite	6	13	18	1	3	7	4	13	13	8	7	6	8	12	13	22	10
Anatase	.	.	.	.	.	.	.	.	.	.	.	.	.	.	.	.	.
Anadalusite	.	.	.	.	.	.	.	.	.	.	.	.	.	.	.	.	.
Apatite	1	1	1	.	.	.	.	.	.	.	.	.	.	.	.	1	.
Augite	.	.	.	.	.	.	.	.	.	.	.	.	.	.	.	.	.
Biotite-Muscovite	.	.	.	.	.	.	.	.	.	.	.	.	.	.	.	.	.
Brookite	.	.	1	.	.	.	.	.	.	.	.	.	.	.	.	.	.
Chlorite	1	.	2	.	.	.	.	.	1	.	.	.	.	.	.	.	.
Corundum	1	.	.	.	1	.	1	.	.	1	.	.	.	.	.	.	.
Epidote	8	5	10	1	3	6	3	5	11	6	6	5	8	7	9	3	7
Garnet	35	38	28	59	55	59	66	54	52	55	50	52	49	38	47	36	47
Hornblende	19	26	38	1	7	11	9	21	14	13	17	18	27	27	18	31	24
Hypersthene	4	9	3	1	1	2	2	7	2	1	1	1	.	9	2	7	2
Kyanite	1	1	1	.	1	.	.	.	1	1	1	1	.	1	1	1	1
Magnetite-Ilmenite	20	11	8	36	30	17	15	8	12	16	18	18	8	8	17	13	13
Monazite	.	.	.	1	1	.	1	1	1	1	1	.	1	.	.	.	.
Rutile	1	.	.	.	.	.	.	.	.	.	1	.	.	1	.	1	.
Sillimanite	1	.	1	.	.	.	.	.	1	1	.	1	1	.	.	.	1
Spinel	.	.	.	.	.	.	.	.	.	.	.	.	.	.	.	.	.

Minerals	Sample Stations																
	68	69	70	71	72	73	74	75	76	77	78	79	80	81	82	83	84
Staurolite	1	.	1	.	.	.	.	.	1	1	1	.	1	.	1	.	1
Topaz	1	.	1	.	.	.	.	.	.	.	.	1	1	.	.	.	.
Tourmaline	1	1	2	.	.	1	1	1	1	1	1	.	1	.	1	1	1
Zircon	5	8	3	1	1	4	2	3	3	3	3	3	3	9	4	6	3

APPENDIX VI

Relation between Number % of Grains and accuracy of Counts

Sample Nr. 115

Minerals	Number % in Counts of								
	100	200	300	400	500	600	1000	2000	3000
Alterites	2	3	3	3	3	3	3	3	3
Anatase	.	.	.	.	.	.	.	.	.
Andalusite	.	.	.	.	.	.	.	.	.
Apatite	1	.	.	.	.	.	.	.	.
Augite	.	.	.	.	.	.	.	.	.
Biotite & Muscovite	.	.	.	.	.	.	.	.	.
Brookite	.	.	.	.	.	.	.	.	.
Chlorite	2	1	1	1	1	1	1	1	1
Corundum	.	.	.	.	.	.	.	.	.
Epidote	2	2	1	1	1	1	1	1	1
Garnet	67	69	68	68	69	69	67	68	67
Hornblende	10	10	10	9	7	8	7	8	8
Hypersthene	1	1	1	1	1	1	1	1	1
Kyanite	1	1	.	1	1	.	1	1	1

Minerals	Number % in Counts of								
	100	200	300	400	500	600	1000	2000	3000
Magnetite & Ilmenite	11	14	16	15	16	16	19	18	19
Monazite	.	.	.	.	.	.	.	.	.
Rutile	.	.	.	.	.	.	.	.	.
Sillimanite	1	.	.	.	.	.	.	.	.
Spinel	.	.	.	.	.	.	.	.	.
Staurolite	1	1	1	1	1	1	1	1	1
Topaz	.	.	.	.	.	.	.	.	.
Tourmaline	1	.	.	1	1	1	.	.	.
Zircon	2	2	2	2	2	2	2	1	1

APPENDIX V11

Fraction Analyses of Two Samples from the Area

	Sample No. 8							Sample No. 74						
	Size Grade in Microns													
Minerals	500 to 297	297 to 251	251 to 178	178 to 149	149 to 124	124 to 74	74 to 33	500 to 297	297 to 251	251 to 178	178 to 149	149 to 124	124 to 74	74 to 33
Alterites	41	18	16	21	23	10	5	33	25	24	9	8	5	3
Anatase	.	.	.	.	.	.	.	.	.	.	.	.	.	.
Andalusite	.	.	.	.	.	.	.	.	.	.	.	.	.	.
Apatite	1	.	.	1	.	2	4	.	1	1	2	.	.	.
Augite	3	2	1	.	.	.	.	.	.	.	.	.	.	.
Biotite & Mucovite	7	9	2	.	.	.	.	.	.	.	.	.	.	.
Brookite	.	.	.	.	.	.	.	.	.	.	.	.	.	.
Chlorite	20	2	20	6	12	3	.	3	.	1	.	.	.	.
Corundum	.	.	.	.	.	.	.	.	.	.	.	.	.	.
Epidote	.	.	.	11	15	9	1	13	16	11	16	9	3	1
Garnet	7	32	44	30	22	31	39	27	41	37	35	55	63	7
Hornblende	60	54	30	34	34	33	12	46	33	40	27	19	7	1
Hypersthene	1	.	.	7	7	5	2	1	1	2	1	2	.	.

Minerals	Size Grade in Microns													
	500 to 297	297 to 251	251 to 178	178 to 149	149 to 124	124 to 74	74 to 33	500 to 297	297 to 251	251 to 178	178 to 149	149 to 124	124 to 74	74 to 33
Kyanite	.	.	.	2	1	3	.	.	.	.	.1	1	.	.
Magnetite & Ilmenite	.	1	2	4	5	8	25	8	8	5	4	8	23	64
Monazite	.	.	.	.	.	.	.	.	.	.	.	.	.	.
Rutile	.	.	.	.	.	.	.	.	.	.	.	.	.	.
Sillimanite	.	.	.	.	.	.	.	.	.	.	.	.	.	.
Spinel	.	.	.	.	.	.	.	.	.	.	.	.	.	.
Staurolite	1	.	.	.	1	.	.	.	.	1	1	1	1	.
Topaz	.	.	.	.	.	.	.	.	.	.	.	.	.	.
Tourmaline	.	.	.	1	1	.	1	1	.	1	2	1	.	.
Zircon	.	.	1	4	2	6	16	1	.	1	2	4	3	27

APPENDIX VIII

Program 1 for Moment Measures Computation

```
JOB

U EDIN, GEO, MISHRA PROGRAM 1

COMPILER ATLAS AUTOCODE


begin

real x, f, fc, fx, fxs, fxc, fxu, a, b, c, d, e, g

integer i, j

array X(1 : 83, 1 : 13)


cycle i = 1, 1, 83

cycle j = 1, 1, 13

read (X(i, j))

repeat

repeat

cycle i = 2, 1, 83

j = 1

fc = 0; fx = o; fxs = o; fxc = o; fxu = o; a = o; b = o; c = o; d = o; e = o; g = o
```

```
1 : x = x (1, j)

j = j + 1

2 : unless X (i, j) = 999999 then→3

j = j + 1

→2

3: x = (x+X (1, j)) / 2

f = X (i, j)

fc  =  fc + f

fx = fx + f * x

fxs = fxs + f * x^2

fxc = fxc + f * x ↑ 3

fxu = fxu + f * x ↑ 4

unless j = 13 then →1


a = fx / fc

b = sq rt (fxs / fc - a^2 )

c = fxc / fc - 3 *a*fxs / fc + 2 *a↑3

d = fxu/fc - 4 *a* fxc / fc + 6 *a^2* fxs / fc - 3 *a↑ 4

e = c /b↑ 3

g = d / b↑ 4


print (i, 2, 0)

caption s̸ b̸ b̸ b̸ mean b̸ b̸;

print (a, 2, 4)
```

```
caption ƀ ƀ ƀ sd ƀ ƀ;

print (b, 2, 4)

caption ƀ ƀ ƀ m3 ƀ ƀ; print (c, 2, 4)

caption ƀ ƀ ƀ m4 ƀ ƀ; print (d, 2, 4)

newline

caption skewness ƀ ƀ; print (e, 2, 4)

caption ƀ ƀ ƀ kurtosis ƀ ƀ; print (g, 2, 4)

newline

repeat


end

***z
```

APPENDIX IX

Program 2 for Moment Measures Computation

```
JOB

U EDIN, GEO MISHRA, PROGRAM 2 21-8-63 TRANS. 217

COMPUTING 5000 INSTRUCTIONS

OUTPUT O TELETYPE 100 LINES

COMPILER AA


begin

real x, f, fc, fx, fxs, fxc, fxu, a, b, c, d, e, g

integer i, j

array X (1 : 36, 1 : 9)


newline

Caption data date

cycle i = i, 1, 3

read (j)

print (j, 1, p)

space

repeat

newline; spaces (5)
```

```
caption mean ₺₺₺₺ sd ₺₺₺₺₺₺ skewness ₺₺ kurtosis ₺₺₺₺ m3 ₺₺₺₺₺₺ m4

cycle i = i, 1, 36
cycle j - 1, 1, 9
read (X(i,j))
repeat
repeat
cycle i = 2, 1, 36
j = 1
fc = o; fx = o; fxs = o; fxc = o; fxu = o; a = o; b = o; c = o; d = o; e = o; g = o
1 : x = X (1, j)
j = j + 1
2 : unless X (i, j) = 999 then →3
j = j + 1
→2
3: x = (x+X (1, j)) / 2
f = X(i, j)
fc = fc + f
fx = fx + f * x
fxs = fxs + f * x^2
fxc = fxc + f * x↑3
fxu = fxu + f * x↑4
unless j = 9 then →1
```

```
a = fx / fc

b = sq rt (fxs / fc - a^2)

c = fxc / fc - 3 *a*fxs / fc + 2 *a↑3

d = fxu / fc - 4 *a* fxc / fc + 6 *a^2* fxs / fc - 3 *a↑ 4

e = c / b↑ 3

g = d / b↑ 4


newline


print (i-1, 3, o); space

print (b, 2, 4); space

print (b, 2, 4); spaces (3)

print (e, 2, 4); space

print (g, 2, 4); spaces (5)

print (c, 2, 4); space

print (d, 2, 4)

repeat


end of program


***T
```

APPENDIX X

Regression Program for Estimating Relationship Between Variables (Moment Measures)

```
JOB

U  EDIN, GEO MISHRA, PROGRAM REGRESSION 2 TRANS. 320

COMPUTING 5000 INSTRU CTIONS

OUTPUT O TELETYPE 100 LINES

COMPILER AA


begin

real x, y, xi, x2, x3, cy, ci, c2, c3, c

cyy, cyl, cy2, cy3, c11, c12, c13, c33, c

c22, c23, s11, s12, s13, s22, s23, s33


integer i,j

array X (1:4, 1:82)

cycle j = 1,1,82

cycle i = 1,1,4

read (X (i,j))

repeat

repeat
```

```
x=o; cyy=o; cy1=o; cy2=0; cy3=o; c11=o
c12=o; c13=o; c22=o; c23=o; c33=o
cycle j = 1, 1, 82
X(2, j) = X(2, j)/X(1, j)
repeat
cycle i = 1, 1, 4; x=o
cycle j = 1, 1, 82
x=x+X(i, j)
repeat
if i = 1 then y = x/82
if i = 2 then x1 = x/82
if i = 3 then x2 = x/92
if i = 4 then x 3 = x/82
repeat
cycle j = 1, 1, 82
cy = X(1, j)-y
ci = X(2, j)-xi
c2 = X(3, j)-x2
c3 = X(4, j)-x3

cyy = cyy + cy^2
cy1 = cy1 + cy*ci
cy2 = cy2 + cy*c2
```

```
cy3 = cy3 + cy*c3
c11 = c11 + c1*c1
c12 = c12 + c1*c2
c13 = c13 + c1*c3
c22 = c22 + c2*c2
c23 = c23 + c2*c3
c33 = c33 + c3^2
repeat
caption normal ƀ equations ƀƀ; newline
print (cy1,4,4); spaces (3); print (c11,4,4); space
print (c12,4,4); space; print (c13,4,4); newline
print (cy2,4,4); spaces (3) ; print (c12,4,4); space
print (c22,4,4); space; print (c23,4,4); newline
print (cy3,4,4); spaces (3); print (c13,4,4); space
print (c23,4,4); space; print (c33,4,4); newline
s11 = sqrt (c11)
s12 = c12/s11
s13 = c13/s11
s22 = sqrt (c22-s12^2)
s23 = (c23-s12*s13)1s22
s33 = sqrt (c33-s13^2-s23^2)
```

```
c33 = 1/ s33²
c23 = (-c33*s23)/ s22
c13 = (-c33*s13-c23*s12)/ s11
c22 = (1/ s22-c23*s23)/ s22
c12= (-c23*s13-c22*s12)/ s11
c11= (1/ s11-c13*s13-c12*s12)/ s11
caption inverse ¢ matrix ¢l ; newline
print (c11, 4, 7); print (c12, 4, 7); print (c13, 4, 7); newline
spaces (12); print (c22, 4, 7); print (c23, 4, 7); newline
spaces (24); print (c33, 4, 7); newline; newline
c1= c11*cy1+c12*cy2+c13*cy3
c2 = c12*cy1+c22*cy2+c23*cy3
c3 = c13*cy1+c23*cy2+c33*cy3
x = sqrt ((cyy-c1*cy1-c2*cy2-c3*cy3)/ 77)
caption regression ¢ equation ¢l¢¢ mean ¢=¢
print (y, 2, 3)
caption ¢+¢; print (c1, 2, 4)
caption ¢+or -¢; print (1.66*x*sqrt(c11), 2, 4)
caption ¢ (sd ¢-¢; print (x1, 2, 3)
caption )¢+¢; print (c2, 2, 4)
caption ¢+ or -¢; print (1.66*x*sqrt(c22), 2, 4)
caption (skewness - ¢; print (x2, 2, 3)
caption )¢ +¢; print (c3, 2, 4)
caption ¢+ or -¢; print (1.66*x*sqrt(c33), 2, 4)
caption (kurtosis ¢-¢; print (x3, 2, 3)
```

```
caption ); newline; newline
caption deviations bldd
cycle j= 1,1,82
x=x (1,j)-y-cl*(X(2,j)-xl)-c2*(X(3,j)-x2)-c3*(X(4,j)-x3)
print (j,2,0); space
print (x,3,4)- spaces (3)
repeat ; newline
end of program
```

APPENDIX XI

Variance Analysis Program

```
JOB

U  EDIN, GEO MISHRA, PROGRAM VARIANCE ANALYSIS TRANS. OOO

OUTPUT

O SEVEN-HOLE PUNCH 2000 LINES

COMPUTING 5000 INSTRUCTIONS

STORE

COMPILER AA


begin

real  x, y, z

integer  catgrs, factors, items, variates, c, f, i, j, v

comment  insert values appropriate to data in next two lines

factors = 3; variates = 11

items = 82; catgrs = 4

real array  Var (1: variates, 1: items), m, s (1: catgrs)

integer array  Cat (1: factors, 1: items), n (1: catgrs)

cycle i=1, 1, items

cycle f=1, 1, factors

read (Cat(f, i))
```

```
repeat
cycle v=1, 1, variates
read (Var(v, i))
repeat
repeat
newline
caption Check: ƀ last ƀ rowƀ of ƀ data
cycle f=1, 1, factors
print (Cat(f, items), 2, o)
repeat
cycle v=1, 1, variates
print (Var(v, items), 2, 2)
repeat
newline
cycle v=1, 1, variates
newline
caption Variates
print (v, 2, 0)
newline
cycle f=1, 1, factors
caption Factors
print (f, 2, 0)
newline
```

```
cycle c=1, 1, catgrs
s (c) = o; n (c) = o
repeat
cycle i=1, 1, items
c = Cat (f, i)
s (c) = s (c) + Var (v, i)
n (c) = n (c) + 1
repeat
j=0; y=o
caption Means ␢ of ␢ categiries
cycle c = 1, 1, catgrs
if n (c) = o then → 1
print (c, 4, 0)
m (c) = s (c) / (c)
j = j + 1
y = y + m (c)
print (m(c), 2, 4)
1 : repeat
caption grand ␢ mean
print ((y/j), 2,4)
newline
caption variance ␢ within ␢ categories
x = o
cycle i = 1, 1, items
```

```
c = Cat (f, i)

x = x + (Var(v, i) - m (c))^2

repeat

x = x / (items - j)

print (x, 2, 4)

caption d.f.

print ((items - j), 2, 0)

newline

caption variance ƀ between ƀ categories

y = y / j; z = o

cycle c = 1, 1, catgrs

z = z + (n (c) * (m (c) - y)^1)

repeat

z = z / (j-1)

print (z, 2, 4)

caption d.f.

print ((j - 1), 2, 0)

spaces (4)

caption variance ƀ reatio ƀ F

print ((z/x), 2, 4)

repeat

repeat

end of program
```

PLATE 1.

A. Tray sample showing pebble-conglomerate with laminated silty sands. Sample from the tidal flats near Ballinbreich.

B. Tray sample showing marsh sediments with rootlets lying over Boulder Clay deposit in the section near Ballinbreich.

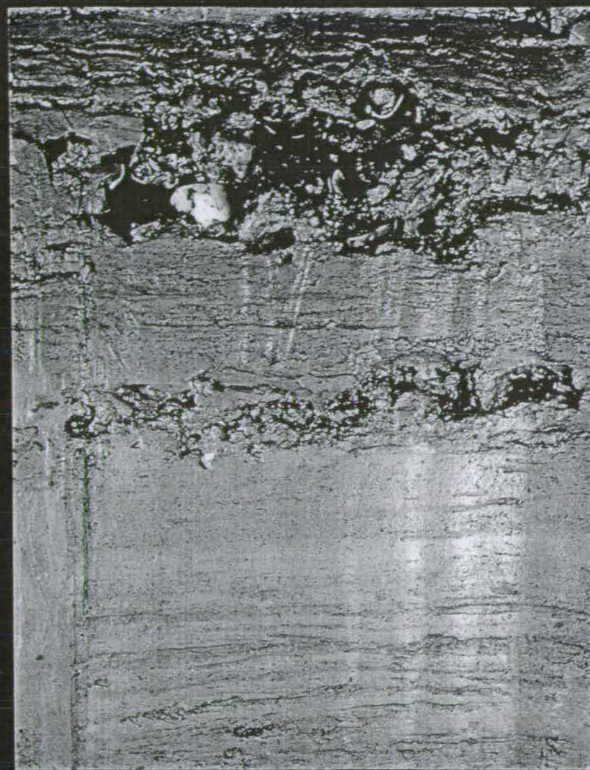

A

B

PLATE 2.

A. Cliffed marsh edge with underlying Boulder Clay deposit near Ballinbreich.

B. Pebble conglomerate in the upper mud flats near Ballinbreich.

A

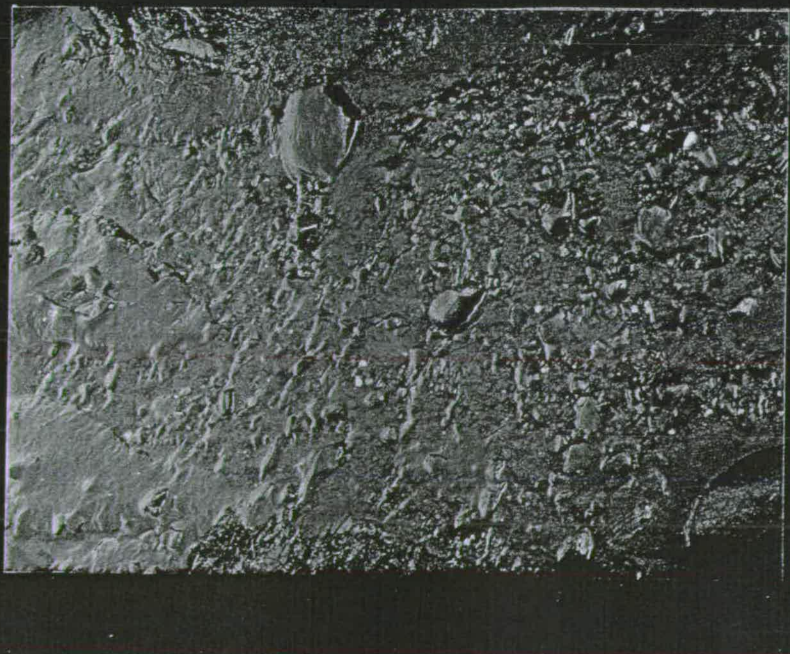

B

PLATE 3.

Aerial photographs of the longitudinal mega - ripples in the Tayport sands. Approximate wave lengths between 5 - 20 metres and amplitudes in a few dm.

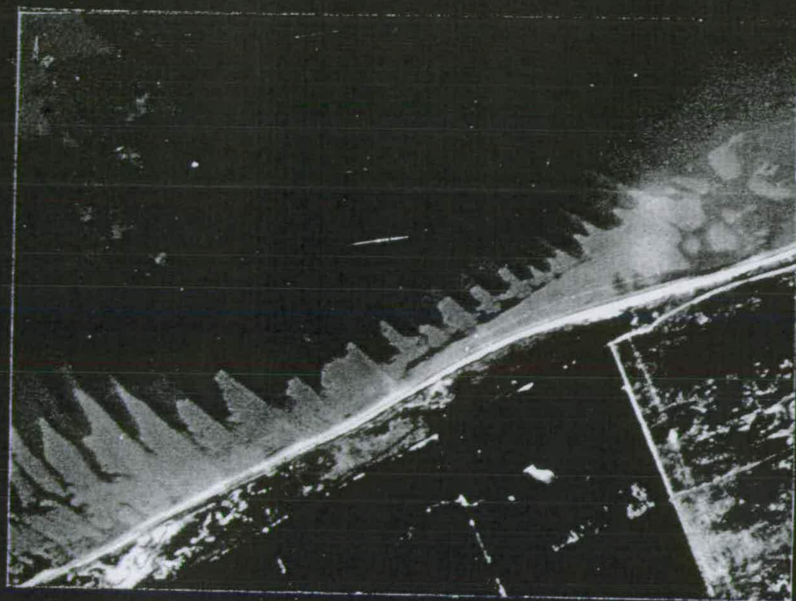

A

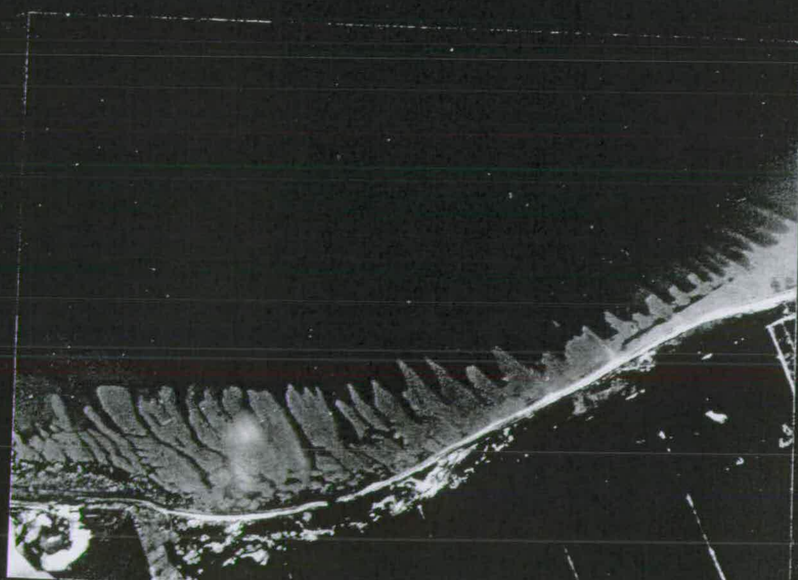

B

PLATE 4.

Aerial photograph of transverse mega - ripples in the sand bank off Wormit. Ripples have steep sides towards downstream and well rounded crests due to ebb - and flood - tidal currents. The wave length vary approximately between 5 - 15 metres and amplitudes from 1 - 2 metres.

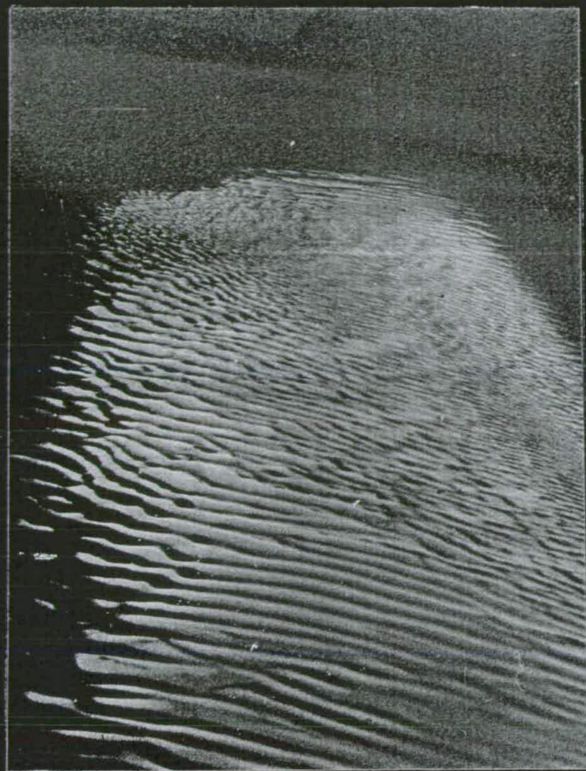

A

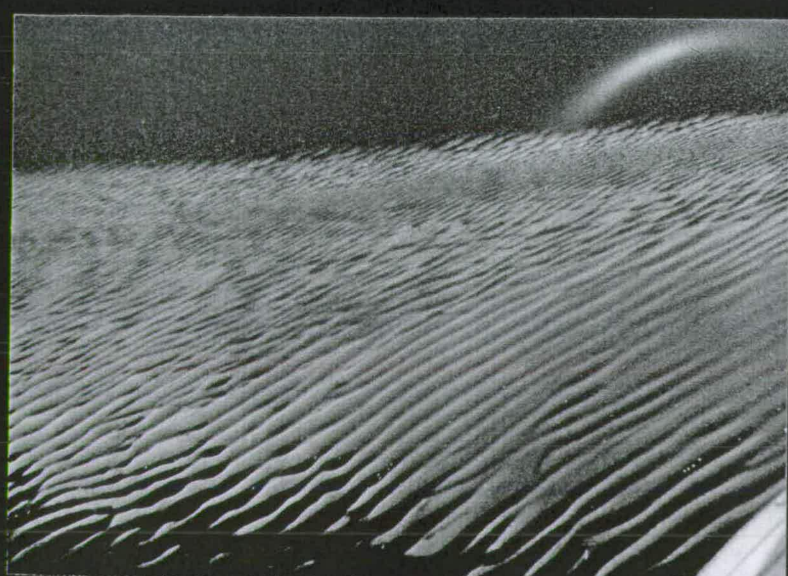

B

PLATE 5.

A. Aerial photograph showing poorly developed asymmetrical mega - ripples off Broughty Ferry. Ripples have steeper sides towards upstream.

B. Aerial photograph of Abertay spit showing mega - ripples in the southern curved part of the spit. Ripples have steep sides towards shore (West). Ripples formed by the westward waves.

A

B

PLATE 6

Aerial photographs of northern side of the Abertay spit. Irregular sand ridges with crescentic depressions, small mounds and smooth surface of the spit.

a - small mound

b - crescentric depression

c - minor ripples at the edge of the sand bank

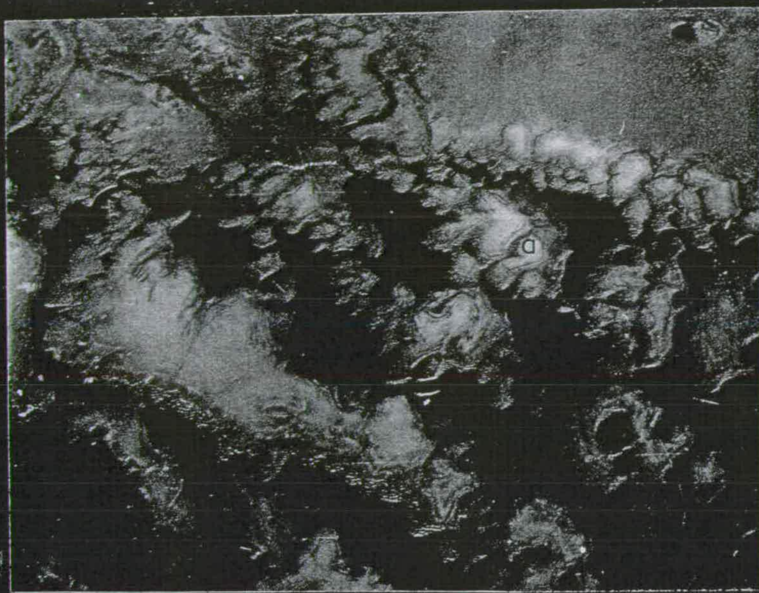

A

B

PLATE 7

Cycle of development of mound and mega - ripple structures in the Budden Ness and Gaa sands.

(Plates 7 to 13)

Aerial photographs of semi - linguoid mega - ripples in the Budden Ness sands. Ripples formed by the westward currents.

A

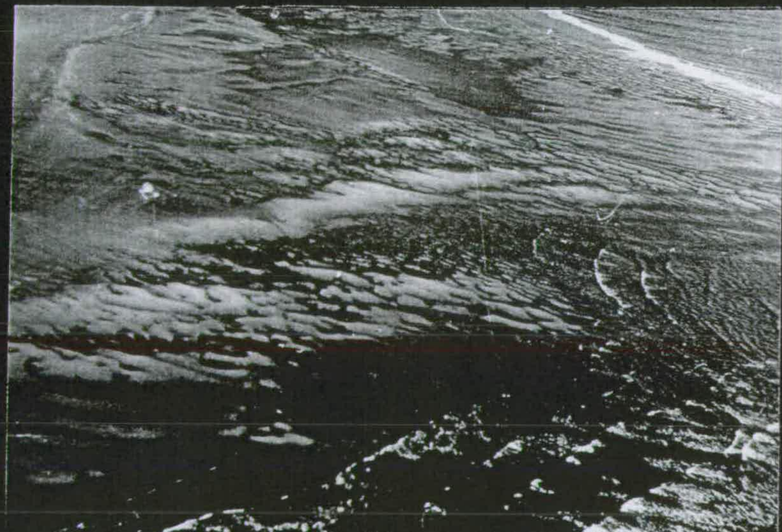

B

PLATE 8

Cycle of development of mound and mega - ripple structures in the Budden Ness and Gaa sands.

Mega - ripples in the process of destruction by change in the tidal cycle and waves. Budden Ness sands.

A

B

PLATE 9

Cycle of development of mound and mega - ripple structures in the Budden Ness and Gaa sands.

A. Mega - ripple crests with various sets of superposed minor ripples.

B. Mound structures appearing in the same area at a later stage by the reworking of the sediment in the area

B

A

PLATE 10

Cycle of development of mound and mega - ripple structures in the Budden Ness and Gaa sands.

A. Aerial photograph showing linear NW - SE pattern of mound structures in the Budden Ness sands.

B. Aerial photograph showing NE - SW trend of mound structures in the Budden Ness sands.

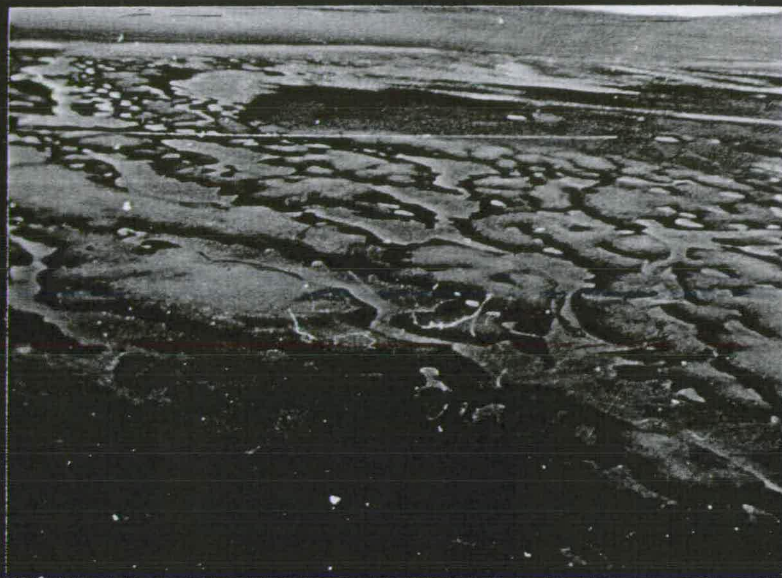

A

B

PLATE 11.

Cycle of development of mound and mega - ripple structures in the Budden Ness and Gaa sands.

Aerial photographs of well rounded mound structures in the Gaa sands. Mounds showing two linear trends; NW - SE trend is better developed than the NE - SW trend.

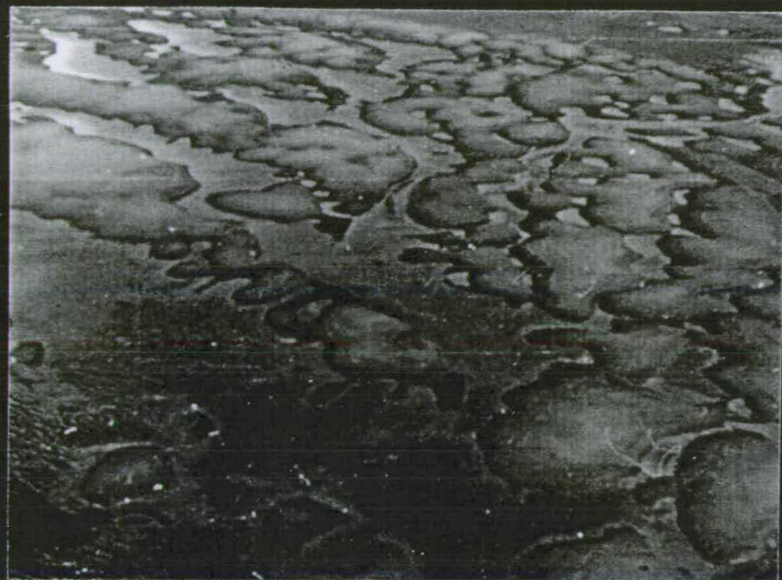

A

B

PLATE 12

Cycle of development of mound and mega - ripple structures in the Budden Ness and Gaa sands.

Mound structures partly obscure due to the deposition in the troughs at a later stage. Smooth unrippled top surfaces of the mounds with backwash striations.

A

B

PLATE 13

Cycle of development of mound and mega - ripple structures in the Budden Ness and Gaa sands.

Highly rippled mound structures being changed by the gradual filling of the troughs.

PLATE 14

Aerial photograph of the two directional wave interference pattern (NW - SE and SW - NE) off Budden Ness.

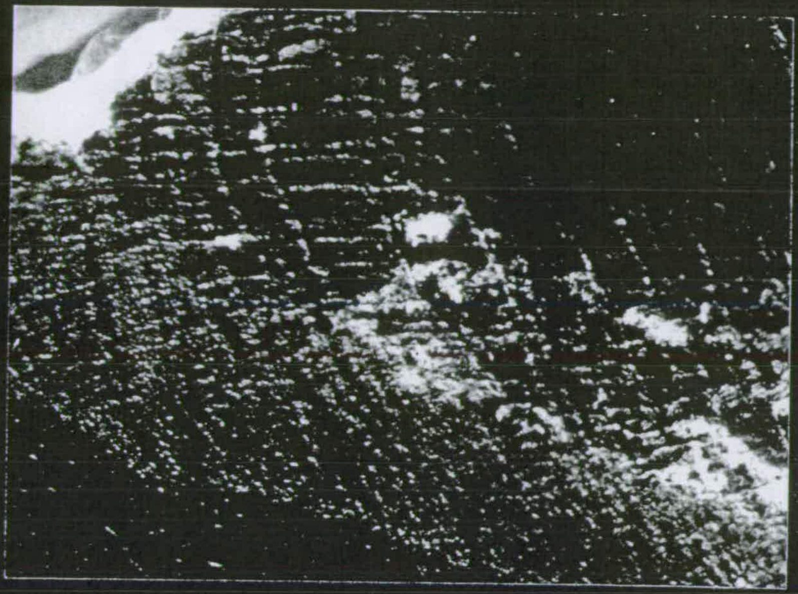

A

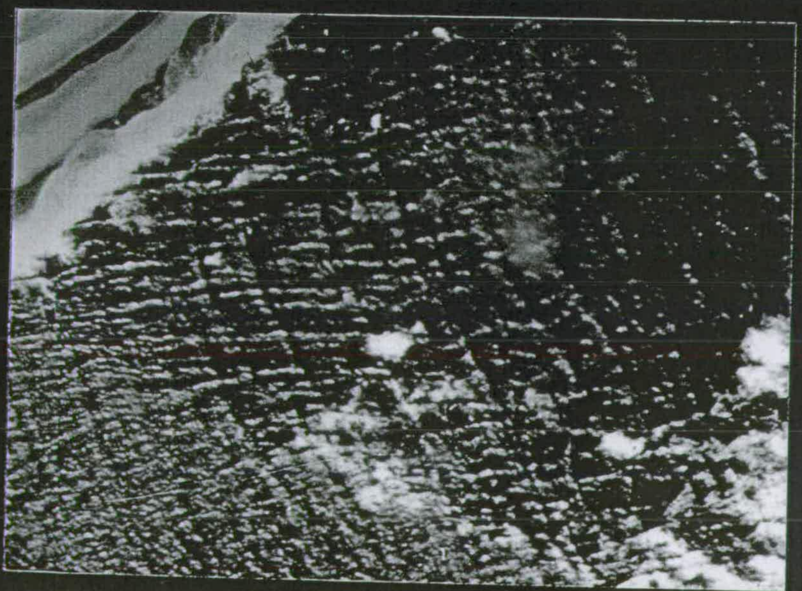

B

PLATE 15

A. Tidal pools formed by the sand ridges in a channel in the Budden sands.

B. Beach cusps developed in the same area after an interval of three weeks at a later stage.

A

B

PLATE 16

A. Section through mound structures. Both sections show irregular scours cutting regular foreshore lamination and filled with cross laminated sands.

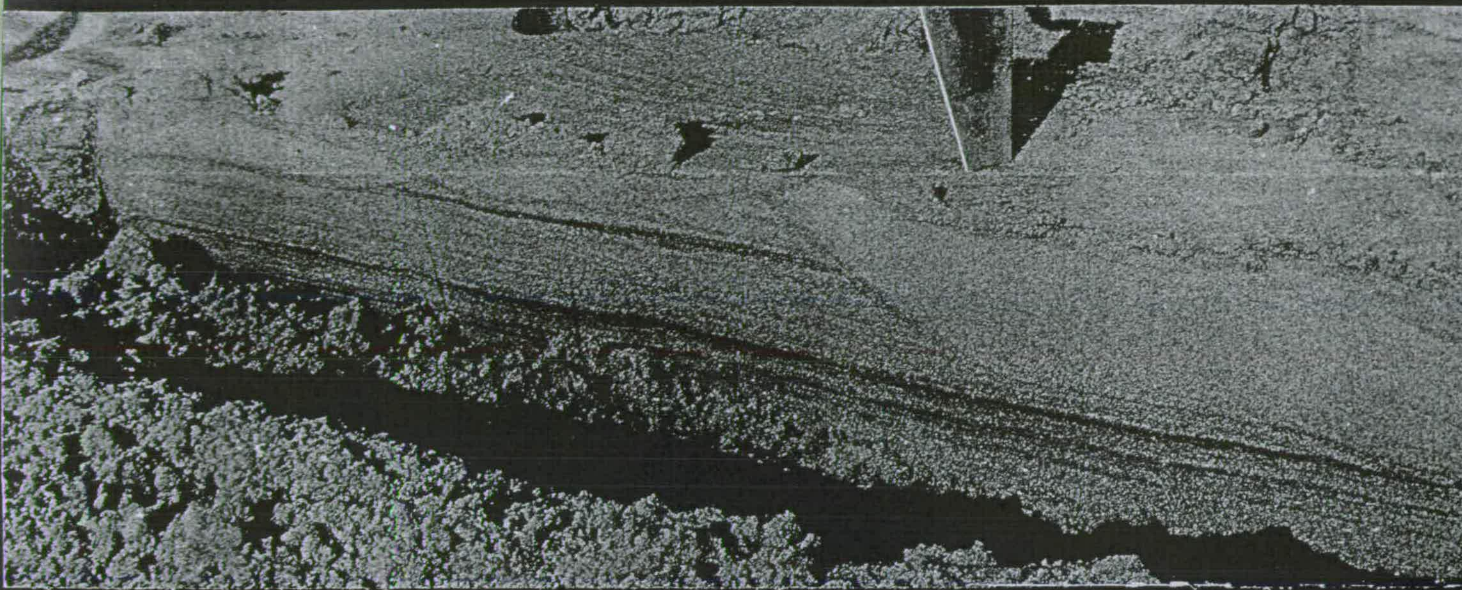

A

B

PLATE 17

Sections in the mound structures.

A. Two sections right angles to each other. Irregular scouring in both directions.

B. Close up of irregular laminations in the mound structures.

A

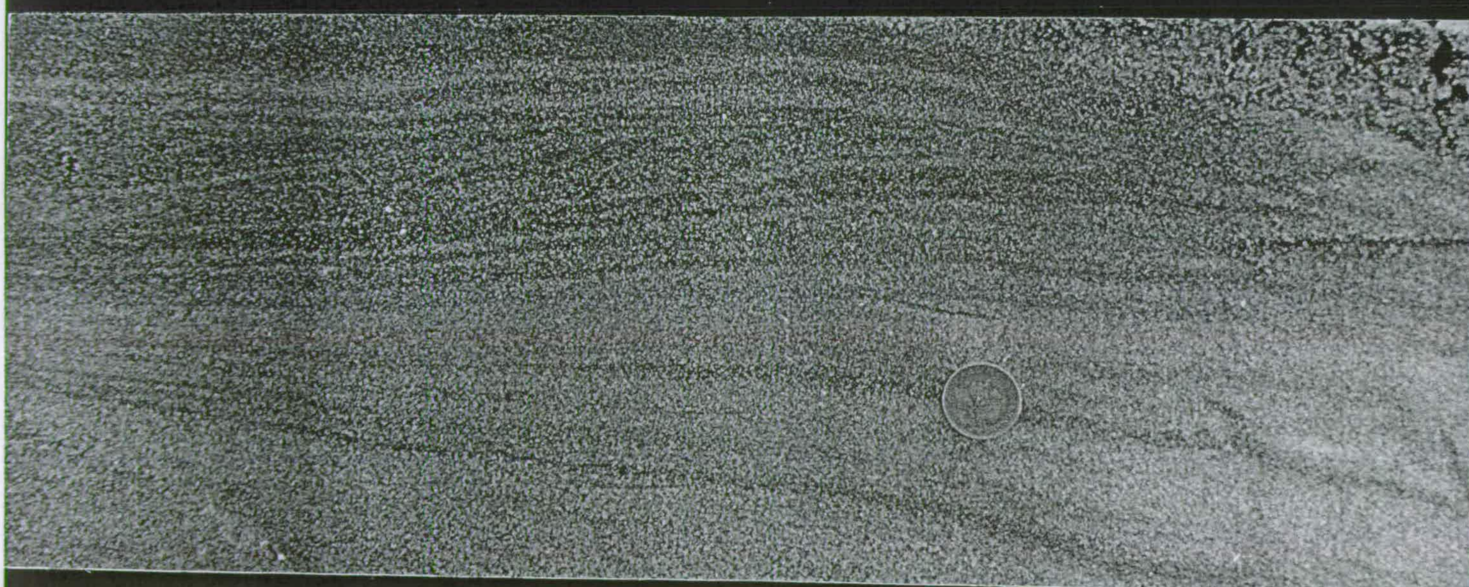

B

PLATE 18

A. Middle foreshore lamination in the Barry sands with rippled laminae near the surface.

B. Rhomboid ripple marks with a crescent mark around a shell in the upper foreshore Tentsmuir sands.

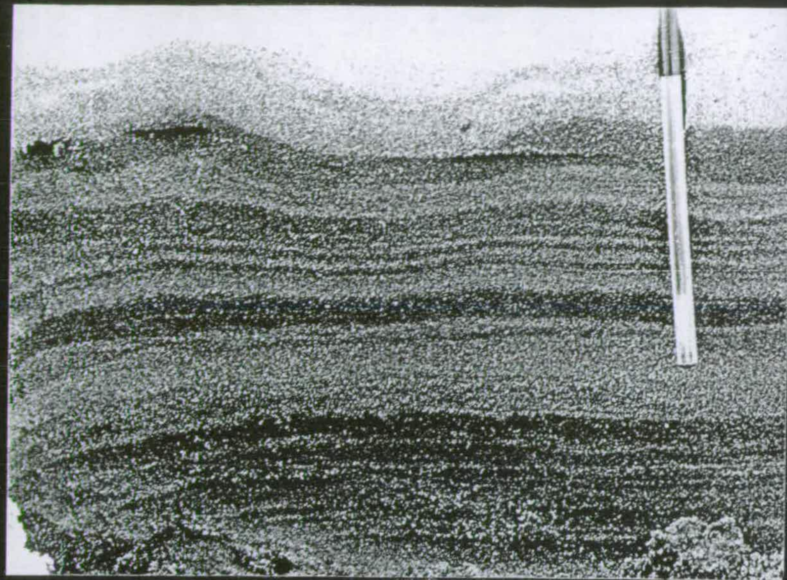

A

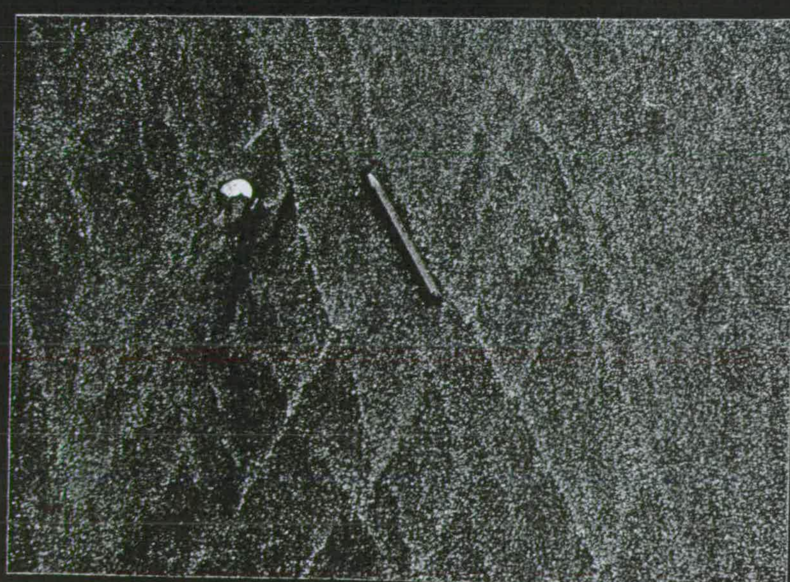

B

PLATE 19

A. Regular asymmetrical transverse ripples with sub-lunate pattern in the Barry sands. Ripples formed by flood tides.

B. Regular asymmetrical transverse ripples in the Barry sands with small longitudinal ridges developed on the ripples. In places crests of the ripples broken by stronger effect of longitudinal ridges.

A

B

PLATE 20

Flat asymmetrical ripples in the upper foreshore Barry sands. Ripples formed by a thin sheet of water during ebb-period.

A

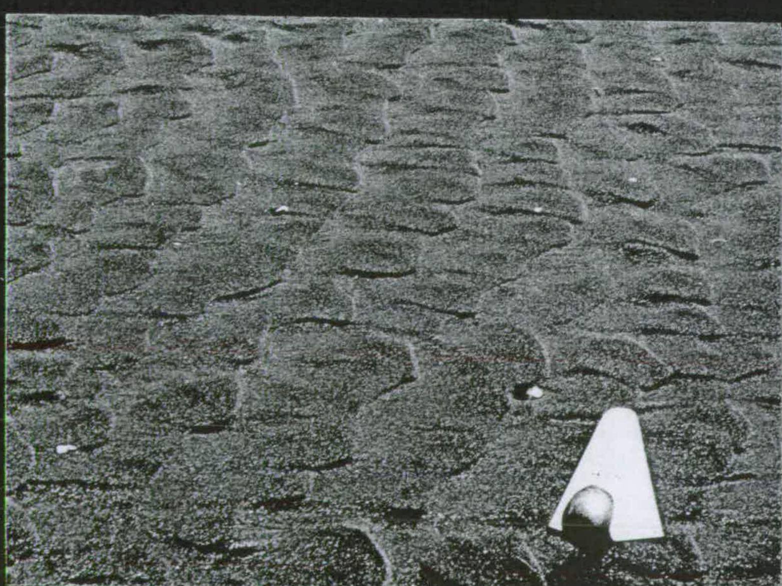

B

PLATE 21

A. Ripple structures flattened by wind - generated waves in the tidal pools. Barry sands.

B. Linguoid ripples flattened by the ebb-tide in the lower foreshore sands.

A

B

PLATE 24

A. Superposed ripples in the Barry sands. Primary set has larger wave lengths and is developed by westward waves. Secondary set is best developed in the troughs of the primary set by the ebb-tide. Southward ebb-tide has flattened the crests of the primary ripple train.

B. Superposed ripples 20 metres west of locality in A. Secondary set is better developed than the other set. In this part of the beach primary ripples have smaller wave lengths than in the locality A.

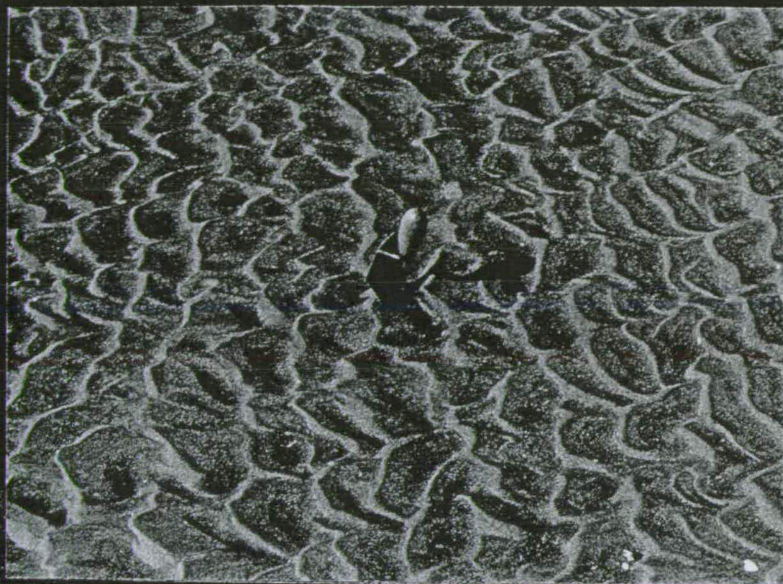

A

B

PLATE 22

A. Semi - linguoid ripples in the middle foreshore Barry sands. Ripples formed by the ebb-tide.

B. A set of well developed linguoid ripples in the lower foreshore sands; a few metres towards the low tide line from the semi - linguoid pattern of A.

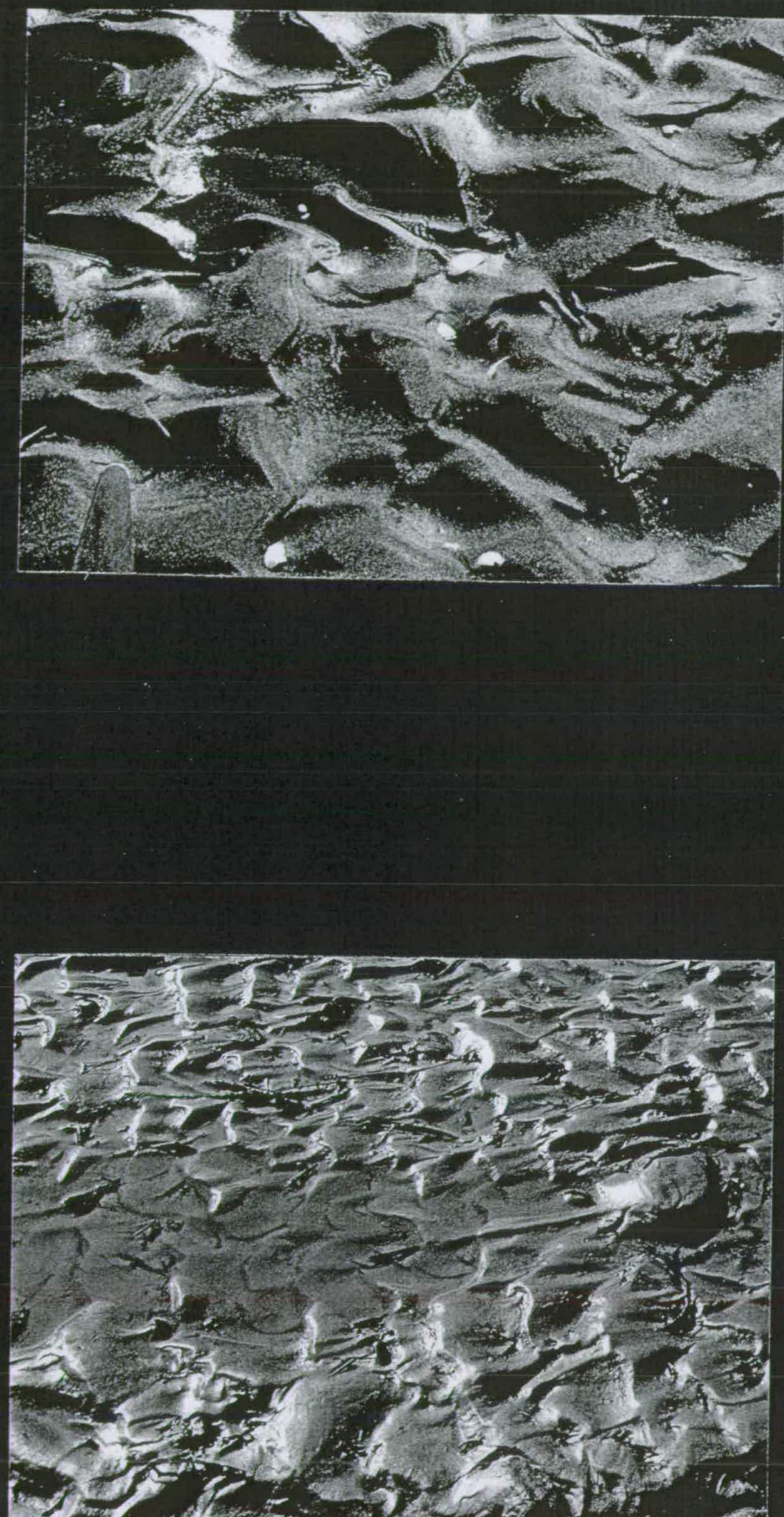

A

B

PLATE 23

A. A set of linguoid ripples in a channel in the lower foreshore Barry sands.

B. Asymmetrical ripple structures in the sand bank off Ballinbreich. Linguoid and sub-lunate patterns.

A

B

PLATE 25

A. Small asymmetrical ripples developed by the ebb-tide in the troughs of larger transverse ripples. Larger ripples have rounded crests modified by the later tidal currents. Structures in Tayport sands.

B. Lineations on the asymmetrical ripples of the Barry sands.

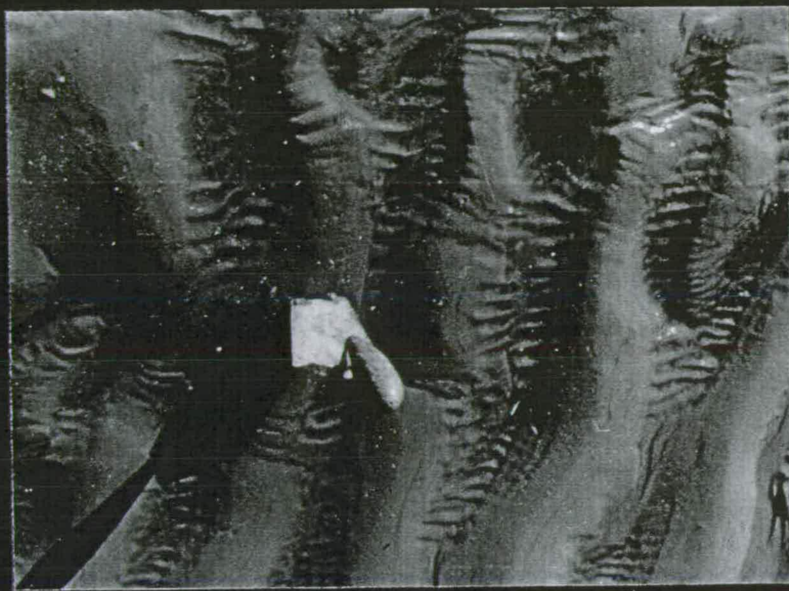

A

B

PLATE 26

A. Longitudinal striations produced in the lower foreshore sands by the backwash.

B. Crescent marks around shells produced by the backwash in the upper foreshore Barry sands.

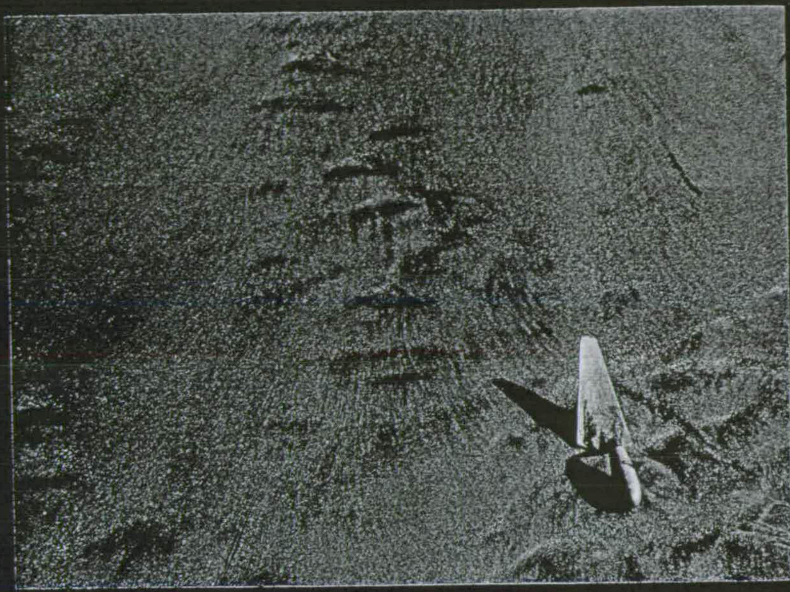

A

B

PLATE 27

A. Rill marks in silty sands in the estuary near Ballinbreich. Dendritic rills developed in the sands with organic debris.

B. Braided rill marks in Barry sands. Rills with current scoop marks; some of the ripple marks cut through by current scoops.

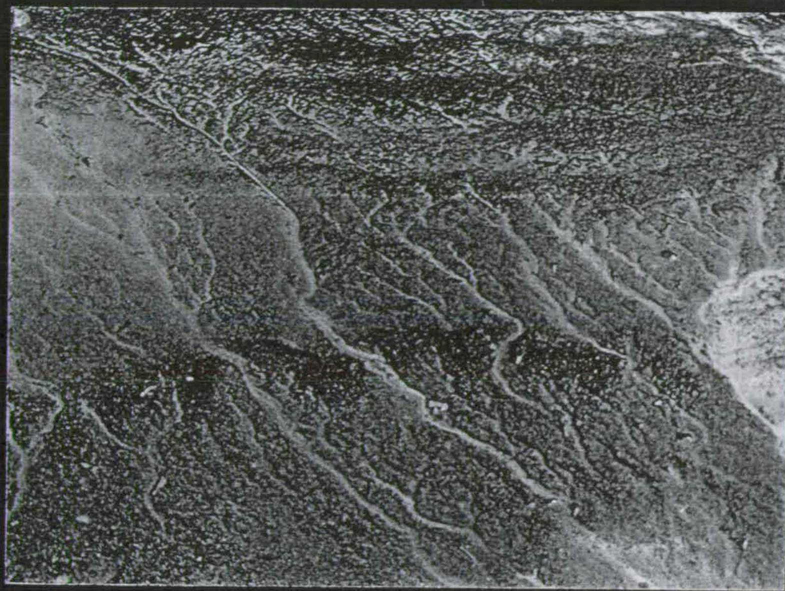

A

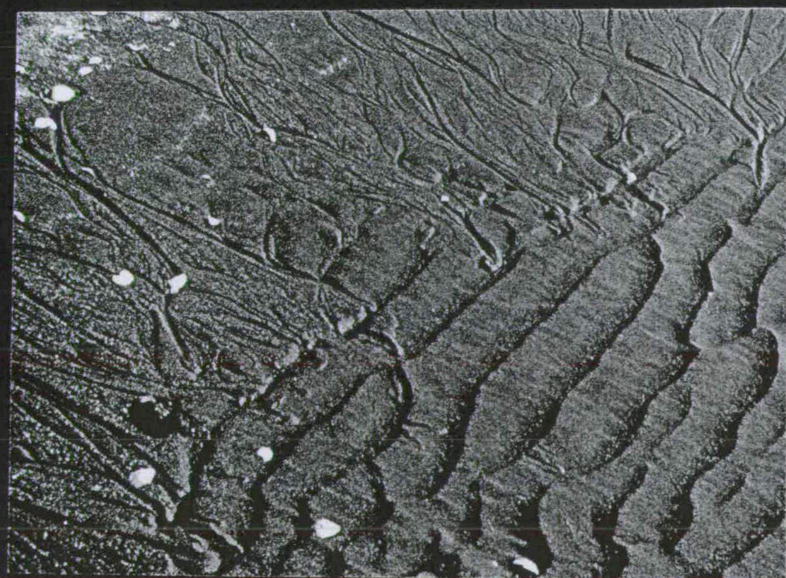

B

PLATE 28

A. Pitted texture developed in the upper foreshore Barry sands.

B. Surface features in a beach chute in the Budden Ness sands (note flow marks and current scoops at the bottom of the chute).

(a) - direction of flow

(b) - current scoops

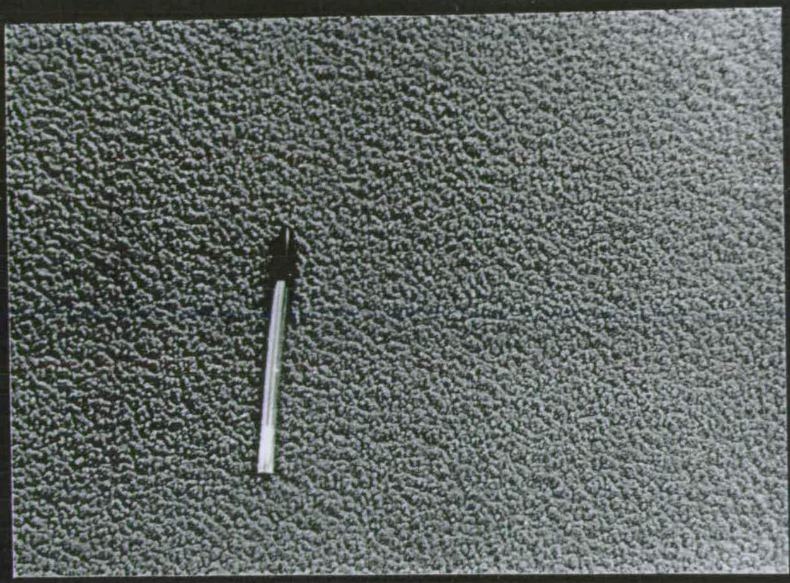

A

B

PLATE 29

Relationship between forms of bed roughness and flow conditions in open channels. (Allen, 1963).

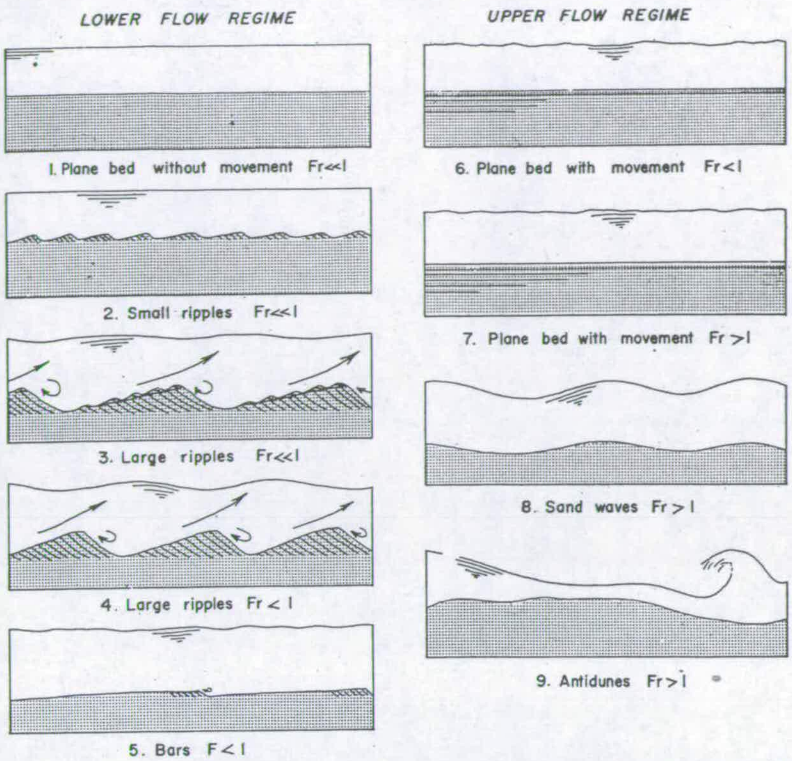

Fig. 1 — Forms of bed roughness in open channels (after Simons and Richardson, 1961; Simons and others, 1961).

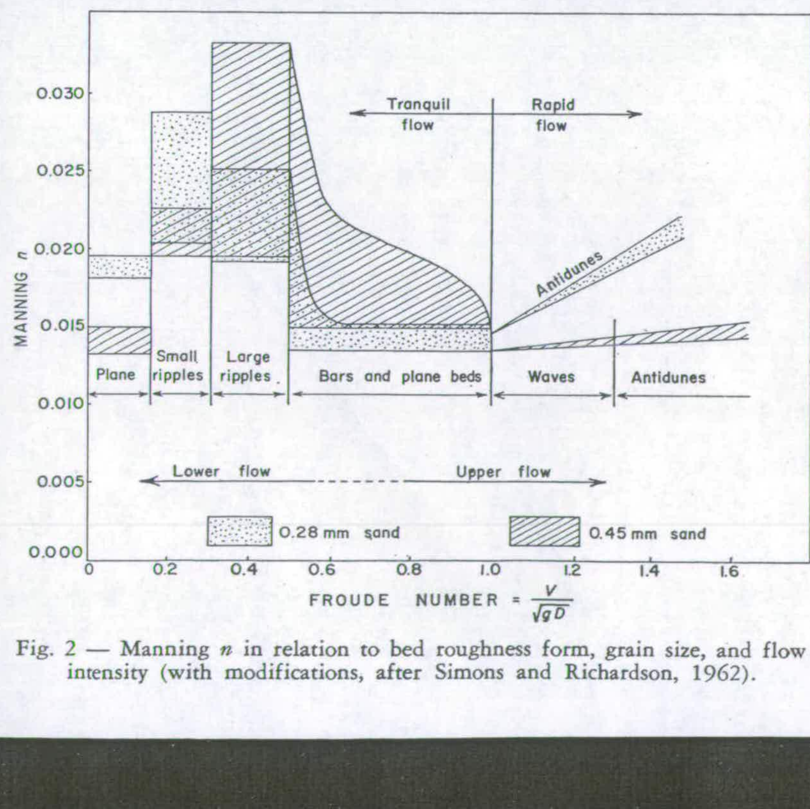

Fig. 2 — Manning *n* in relation to bed roughness form, grain size, and flow intensity (with modifications, after Simons and Richardson, 1962).

PLATE 30

A. Diagram showing range in phi units for various percentiles from the cumulative curves of repeated analyses of each of several samples. There is a wide range for percentiles less than 5 and greater than 95.

B. Diagram showing the fluctuations of sampling on the accuracy of various percentile measurements for a normal distribution. The errors are greatly increased for percentiles below 5 and above 95.
(Inman, 1952.)

A

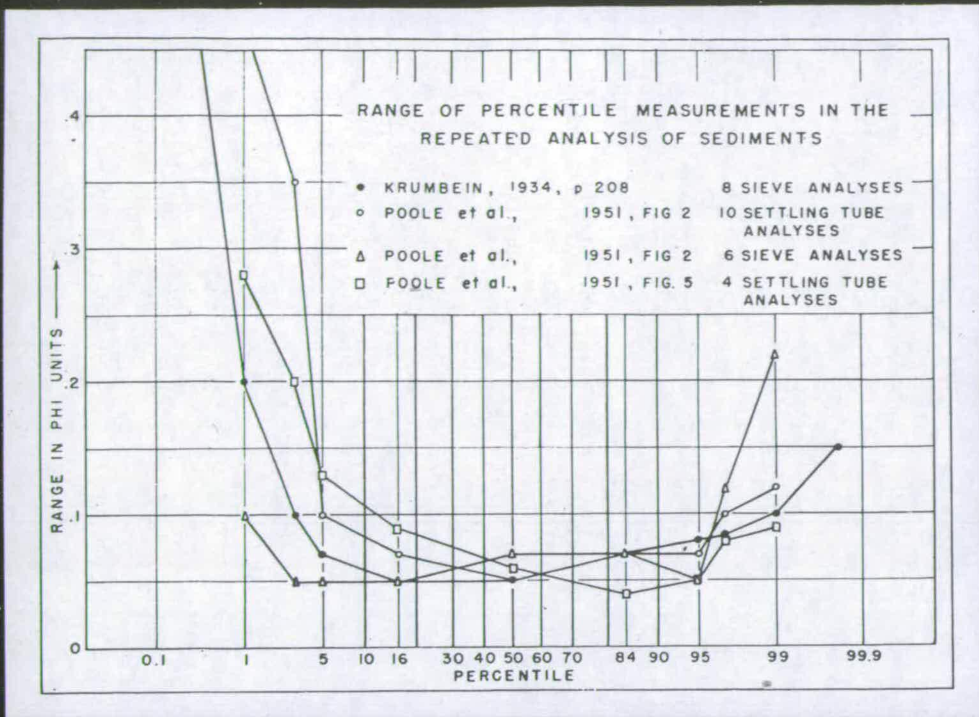
RANGE OF PERCENTILE MEASUREMENTS IN THE REPEATED ANALYSIS OF SEDIMENTS
● KRUMBEIN, 1934, p 208 8 SIEVE ANALYSES
○ POOLE et al., 1951, FIG 2 10 SETTLING TUBE ANALYSES
Δ POOLE et al., 1951, FIG 2 6 SIEVE ANALYSES
□ POOLE et al., 1951, FIG. 5 4 SETTLING TUBE ANALYSES
RANGE IN PHI UNITS
PERCENTILE
0.1 1 5 10 16 30 40 50 60 70 84 90 95 99 99.9
0 .1 .2 .3 .4

B

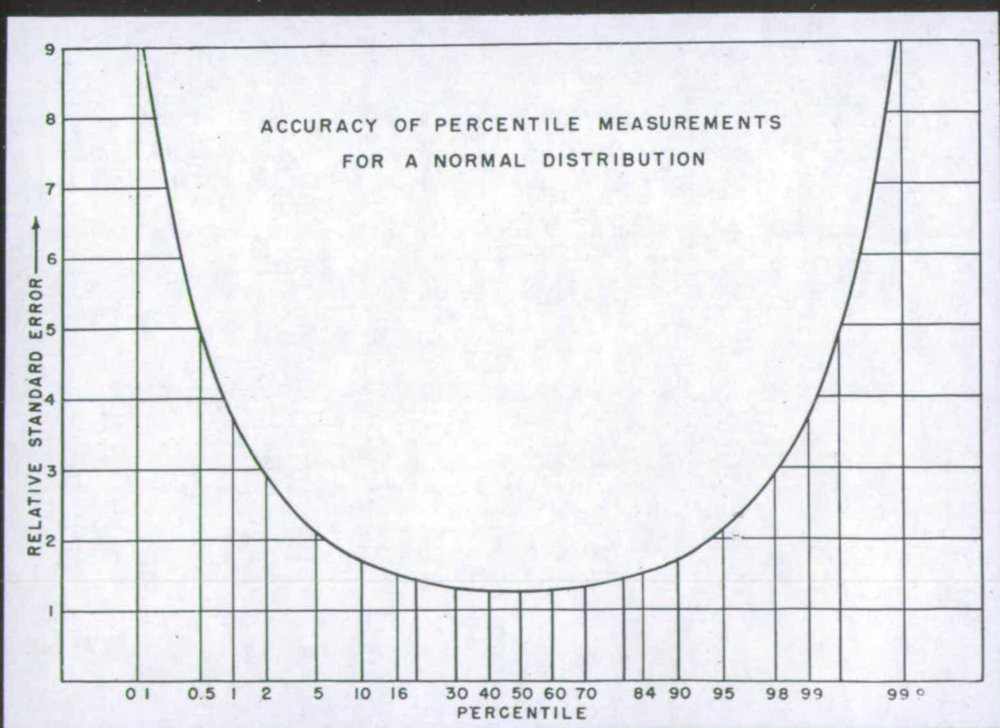
ACCURACY OF PERCENTILE MEASUREMENTS FOR A NORMAL DISTRIBUTION
RELATIVE STANDARD ERROR
PERCENTILE
0.1 0.5 1 2 5 10 16 30 40 50 60 70 84 90 95 98 99 99.9
1 2 3 4 5 6 7 8 9

PLATE 31

I A. Origin of river sediments from mixtures between bottom sediment (a) and fine suspended material (b) (after Doeglas. 1946).

B. Example of river sediment mixing from the Gulf of Paria sediments (F - group) (after Van Andel & Postma, 1954).

II A. Differentiation of transported material (Doeglass, 1950).

B. Example of differentiation of transported material from the Gulf of Persia (after Van Andel & Postma, 1954).

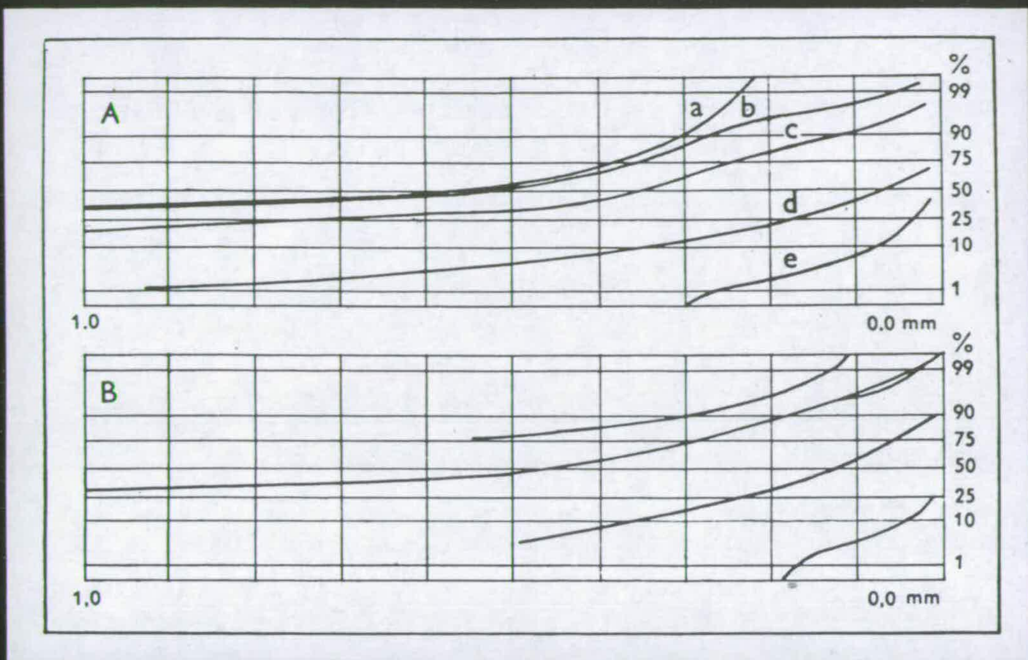
A
a
b
c
d
e
%
99
90
75
50
25
10
1
1.0
0.0 mm
B
1,0
0,0 mm

I

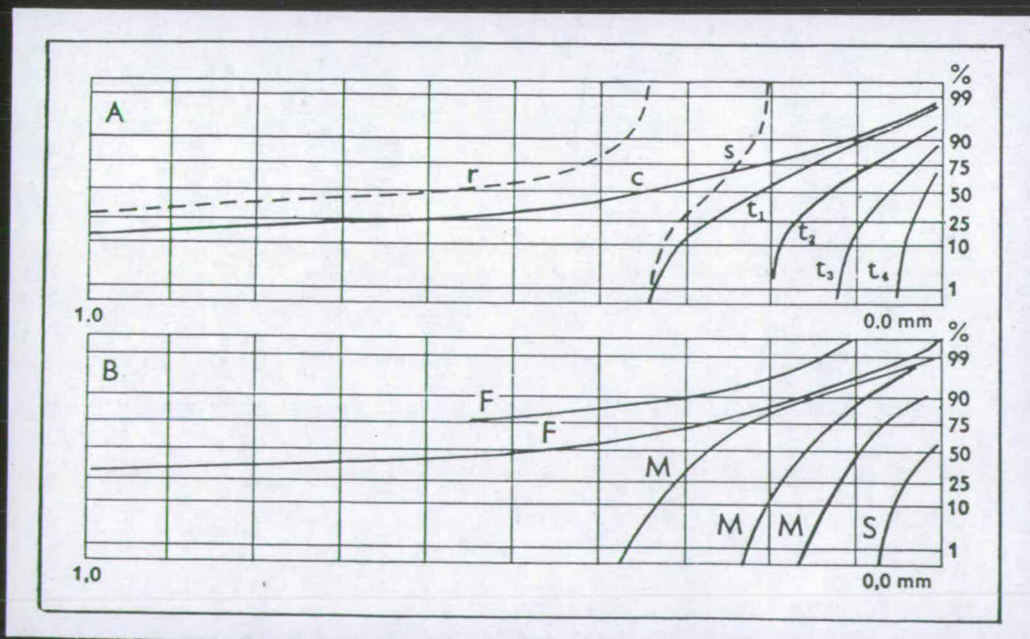
A
r
c
s
t_1
t_2
t_3
t_4
%
99
90
75
50
25
10
1
1.0
0.0 mm
B
F
F
M
M
M
S
1,0
0,0 mm

II

PLATE 32

A. Zone diagram of B - C series. (Van Andel & Postma, 1954)

B. The variation in grain size distribution of beach sands from the Rhone delta. There is a wider variation especially in the finer end due to the acid treatment. (from Kruit and Van Andel, 1955)

A

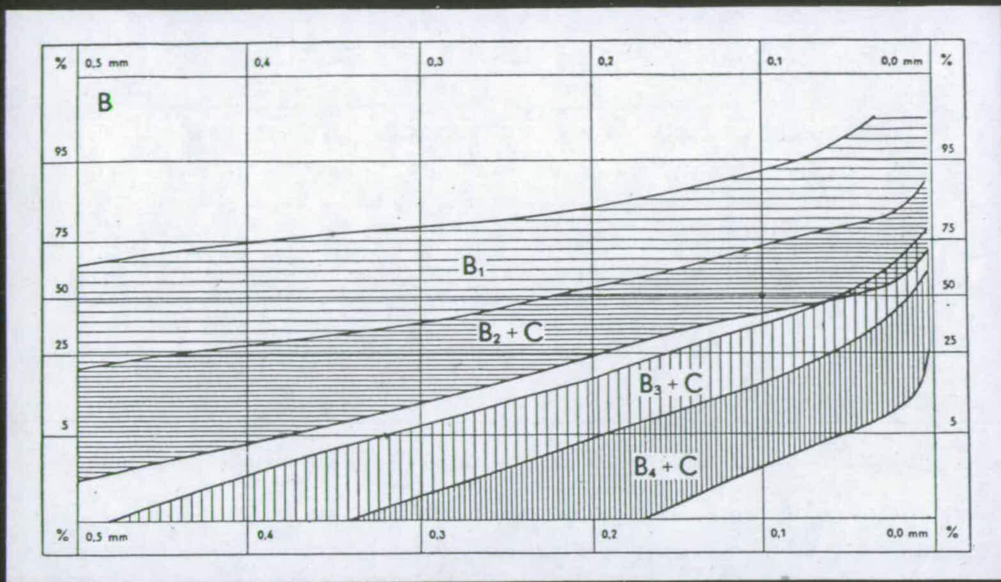

%
0,5 mm
0,4
0,3
0,2
0,1
0,0 mm
B
95
75
50
25
5
B_1
$B_2 + C$
$B_3 + C$
$B_4 + C$

B

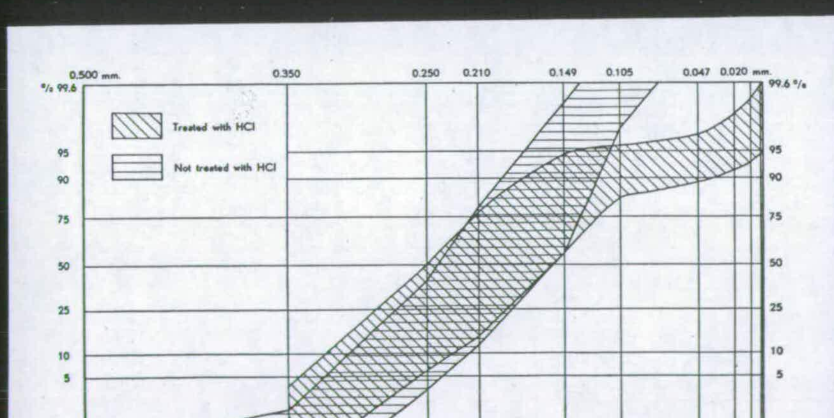

0.500 mm.
0.350
0.250
0.210
0.149
0.105
0.047
0.020 mm.
% 99.6
99.6 %
Treated with HCl
Not treated with HCl
95
90
75
50
25
10
5
% 0.4
0.4 %

PLATE 33

B. Zone diagram of F - S series

C. Zone diagram of M - S series

(from Van Andel & Postma, 1954)

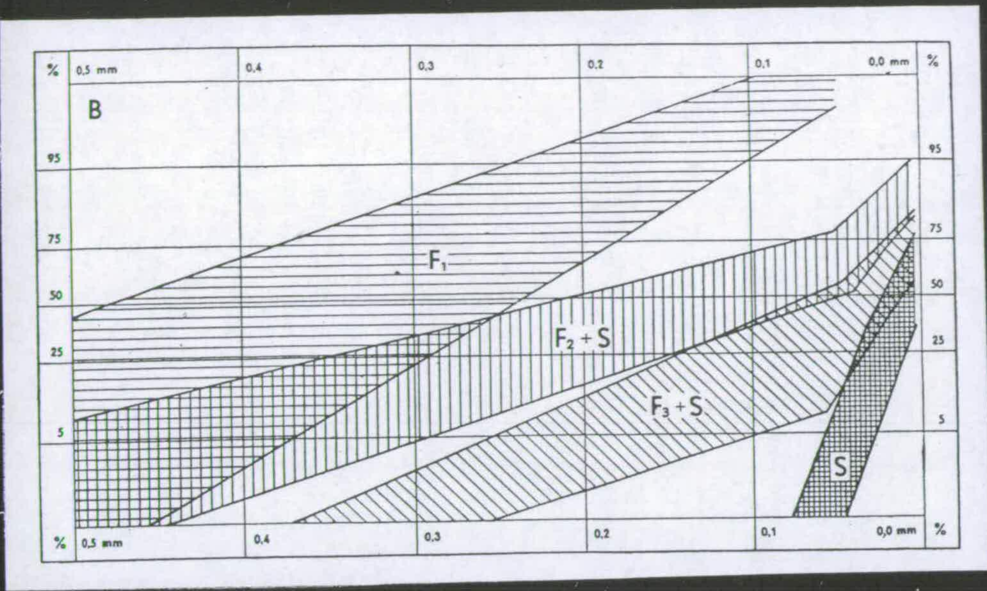
B
F1
F2 + S
F3 + S
S
0,5 mm
0,4
0,3
0,2
0,1
0,0 mm
%
95
75
50
25
5

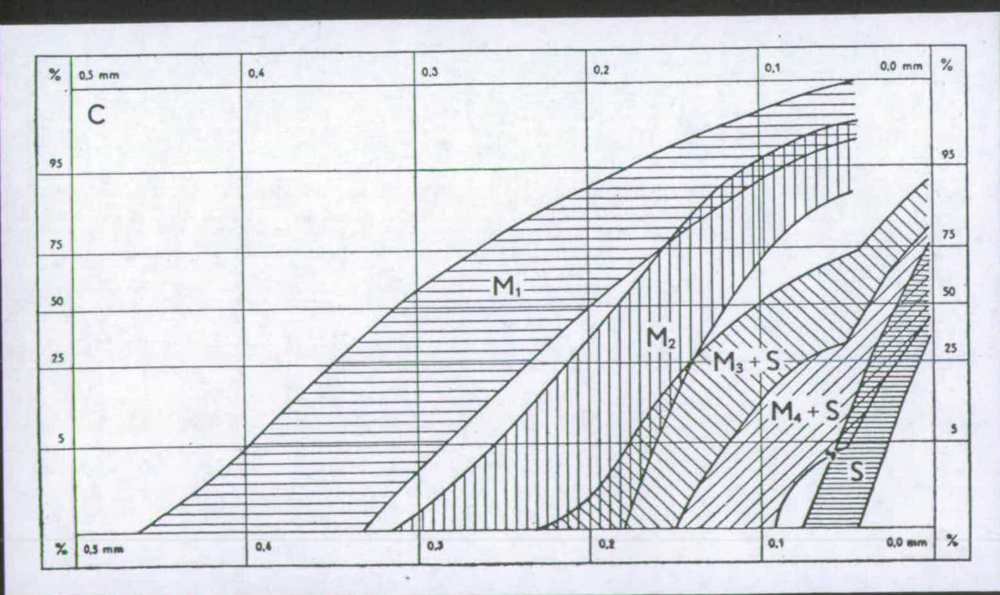
C
M1
M2
M3 + S
M4 + S
S
0,5 mm
0,4
0,3
0,2
0,1
0,0 mm
%
95
75
50
25
5

PLATE 34

Visual estimation chart used for roundness determinations.
(from Shepard & Young, 1961)

A - Very angular
B - Angular
C - Sub-angular
D - Sub-rounded
E - Rounded
F - Well-rounded

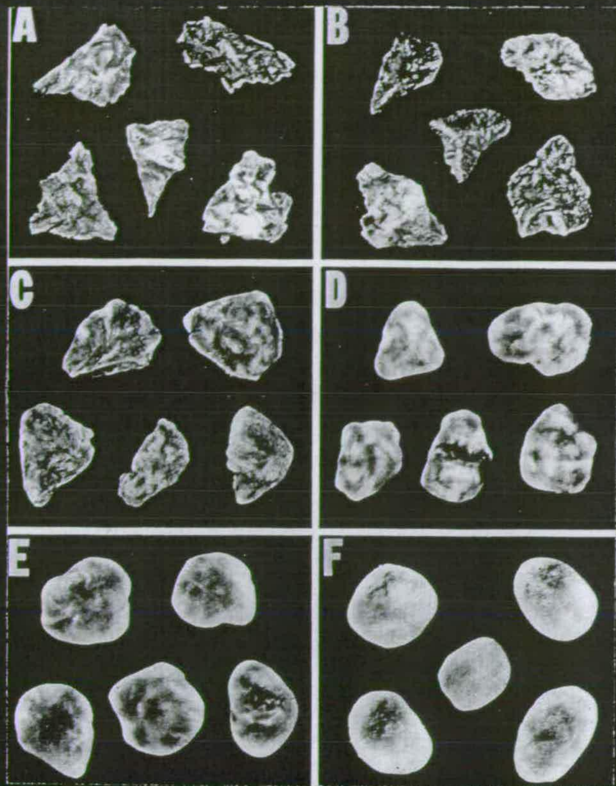
A
B
C
D
E
F

ABSTRACT OF THESIS

Name of Candidate: Sharad Kumar Mishra

Address: Grant Institute of Geology, West Mains Road, Edinburgh, 9.

Degree: Ph. D. Date: 20th August, 1964.

Title of Thesis: Recent sediments in the Firth of Tay Region.

This thesis presents a study of some aspects of recent sedimentation in the Tay estuary region, greater emphasis being placed on the environments of deposition and their relationship with sedimentary structures, grain size and heavy mineral distribution.

The Fluvial sediments are characterised by their medium to medium-fine sands with F-type distribution curves. The sediments show a gradual decrease in mean size towards the estuary.

The estuarine sediments have fine sand to coarse silt size material with mixed FM-MS-type distribution curves which gradually change to M-type curves towards the lower reaches of the estuary. Cliff falls have given B - and BS - type curves in the southern cliffed parts of the estuary. The estuarine sediments have the highest silt/clay content in the area. The marsh sediments are characterised by undulating, nodular laminae, mostly composed of silty sands and sandy silts with abundant rootlets. Rippled laminae are absent. The tidal flat laminations are more regular and are composed of fine to very fine silty sands. Rippled laminae are present but the heavy-mineral laminae are not observed here. Various types of current structures are found in the flats, while the tidal channels with sand banks show transverse megaripples.

The beach sediments consist of fine to very fine sands with M-type distribution curves. Silt-clay fraction is always less than one per cent. Here, three types of laminations are found. The backshore laminae have low landward dips while the upper foreshore laminae have low seaward dips. Both types of laminations are characterised by well sorted sands with well-developed heavy-mineral laminae. Rippled laminae are frequent. The lower foreshore sediments have coarser sands than the other two and irregular laminae have high values of seaward dips. In this zone of the beach the heavy mineral laminae are not so well developed as in the other two zones.

There is a maximum development of current-formed minor and major structures in the beach sands. The beach sediments can be distinguished from the sediments from other environments by the shapes of the distribution curves, moment measures and scatter plots.

Coastal dune sediments have an abundance of cross-laminations with varying orientations and amounts of dip. The laminae are very thin and consist of fine to very fine sand with streaks of heavy-minerals.

Use other side if necessary.

Normally, the dune sands have a higher heavy-mineral content than the other sands. Dune sands can be distinguished from the other sands by the shape of distribution curves and moment measure plots.

Variance analysis and scatter plots show that the moment measures are the best statistical parameters to distinguish between various environments. Inman's graphic parameters are of little use in determining the various environments. Thus a combination of distribution curves and moment measures should give the best picture of the size-frequency distribution of sediments. In the open-end curves, the moment measures are approximate, so in these cases graphic parameters can give a better approximation of the size distribution with less computation.

Heavy mineral studies do not reveal any significan relationship between the mineralogical composition of a sample and its grain size parameters. Three types of heavy-mineral associations are found and they are all derived from the same mineral province. The source area consists of the Moine and Dalradian metamorphics with associated igneous rocks together with Old Red Sandstone sediments and lavas, and local carboniferous sediments.